## DOCTOR OF PHILOSOPHY

# Investigation of the recognition and host target of the Phytophthora infestans effector PiAVR2

Breen, Susan Anne

*Award date:*
2012

DOCTOR OF PHILOSOPHY

# Investigation of the recognition and host target of the Phytophthora infestans effector PiAVR2

Susan Anne Breen

2012

University of Dundee

# Investigation of the recognition and host target of the *Phytophthora infestans* effector PiAVR2

**Susan Anne Breen**

Doctor of Philosophy

College of Life Sciences
The University of Dundee
and
Cell and Molecular Sciences
The James Hutton Institute



April 2012

# Declaration

The results presented here are of investigations conducted by myself. Work other than my own is clearly identified with references to relevant researchers and/or their publications. I hereby declare that the work presented here is my own and has not been submitted in any form for any degree at this or other university.

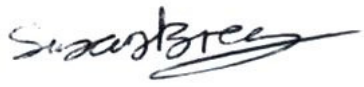

Susan A. Breen

We certify that Susan Breen has fulfilled the relevant Ordinance and Regulations of the University Court and is qualified to submit this thesis for the degree of Doctor of Philosophy.

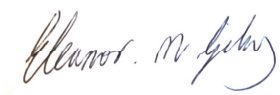

Dr Eleanor M. Gilroy
Cell and Molecular Sciences
The James Hutton Institute

Prof. Paul R J Birch
College of Life Sciences
University of Dundee

# Table of Contents

# List of Figures

# List of Tables

# Acknowledgments

I would like to begin by thanking Paul Birch and Eleanor Gilroy for arranging this PhD project, finding the funding and to the BBSRC for providing the financial support. I would also like to thank Paul and Elli for all their support, guidance and faith in me during this project which is what has allowed me to complete this work. Also, for all the amazing opportunities they have provided me with and for their extremely valued friendship both in and out of the lab. I am extremely grateful for all they have done for me.

I would also like to thank all of those within the James Hutton Institute, too numerous to mention, who have advised me, guided me and supported me throughout this PhD. A special thanks to Hazel, Ingo, Amar, Miles, Stefan, Petra, Tanya, Eva and Steve who have kept me smiling in the lab, even during the tough days, and for all your help, advice and friendship.

I would like to thank my family, but especially my parents, Anne and Paul, and my brother Alan who have had to deal with me through-out this PhD. Also a very special thanks to Craig who has had to deal with most of my ups and downs, I know that has not been easy, and I thank you for sticking with me.

I could not have achieved this without all of this support from everyone, so thank you!

# Publications arising from this work

Diane G O Saunders, **Susan Breen**, Joe Win, Sebastian Schornack, Ingo Hein, Tolga O Bozkurt, Nicolas Champouret, Paul R J Birch, Eleanor M Gilroy, Sophien Kamoun. (2012) *Indirect recognition of Phytophthora infestans RXLR effector PiAVR2 by the host immune receptor R2.* In preparation

Eleanor M Gilroy, **Susan Breen**, Stephen C Whisson, Julie Squires, Ingo Hein, Anoma Lokossou, Petra C Boevink, Juan Morales, Anna O Avrova, Leighton Pritchard, Dionne Turnbull, Maciej Kaczmarek, Liliana Cano, Eva Randall, Francine Govers, Pieter van West, Sophien Kamoun, Vivianne G A A Vleeshouwers, David E L Cooke, Paul R J Birch. (2011**)** *Presence/absence polymorphism and differential expression of two diverged forms of PiAVR2 in* Phytophthora infestans *determine virulence on R2 plants*. **New Phytologist, 191**:763-776

# Abstract

This was a project joint between the University of Dundee and The James Hutton Institute where both parties were interested in further understanding the interactions between plant host proteins and pathogen effector proteins. An objective of this thesis was to determine the host target of the *Phytophthora infestans* effector PiAVR2 and the means by which this avirulence protein is recognised by the potato resistance protein, R2.

Prior to this PhD, forward genetic studies identified three RXLR effector encoding genes within the *AVR2* locus. By use of transient co-expression with the resistance gene *R2* it was determined which of these genes was *PiAVR2*. A virulent form of PiAVR2, named PiAVR2-like, was found within isolates of *P. infestans*. Isolates which only express *PiAVR2-like* are virulent on potato cultivars expressing *R2*. Isolates which express both forms, or only the *PiAVR2* form, are avirulent on cultivars expressing *R2*. This suggests that expressing only *PiAVR2-like* is key to the virulence of the pathogen on *R2* expressing cultivars. There are 10 known orthologues of *R2* which all recognise PiAVR2. However none can recognise PiAVR2-like. The characterisation of the means by which *P. infestans* overcomes *R2* resistance has provided a strategy, based on identifying *R* genes that recognise *PiAVR2-like*, to provide durable late blight disease resistance.

It was also discovered that both PiAVR2 and PiAVR2-like physically interact with the same host target proteins, BSL1, BSL2a and BSL2b. The BSLs are part of a family of Kelch repeat containing Ser/Thr phosphatases which function as activators of the brassinosteroid signal transduction pathway. It was shown that silencing of the *BSL1* and *BSL2a* genes within plants results in the attenuation of PiAVR2 recognition by R2. In the case of BSL1 it was further shown that an interaction between R2 and BSL1 only occurs in the presence of PiAVR2. This implies that R2 recognises PiAVR2 by an indirect mechanism, utilising

either the Guard or Decoy Hypotheses, and that BSL1 is essential for this recognition. This is the first reported demonstration of indirect recognition of an intracellular eukaryotic plant pathogen effector protein.

# Abbreviations

| | |
|---|---|
| ABA | abscisic acid |
| AL | activation loop |
| At | *Arabidopsis thaliana* |
| AVR | avirulence |
| BAC | bacterial artificial chromosome |
| BBH | best blast hits |
| BCTV | beet curly top virus |
| BLAST | basic local alignment search tool |
| BL | brassinolide |
| BR | brassinosteroid |
| CBEL | cellulose binding elicitor lectin |
| CK | cytokinin |
| CPC | Commonwealth Potato Collection |
| CT | C-terminal domain |
| DNA | deoxyribonucleic acid |
| EBL | epi-brassinolilde |
| EF-Tu | elongation factor Tu |
| EST | expressed sequence tag |
| ET | ethylene |
| ETI | effector triggered immunity |
| ETS | effector triggered susceptibility |
| FLAG | phenylalanine, leucine, alanine, glycine |
| Flg22 | 22 amino acid section from bacterial flagellin |
| GA | gibberellic acid |
| GFP | green fluorescent protein |
| GM | genetic modification |
| GSK3 | glycogen synthase kinase 3 |
| HA | haemagglutinin |
| Hp | *Hyaloperonospora parasitica* |
| HR | hypersensitive response |
| HSP | high-scoring segment pairs |
| ID | island domain |
| INF1 | elicitin infestin 1 |
| JA | jasmonic acid |
| JM | juxtamembrane region |
| KD | kinase domain |
| KO | knock out lines |
| LFLAK | leucine, phenylalanine, leucine, alanine, lysine |
| LPS | lipopolysaccharides |
| LRR | leucine rich repeats |
| MAPK | mitogen activated protein kinase |
| MES | 2-[N-Morpholino]ethanesulfonic acid |
| MS | mass spectrometry |
| myc | myc epitope from the c-myc gene |
| *nahG* | salicylate hydroxylase gene |
| Nb | *Nicotiana benthamiana* |
| NBS | nucleotide binding site |
| NOI | reactive nitrogen oxide intermediates |
| NPP1 | necrosis-inducing, *Phytophthora* protein 1 |
| OD | optical density |
| PAMPs | pathogen associated molecular patterns |
| PCD | programmed cell death |
| PCR | polymerase chain reaction |
| Pepl3 | 13-amino acid pattern |
| Pi | *Phytophthora infestans* |

| | |
|---|---|
| PI3P | phosphatidylinositol-3-phosphate |
| PI4P | phosphatidylinositol-4-phosphate |
| *PR* | pathogenesis-related |
| PRR | pathogen recognition receptors |
| Ps | *Phytophthora sojae* |
| PS | Ponceau stain |
| PTI | pathogen triggered immunity |
| PVM | parasitophorous vacuole membrane |
| PVX | potato virus X |
| qRT-PCR | quantitative reverse transcription polymerase chain reaction |
| QTL | quantitative trait locus |
| *R* gene | resistance gene |
| RACE | rapid amplification of cDNA ends |
| RFP | red fluorescent protein |
| RNA | ribonucleic acid |
| ROS | reactive oxygen species |
| RT-PCR | reverse transcription polymerase chain reaction |
| RXLR-EER | arginine, any amino acid, leucine, arginine, glutamic acid, glutamic acid, arginine motif |
| SA | salicylic acid |
| SAR | systemic acquired resistance |
| SCR | small cysteine rich |
| SDW | sterile distilled water |
| Sl | *Solanum lycopersicum* |
| SNP | single nucleotide polymorphism |
| St | *Solanum tuberosum* |
| TAIR | The *Arabidopsis* Information Resource |
| TF | transcription factor |
| TM | transmembrane domain |
| TPR | tetratricopeptide repeat |
| TRV | tobacco rattle virus |
| T3SS | type three secretion system |
| VIGS | virus-induced gene silencing |
| YC | C-terminal section of YFP |
| YFP | yellow fluorescent protein |
| YN | N-terminal section of YFP |
| Y2H | Yeast Two Hybrid |
| bp | basepairs |
| kb | kilobase |
| kDa | kilodaltons |
| µg | micrograms |
| µl | microlitres |
| ml | millilitres |
| hpi | hours post-inoculation |
| dpi | days post-inoculation |
| rpm | revolutions per minute |

# 1 - Introduction

## 1.1 - *Phytophthora infestans*

*Phytophthora infestans* belongs to the class of Oomycetes and is the causative agent of late blight in potato and tomato plants. It is an economically important plant pathogen and became widely known in the 1840s for causing the Irish potato famine. This is a particularly important pathogen to understand as it is estimated to cost approximately £9 billion per annum in crop loss and damages and in epidemic years can cause farmers' businesses to fail (Haverkort *et al.*, 2008). Even now, with new technology and a greater understanding of resistance, there are no fungicides that can overcome *P. infestans* once it infects a plant*;* instead, they are used as a preventative measure to try and stave off infection. There is also no fully resistant potato cultivar in existence that can withstand infection from the most virulent isolates.

*P. infestans* populations have a large range of genetic diversity, particularly in Central Mexico where *P. infestans* has co-evolved with diverse wild *Solanum* species (Fry, 2008). Agricultural selection pressures result in isolates of *P. infestans* that can overcome the cultivated potato lines, becoming more prevalent, and the pathogen emerges triumphant time and time again. *P. infestans* is a hemibiotrophic pathogen; the first two days of infection are biotrophic but after 48 hours the transition to necrotrophy begins. *P. infestans* is a eukaryotic fungus-like micro-organism which belongs to the kingdom Chromista within the group Stamenopiles (Grenville-Briggs and West, 2005; Fry, 2008). The Oomycetes cluster within a super-group called Chromalveolata which also contains the protist *Plasmodium* (Fry, 2008). Unlike fungi which have chitinous cell walls, the mycelia produced by oomycetes contain predominantly cellulose and β-1,3-glucans, with little or no chitin (Grenville-Briggs and West, 2005). Oomycetes are a diverse group which contain

saprophytes and pathogenic members (Grenville-Briggs and West, 2005). Plants, fish, vertebrates and fungi are some examples of hosts for pathogenic oomycetes (Grenville-Briggs and West, 2005).

### 1.1.1 – Asexual *P. infestans* life cycle

Oomycetes have a life cycle in which they remain diploid for the majority of the time with a distinct sexual stage. The asexual stage of the life cycle has clearly defined biotrophic (for the first 48 hours of infection) and necrotrophic (from 72 hours) stages. In the asexual stage spores are non-motile sporangia which can either undergo direct or indirect germination (Grenville-Briggs and West, 2005). Direct germination usually occurs at higher temperatures (>12$^{o}$C) when a germ tube forms directly from the sporangium. Indirect germination occurs at lower temperatures (<12$^{o}$C) and in wet conditions. This germination step involves the cleavage of multinucleated sporangia to release single-nucleated motile zoospores (Grenville-Briggs and West, 2005). Zoospores are biflagellate and can move around within droplets of water on leaf surfaces (Fry, 2008). The zoospores then encyst and infection begins with the formation of an appressorium which can penetrate the leaf cuticle (Figure 1.1.1). It is believed that a combination of turgor pressure and cell wall degrading enzymes are used to penetrate the plant cell wall (Kamoun, 2003). Proteins resembling mammalian mucins were identified on the surface of germinating *P. infestans* spores. These proteins may form a mucosal layer protecting the germinating spore from physical damage and host defence mechanisms, but they may also assist in spore adhesion to the leaf surface (Gornhardt *et al.*, 2000). Penetrating hyphae form from the appressorium that can grow inter-cellularly within the mesophyll layer, producing intracellular haustoria (Grenville-Briggs and West, 2005).

Haustoria bud from the hyphae and have the closest interaction with the plant cell. They protrude into the cell but never puncture the host membrane. An extrahaustorial matrix is formed between the haustorial cell wall and the plant cell membrane. It is known that effectors can be found at the base of the haustoria and are released into the extrahaustorial matrix during an infection of plant leaves (Whisson *et al.*, 2007). Translocation mechanisms across the plant cell membrane are still being investigated.

Between three and seven days after infection began, asexual spores are produced. Sporangia are formed on sporangiophores, usually at night, which grow through the stomata on the underside of the leaf surface (Grenville-Briggs and West, 2005).

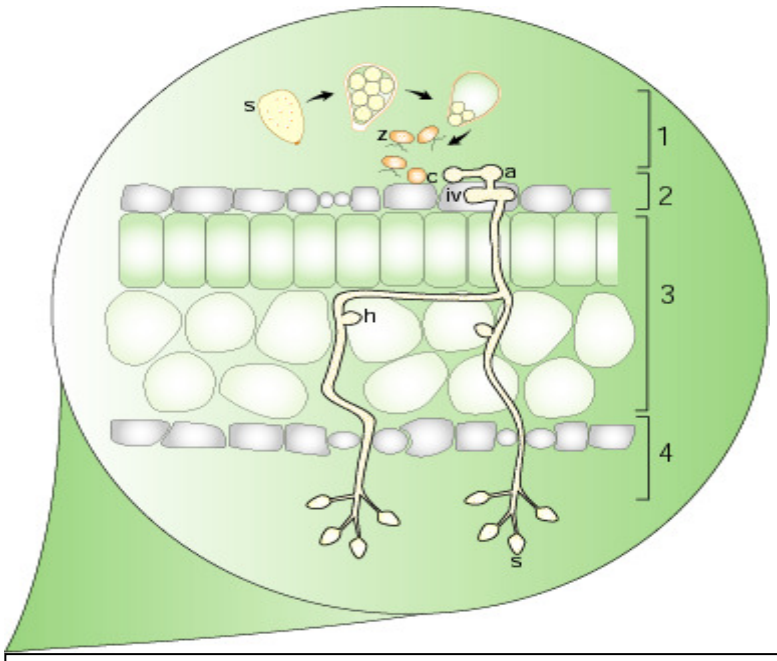


**Figure 1.1.1: Asexual life cycle of *P. infestans*.** Image from P. Birch. Sporangia (s) are released from hyphae and blown or splashed onto leaf surfaces. They release motile zoospores (z) which then encyst (c). This cyst forms an appressorium (a) which penetrates the leaf cuticle and forms an infection vesicle (iv). Hyphae from the infection vesicle spread throughout the leaf moving between its cells. The protrusions that form from the hyphae are called haustoria (h). Haustoria push into the plant cell but do not penetrate the plasma membrane. However, they do form a very close physical interaction. The hyphae continue moving throughout the leaf and eventually reappear outside the leaf through stomata. Sporangia that develop are on the tips ready to get dispersed by the wind again.

### 1.1.2 – *P. infestans sexual* lifecycle

The spores of the sexual stage are defined as oospores and can survive dormant in the soil for several years (Grenville-Briggs and West, 2005). There are two mating types, A1 and A2. Both are required for sexual sporulation and each mating type produces different hormones, making them compatible (Judelson, 1997). A1 and A2 mating types are bisexual and can produce both oogonia (the female gamete) and antheridia (the male gamete) (Judelson, 1997). Some isolates have shown a preference to develop either female or male gametes but some isolates vary depending on which isolate it is crossed with (Judelson, 1997). Sexual sporulation takes place six to ten days after inoculation and occurs in the mesophyll layer (Grenville-Briggs and West, 2005). The intertwining of hyphae from A1 and A2 mating type initiates reproduction. These hyphae differentiate to form oogonia and antheridia initials. A receptive papilla is formed by attachment of the mature oogonia and antheridia. Through this papilla a nucleus is released *via* a fertilisation tube from the antheridia into the oogonia (Grenville-Briggs and West, 2005). The two nuclei fuse forming a diploid oospore. This oospore matures within the leaf and once the leaf tissue breaks down, due to decay, the oospores are released into the soil where they can survive for years (Grenville-Briggs and West, 2005). These oospores can infect the roots of plants only when there is direct contact as they are non-motile. Colonisation occurs by the same mechanism described for asexual colonisation after the hyphae have grown up the root to leaf or stem tissue (Grenville-Briggs and West, 2005).

### 1.1.3 – *P. infestans* effect on crop losses

*P. infestans* is the number one disease on the world's most important non-cereal crop and causes annual losses within the UK of approximately £55 million (Twining *et al.*, 2009). On a world scale this pathogen costs approximately £9 billion due to crop loss and the need for chemical control by means of fungicide applications (Haverkort *et al.*, 2008). The

current chemical control methods used against *P. infestans* involve up to as many as 20 applications, per season (Hansen *et al.*, 2007). It has been demonstrated that some isolates of *P. infestans* have become resistant to the chemical metalaxyl, which is a key agent in some fungicides (Hansen *et al.*, 2007). The development of this resistance means that isolates which can overcome metalaxyl will become more prevalent within field populations. Other chemicals currently used to control blight include Ethylenebisdithiocarbamates (EBDCs), which are a group of non-systemic (surface acting) fungicides. The active ingredients in these chemicals include mancozeb and maneb. The specific mode of action of these fungicides is currently not known. These chemical agents that farmers rely on so heavily are coming under threat from EU directive (91/414/EEC). This directive aims to reduce the amount of chemicals used within the farming community within the next 10 years. Since the potato industry relies heavily on these chemical applications a study investigating the effect of a reduction of their use on yield losses was undertaken. It was discovered that most of the losses would be due to poor control of *P. infestans* with the total losses increasing from the current £55 million within the UK to approximately £363 million (Twining *et al.*, 2009). This shows there is an urgent need over the next few years to develop a cultivar of potato that has an increased resistance to *P. infestans*.

## 1.2 – Molecular Plant-Pathogen Interactions – PTI, ETS and ETI

Plants are not defenceless against the pathogens that attack them. They have an immune system that is able to withstand attacks from diverse pests and pathogens such as fungi, bacteria, oomycetes, viruses, nematodes and insects. The first line of defence includes physical barriers, such as the cuticle and cell wall (Dangl and Jones, 2001). To cause disease in a plant, pathogens first have to be able to penetrate through the waxy layer on

the leaf surface and then through the cell wall. Such permanent physical defences are effective against a number of would-be pathogens. However, if a pathogen does manage to get through these, the plant needs to be able to defend itself against them.

### 1.2.1 – Pattern-Triggered Immunity (PTI)

Pathogen Associated Molecular Patterns (PAMPs) are conserved, secreted or exposed molecules that are present on all micro-organisms, not just on pathogens. These PAMPs are responsible for the initial plant immune response, called Pattern-Triggered Immunity (PTI) (Jones and Dangl, 2006) (Figure 1.2.1; tailored to oomycete plant interactions). Examples of PAMPs include flagellin, elongation factor Tu (EF-Tu), cold shock proteins and LPS from bacteria, chitin, β-glucans and ergosterol from fungi (Ingle *et al.*, 2006) and β-glucans, elicitin family members, like INF1, cellulose binding elicitor lectin (CBEL) and transglutaminase GP42 from oomycetes (Hein *et al.*, 2009). PAMPs are usually essential to the microbe and, as such, are under strong selective pressure to remain conserved. They are not found in the host they intend to infect. The fact that they are essential means these compounds cannot be lost, making them good detection patterns for the plant to recognise. In most cases it is not the whole protein or molecule that is needed for recognition. For example, a 22 amino-acid peptide of flagellin known as flg22, and the RNA-binding motif, RNP-1 of bacterial cold-shock proteins (Felix and Boller, 2003) are enough to trigger recognition by the plant (Felix *et al.*, 1999).

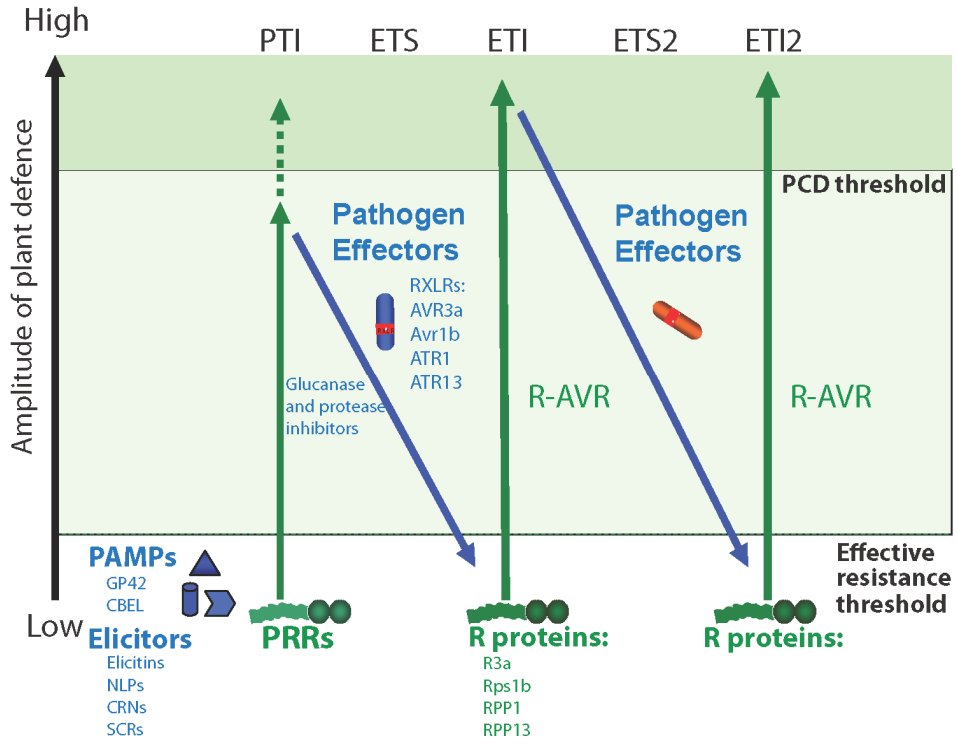


**Figure 1.2.1: The zig-zag-zig model for oomycete-plant interactions.** (taken from Hein *et al*., 2009). It describes the arms race between the pathogen and the plant. Pathogen associated molecular patterns (PAMPs) on micro-organisms activate PAMP triggered immunity (PTI); this is then counteracted with effectors to suppress PTI known as effector triggered susceptibility (ETS). The plants R proteins then counteract this known as effector triggered immunity (ETI). Again the pathogens release more effectors to suppress ETI known as ETS2 but the plant may have another defence layer with ETI2. The examples mentioned in the figure are specific to oomycetes-plant interactions.

PAMPs are recognised by the plant at the cell surface by pattern recognition receptors (PRRs) (Jones and Dangl, 2006). PRRs are transmembrane receptors analogous to Toll-like receptors in the mammalian innate immune system (Hein *et al*., 2009). However, not all PAMPs are recognised by all plant species; for example, only members of the *Brassicaceae* possess the EF-TU RECEPTOR (EFR) and thus respond to EF-Tu (Felix and Boller, 2003). Many of the receptors for the identified PAMPs were not discovered until recently but the most studied example is that of FLAGELLIN-SENSITIVE 2 (FLS2) which recognises flg22.

FLS2 is a receptor-like kinase that has an extracellular ligand binding domain, one membrane-spanning domain and an intracellular serine/threonine kinase domain (Ingle *et al.*, 2006). Most PRRs induce the general first line defence system of plants which consists of ethylene (ET) production, production of reactive oxygen species (ROS), callose deposition, the activation of a mitogen-activated protein kinase (MAPK) cascade and induction of pathogenesis related (*PR*) defence genes which are often regulated by WRKY transcription factors (Ingle *et al.*, 2006). This stage of the immune system is thought to halt all microbes from colonising the plant further if they have not co-evolved additional weaponry to suppress it (Jones and Dangl, 2006). Once flg22 interacts with FLS2, internalisation of the surface receptor occurs via endocytosis (Robatzek *et al.*, 2006). Internalisation of this receptor induces the PTI defence responses, described above (Robatzek *et al.*, 2006). Mutant *fls2* plants have increased disease susceptibility to bacterial spray infection but not to bacterial infiltration into the apoplast. This implies that the receptor plays a key role in early PTI signalling (Robatzek *et al.*, 2006). It has been shown that FLS2 forms a complex with BRI1-ASSOCIATED RECEPTOR KINASE 1 (BAK1) within minutes of flg22 binding (Chinchilla *et al.*, 2007). It appears that BAK1 is a positive regulator of signalling, as *bak1* mutant plants have abnormal early and late flagellin-triggered responses, but normal binding to flagellin (Chinchilla *et al.*, 2007). This implies that these two proteins are both important components of PTI.

The BAK1 co-receptor is thought to bind other PTI-related cell surface receptors to aid in the activation of early defence responses. Another PAMP, EF-Tu, the receptor for which also binds BAK1, activates nearly identical gene expression to flg22, implying similarity in their defence response mechanisms (Jones and Dangl, 2006; Roux *et al.*, 2011). EF-Tu is recognised by a LRR-kinase called EFR in *Arabidopsis thaliana*. Not only do FLS2 and EFR induce similar gene expression when they recognise flg22 and EF-Tu, respectively, but recognition of flg22 induces the transcription of EFR (Jones and Dangl, 2006). These

two PRRs indicate that the signalling responses to different PAMPs may lead to a similar set of genes being expressed, which is collectively known as PTI (Jones and Dangl, 2006). Each PAMP and PRR varies from species to species and some plant species can only recognise a subset of PAMPs. Flagellin from *Pseudomonas syringae* is more active at triggering PTI in *A. thaliana* than the flagellin from *Agrobacterium tumefaciens* (Jones and Dangl, 2006).

### 1.2.2 – Oomycete-specific PAMPs and elicitors

Most characterised PAMPs and elicitors of oomycetes are secreted proteins which is how they are exposed to plant cell surface receptors. However, the β-glucans in the cell walls of oomycetes also act as PAMPs and are recognised by a β-glucan elicitor binding protein (GEBP) found in the plasma membrane of soybean roots (Umemoto *et al.*, 1997). The signal transduction pathways downstream of this PAMP receptor have not been investigated in detail. Another oomycete PAMP is the protein GP42 which is a calcium-dependent transglutaminase (TGase) found in the cell wall of *P. sojae* (Brunner *et al.*, 2002). A 13-amino acid pattern, called Pep-13, is sufficient to trigger PTI within parsley cells (Brunner *et al.*, 2002). The Pep-13 motif is highly conserved and present in many *Phytophthora* species (Brunner *et al.*, 2002). A further PAMP of oomycetes is the cellulose binding elicitor lectin (CBEL), which can trigger necrosis and PTI (Mateos *et al.*, 1997). The conserved region from CBEL that is sufficient to trigger PTI comprises two cellulose-binding domains (CBDs). A single mutation in either CBD leads to the elicitor activity being abolished (Gaulin *et al.*, 2006). CBEL is thought to be perceived in the plant by the destabilisation of cellulose caused by its binding to the plant cell wall. A mutation in both CBD domains is needed to disrupt the cell wall binding activity (Gaulin *et al.*, 2006). In transgenic strains of *P. parasitica* that have the expression of CBEL suppressed, virulence was not seriously altered, which was unexpected considering CBEL contributes

to the adhesion of pathogen to plant, and PAMPs are generally considered to be highly conserved due to their essential nature (Gaulin *et al.*, 2006). It was discovered, using protoplasts, that the plant cell wall is necessary for CBEL to alter cytosolic calcium levels in tobacco cells (Ellis and Turner, 2001).

Small cysteine-rich (SCR) molecules secreted by oomycetes can trigger necrosis and plant defence responses. These SCRs include elicitins and phytotoxins (Hein *et al.*, 2009). The phytotoxic protein *Phytophthora cactorum*-Fragaria (PcF) from *P. cactorum* is one example of an SCR. There are two PcF-like proteins that are secreted from *P. infestans* called SCR74 and SCR91 (Hein *et al.*, 2009). It has been shown that the *Scr74* gene family is induced during infection and appears to have undergone diversifying selection by means of gene duplication and recombination (Liu *et al.*, 2005). This type of diversifying selection usually occurs during co-evolution; and implies that the Scr74 protein family could be targets for the plant detection system.

Elicitins are approximately 10 kDa in size, are conserved amongst most *Phytophthora* species and can induce plant defence responses, including the formation of an HR (Hein *et al.*, 2009). One of the most studied elicitins is INF1 from *P. infestans*. The HR that is triggered by INF1 requires the heat shock proteins HSP70 and HSP90, a MAPK kinase and the ubiquitin ligase-associated protein NbSGT1 (Hein *et al.*, 2009). It has recently been discovered that NbLRK1, a lectin-like receptor kinase, interacts with INF1. When this receptor is silenced using VIGS there is a delay in the development of the INF1 HR implying that NbLRK1 is part of the signal perception complex, or transduction pathway, for INF1 (Kanzaki *et al.*, 2008).

Another well studied family of elicitors contains the necrosis and ethylene-inducing peptide1 (Nep1)-like proteins which include NPP1 (necrosis-inducing, *Phytophthora*

protein 1) from *P. parasitica.* Nep1 induces necrosis and ethylene synthesis in plants. NPP1 is able to induce PTI in a similar manner to Pep-13 but it also induces cell death (Hein *et al.*, 2009). A list of oomycete PAMPs and elicitors is provided in Table 1.2.1.

**Table 1.2.1: PAMPs, secreted elicitors and apoplastic effector proteins from oomycetes.**

| Protein | Function | Reference |
|---|---|---|
| β-glucan | PAMP | (Umemoto *et al.*, 1997) |
| GT42 (calcium-dependent transglutaminase) | Pep-13, PAMP | (Brunner *et al.*, 2002) |
| CBEL family | Cellulose binding domain, PAMP | (Mateos *et al.*, 1997; Gaulin *et al.*, 2006) |
| Small cysteine-rich (SCR)<br>PcF<br>SCR74<br>SCR91 | Elicitors | (Orsomando *et al.*, 2001; Liu *et al.*, 2005) |
| INF1 | Elicitor | (Kamoun *et al.*, 1997) |
| Nep1-like proteins | Elicitor | (Fellbrich *et al.*, 2002) |
| GIP1 and GIP2 | glucanase inhibitors | (Rose *et al.*, 2002) |
| EPI1-14 and EPIC1-4 | protease inhibitors | (Tian *et al.*, 2004; Tian *et al.*, 2005 ; Tian et al., 2007) |

**Table 1.2.1: PAMPs, secreted elicitors and apoplastic effector proteins from oomycetes.** Known PAMPs, elicitors and inhibitors secreted by oomycetes to combat plant defence systems.

## 1.2.3 – Effector Triggered Susceptibility (ETS)

Plant pathogens are able to suppress PTI by delivery of so-called effector proteins, that act either inside or outside plant cells. Collectively, the promotion of disease by effectors is known as Effector-Triggered Susceptibility (ETS) (Figure 1.2.1).

Oomycetes have a large repertoire of effectors which are secreted into the plant apoplast. Plants secrete hydrolytic enzymes such as glucanases, chitinases and proteases to defend themselves against pathogen attack. *Phytophthora* species secrete inhibitory proteins that target and block these plant glucanases and proteases. In *P. sojae,* two

glucanase inhibitor proteins, GIP1 and GIP2, have been shown to inhibit the endo-β-1,3-glucanase EgaseA from soybean. GIP1 and GIP2 are classed as extracellular effectors as they function within the apoplast of infected plant tissues, (reviewed in Hein *et al.,* 2009).

Two major classes of extracellular protease inhibitors (EPIs) have been identified in *P. infestans;* Kazal-like serine protease inhibitors (EPI1-14), and cystatin-like cysteine protease inhibitors (EPIC1-4) (Hein *et al*., 2009). It has been shown that EPI1 and EPI10 are able to interact with and inhibit the PR protein P69B from tomato; the activity of EPI1 has been shown to occur within the apoplast (Tian *et al*., 2004; Tian *et al*., 2005). It has also been shown that EPIC2 interacts with a novel papain-like extracellular cysteine protease which has been called *Phytophthora*-inhibited protease 1 (PIP1) (Tian *et al*., 2007). These apoplastic effectors can also be found in Table 1.2.1.

In addition to apoplastic effectors, some pathogens have evolved effectors that are delivered into plant cells to help them overcome PTI. In the case of Gram-negative bacterial pathogens, delivery of effectors into plant cells is achieved via a type three secretion system (T3SS). This secretion system acts as a molecular syringe which injects the effectors directly into the host cell. It is composed of inner and outer membrane components and a cytoplasmic region. This structure is combined with an extracellular needle which provides an effective mechanism for the translocation of effectors (Zenk *et al*., 2007). Approximately 30 bacterial effectors from *Pseudomonas syringae* pv. tomato are secreted through the T3SS which cause virulence by mimicking, manipulating or inhibiting normal host cellular functions (Jones and Dangl, 2006).

The bacterial effector HopU1 from *P. syringae* has the ability to suppress the plant defence system by suppressing the development of the non-host HR (Fu *et al*., 2007). Another study has shown that a total of 9 effectors from *P. syringae* have the ability to suppress the

development of flagellin-induced NHO1 expression (Li *et al.*, 2005). These 9 effectors are HopS1, HopAI1, HopAF1, HopT1-1, HopT1-2, HopAA1-1, HopF2, HopC1, and AvrPto (Li *et al.*, 2005). In addition, multiple effectors targeting one host protein that is important in defence has been shown for AvrPto and AvrPtoB, which both target and inhibit the function of BAK1 (Shan *et al.*, 2008), the co-receptor to multiple cell surface receptors, including PRRs. This shows an important role for ETS in pathogen disease development.

There is much more information available on bacterial effectors than fungal or oomycete effectors, but these are now being more widely studied. A number of proteins secreted by oomycetes are delivered into the plant cell where they are recognised by plant defence systems (then called avirulence, AVR, proteins) (see ETI below). A few examples are *PiAVR3a* (Armstrong *et al.,* 2005) and *PiAVR4a* (van Poppel *et al.,* 2008) from *P. infestans; PsAVR1b* (Shan *et al.,* 2004), and *PsAVR3c* (Dong *et al.,* 2009) from *Phytophthora sojae*; *ATR1* (Rehmany *et al.,* 2005) and *ATR13* (Allen *et al.,* 2004) from *Hyaloperonospora arabidopsidis*. All of these effectors, and many more proteins from oomycetes, share a conserved motif on the N-terminal end known as the RXLR motif (Rehmany *et al.,* 2005). Some of these effectors also have a second conserved region downstream of the RXLR motif called the EER motif but this is not present in all. The regions in between these conserved motifs are made up of mainly acidic amino acids. Another class of effectors, called crinklers, is characterised by a second type of conserved motif known as an LFLAK domain (Haas *et al.,* 2009). Both of these motifs, RXLR and LFLAK, have been shown to be required for translocation of these effectors inside host cells (Whisson *et al.,* 2007; Schornack *et al.,* 2010) (see below).

It is known that in the *P. infestans* genome there are 563 RXLR encoding genes and 196 LFLAK encoding genes (Haas *et al.*, 2009). This number is far larger than the 30 T3SS effectors from *Pseudomonas syringae,* so why is there such a big difference? The large

effector repertoire from *P. infestans* suggests that there may be a lot of redundancy if bacteria can achieve the same effect with only 30. Furthermore the large number of effectors potentially entering the host cell may give the plant more targets for detection (Hein *et al.*, 2009).

1.2.4 – Translocation of RXLR effectors

Whisson *et al.* (2007) showed that translocation of the oomycete effector PiAVR3a, across the cell wall and plasma membrane of host plant cells after secretion from haustoria of *P. infestans*, is determined by the RXLR motif. To demonstrate this, the *Escherichia coli* gusA gene was fused to the C-terminus of the RXLR. The gusA gene product is inactive in the plant apoplast but active within plant cells, its activity could report the translocation of the effector PiAVR3a. In a subsequent experiment, the RXLR motif was modified to four alanines (AAAA) and this inhibited the translocation of the effector (Whisson *et al.,* 2007). The mechanism by which *P. infestans* translocates the RXLR effectors into the plant cells remains unclear.

It has been previously found that a similar motif, RXLX (E, D or Q), was present in the effectors of the human malaria parasite *Plasmodium falciparum* and was demonstrated to be a host-targeting sequence (Lopez-Estrano *et al.,* 2003). This similar motif in the *P. falciparum* effectors is needed for their delivery into the cytoplasm of host blood cells. Bhattacharjee *et al.* (2006) showed that the RXLR motif of *P. infestans* could be used in place of the malaria motif and translocation of the malaria effectors would still occur. In a reciprocal experiment, the motif from the virulence protein PfHRPII from *P. falciparum* replaced the RXLR-EER motif of PiAVR3a and was found to function in translocation into plants cells. In addition, the equivalent motifs from *H. arabidopsidis* (an obligate biotroph oomycete) ATR1NdWsB and ATR13 replaced the RXLR-EER motif of AVR3a and it was concluded that translocation occurred (Grouffaud *et al.,* 2008). This therefore implies that

there is a common mechanism for the translocation of proteins in both oomycete and malaria systems (Grouffaud *et al.,* 2008).

A recent publication implicated a translocon for exported proteins (PTEX) in *P. falciparum* (de Koning-Ward *et al.,* 2009). It is believed that this translocon may work in an ATP-dependent manner with the core component being HEAT SHOCK PROTEIN 101, (HSP101). This protein is part of a family that are components of many secretion systems in bacteria (de Koning-Ward *et al.,* 2009). Other components that this group discovered to be important in this translocon are EXPORTED PROTEIN 2, (EXP2), which is a known parasite protein, and a novel protein they named PTEX150 (de Koning-Ward *et al.,* 2009). It was discovered that PTEX150 contains an ER signalling sequence and this protein can be found in complex with HSP101 (de Koning-Ward *et al.,* 2009). EXP2 was previously discovered to be associated with the parasitophorous vacuole membrane (PVM) possibly by the N-terminal section of the protein (Fischer *et al.,* 1998). It has been shown that EXP2 interacts with PTEX150 and localises with PTEX150 and HSP101 in large foci in the ring stage PVM (de Koning-Ward *et al.,* 2009). If this does prove to be the method used by *P. falciparum* to transfer its RXLXE/D/Q effectors into erythrocytes, the system for the uptake of P. infestans RXLRs into the plant cell may be similar.

There have been studies in recent years which investigated the use of cell surface components to facilitate entry by RXLR effector molecules into plant cells. One such study investigated phosphatidylinositol-3-phosphate (PI3P) and beta-type phosphatidylinositol-4-phosphate (PI4P) (Kale *et al.,* 2010). These are phospholipids that can be found on the outer surface of plant cell plasma membranes. It was reported that the RXLR motif from the *P. sojae* effectors PsAVR1b, PsAvh331 and PsAvh5 bind to phospholipid PI3P and PI4P and are internalised by means of lipid raft-mediated endocytosis (Kale *et al.,* 2010). The specificity of the RXLR motif was investigated by substituting amino acids in this motif,

for example RXLR to (RFLR-> FRLR or RFLR-> RFRL). These mutations led to the loss of the effector binding to the phospholipids (Kale *et al.,* 2010). None of the RXLR-dEER proteins tested could bind liposomes, therefore the binding appears specific to the phospholipids (Kale *et al.,* 2010).

Another group has been investigating the translocation of a putative RXLR effector from the oomycete *Saprolegnia parasitica*, SpHtp1, into trout cells (Wawra *et al.,* 2012). *S. parasitica* is an oomycete that is pathogenic to fish causing a decline in wild fish stocks and salmon and trout within fish farms. This putative effector contains an RXLR domain but no dEER domain. The N-terminus of the putative effector and a mutated N-terminal domain were fused to an mRFP protein. The mutated domain contained GGHLG mutation instead of KRHLR (Wawra *et al.,* 2012). This showed that the RXLR domain is crucial for the uptake of SpHtp1 into trout cells (RTG-2 cell line) as the mutated mRFP fusion no longer entered the RTG-2 cells (Wawra *et al.,* 2012). This work also showed that the translocation of SpHtp1 is mediated by a cell surface receptor molecule that is modified by tyrosine-O-sulphate and not phosphoinositol phosphate (Wawra *et al.,* 2012). This contradiction implies that there may be differences between oomycete pathogens of plants and animals.

### 1.2.5 – Genetics and expression of RXLR effector genes

The number of potential RXLR-dEER containing proteins encoded by the *P. infestans* genome is estimated to be >500. This is substantially larger than other *Phytophthora* species, *P. sojae* and *P. ramorum*, which contain approximately 60% fewer predicted RXLR genes (Haas *et al.,* 2009). The genomes of *P. sojae* and *P. ramorum* are 95 Mb and 65 Mb respectively, compared to *P. infestans* which is 240 Mb. The larger genome of *P. infestans* shows substantial expansion of the RXLR genes compared to other *Phytophthora* species and these RXLR genes are found in gene-sparse areas of the

genome which are repeat-rich (Haas *et al.,* 2009). The gene-dense regions of the genome contain the housekeeping genes for growth and regulation (Haas *et al.,* 2009). The genes within the repeat-rich area do not have a conserved gene order with the other *Phytophthora* species and show presence/absence polymorphisms (Haas *et al.,* 2009). These expanded gene-sparse areas contain large numbers of mobile elements. It is thought that the dynamic nature of these regions has facilitated the evolution of effector gene families due to higher than average rates of non-allelic homologous recombination and tandem gene duplication (Haas *et al.,* 2009).

More than 80 RXLR-dEER effector genes have been shown to be up-regulated during the pre-infection and biotropic stages of the life cycle of *P. infestans* (Armstrong *et al.,* 2005; Whisson *et al.,* 2007; Haas *et al.,* 2009). The transcription of these genes at these early stages in the *P. infestans* life cycle is thought to aid in the infection of host cells. It has been shown that the expression of some RXLR genes at this early time point results in their accumulation at the haustoria before translocation into the plant cells (Whisson *et al.,* 2007). The functions and targets of these *RXLR* genes once inside the plant cell are important to investigate, as this will lead to a greater understanding of how the pathogen interferes with normal physiological regulation of the plant.

### 1.2.6 - Function of oomycete *RXLR* genes

Only a few RXLR effectors have been studied in detail so far, the most detailed of which is AVR3a from *P. infestans*. It has been shown that there are two alleles of *AVR3a* in isolates of *P. infestans*, $AVR3a^{KI}$ and $AVR3a^{EM}$ (Armstrong *et al.,* 2005). AVR3a has been shown to target a U-box E3 ligase within the plant called CMPGI (Bos *et al.,* 2010). AVR3aKI is recognised by the resistance protein R3a and has the ability to strongly suppress programmed cell death (PCD) induced by the *P. infestans* elicitin infestin 1 (INF1) (Armstrong *et al.,* 2005; Bos *et al.,* 2006). The $AVR3a^{EM}$ allele is very weakly

recognised by *R3a* and does not suppress INF1-mediated cell death as efficiently (Armstrong *et al.,* 2005; Bos *et al.,* 2006; Bos *et al.,* 2009). Intriguingly, *AVR3a*$^{EM}$ is the more commonly occurring allele in *P. infestans* populations, possibly due to selection pressure against *AVR3a*$^{KI}$ from R3a in potato populations.

The recognition of AVR3a$^{KI}$ by R3a and the ability to suppress PCD caused by INF1 can be separated. AVR3a$^{KI}$ recognition by R3a is not altered by mutation of the last amino acid tyrosine to a phenylalanine (Y147F). However, this mutation abolishes its suppression of INF1-mediated cell death. This indicates that the last amino acid of AVR3a is important for its CMPG1-related virulence function but not for recognition by *R3a* (Bos *et al.,* 2009). The best characterised target of AVR3a, CMPG1, is important for the activation of INF1-mediated cell death and the activation of plant defence and disease resistance (Gonzalez-Lamothe *et al.,* 2006; Gilroy *et al.,* 2011b). The strong interaction of AVR3a$^{KI}$ with CMPG1 prevents the latter's turnover by the 26S proteasome which is thought to be connected to AVR3a function in suppression of INF1-mediated cell death. The interaction and stabilisation of CMPG1 and suppression of INF1-mediated cell death by AVR3a$^{EM}$ is much weaker (Bos *et al.,* 2010). This implies that the suppression of INF1-mediated cell death is closely associated with the ability of AVR3a to stabilise CMPG1 (Bos *et al.,* 2010). It was concluded that the virulence function of Avr3a$^{KI}$ includes the suppression of CMPG1–mediated host cell death during the early biotrophic phase. Since AVR3a$^{EM}$ is a weaker suppressor of CMPG1-mediated cell death but is still highly conserved in *P. infestans* populations it is thought to give an advantage *to P. infestans* in the necrotrophic phase (Bos *et al.,* 2010). These data imply that CMPG1 is a key virulence target early during infection (Bos *et al.,* 2010; Gilroy *et al.,* 2011b).

The secreted RXLR protein, Avr3b, from *P. sojae* contains a W motif and a Nudix hydrolase domain in its C-terminus (Dong *et al.,* 2011). The Nudix domain has been

confirmed to be functional by the use of biochemical assays; Avr3b is therefore an ADP-ribose/NADH pyrophosphorylase (Dong *et al.,* 2011). It does not appear that the enzyme activity is related to the recognition of this effector protein by the *R* gene *Rps3b*, as mutations in the Nudix motif reduce the virulence of the effector but do not alter the recognition by Rps3b (Dong *et al.,* 2011). It is known that some Nudix hydrolases can act as negative regulators of plant defence systems. Therefore Avr3b may contain a Nudix motif in order to alter the host defence system.

Other effectors from *P. sojae* have been discovered that can suppress the plant immune system. For example, immediate-early effectors, Avh172, that are strongly expressed can suppress the cell death that is triggered by some early effectors, such as Avr4/6 (Wang *et al.,* 2011). Some of these early effectors, for example Avh5, can suppress INF1-mediated cell death as described for AVR3a from *P. infestans* (Wang *et al.,* 2011). This implies that there are at least two classes of effectors from *P. sojae* which may target different branches of the plant immune response. There is evidence to support this hypothesis, as when key immediate-early and early effectors are miss-expressed then the isolate of *P. sojae* appears less virulent (Wang *et al.,* 2011). It stands to reason that if *P. sojae* contains effectors that target different stages of the plant immune system then other oomycete plant pathogens may also have adopted this strategy.

### 1.2.7 – Effector Triggered Immunity (ETI)

Effector Triggered Immunity (ETI) is the recognition of pathogen effectors or effector activity by host resistance (R) proteins (Jones and Dangl, 2006; Hein *et al*., 2009) (Figure 1.2.1). Resistance genes often encode nucleotide binding leucine rich repeat (NB-LRR) proteins. The nucleotide binding domain is involved in their activation, and their stability is regulated by a chaperone complex which contains HSP90 and SGT1 (Coll *et al*., 2011).

There are two main classes of NB-LRRs: CC-NB-LRRs which contain a predicted coiled-coil N-terminal domain, and TIR-NB-LRRs which have N-terminal homology to the intracellular TIR domain of Toll-like receptors (TLRs) (Coll *et al.*, 2011).

Genetic studies have shown that there is selection pressure on the evolution of new NB-LRR proteins and that this selection pressure is often focussed on the LRR domain of the proteins (Hein *et al.*, 2009). Two different selection pressures apply to *R* genes; purifying selection where no gene variation is wanted in order to maintain the protein function; and diversifying selection where recognition of new effector forms is generated (Hein *et al.*, 2009).

There are two ways by which NB-LRRs can detect effector proteins from the pathogen. The first of these is direct interaction, as suggested by the gene-for-gene hypothesis (Flor, 1971). This hypothesis implies that direct interaction occurs between an R protein from the plant and a corresponding effector protein from the pathogen to trigger defences. For simplicity, throughout this thesis the Gene-for-Gene Hypothesis will be refered to in the context of direct R-AVR interaction. The second mode of recognition, indirect, is exemplified by the Guard Hypothesis, which suggests that (avirulence) effector detection occurs via an intermediate plant protein in which the R protein recognises a change (Dangl and Jones, 2001). Both of these hypotheses have since been proven experimentally to occur and will be described in detail in Section 1.2.11.

The term ETI is synonymous with the hypersensitive response (HR) (Hein *et al.*, 2009). The *P. infestans* effector *AVR3a* is recognised within the plant cell by the resistance protein R3a as described above (Armstrong *et al.*, 2005). There are many additional well documented examples of bacterial and fungal effectors that are recognised by the plant and trigger ETI (Table 1.2.2). AvrRpm1 and AvrB from *P. syringae* are detected by the

resistance gene *RPM1* in *A. thaliana*. Another effector from *P. syringae,* AvrRpt2, which has five different protein targets within *A. thaliana,* is detected by the resistance gene *RPS2* (Jones and Dangl, 2006). *Prf* is a resistance gene from *Solanum lycopersicum* (tomato) that is able to recognise the avirulence proteins AvrPto and AvrPtoB from *P. syringae* and trigger the development of ETI. AvrPto is a kinase inhibitor that binds the tomato kinase Pto but can also inhibit the kinase domains of the PRRs FLS2 and EFR to suppress PTI (Hogenhout *et al.*, 2009). The fungal apoplastic effector Avr2 from *Cladosporium fulvum* is recognised by the *S. lycopersicum* Cf-2 resistance gene (Rooney *et al.*, 2005). The effector ATR1 from the oomycete *H. arabidopsidis* is recognised by the *RPP1* resistance gene from *A. thaliana* (Krasileva *et al.*, 2010). The resistance gene *Pi-ta* from rice recognises *AVR-Pita* from *Magnaporthe grisea* (Jia *et al.*, 2000). The flax rust fungus (*Melampsora Lini*) also triggers ETI by the expression of AvrL567 in flax (*Linum usitatissimum*) plants that contain the resistance genes L5, L6 and L7 (Dodds *et al.*, 2006). Some of these resistance genes will be described in more detail in Section 1.2.11.

**Table 1.2.2: Recognition of avirulence genes by resistance genes**

| Avirulence gene | Pathogen | Resistance gene | Plant | Reference |
|---|---|---|---|---|
| *AvrRpm1* | *P. syringae* | *RPM1* | *A. thaliana* | (Mackey *et al.*, 2002) |
| *AvrB* | *P. syringae* | *RPM1* | *A. thaliana* | (Mackey *et al.*, 2002) |
| *AvrRpt2* | *P. syringae* | *RPS2* | *A. thaliana* | (Jones and Dangl, 2006) |
| *AvrPto* | *P. syringae* | *Prf* | *S. lycopersicum* | (Mackey *et al.*, 2003) |
| *AvrPtoB* | *P. syringae* | *Prf* | *S. lycopersicum* | (Mackey *et al.*, 2003) |
| *Avr2* | *Cladosporium fulvum* | Cf-2 | *S. lycopersicum* | (Rooney *et al.*, 2005) |
| *ATR1* | *H. arabidopsidis* | *RPP1* | *A. thaliana* | (Krasileva *et al.*, 2010) |
| *AVR-Pita* | *Magnaporthe grisea* | *Pi-ta* | Rice | (Jia *et al.*, 2000) |
| *AvrL567* | *Melampsora lini (Flax rust)* | L5, L6 and L7 | *Linum usitatissimum (Flax)* | (Dodds *et al.*, 2006) |

**Table 1.2.2: Recognition of avirulence genes by resistance genes.** This table shows some of the published effector *R* gene interactions.

1.2.8 – Plant *R* genes effective against oomycetes

*R* genes are an important line of defence against the oomycetes and their co-evolution with effectors is thought to be highly competitive. Some known *R* genes against *P. infestans* are shown in Table 1.2.3. Most recognise RXLR effectors. It has been shown that many RXLRs are found within families and members of these families can be paralogous (Win *et al.*, 2007). The selection pressure for mutations within RXLRs is thought to occur within the C-terminal 'effector' domain while the N-terminal domain is used for secretion and translocation (Win *et al.*, 2007). This selection pressure is similar to that seen in *R* genes which often undergo selection pressure within the LRR-encoding domain (Hein *et al.*, 2009). As mentioned previously *R* genes are can be found individually or within clusters (Hulbert *et al.*, 2001). The selection pressures on resistance genes mean that genes and clusters will evolve at different rates. *Rpi-blb2* is a resistance gene against *P. infestans* found in *S. bulbocastanum* within a cluster of *R* genes situated on chromosome 6 (Hein *et al.*, 2009). The *Rpi-blb2* resistance gene is similar to *Mi-1* gene from tomato, which mediates resistance to root-knot nematodes, aphids and white flies (van der Vossen *et al.*, 2005). The *I2* locus, which the *Mi-1* gene is situated within, shows slow evolution in tomato. However, the cluster containing *Rpi-blb2* has undergone a fast rate of evolution (van der Vossen *et al.*, 2005). Another resistance gene from *S. bulbocastanum, Rpi-blb1,* is thought to have undergone slow evolution with large numbers of synonymous substitutions. This has led to speculation that this is an ancient gene (Hein *et al.*, 2009). It has also been suggested that this resistance gene is restricted geographically to germplasm originating in Mexico (Vleeshouwers *et al.*, 2011).

Some *R* gene clusters show expansion within the genome and become *R* gene hot spots. The *R3* locus found on chromosome 11 of potato is one such hot spot. This locus contains the resistance genes *R3a* for *P. infestans* resistance, *R3b* and possibly *R5-R11;* it also contains *R* genes against *Stemphylium* species, yellow leaf curl virus and tobacco

mosaic virus as well as some resistance to *Globodera rostochiensis,* a cyst nematode (Hein *et al.*, 2009). Another example of complex clustering comes from potato chromosome 5 where the *R1* gene for *P. infestans* resistance is found along with other resistances to *P. infestans,* resistances towards potato virus X (*X*, *Rx2* and *Nb*), *G. pallida* (*Gpa* and *Gpa5*) and *G. rostochiensis* (*Gpr1)* (Hein *et al.*, 2009). The *R2* locus found on chromosome 4 contains the dominant resistance gene *R2* but also contains many other NB-LRR genes which may function in unknown or weak recognition events. For example, a known quantitative trait locus (QTL) on linkage group IV (LGIV), partially responsible for field resistance to late blight in the tetraploid cultivar Stirling, has been positioned close to of the *R2* gene cluster (Bradshaw *et al.*, 2004; Hein *et al.*, 2007). Field resistance or non-race-specific resistance is hypothesised to be controlled by multiple but weak or partial *R* genes that are spread over many QTLs. These *R* genes are much slower to trigger PCD resulting in a trailing HR behind the spreading pathogen but still provide some resistance to the plant (Avrova *et al.*, 2004).

**Table 1.2.3: Cloned *R* genes**

| ***R* genes** | ***Solanum* species** | **Chromosome** | **Effector recognised by *R* gene** |
|---|---|---|---|
| *R1* | *S. demissum* | V | *AVR1* |
| *R2* | *S. demissum* | IV | *AVR2* |
| *R3a* | *S. demissum* | XI | *AVR3a* |
| *R4* | *S. demissum* | XI | *AVR4* |
| *Rpi-blb1* | *S. bulbocastanum* | VIII | *AVRblb1* |
| *Rpi-blb2* | *S. bulbocastanum* | VII | *AVRblb2* |
| *Rpi-vnt1* | *S. bulbocastanum* | IX | *AVRvnt1* |

**Table 1.2.3: Cloned *R* genes.** The cloned *R* genes are shown and the species of *Solanum* and which chromosome they were isolated from. The cloned orthologues of some of these genes are not listed. The *AVR* gene recognised by each *R* gene is also given.

1.2.9 - Effector Triggered Susceptibility 2 (ETS2)

Some effectors secreted by pathogens have been found to target ETI; these effectors lead to ETS2 (Hein *et al.*, 2009) (Figure 1.2.1). For example bacterial effectors have been identified that have the ability to suppress PCD triggered by other effectors, such as AvrPto, AvrPtoB and AvrPtoD2 from *P. syringae* (Bos *et al.*, 2006; Gohre and Robatzek, 2008). It is thought that if there are effectors for ETS2 the plant may evolve additional *R* genes to combat them, leading to ETI2.

1.2.10 – How oomycete *AVR* genes evolve to evade the plant defence system

Many *AVR* genes from *P. infestans, P. sojae* and *H. arabidopsidis* have evolved to evade recognition by the plant defence system (summarised in Table 1.2.4). In the case of AVR3a from *P. infestans* a change in two amino acids K80E and I103M is enough to cause the evasion of the resistance gene *R3a* (Armstrong *et al.*, 2005), whilst retaining virulence function (Bos *et al.*, 2010). There are other RXLR genes that also evade recognition by single nucleotide mutations. These include *PsAvr1b* (Shan *et al.*, 2004) and *PsAvr3c* (Dong *et al.*, 2009) from *P. sojae, PiAVR-blb1* (Vleeshouwers *et al.*, 2008) from *P. infestans* and *HpATR13* (Allen *et al.*, 2004) and *HpATR1* (Rehmany *et al.*, 2005) from *H. arabidopsidis.*

Other mechanisms of evasion have evolved in oomycetes in order to promote virulence. *PiAVR1* from *P. infestans* has been lost from some isolates, presumably to evade recognition by the resistance gene *R1* (Vivianne Vleeshouwers, David Cooke; personal communication). The loss of *PiAVR1* implies that it is not a key effector protein, or that functional redundancy exists within the effector repertoire that has allowed this gene to be lost from the genome of some isolates.

*PsAvr3a* and *PsAvr1a* (Qutob *et al.*, 2009) from *P. sojae* and *PiAVR4* (van Poppel *et al.*, 2008) from *P. infestans* evade the plant immune system by undergoing transcriptional inactivation. *PsAvr3a* and *PsAvr1a* show copy number variation in different strains of *P. sojae* (Qutob *et al.*, 2009). *PsAvr1a* has two copies deleted from some strains which causes a change in virulence while other strains have a change in the transcription of the gene which causes an increase in virulence (Qutob *et al.*, 2009). Some isolates of *P. sojae* have one copy of *PsAvr3a* while other strains have four copies and it is the transcriptional regulation of these genes which causes changes to virulence (Qutob *et al.*, 2009).

*PiAVR4* (van Poppel *et al.*, 2008) from *P. infestans* can also undergo truncation in order to evade recognition by *R4*. Virulent isolates of *P. infestans* contain deletions in the *PiAVR4* gene which cause premature stop codons resulting in a truncated protein which is probably non-functional (van Poppel *et al.*, 2008). This alteration and formation of a truncated protein does not appear to have an effect on the fitness of these isolates (van Poppel *et al.*, 2008). The transcriptional inactivation and truncation to avoid detection by the plant immune system suggests that this *AVR* gene is not essential to the survival of a *P. infestans* isolate. Effectors that are not essential to the pathogen can therefore be lost to enhance the virulence of the pathogen. However there are some effectors, for example *PiAVR3a,* which appear to be essential to the pathogen.

**Table 1.2.4: Cloned oomycete *AVR* genes**

| ***AVR* gene** | **Species** | **Method used to evade R gene** | **Reference** |
|---|---|---|---|
| *PiAVR1* | *P. infestans* | Deletion | (unpublished) |
| *AVR3a* | *P. infestans* | SNPs | (Armstrong *et al.*, 2005) |
| *AVR4a* | *P. infestans* | Transcriptional inactivation/Truncation | (van Poppel *et al.*, 2008) |
| *PiAVR-blb1* | *P. infestans* | SNPs | (Vleeshouwers *et al.*, 2008) |
| *Avrblb2* | *P. infestans* | Unknown | (Oh *et al.*, 2009) |
| *AVR1a* | *P. sojae* | Transcriptional inactivation | (Qutob *et al.*, 2009) |
| *AVR1b* | *P. sojae* | SNPs/Transcriptional inactivation | (Shan *et al.*, 2004) |
| *AVR3a* | *P. sojae* | Transcriptional inactivation | (Qutob *et al.*, 2009) |
| *AVR3b* | *P. sojae* | SNPs/Reduced transcription | (Dong *et al.*, 2011) |
| *AVR3c* | *P. sojae* | SNPs | (Dong *et al.*, 2009) |
| *ATR1* | *H. parasiticaa* | SNPs | (Rehmany *et al.*, 2005) |
| *ATR13* | *H. parasiticaa* | SNPs | (Allen *et al.*, 2004) |

**Table 1.2.4: Cloned oomycete *AVR* genes.** Known *AVR* genes, their species and how they avoid detection by the *R* genes.

1.2.11 – Mechanisms of AVR effector recognition by R proteins

The initial proposal for the *R* gene defence response to *Avr* genes was suggested in the 1950s by Flor, who described a gene-for-gene hypothesis. This initially postulated a direct interaction between the products of *AVR* alleles and corresponding *R* alleles (Flor, 1971) (Figure 1.2.2). This has been widely researched and for some fungal pathogens this hypothesis has been confirmed. The resistance protein Pi-ta found in some cultivars of rice binds directly to the AVR_Pita effector protein upon infection of the plant (Jia *et al.*, 2000). The *Pi-ta* gene encodes a putative cytoplasmic receptor at the N-terminus with a nucleotide binding site in the centre of the protein and a LRR domain at the C-terminus (Jia *et al.*, 2000). It was shown that the AVR_Pita$_{176}$ effector protein lacking a signal peptide and pro-protein sequences was able to bind directly to the leucine-rich domain of the Pi-ta resistance protein which initiated the defence responses (Jia *et al.*, 2000). The proposed gene-for-gene model also holds true for the flax rust fungus, (Dodds *et al.*, 2006). 12 variants of the *AvrL567* gene have been found in six different rust strains. Seven of these AvrL567 proteins are virulent on flax plants that express the resistance

genes L5, L6 and L7, but five are avirulent (Dodds *et al.*, 2006). It was shown that these three resistance proteins can directly interact with the five avirulent AvrL567 proteins both *in vivo* and *in vitro* (Dodds *et al.*, 2006). The virulent and avirulent forms of AvrL567 had a conserved structure, which implies that it is the amino acid changes between the virulent and avirulent forms that affect the binding to the resistance protein (Dodds *et al.*, 2006).

Plants encode a large number of NB-LRR *R* genes within their genomes. These are either found individually or in clusters (Hulbert *et al.*, 2001). The clusters are thought to have arisen through rapid *R* gene evolution (Hulbert *et al.*, 2001). It has been shown that some pathogens, such as *Phytophthora,* contain a large effector repertoire. It therefore appears that plant genomes do not contain enough *R* genes to combat all pathogens they come into contact with if the gene-for-gene model were true in all cases.

This knowledge, combined with the lack of evidence for direct AVR-R protein interactions, led to an indirect interaction model being devised. The guard hypothesis suggests that R proteins may be guarding, or monitoring key host proteins that are manipulated by AVR effectors to aid pathogen virulence (Dangl *et al.*, 2001) (Figure 1.2.2). There are two possible ways this could occur: 1) through monitoring of the conformational state of the target protein, (binding of the effector to the target); 2) the R protein is permanently bound to the target protein and, when the effector binds, the R protein is released and activated (Dangl *et al.*, 2001) (Figure 1.2.2). The activation of R proteins causes defence responses to be triggered and therefore resistance occurs. If there is no *R* gene product within a cell, the changes triggered by the effector activity are not detected, the targeted protein is successfully manipulated and disease occurs. Neither of the above options for guarding of the target protein involve the R protein actually interacting with the effector. This model explains how many different effectors could be detected by one R protein. An example of this is the *RIN4* gene from *A. thaliana*. The R protein RPM1 activates resistance when the

plant is infected with *P. syringae*. RPM1 recognises the phosphorylation of RIN4 by the *P. syringae* effectors AvrRpm1 or AvrB (Mackey *et al.*, 2002). RPM1 appears to monitor the phosphorylation state of the RIN4 protein (Mackey *et al.*, 2002). Another example from *A. thaliana* is RPS2 which also monitors RIN4. This R protein detects disappearance of RIN4 when the AvrRpt2 effector, also from *P. syringae*, proteolytically cleaves RIN4 (Mackey *et al.*, 2003). These examples show two R proteins guarding one host protein and detecting three effector proteins, indicating that a smaller number of *R* genes could be responsible for detecting a range of effectors (Dangl and Jones, 2001).

An example from fungi, which implies that the guard hypothesis is not restricted to bacteria, comes from *C. fulvum.* This fungus secretes the effector Avr2 when infecting tomato plants. It has been shown that Avr2 targets the plant proteins RCR3 and PIP1 which are papain-like cysteine proteases (PLCPs) (Rooney *et al.*, 2005; Shabab *et al.*, 2008). Avr2 is able to bind to and inhibit these proteases, which are up-regulated by the SA pathway during defence responses to biotrophic pathogens (Rooney *et al.*, 2005; Shabab *et al.*, 2008). Avr2 from *C. fulvum* is recognised by the resistance Cf-2. However there has been no proof of interaction between Cf-2 with the target proteins RCR3 and PIP1 or the effector protein Avr2.

The guard hypothesis has since been adapted to include a decoy model. The principle of the Decoy model is that a host protein has evolved that can mimic the original target protein but it has no function in the development of disease (van der Hoorn and Kamoun, 2008) (Figure 1.2.2). This means that the decoy protein undergoes an effector-induced conformational change, as the genuine target protein would, allowing the R protein to detect it and trigger resistance (van der Hoorn and Kamoun, 2008). An example of this is the protein kinase Pto from tomato. This appears to act as a decoy for the receptor-kinase FLS2 (Chang *et al.*, 2000). *P. syringae* effector AvrPto blocks the kinase activity of its

target FLS2, but resistance is conferred in strains that contain the protein Pto. However, in the absence of Pto, AvrPto still enhances virulence of *P. syringae*, indicating that Pto may be a decoy and FLS2 the functional target (Chang *et al.*, 2000). This decoy model may also be true for the Avr2/Cf-2 interaction in tomato. It has been suggested that RCR3 may be a decoy whereas PIP1 is the genuine target of Avr2, as a role for RCR3 in plant defence has not been found (Shabab *et al.*, 2008). The avirulence protein will interact with these decoys in the presence or absence of an R protein (van der Hoorn and Kamoun, 2008). The decoy model has not been experimentally verified but it does give an alternative view to the guard hypothesis.

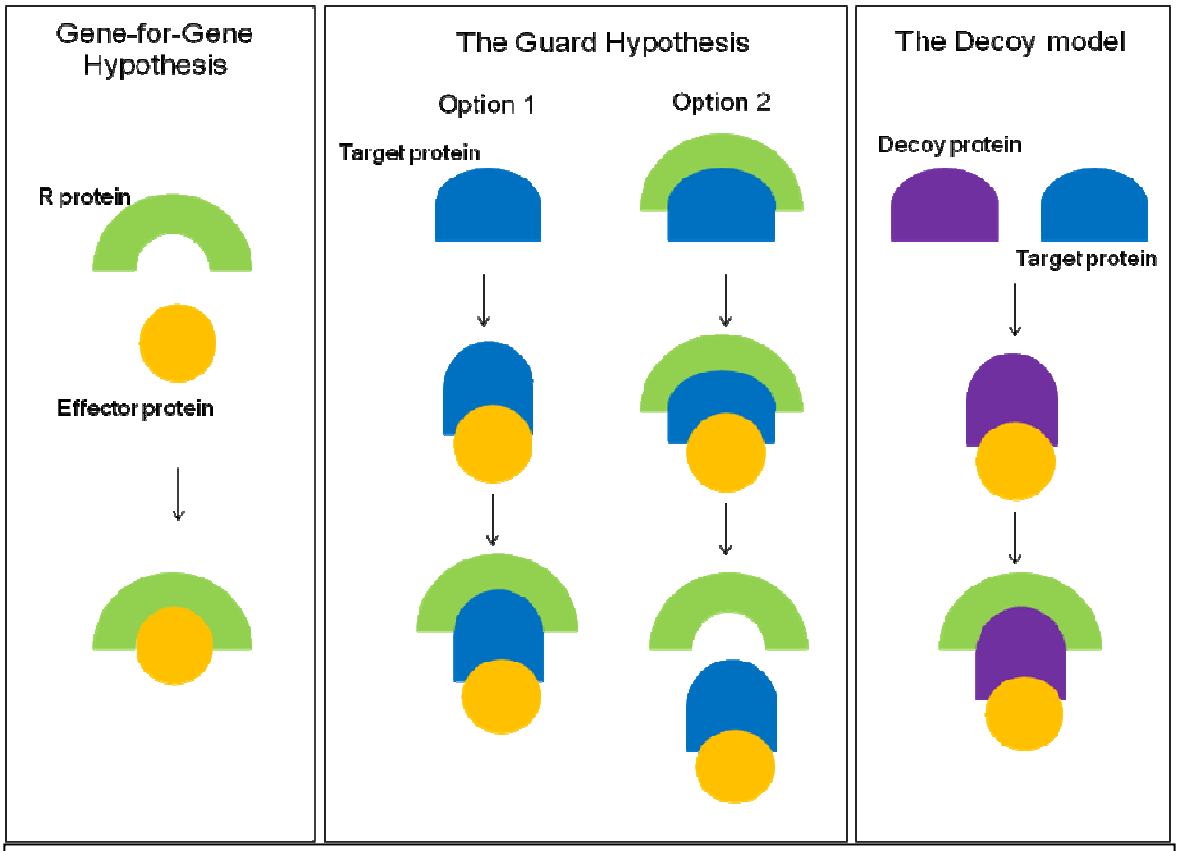


**Figure 1.2.2: Mechanisms of AVR effector recognition by R proteins.** A diagram depicting three models for effector recognition; Gene-for-Gene Hypothesis, The Guard Hypothesis and the Decoy model. The Guard Hypothesis Option 1 refers to a change in confirmation allowing the R protein to recognise the presence of the effector. Option 2 refers to the R protein being already bound to the target, the binding of the effector causes the release and activation of the R protein. All modes of recognition result in the activation of the defence system

1.2.12 – Development of the Hypersensitive Response (HR)

The events triggered by PTI and ETI are similar, i.e. accumulation of reactive oxygen species (ROS), reactive nitrogen oxide intermediates (NOI) and the hormone salicylic acid (SA), the activation of MAPK cascades and changes in transcriptional reprogramming, but it appears that these responses are amplified and accelerated in ETI. The HR is a form of programmed cell death (PCD) associated with some PTI, but mainly ETI, defence responses, implying that it is the quantity and strength of the responses that trigger the development of an HR (Coll *et al.*, 2011). The HR usually occurs around the site of biotrophic pathogen infections to prevent their spread, as they need the host cells alive to survive (McLellan *et al.*, 2009). Necrosis is a form of cell death usually caused by toxins or trauma and is uncontrolled, whereas the HR is an active process under strict genetic control that requires metabolically functioning cells which can still undergo transcription and translation (Coll *et al.*, 2011).

The genetic control of HR development has been examined using lesion mimic mutants (LMMs). One null mutant plant, *lsd1,* presents runaway cell death (Lorrain *et al.*, 2003). This mutant still presents spontaneous lesions in a salicylic acid deficient NahG background but overall cell death is reduced which implies that the SA pathway regulates the formation of the HR (Lorrain *et al.*, 2003).

There are many signalling components and proteins involved in the formation of an HR. One protein that has been investigated is the papain cysteine protease cathepsin B. It has been shown that cathepsin B is key for the development of some HRs (Gilroy *et al.*, 2007). When *cathepsin B* is silenced the R3a/AVR3a HR failed to be produced, although the HR from *C. fulvum* AVR4 with tomato Cf-4 was unaffected. This implies that cathepsin B is needed for R3a HR but not Cf-4, indicating that there could be at least two mechanisms for HR formation (Gilroy *et al.*, 2007).

The production of SA during an HR is associated with a systemic induction of defence response genes within distal plant tissue known as systemic acquired resistance (SAR) (Dangl *et al.*, 1996). During the formation of an HR, specific characteristic morphological and physiological changes occur, including cytoplasmic shrinkage, chromatin condensation, mitochondrial swelling, vacuolisation and chloroplast disruption (Coll *et al.*, 2011). These changes are mainly caused by a second, sustained burst of ROS which causes irreparable damage to DNA, proteins and lipids of the invading pathogen and host cells. However, ROS can also act as signalling molecules that lead to induction of defence response genes and to cross-linking of cell walls surrounding the HR and in close proximity to it (Dangl *et al.*, 1996).

The chloroplast is a very important site for production of plant defence signalling molecules such as ROS and NOI, but also of defence hormones such as SA and jasmonic acid (JA) (Coll *et al.,* 2011). The formation of ROS is not solely localised to the chloroplast; it has been shown that apoplastic ROS which is generated by the plasma membrane NADPH oxidases are essential to the development of the HR (Torres and Dangl, 2005). It appears that ROS signalling might be compartmentalised to the various organelles and this compartmentalisation is key to the formation of the defence responses (Coll *et al.*, 2011).

### 1.2.13 – *R* gene signaling

The signalling events that lead to the development of the HR and plant defence responses after the recognition of an effector by the NB-LRR protein are not fully understood. It is known that the CC-NB-LRR and the TIR-NB-LRR use different signalling molecules. The CC-NB-LRRs are regulated by NON-RACE-SPECIFIC DISEASE RESISTANCE 1 (NDR1) and a complex of three proteins mediates activity of the TIR-NB-LRR proteins. The three proteins within this complex are ENHANCED DISEASE SUSCEPTIBILITY 1 (EDS1),

PHYTOALEXIN DEFICIENT 4 (PAD4) and SENESCENCE-ASSOCIATED GENE 101 (SAG101) (Coll *et al.*, 2011). It is known that these two different regulation mechanisms of the NB-LRRs utilise redox signalling which leads to SA accumulation. The resulting ROS and SA are known to act synergistically to form the development of the HR (Coll *et al.*, 2011). Two other key components of *R* gene signalling are REQUIRED FOR MLA12 RESISTANCE, (RAR1) and SUPPRESSOR OF G2 ALLELE OF SKP1, (SGT1). These proteins interact in a yeast two hybrid system and can both complement *sgt1* yeast KO mutants (Azevedo *et al.*, 2002). When loss of function mutations were made in *RAR1* this resulted in a loss of the resistance protein RPM1 function, implying RAR1 is important for the stability of RPM1 (Tornero *et al.*, 2002). Virus-Induced Gene Silencing and KO studies of SGT1 suggest this protein is a key component of *R* gene-mediated resistance (Tor *et al.*, 2002; Austin *et al.*, 2002).

The localisation of some R proteins has been investigated to try and shed light on downstream signalling mechanisms. RPS4 is a TIR-NB-LRR resistance protein found in *A. thaliana* that is important for resistance against multiple pathogens including *Ralstonia solanacearum, Colletotrichum higginsianum* and *P. syringae* (Eitas and Dangl, 2010). RPS4 accumulates in the nucleus in order to trigger the development of an HR (Eitas and Dangl, 2010). Another R protein which localises to the nucleus to trigger defence responses is the barley NB-LRR MLA10 (Bernoux *et al.*, 2011). This resistance protein detects the effector AvrA10 from barley mildew and then accumulates in the nucleus, where it associates with two WRKY transcription factors that act as transcriptional repressors of PTI (Bernoux *et al.*, 2011). The resistance protein Rx has been shown to shuttle between the cytosol and the nucleus, dependent on interaction with Ran GTPASE ACTIVATING PROTEIN 2 (RanGAP2), resulting in immune signalling (Bernoux *et al.*, 2011). However, more recently the resistance protein RPM1 was discovered to trigger immune signalling from the plasma membrane (Bernoux *et al.*, 2011). This implies that

there is no uniformity in the signalling of resistance proteins and also that there is no single signalling pathway for the production of the HR after AVR effector recognition.

1.2.14 – Durable resistance

The potato cultivar Stirling has proven to express high levels of resistance to *P. infestans* nationally and internationally but the tubers produced are not of suitable quality for consumer purposes (Hein *et al.*, 2007). For this reason Stirling was used as a base for creating genetic crosses which gave rise to the popular organic cultivar Lady Balfour. Stirling, until recently, was resistant to all known isolates of *P. infestans.* However, with the recent emergence of the *P. infestans* genotype 13_A2 the resistance in Stirling failed. Genotype 13_A2 is highly aggressive and has spread throughought the UK *P. infestans* population to become the dominant genotype found in 2007 and 2008 (David Cooke, the JHI, personal communication). The difference in aggressiveness of isolates is down to a number of factors, including the secretion of different RXLR effectors, optimal temperature growth range, and faster or slower life cycles. The isolate 06_3928A from the 13_A2 genotype is highly virulent but T30-4, the genome-sequenced isolate, is less aggressive (David Cooke, the JHI, personal communication; Haas *et al.*, 2009).

The resistance genes *R1*, *R3* and *R10* have been bred into many European potato cultivars. *R1* and *R3* genes have a narrow range of resistance to *P. infestans* and many isolates have overcome them. Therefore their usefulness is limited within the field (Vleeshouwers *et al.*, 2011). Most resistance genes to date have been overcome by effector varients expressed from some isolates of *P. infestans;* this implies a new strategy to generate durable resistance must be put in place to reduce the amount of crop losses suffered each year. Some resistance genes have only been partially defeated and these

will still be useful in crop plants especially when they are used in combination with other *R* genes (Vleeshouwers *et al.*, 2011).

Durable resistance is an important objective of many research groups and there are several different approaches being taken. The first approach has been made possible by the availability of cloned effector proteins from the pathogen. These effector proteins can be co-expressed *in planta* using *A. tumefaciens* with candidate cloned *R* genes. This allows recognition of the effector by the R protein to be visualised by the development of an HR and then allows rapidly identification new sources of resistance that can be used in breeding or transgenic approaches. (Vleeshouwers *et al.*, 2011).

Another useful method using these cloned effectors is to screen virulent forms for recognition in wild *Solanum* species, again via *A. tumefaciens,* in order to try and discover any novel *R* genes that are not in the crop plants currently used. Discovery of these could lead to novel breeding programmes to introduce these resistances into the crop (Vleeshouwers *et al.*, 2011). This approach is being used at the James Hutton Institute with the Commonwealth Potato Collection (CPC), which contains about 1800 accessions made up of >80 wild and cultivated potato species. These accessions can be traced back to tubers from Solanum species in South or Central America.

A further approach being used to generate new resistance proteins utilises gene shuffling techniques. This approach involves artificially introducing SNPs into the LRR domain of characterised *R* genes in order to expand their recognition spectrum to the virulent alleles of recognised effectors (Vleeshouwers *et al.*, 2011). For example, *R3a* can recognise $AVR3a^{KI}$ but not $AVR3^{EM}$ but a shuffled *R3a* gene may recognise both. This strategy has previously been successfully applied to the potato virus X (PVX) *R* gene, *Rx.* Before mutagenesis the Rx protein only recognised strains of PVX with a threonine and lysine at

positions 121 and 127 within the coat protein (Farnham and Baulcombe, 2006). After an error prone PCR was used to introduce SNPs into the LRR domain, recognition of previously unrecognised strains which contained lysine and arginine at positions 121 and 127 was generated (Farnham and Baulcombe, 2006). If this method was successful in generating novel resistance genes against late blight then they would have to be introduced into the plant using genetic modification (GM).

The effectiveness of *R* genes needs to be explored in relation to where they will be deployed. For example the *P. infestans* populations found within Europe are quite complex and fast evolving compared to populations found in Africa which are dominated by a few local isolates (Vleeshouwers *et al.*, 2011). This means that deploying the same *R* genes in these two different areas may not be sensible as the pathogen populations are so different. The more information known and understood about the effectors conserved in pathogen populations, the better we can assess the effectiveness of an *R* gene before it is deployed. For example, there is little use in deploying *R1* in potato cultivars if populations of *P. infestans* isolates within that particular geographical location do not express *AVR1.* The methods described above are useful for identifying potential durable *R* genes. Many different potentially durable *R* genes may need to be stacked and expressed simultaneously within one cultivar to provide the best chance of engineering a long term solution to late blight infection. Sadly, current political and consumer attitudes to genetically modified crops prevent many of these strategies being deployed in Europe.

## 1.3 – The Brassinosteroid Pathway

During the work in this thesis it was discovered that the PiAVR2 effector protein from *P. infestans* was interacting with a phosphatase found to function within the brassinosteroid

signal transduction pathway. This section describes the current knowledge for the signal transduction of this pathway and the main components that function within this pathway

Cell growth, division, elongation and differentiation, leading to plant growth and development, are regulated by the brassinosteroid pathway. Brassinosteroids (BRs) are small growth promoting molecules that bind to leucine-rich-repeat receptor kinases (LRR-RK) on the cell surface and initiate a signal transduction pathway (Belkhadir and Chory, 2006). The most abundant BR is called brassinolide (BL) and was first identified in the 1970s when a crystal structure was made from *Brassica napus* (oilseed rape) pollen (Grove *et al.*, 1979). It was not until the mid 1990s that the role of BRs was clarified, when it was discovered that *A. thaliana* mutants deficient in BR synthesis were severely stunted in growth, with small, curled leaves (Li *et al.*, 1996; Szekeres *et al.*, 1996). Since then this pathway has been investigated extensively in *A. thaliana* using forward genetic screens, protein-protein interactions, proteomics and biochemical studies. These techniques have led to the discovery of most of the components of this pathway and the clear signalling steps involved in the regulation of growth and development of the plant. Below the pathway is described as it is currently known in *A. thaliana*.

The cell surface receptor that BRs bind to is called BRASSINOSTEROID INSENSITIVE 1 (BRI1). This receptor was first discovered in the 1990s by the identification of a *bri1* mutant which resulted in a dwarfed phenotype that was insensitive to BR treatment (Clouse *et al.*, 1996). This receptor is composed of an extracellular domain which contains an N-terminal signal peptide, 24 LRRs and an island domain (ID) located between LRR domains 20 and 21 (Belkhadir and Chory, 2006; Kim and Wang, 2010). The receptor has one transmembrane domain next to which a juxtamembrane region (JM) lies, an intracellular serine/threonine kinase domain (KD) and a C-terminal region (CT) (Figure 1.3.1) (Belkhadir and Chory, 2006). Several studies have shown that BRI1 is the cell surface receptor for BR. One of these showed that BRI1, immunoprecipitated from *A.*

*thaliana* or purified from *E. coli*, bound to tritium-labelled BL and induced BRI1 auto-phosphorylation (Kinoshita *et al*., 2005; Kim and Wang, 2010). It was also shown that a 94 amino acid section, which contained the ID domain and the LRR21 domain, was sufficient for BR binding (Kinoshita *et al*., 2005). The BRI1 receptor is found as a homo-dimer in the plasma membrane 20% of the time. However, BR treatment increased the number of homo-dimers observed, which suggests that BR promotes stability of these dimers (Kim and Wang, 2010). The crystal structure of BRI1 (LRR) has been generated for this receptor, free and brassinolide bound structures have been generated (She *et al.,* 2011). These crystal structures show that brassinolide binds to a hydrophobicity-dominating surface groove and that recognition of the hormone is through the stabilisation of two interdomain loops creating a non-polar surface which the hormone binds too (She et al., 2011). This grove is the island domain situated between LRRs 21 and 22 (Hothorn et al., 2011). This island domain folds back into the superhelix creating the surface grove for the binding of brassinolide (Hothorn *et al.,* 2011).

In the absence of BRs, another plasma-membrane associated phosphoprotein called BRI1 KINASE INHIBITOR 1 (BKI1) interacts with the kinase domain of BRI1. This interaction interferes with the kinase activation of BRI1 and prevents the receptor from becoming fully active. It is thought this interference occurs by BKI1 physically blocking BAK1 association (Wang and Chory, 2006). Therefore BKI1 acts as a negative regulator of the BR pathway and may ensure specificity of BRI1 signalling (Wang and Chory, 2006). When BKI1 is over-expressed, a weak dwarf phenotype is observed, while RNAi knockdowns of *bki1* result in enhanced hypocotyl elongation, suggesting enhanced activity of BRI1 (Wang and Chory, 2006; Kim and Wang, 2010). In the presence of hormone, BKI1 rapidly dissociates from BRI1 allowing auto-phosphorylation of the receptor to occur, increasing the interaction between BRI1 and its signalling partner BAK1 (Wang and Chory, 2006). The localisation of BKI1 can be seen to change when BRI1 becomes activated. Prior to BR

treatment, BKI1 localises to the plasma membrane, while post-treatment it is re-localised to the cytosol (Wang and Chory, 2006).

BAK1, also known as SERK3 (SOMATIC EMBRYOGENESIS RECEPTOR KINASE 3) is an LRR-RLK that contains 5 extracellular LRR-domains (Figure 1.3.1) (Wang *et al.*, 2008). BAK1 is a co-receptor to BRI1 (Wang *et al.*, 2008). The BRI1/BAK1 association appears to be mediated by their kinase domains rather than their extracellular domains (Kim and Wang, 2010). Mutations were made in the kinase domains that abolished their activity; and this resulted in minimal interactions between BRI1/BAK1. A kinase-inactive BRI1 mutant did not associate with BAK1 after BR treatment (Li *et al.*, 2002; Wang *et al.*, 2008). When a kinase-inactive BAK1 was tested with a wild type BRI1, the BAK1 still interacted with active BRI1, which implies that the BRI1/BAK1 association is a result of the activation of the BRI1 kinase domain (Wang *et al.*, 2008).

BAK1 does not participate in the binding to BR, as the binding activity of BRI1 was not altered when BAK1 was over-expressed, or in a *bak1* null mutant (Kinoshita *et al.*, 2005). The BRI1/BAK1 complex undergoes trans-phosphorylation which leads to the activation of the plasma membrane- associated BR-SIGNALLING KINASES (BSKs) (Tang *et al.*, 2008). The trans-phosphorylation of BRI1 and BAK1 has been investigated using mass spectrometry (MS). This has shown that BRI1 primarily phosphorylates the kinase domain of BAK1 at S290, T312, T446, T449, T450 and T455 (Figure 1.3.1). Four of these residues are in the activation loop and are required for kinase activity of BAK1 (T446, T449, T450 and T455) (Wang *et al.*, 2008). The phosphorylation of BRI1 by BAK1 does not occur in the kinase domain. Instead the phosphorylation sites can be found in the CT, S1166 and T1180, and the juxtamembrane region (JM), S838, T846 and S858 (Figure 1.3.1) (Wang *et al.*, 2008).

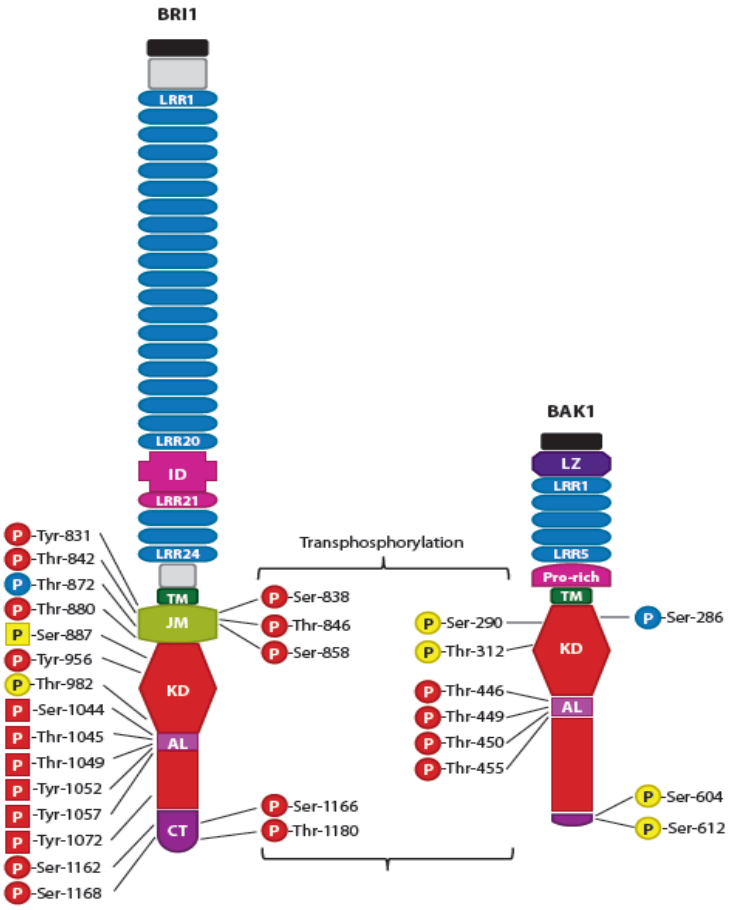


**Figure 1.3.1: The structures of BRI1 and BAK1.** (Taken from Kim and Wang, 2010). The extracellular domain of BRI1 contains 24 leucine rich repeats (LRR) and an island domain (ID) is situated between LRR 20 and 21. One transmembrane domain (TM) is present next to which lies the juxtamembrane region (JM) before the intracellular kinase domain (KD) and C-terminal domain (CT). BAK1 contains 5 LRR domains, 4 leucine zippers and a proline rich domain in its extracellular domain. It contains one TM domain with the intracellular KD and CT domains next to it. AL represents the activation loop. Confirmed phosphorylation sites are represented by circles and putative ones by squares. Red sites show activation while inhibitory sites are blue and sites with no effect are yellow.

There have been three BSKs found in *A. thaliana* that act redundantly in this pathway (BSK1, BSK2 and BSK3). These BSK proteins are composed of a kinase domain at the N-terminus and a tetratricopeptide repeat (TPR) at the C-terminus (Tang *et al.*, 2008). There is no transmembrane domain present but there is a putative N-terminal

myristoylation site that could mediate its membrane localisation (Tang *et al.*, 2008). TPRs can mediate protein-protein interactions and BSKs are thought to be bound to the BRI1 cell surface receptor (Tang *et al.*, 2008). It has been shown that BSK1 undergoes phosphorylation by BRI1 at Ser230 after which it seems to dissociate from BRI1. However, its localisation at the cell surface does not change (Tang *et al.*, 2008). Once dissociation occurs, BSK1 interacts with BRI1 SUPPRESSOR 1 (BSU1) (Kim *et al.*, 2009). Knockout plants of *bsk1* and *bsk2* did not show any developmental phenotype. However, *bsk3* knockout plants showed a slight reduction in BR sensitivity. Over-expression of the BSKs restored normal growth in dwarf plants and BR-regulated gene expression (Tang *et al.*, 2008). The phosphorylation of Ser230 on BSK1 is the trigger for the interaction with BSU1; if a S230A substitution is made then no interaction between BSK1 and BSU1 occurs (Kim *et al.*, 2009). It is not known what physical effect the BSK1-BSU1 interaction has on BSU1.

In addition to BSK1 it has been shown that a receptor-like cytoplasmic kinase named CONSTITUTIVE DIFFERENTIAL GROWTH 1 (CDG1) can also activate BSU1 (Kim *et al.,* 2011). CDG1 is a plasma membrane protein which is activated by the cell surface receptor BRI1. This activation occurs by BRI1 phosphorylating CDG1 at S44, S47 and S234 (Kim et al., 2011). While the mode of activation of BSU1 by BSK1 is not published it has been described that CDG1 activates BSU1 by phosphorylating S764 within the phosphatase domain (Kim *et al.,* 2011). It was shown using bimolecular fluorescence complementation that CDG1 interacts with BSU1 and BSL1 (Kim *et al.,* 2011).

BSU1 is a Ser/Thr phosphatase that contains 6 putative N-terminal Kelch-repeat domains. There are three other family members associated with BSU1: BSU1-like 1, 2 and 3 (BSL1, BSL2 and BSL3). The positive regulation by BSU1 on the BR pathway can be seen when the *BSU1* gene is over-expressed in a *bri1* knock-out line. This over-expression restores

normal growth to the stunted KO line (Mora-Garcia *et al.*, 2004). To support this, when *bri1* plants over-expressing BSU1 are treated with BR hormones, there are also increases in physiological responses, i.e. normal height of plants, normal growth of leaves (Mora-Garcia *et al.*, 2004). It has recently been shown that BSU1 acts to dephosphorylate BR-INSENSITIVE 2 (BIN2) at Tyr200 which results in the inactivation of BIN2 (Kim *et al.*, 2009). The interaction of BIN2 and BSU1 has been shown *in planta* using bimolecular fluorescence, and appears to occur in the nucleus and at the plasma membrane of cells (Kim *et al.*, 2009).

BIN2 is a GLYCOGEN SYNTHASE KINASE-3 (GSK3)-like kinase which is a negative regulator of the BR pathway. When BIN2 is active and the BR pathway is inactive, i.e no hormone is present, BIN2 phosphorylates multiple sites of the transcription factors (TFs) BRASSINAZOLE RESISTANT 1 (BZR1) and bri1-EMS-SUPPRESSOR 1/ BRASSINAZOLE RESISTANT 2 (BES1/BZR2) (Li and Nam, 2002). Six phosphorylation sites for BZR1 were discovered *in vivo*: S102, S171, S173, S177, S181 and S185, while two other sites were discovered *in vitro*; S220 and S224 (Kim and Wang, 2010). The phosphorylation of these two TFs inhibits their activity through several mechanisms, including inhibition of DNA binding and transcriptional activity, accelerated proteasomal degradation and nuclear export, and cytoplasmic retention by a 14-3-3 protein (Gampala *et al.*, 2007). The positive regulation achieved by BSU1 interacting with and inhibiting BIN2 prevents the phosphorylation of the TFs (Kim *et al.*, 2009). BSU1 does not dephosphorylate already phosphorylated TFs - that is the job of a PROTEIN PHOSPHATASE 2A (PP2A) - but it does prevent newly synthesised TFs from becoming phosphorylated by BIN2, allowing them to regulate the BR-responsive genes (Kim *et al.*, 2009; Tang *et al.*, 2011).

PP2A has recently been found to act within this complex pathway as a BZR1-interacting protein (Tang *et al.*, 2011). This interaction takes place between the B' subunit of the PP2A (At3g09880) and the putative PEST (proline, glutamic acid, serine and threonine-rich) domain of BZR1 (Tang *et al.*, 2011). The interaction with BZR1 and its dephosphorylation are abolished if the PEST domain is deleted and enhanced if the *bzr1-1D* mutant is used (Tang *et al.*, 2011). The *bzr1-1D* is a dominant mutant which has a P234L mutation that results in suppression of BR-deficient phenotypes and insensitivity to the BR inhibitor brassinazole (BRZ) (Wang *et al.*, 2002). When the PP2A protein is over-expressed it results in increased activity of BZR1 and suppression of the BR-deficient phenotype (Tang *et al.*, 2011). Another discovery of this work was that dephosphorylation of BZR1 by PP2A abolishes the binding of BZR1 to the 14-3-3 proteins which target the TF for degradation (Tang *et al.*, 2011).

RNAi suppression of the TF genes results in a dwarf phenotype which shows that the suppressed genes are positive regulators of the BR pathway and have redundant roles (Yin *et al.*, 2005). Active BZR1 and BES1/BZR2 bind DNA directly and regulate the expression of BR-responsive genes. The BR-responsive genes that this whole pathway targets are numerous and some are still elusive. However, there are a few known target genes, and a little is known about their regulation. The two TFs BZR1 and BES1/BZR2 target and regulate BR-responsive genes by binding directly to their promoters (Gampala *et al.*, 2007).

Each TF has a different sequence specificity and transcriptional activity. The N-terminal domain of BZR1 binds to the BR-response element (BRRE) which has an optimal binding site of CGTG(T/G)G (Gampala *et al.*, 2007). This sequence is conserved in the promoters of BR repressed genes e.g. *CPD, DWF4* and *ROT3* (He *et al.*, 2005). This means that BZR1 acts as a transcriptional repressor to mediate feedback inhibition of BR biosynthetic

gene expression (Gampala *et al.*, 2007). However, the BRRE motif was also found on the promoters of some BR-induced genes as BZR1 has dual roles in feedback inhibition of BR biosynthesis and BR promotion of plant growth (He *et al.*, 2005). BZR1 works alone to bind the promoters but BES1/BZR2 first binds BES1-INTERACTING MYC-LIKE PROTEIN 1 (BIM1) which is a bHLH-type transcription factor and together they bind to the E-box elements (CANNTG) in the promoter (Gampala *et al.*, 2007). This can be found in the promoter of SAUR-AC1 gene which is up-regulated implying that BES1/BZR2 acts as a transcriptional activator (Yin *et al.*, 2005). The opposite regulation of these two transcription factors is interesting when taken together with the results from gain-of-function mutant studies. *bzr1-1D* and *bes1-D* showed opposite phenotypes when grown in the light; *bzr1-1D* produced a semi-dwarf phenotype while *bes1-D* showed long petioles and pale leaves which resembles BR-treated plants (Wang *et al.*, 2002; Yin *et al.*, 2002). It has been reported that BES1/BZR2 is also able to inhibit the expression of CPD and DWF4 implying that it is difficult to separate the functions of these two transcription factors (Mora-Garcia *et al.*, 2004; Kim and Wang, 2010). The fact that it appears difficult to separate the functions of these TFs is not surprising as they are 89% identical (Belkhadir and Chory, 2006; Gampala *et al.*, 2007).

The BR pathway is complex with many layers of signalling required to have the regulation specificity needed to control plant growth and development. The BR pathway in an inactive and active state is shown in Figure 1.3.2.

Plants use many signalling pathways and the BR pathway is just one of these. How this growth and development pathway is linked to other regulatory pathways is not known but it is thought that cross-talk must occur between regulatory pathways within the plant. Some of the hormone regulatory pathways have the same function. It has been shown that gibberellin, auxin and BR all regulate along longitudinal axes which influence the structure

of plants and their organ size (Jaillais and Chory, 2010). The GSK3-like kinase, BIN2, found within the BR pathway is also found within the auxin pathway (Jaillais and Chory, 2010). This shows that two regulatory pathways share a common signalling component, which could allow cross-talk between them. A diagram has been designed showing the complex interactions thought to occur between gibberellins, auxin, brassinosteroids, ethylene, cytokinins and abscisic acid. However, there is no experimental evidence currently available to prove or disprove there interactions (Figure 1.3.3) (Jaillais and Chory, 2010).

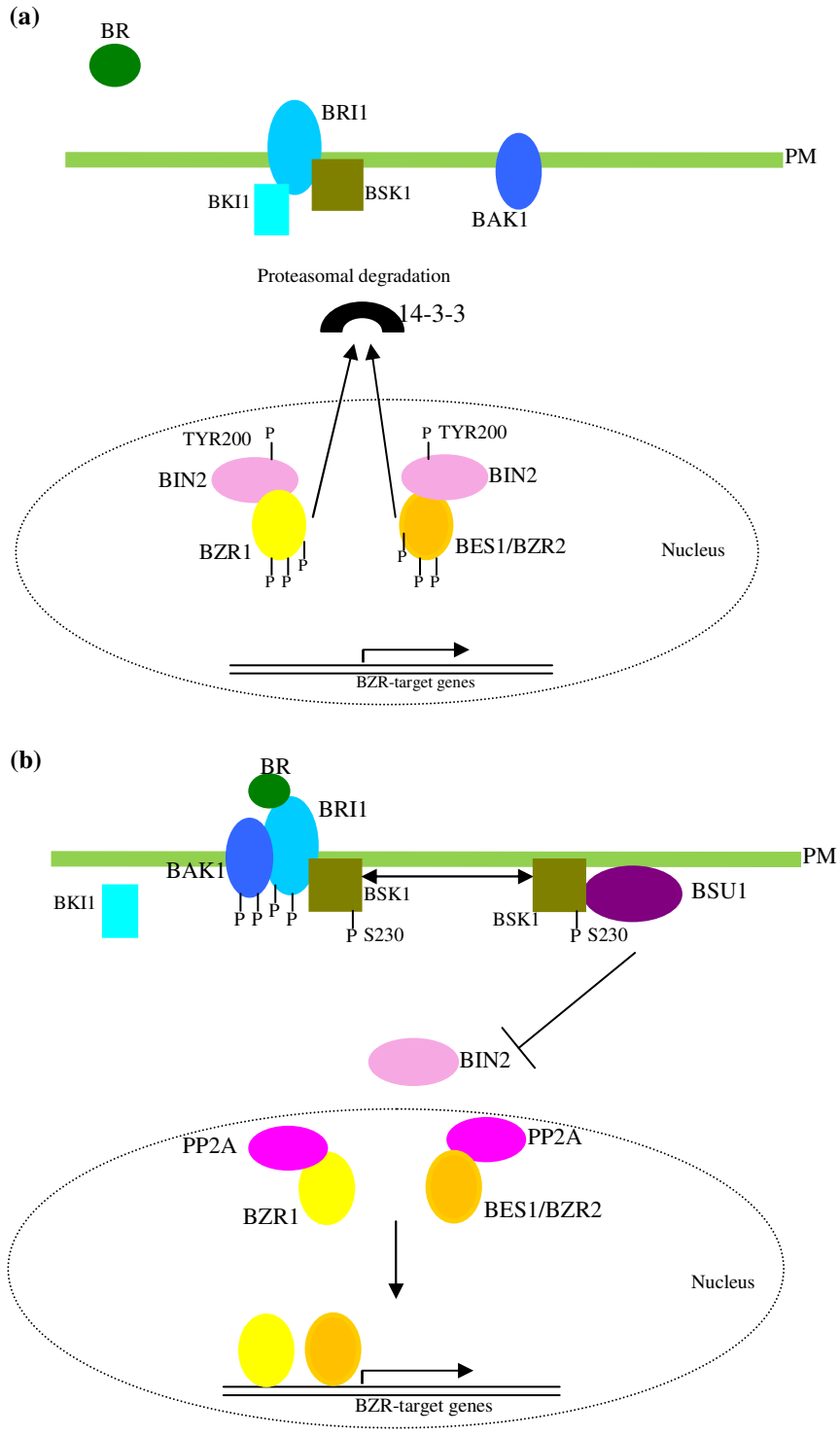


**Figure 1.3.2: The BR pathway.** **(a)** Shows the inactive pathway with BKI1 bound to BRI1 and the transcription factors heading for proteasomal degradation. **(b)** Shows the active pathway with BAK1 bound to BRI1, BSK1 dissociating and activating BSU1, BIN2 being inactivated, PP2A activating the transcription factors which leads to transcription of BR responsive genes.

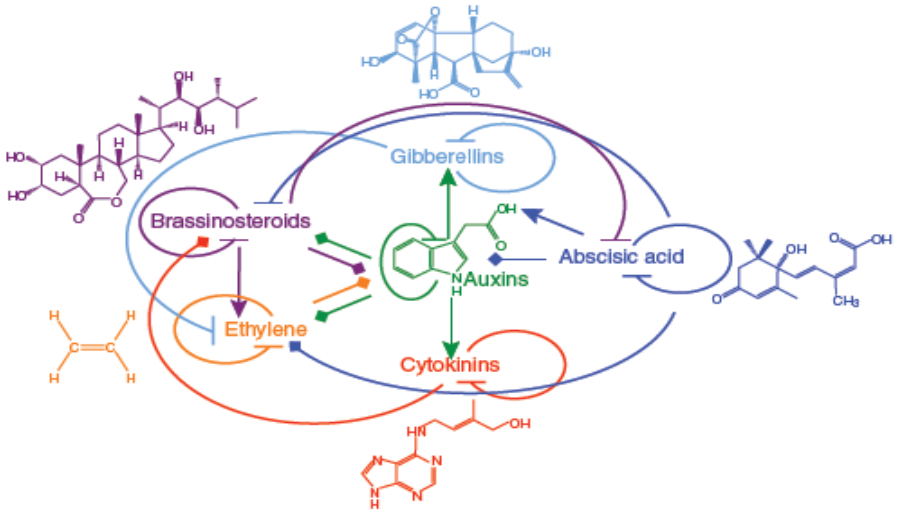


**Figure 1.3.3: Complex interactions between hormone pathways.** This image is taken from Jaillais and Chory, (2010). It shows the complex interactions that are thought to occur between a few of the hormone pathways. Some pathways are missing from this image for example, SA and JA.

## 1.4 – Aims and Objectives

The avirulence gene *PiAVR2* is recognised by the potato resistance gene *R2*. In this project the model crop plant *Nicotiana benthamiana* was used to perform the majority of experiments. Confirmation of the R2/PiAVR2 recognition was sought and any alleles/paralogues of *PiAVR2* investigated. Using *in vitro* and *in vivo* techniques the host target of this avirulence protein was investigated in order to gain more understanding of the recognition of oomycete effector proteins by the plant defence system.

The specific aims of this project were to:

- Determine the gene that encodes *PiAVR2* and the virulence of any alleles/paralogues found within *P. infestans* populations.
- Determine the host target of PiAVR2.
- Investigate how the host target protein mediates the resistance of *R2* plants to *P. infestans* infection.

# 2 – Materials and Methods

Unless otherwise stated, all chemicals were purchased from VWR (VWR International Ltd, UK) and antibiotics were purchased from Sigma-Aldrich (Sigma-Aldrich Company Ltd, UK).

## 2.1 – Cloning and recombination

Gateway® recombination cloning technology (Invitrogen, Paisley, UK) was used for the cloning of genes from both *P. infestans* and *S. tuberosum*. A nested two step PCR was used for this cloning method using KOD Hot Start DNA Polymerase (Novagen, Germany). The first primer pair used is gene-specific with half of the gateway attB site present at the 5' end of the primer and is mentioned in tables relevant to each methods section. A second amplification using the first gene-specific PCR product as a template, again with KOD Hot Start DNA Polymerase, was undertaken using the universal primer pair (AttB1/2), this completes the gateway attB site (Table 2.1.1). Once amplification of the required gene had been achieved the final PCR product was run on a 1% agarose, 1x TBE gel and the bands of the expected size cut out and gel purified using the QIAquick® Gel Extraction Kit (Qiagen Ltd, UK) following the manufacturer's instructions. The resulting purified PCR product was recombined into the entry plasmid pDONR201 using the Gateway® BP Clonase® II kit (Invitrogen, Paisley, UK). This entry plasmid allows the movement of the genes of interest to all other Gateway® vectors using the att recombination sites, which is achieved by the use of the Invitrogen LR Clonase® II kit (Invitrogen, Paisley, UK). The methods for both the BP and LR Clonase® II kits were followed as per the manufacturer's instructions.

2.1.1 – *P. infestans* genes

*PiAVR2*$^{N31/K31}$, *PiAVR2* N-terminus, *PiAVR2* C-terminus and *PITG_08949* were cloned without the signal peptide from cDNA using primers specific to each gene (Table 2.1.1). The cDNA was prepared from RNA extracted from susceptible potato cultivar, Bintje leaf material infected with *P. infestans* isolates at 24 hpi. The PCR product was recombined into the pDONR201 entry vector after purification as described above. The *PiAVR2-like*, *PiAVR2-like* C-terminus, *PiAVR2* mutated dEER and *PiAVR2* V83G C-term were synthesised plus and minus a stop codon by GenScript USA Inc with the Gateway® attB site in place allowing the recombination of these genes into the pDONR201 entry vector with the BP Clonase® II kit.

**Table 2.1.1: *P. infestans* cloning primers**

| Gene | Primer name | Primer sequence |
|---|---|---|
| *PiAVR2*$^{N/K31}$ *-SP* | PiAVR2 For | 5'-AAAGCAGGCTTCACC**ATGCTGCATGCAGCTCCAGGTG**-3' |
| | PiAVR2 Rev | 5'-GAAAGCTGGGTC**TTAACTCCTCTTGTCACCCTTAAT**-3' |
| *PiAVR2* N-terminus | PiAVR2 For | 5'-AAAGCAGGCTTCACC**ATGCTGCATGCAGCTCCAGGTG**-3' |
| | PiAVR2 Nt Rev | 5'-GAAAGCTGGGTC**TTAACTCTCTTCCTCGATCTCAAA**-3' |
| *PiAVR2* C-terminus | PiAVR2 Ct For | 5'-AAAGCAGGCTTCACC**ATGGGATTCAGTCTGAAGGATAC**-3' |
| | PiAVR2 Rev | 5'-GAAAGCTGGGTC**TTAACTCCTCTTGTCACCCTTAAT**-3' |
| *PITG_08949 -SP* | 08949 For | 5'-AAAGCAGGCTTCACC**ATGTTGCATGCCGTC**-3' |
| | 08949 Rev | 5'-GAAAGCTGGGTC**TTATTTAATGGGATTGAG**-3' |
| attB sites | AttB1 For | 5'-GGGGACAAGTTTGTACAAAAAAGCAGGCTTCACC-3' |
| | AttB1 Rev | 5'-GGGGACCACTTTGTACAAGAAAGCTGGG-3' |

2.1.2 – *S. tuberosum* genes

*StBSL1*, *StBSL1* C-terminus, *StBSL2*, *StBSL3*, *StBIN2* and *StBSK2* were cloned from *S. tuberosum* cDNA using gene specific primers (Table 2.1.2). Due to the length of *StBSL1*, *StBSL2* and *StBSL3* internal sequencing primers were designed to ensure sequence integrity over the full length of the gene (Table 2.1.2). The resistance genes from the *R2-like* family were received from Vivianne Vleeshouwers in Wageningen University, The Netherlands. These were already cloned into plant expression vectors; however R2 was cloned out of this vector and placed in pDONR201 using the attB primers. Internal sequencing primers were generated to ensure the correct sequence was present in

subsequent recombinations (Table 2.1.2). Sequence analysis was conducted using the BioEdit software package.

**Table 2.1.2: *S. tuberosum* cloning and sequencing primers**

| Gene | Primer name | Purpose | Primer sequence |
|---|---|---|---|
| *StBSL1* | StBSL1 FL_F | Amplification | 5' AAAGCAGGCTTC**ATGGGTTCAAAGCCATGG** 3' |
| | StBSL1 FL _R | Amplification | 5' GAAAGCTGGGTA**TTAAATATAGGCAAGTGAGCT** 3' |
| | StBSL1 -ST_R | Amplification | 5' GAAAGCTGGGTA**AGCAATATAGGCAAGTGATCT** 3' |
| | StBSL1_F2 | Sequencing | 5' ATCTGGTAACTGTCAGTGGCA 3' |
| | StBSL1_R2 | Sequencing | 5' TGCTCAACTGAATTTATTGAC 3' |
| | StBSL1_F3 | Sequencing | 5' TCTGGTTGCAGAAAATTCTCC 3' |
| | | | |
| *StBSL1* C-terminus | StBSL1 C-term F | Amplification | 5' AAAGCAGGCTTC**ATGGTGAGGCAATTGTCA** 3' |
| | StBSL1 FL _R | Amplification | 5' GAAAGCTGGGTA**TTAAATATAGGCAAGTGAGCT** 3' |
| | | | |
| *StBSL2* | StBSL2 FL _F | Amplification | 5' AAAGCAGGCTTCACC**ATGGATGTGGATTCAACGATG** '3 |
| | StBSL2 FL _R | Amplification | 5'GAAAGCTGGGTC**TTAAGTCCAAGCAACAGAAC** '3 |
| | StBSL2_F1 | Sequencing | 5' CTAGGATGACCCCAATAGGA 3' |
| | StBSL2_F2 | Sequencing | 5' CTGTTTTTGTTAATGCTCGGC 3' |
| | StBSL2_R1 | Sequencing | 5' CCATAGTAATAGGGCGTTGGA 3' |
| | StBSL2_R2 | Sequencing | 5' TTAGGAACAGTGTTGATGGACA 3' |
| | | | |
| *StBSL3* | StBSL3 FL_F | Amplification | 5'AAAAAGCAGGCTGT**ATGGATGTGGATTCAACTATGGTATCGG** '3 |
| | StBSL3 FL_R | Amplification | 5'AGAAAGCTGGGT**CTAAGTCCAAGCAAAAGAACCTCGATCG** '3 |
| | StBSL3_5' Ra | Sequencing | 5' TTCCATAACTGACTCGCCGGCCTTC '3 |
| | StBSL3_5'Ra-F2 | Sequencing | 5' CCAGCTGGTTTGTCAG '3 |
| | StBSL3_5'Ra-R2 | Sequencing | 5' CCCAGTACAACAGAACCA 3' |
| | StBSL3_5'Ra-R3 | Sequencing | 5' ACCACCAAGTGCCCCTC 3' |
| | StBSL3_5'Ra-R4 | Sequencing | 5' GCACATCAGCAGAGCGG 3' |
| | StBSL3_orig Y2H section - F | Sequencing | 5' GGGATGGTGGAGCAGAGAC 3' |
| | StBSL3_orig Y2H section - R | Sequencing | 5' CTCAATCAGGGGAGCCAG 3' |
| | StBSL3_F1 | Sequencing | 5' TACTCTTCTCCTTGCTTTAAAGGTC '3 |
| | StBSL3_F2 | Sequencing | 5' TTCAACTAATAGTCCGTGCCCAC '3 |
| | | | |
| *StBIN2* | StBIN2GW_for: | Amplification | 5' AAAGCAGGCTTCACC**ATGATGGCTGATGATAAGGAGATG** '3 |
| | StBIN2GW+sc_Rev: | Amplification | 5' GAAAGCTGGGTC**TCACGTCATGTCACCGTGGG** '3 |
| | | | |
| *StBSK2* | StBSK2GW_for: | Amplification | 5' AAAGCAGGCTTCACC**ATGGGCTGTTTACAGTCC** '3 |
| | StBSK2GW+sc_Rev: | Amplification | 5' GAAAGCTGGGTC**TCAGTTACGCCAACTGTTTAAC** '3 |
| | | | |
| *StR2* | StR2_F1 | Sequencing | 5' GGCTGGTAAAGGTGCTAGTCG 3' |
| | StR2_F2 | Sequencing | 5' GAATGCAAATACCTTGTGGTG 3' |
| | StR2_F3 | Sequencing | 5' CTGACGGCTTCTTGAATG 3' |

## 2.2 – Generation of *S. tuberosum* sequence information

In order to design the gene specific primers for amplification of the *S. tuberosum* genes shown in Table 2.1.2 sequence information was first needed. This was generated for *StBSL2*, *StBIN2* and *StBSK2* by using the *A. thaliana* gene sequence from the TAIR database and searching the *S. tuberosum* cv. *phureja* genome database. The database searched for the *S. tuberosum* cv. *phureja* sequences was version 3.4 which was downloaded from the following webpage ftp://ftp.plantbiology.msu.edu/pub/sgr/other/. Best BLAST hits (BBH) were found for *StBSL2*, *StBIN2* and *StBSK2* by using the following method:

1. BLASTX *A. thaliana* data against the *S. phureja* database, finding the most similar sequence in each case.
2. Generate a multiple FASTA file of these similar sequences, and BLASTP them against the *A. thaliana* database, finding the most similar sequence in each case.
3. Accession numbers of these similar sequences were compared to the original set used in the BLASTX. If the reciprocal blast sequence matches the original *A. thaliana* gene then a BBH has been generated.

*StBSL1* sequence information to allow primer design was generated by using the *A. thaliana BSL1* nucleotide sequence to search The Gene Index Project *Solanum lycopersicum* database in April 2009. This yielded a full length EST (TC194541 TC187939) for *SlBSL1*.

*StBSL3* sequence information was generated by sequencing the Y2H interactor which generated the 3' end of the gene and by using a 5' RACE. Sequencing of the 3' end was undertaken as described in Armstrong *et al.*, (2005) and Gilroy *et al.*, (2007) using the sequencing primers StBSL3_F1 and StBSL3_F2 (Table 2.1.2). This generated sequence

information for the end of the gene allowing the design of the reverse amplification primer. 5' RACE was carried out following the SMART™ RACE cDNA Amplification Kit manual from Clontech (Clontech, France). The 5' RACE product was dA tailed using the following mix – purified 5' RACE product, 10x molecular Taq buffer, 2mM dATP, molecular Taq polymerase and sterile distilled water, incubated at 72°C for 30 min. This product was then ligated to pGEM-T easy overnight at 4°C following the Promega protocol (Promega, Southampton, UK) and transformed into DH10B electrocompetent *E. coli* cells before being plated on LB AIX. Clones were sequenced using the 5' RACE primer, StBSL3_5' Ra (Table 2.1.2) and M13F primer (Table 2.6.2) for the pGEM-T easy vector. These allowed the whole potato sequence of *StBSL3* to be generated and a primer for the beginning of the gene to be designed for amplification of this gene.

## 2.3 – Blast and phylogenetic analysis

*StBSL* genes amplified from *S. tuberosum* cDNA were used to search the TAIR website. The BLASTN tool was used to search the TAIR10 database with the coding sequence of the amplified genes. This BLASTN search used the default setting with one exception, the nucleotide mismatch was changed from the default of -3 to -1. The BLASTX tool was also used to search the TAIR10 database; this time the default settings were used. The percentage coverage and percentage identities were calculated from the Blast outputs.

Percentage coverage - The percentage identities taken for each high scoring pair (HSP). The number of base pairs or amino acids per HSP is totalled and divided by the length of the query, for example: percentage identities for each HSP - 641/786, 578/726, 17/17

Query sequence length is: 2637 letters

Percentage coverage = ((786+726+17)/2637)*100 = 58%

Percentage identities – Total the number of identities for each HSP and this is divided by the total number of base pairs or amino acids covered, for example: percentage identities for each HSP - 641/786, 578/726, 17/17

Total identities is 641 + 578 + 17 = 1236

Total coverage is 786+726+17 = 1529

Percentage identities = (1236/1529)*100 = 81%

The protein sequences for all St and AtBSLs and AtPP2B'alpha were aligned using the software package T-COFFEE; this protein alignment was then back-translated to the nucleotide sequences using the original coding sequences as a scaffold in T-COFFEE. These nucleotide and protein alignments were imported into TOPALi v2.5 for phylogenetic analysis. Maximum likelihood trees were generated with a bootstrap of 100 on the full length of the nucleotide and protein alignments. The trees were then imported into FigTree in order to re-root them to the outlier AtPP2B'alpha.

Smaller alignments, that contain only a few sequences for visual comparison are shown in the results sections, these were generated using the software package BioEdit.

## 2.4 – *R* gene / *AVR* gene recognition in *N. benthamiana and S. tuberosum*

*Agrobacterium tumefaciens* cultures were grown for 2 days, with shaking at 27°C in Luria-Bertani (LB) broth with the designated antibiotic (Table 2.4.1).

*N. benthamiana* recognition experiment:

The cultures were diluted to an $OD_{600}$ of 1.5 for the *R* genes and $OD_{600}$ of 0.75 for the *AVR* gene using a 10 mM $MgCl_2$ 10 mM 2-[morpholino]ethanesulfonic acid (MES) solution. The

two cultures were mixed in a 1:1 ratio to give a final $OD_{600}$ of 0.75 for the *R* genes and 0.375 for the *AVR* genes. A final concentration of 200 nM of acetosyringone was added to each culture and they were incubated at room temp in the dark for 3-4 h. Wild-type and VIGS *N. benthamiana* were used for these experiments.

*S. tuberosum* recognition experiments:

*AVR* cultures that were infiltrated into potato cultivars which naturally express an *R* gene were not mixed with *R* genes. A final $OD_{600}$ of 0.3 was used for the *AVR* gene with a final concentration of 200 nM of acetosyringone added to each culture which were incubated at room temp in the dark for 3-4 h before infiltration.

For infiltration the underside of the leaf was scored using a needle and the *Agrobacterium* infiltrated into the leaf using a 1 ml syringe to make a circular infiltration site. Leaves were left for 6 dpi before HRs were counted.

**Table 2.4.1: *A. tumefaciens* cultures used for recognition assays**

| ***PiAVR2* Alleles** | **Agrobacterium Strain** | **Vector** | **Antibiotic/ Antifungals** | **Working Concentration in Cultures** |
|---|---|---|---|---|
| *PiAVR2*$^{N31}$ | AGL1:pVIRG:pSOUP | pGRAB | Kanamycin<br>Chloramphenicol<br>Rifampicin<br>Tetracycline | Kan - 50 µg/ml<br>Chlor – 25 µg/ml<br>Rif - 50 µg/ml |
| *PiAVR2*$^{K31}$ | AGL1:pVIRG:pSOUP | pGRAB | Kanamycin<br>Chloramphenicol<br>Rifampicin<br>Tetracycline | Kan - 50 µg/ml<br>Chlor – 25 µg/ml<br>Rif - 50 µg/ml |
| *PiAVR2 C-terminal* | AGL1:pVIRG:pSOUP | pGRAB | Kanamycin<br>Chloramphenicol<br>Rifampicin<br>Tetracycline | Kan - 50 µg/ml<br>Chlor – 25 µg/ml<br>Rif - 50 µg/ml |
| *PiAVR2 N-terminal* | AGL1:pVIRG:pSOUP | pGRAB | Kanamycin<br>Chloramphenicol<br>Rifampicin<br>Tetracycline | Kan - 50 µg/ml<br>Chlor – 25 µg/ml<br>Rif - 50 µg/ml |
| *PiAVR2-like* | AGL1:pVIRG:pSOUP | pGRAB | Kanamycin<br>Chloramphenicol<br>Rifampicin<br>Tetracycline | Kan - 50 µg/ml<br>Chlor – 25 µg/ml<br>Rif - 50 µg/ml |
| *PiAVR2-like C-terminal* | AGL1:pVIRG:pSOUP | pGRAB | Kanamycin<br>Chloramphenicol<br>Rifampicin<br>Tetracycline | Kan - 50 µg/ml<br>Chlor – 25 µg/ml<br>Rif - 50 µg/ml |

| | | | | |
|---|---|---|---|---|
| *PiAVR2 mutated dEER* | AGL1:pVIRG:pSOUP | pGRAB | Kanamycin<br>Chloramphenicol<br>Rifampicin<br>Tetracycline | Kan - 50 µg/ml<br>Chlor – 25 µg/ml<br>Rif - 50 µg/ml |
| *PiAVR2 V83G C-term* | AGL1:pVIRG:pSOUP | pGRAB | Kanamycin<br>Chloramphenicol<br>Rifampicin<br>Tetracycline | Kan - 50 µg/ml<br>Chlor – 25 µg/ml<br>Rif - 50 µg/ml |
| *PITG_08949* | AGL1:pVIRG:pSOUP | pGRAB | Kanamycin<br>Rifampicin<br>Tetracycline | Kan - 50 µg/ml<br>Rif - 50 µg/ml |
| *PiAVR3a$^{KI}$* | AGL1:pVIRG:pSOUP | pGRAB | Kanamycin<br>Rifampicin<br>Tetracycline | Kan - 50 µg/ml<br>Rif - 50 µg/ml |
| *Pilpio1* | AGL1:pVIRG:pSOUP | pGRAB | Kanamycin<br>Chloramphenicol<br>Rifampicin<br>Tetracycline | Kan - 50 µg/ml<br>Rif - 50 µg/ml |
| *PVX-CP* | GV3101 | pBIN61 | Kanamycin<br>Rifampicin<br>Gentamycin | Kan - 50 µg/ml<br>Rif - 50 µg/ml |
| | | | | |
| ***R* Gene Alleles** | | | | |
| *R2* | AGL1:pVIRG:pSOUP | pDEST-KGW | Ampicillin<br>Tetracycline<br>Chloramphenicol<br>Spectinomycin<br>Rifampicin | Spec – 100 µg/ml<br>Chlor – 25 µg/ml<br>Rif - 50 µg/ml |
| *R2-like* | AGL1:pVIRG:pSOUP | pDEST-KGW | Ampicillin<br>Tetracycline<br>Chloramphenicol<br>Spectinomycin<br>Rifampicin | Spec – 100 µg/m<br>Chlor – 25 µg/ml<br>Rif - 50 µg/ml |
| *Blb3* | AGL1:pVIRG:pSOUP | pDEST-KGW | Ampicillin<br>Tetracycline<br>Chloramphenicol<br>Spectinomycin<br>Rifampicin | Spec – 100 µg/ml<br>Chlor – 25 µg/ml<br>Rif - 50 µg/ml |
| *Abpt* | AGL1:pVIRG:pSOUP | pDEST-KGW | Ampicillin<br>Tetracycline<br>Chloramphenicol<br>Spectinomycin<br>Rifampicin | Spec – 100 µg/ml<br>Chlor – 25 µg/ml<br>Rif - 50 µg/ml |
| *Rpi-edn1.1* | AGL1:pVIRG:pSOUP | pKGW-MGW | Tetracycline<br>Chloramphenicol<br>Spectinomycin<br>Rifampicin | Spec – 100 µg/ml<br>Chlor – 25 µg/ml<br>Rif - 50 µg/ml |
| *Rpi-snk1.1* | AGL1:pVIRG:pSOUP | pKGW-MGW | Tetracycline<br>Chloramphenicol<br>Spectinomycin<br>Rifampicin | Spec – 100 µg/ml<br>Chlor – 25 µg/ml<br>Rif - 50 µg/ml |
| *Rpi-snk1.2* | AGL1:pVIRG:pSOUP | pKGW-MGW | Tetracycline<br>Chloramphenicol<br>Spectinomycin<br>Rifampicin | Spec – 100 µg/ml<br>Chlor – 25 µg/ml<br>Rif - 50 µg/ml |
| *Rpi-hjt1.1* | AGL1:pVIRG:pSOUP | pKGW-MGW | Tetracycline<br>Chloramphenicol<br>Spectinomycin<br>Rifampicin | Spec – 100 µg/ml<br>Chlor – 25 µg/ml<br>Rif - 50 µg/ml |
| *Rpi-hjt1.2* | AGL1:pVIRG:pSOUP | pKGW-MGW | Tetracycline<br>Chloramphenicol<br>Spectinomycin<br>Rifampicin | Spec – 100 µg/ml<br>Chlor – 25 µg/ml<br>Rif - 50 µg/ml |

| | | | | |
|---|---|---|---|---|
| *Rpi-hjt1.3* | AGL1:pVIRG:pSOUP | pKGW-MGW | Tetracycline<br>Chloramphenicol<br>Spectinomycin<br>Rifampicin | Spec – 100 µg/ml<br>Chlor – 25 µg/ml<br>Rif - 50 µg/ml |
| *R3a* | AGL1:pVIRG:pSOUP | pGRAB | Kanamycin<br>Rifampicin<br>Tetracycline | Kan - 50 µg/ml<br>Rif - 50 µg/ml |
| *Sto1* | AGL1:pVIRG | pBIN | Kanamycin<br>Rifampicin | Kan - 50 µg/ml<br>Rif - 50 µg/ml |
| *Rx-HA* | GV3101 | pBINpBI | Kanamycin<br>Rifampicin<br>Gentamycin | Kan - 50 µg/ml<br>Rif - 50 µg/ml |

## 2.5 - Western blots

*A. tumefaciens* cultures were grown for 2 days, with shaking, at 27°C in Luria-Bertani (LB) broth with the designated antibiotic (Table 2.5.1). A final $OD_{600}$ of 0.25 or 0.4 was used for the genes of interest and a final $OD_{600}$ of 0.01 for P19 (a silencing suppressor) in a 2:1 ratio. The whole leaf was infiltrated with culture to allow 1 cm leaf discs to be cut out at 3 dpi. The GFP positive control was extracted from an endoplasmic reticulum GFP tagged transgenic plant, CB28. There were two different protein extraction methods used for the western blots. The extraction method using protein extraction buffer was used on the GFP tagged proteins, while the split YFP and YFP_StR2 vectors used the 2x SDS loading buffer to extract the proteins directly.

Protein extraction buffer - method used on GFP tagged proteins:

One leaf disc was used for this protein extraction protocol.

**Protein extraction buffer:** 20 mM 4-(2-hydroxyethyl)-1-piperazineethanesulfonic acid (HEPES), 13% sucrose, 1 mM EDTA, 1 mM DTT, proteinase inhibitor cocktail tablet, 0.1% Triton. The DTT, Triton x100 and proteinase inhibitor cocktail tablet (Roche, West Sussex) were added fresh each time.

A leaf disc of ~100 mg was ground in liquid $N_2$, 200 µl extraction buffer was added and left to thaw on ice. 20 µl of the whole lysate was mixed with 20 µl 2x SDS loading buffer. Samples were boiled for 5 min at 95°C.

No extraction buffer – method used on split YFP and YFP samples:

Two, 1 cm diameter leaf discs were used. ~200 mg of leaf material was ground in liquid $N_2$, 200 µl of 2x SDS loading buffer was added and samples were directly boiled for 10 min at 95°C. Samples were cooled on ice before centrifuging at 13,000 rpm [17,900g] for 5 min.

Samples were loaded onto a 12% or gradient 4–12% Bis-Tris NuPAGE® Novex® Mini gel (Invitrogen, Paisley, UK) and this was run at 200 V, 120 mA and 25 W for 1 h; the blotting was done (Sambrook et al., 1989) for 1 h at 130 V. 4% milk was used to block the membrane. The primary antibodies were monoclonal mouse GFP antibody from (Sigma-Aldrich, Dorset, UK), monoclonal rabbit myc antibody (Sigma-Aldrich, Dorset, UK), and a monoclonal rabbit HA antibody (Sigma-Aldrich, Dorset, UK). All primary antibodies were used at 1:1000 dilution. PBS-T 0.1% was used to wash the membrane before addition of the secondary antibody. The secondary antibodies were a goat antimouse Ig horseradish peroxidase and a goat antirabbit Ig horseradish peroxidase (Sigma-Aldrich, Dorset, UK) used at 1:5000 dilution. Phosphate Buffered Saline with Tween (PBS-T) 0.1% was used to wash the membrane before addition of the ECL Detection Reagents. ECL Plus Western Blotting Detection Reagents (GE Healthcare, Hertfordshire, UK) were used for detection; the reagents were used as directed in the manufacturer's instructions.

**Table 2.5.1: *A. tumefaciens* cultures used for western blots**

| Proteins and Tags | Agrobacterium Strain | Vector | Antibiotic/ Antifungals | Working Concentration in Cultures |
|---|---|---|---|---|
| PiAVR2$^{N31}$-GFP | AGL1:pVIRG | pB7FWG2,0 | Rifampicin<br>Spectinomycin<br>Chloramphenicol | Rif - 50 µg/ml<br>Spec – 100 µg/ml<br>Chlor – 25 µg/ml |
| PiAVR2$^{K31}$-GFP | AGL1:pVIRG | pB7FWG2,0 | Rifampicin<br>Spectinomycin<br>Chloramphenicol | Rif - 50 µg/ml<br>Spec – 100 µg/ml<br>Chlor – 25 µg/ml |
| PiAVR2 C-terminal -GFP | AGL1:pVIRG | pB7FWG2,0 | Rifampicin<br>Spectinomycin<br>Chloramphenicol | Rif - 50 µg/ml<br>Spec – 100 µg/ml<br>Chlor – 25 µg/ml |
| PiAVR2 N-terminal -GFP | AGL1:pVIRG | pB7FWG2,0 | Rifampicin<br>Spectinomycin<br>Chloramphenicol | Rif - 50 µg/ml<br>Spec – 100 µg/ml<br>Chlor – 25 µg/ml |
| PiAVR2-like-GFP | AGL1:pVIRG | pB7FWG2,0 | Rifampicin<br>Spectinomycin<br>Chloramphenicol | Rif - 50 µg/ml<br>Spec – 100 µg/ml<br>Chlor – 25 µg/ml |
| PiAVR2-like C-terminal | AGL1:pVIRG | pB7FWG2,0 | Rifampicin<br>Spectinomycin<br>Chloramphenicol | Rif - 50 µg/ml<br>Spec – 100 µg/ml<br>Chlor – 25 µg/ml |
| PITG_08949-GFP | AGL1:pVIRG | pB7FWG2,0 | Rifampicilin<br>Spectinomycin<br>Chloramphenicol | Rif - 50 µg/ml<br>Spec – 100 µg/ml<br>Chlor – 25 µg/ml |
| | | | | |
| YN-PiAVR2$^{N31}$ | AGL1:pVIRG | CL112 | Rifampicin<br>Spectinomycin<br>Chloramphenicol | Rif - 50 µg/ml<br>Spec – 100 µg/ml<br>Chlor – 25 µg/ml |
| YN-PiAVR2$^{K31}$ | AGL1:pVIRG | CL112 | Rifampicin<br>Spectinomycin<br>Chloramphenicol | Rif - 50 µg/ml<br>Spec – 100 µg/ml<br>Chlor – 25 µg/ml |
| YN-PiAVR2 C-terminal | AGL1:pVIRG | CL112 | Rifampicin<br>Spectinomycin<br>Chloramphenicol | Rif - 50 µg/ml<br>Spec – 100 µg/ml<br>Chlor – 25 µg/ml |
| YN-PiAVR2-like | AGL1 | CL112 | Rifampicin<br>Spectinomycin | Rif - 50 µg/ml<br>Spec – 100 µg/ml |
| YN-PiAVR2-like C-terminal | AGL1 | CL112 | Rifampicilin<br>Spectinomycin | Rif - 50 µg/ml<br>Spec – 100 µg/ml |
| YN-PITG_08949 | AGL1:pVIRG | CL112 | Rifampicin<br>Spectinomycin<br>Chloramphenicol | Rif - 50 µg/ml<br>Spec – 100 µg/ml<br>Chlor – 25 µg/ml |
| YN-StR2 | AGL1:pVIRG | CL112 | Rifampicin<br>Spectinomycin<br>Chloramphenicol | Rif - 50 µg/ml<br>Spec – 100 µg/ml<br>Chlor – 25 µg/ml |
| YN-StR3a | AGL1 | CL112 | Rifampicin<br>Spectinomycin | Rif - 50 µg/ml<br>Spec – 100 µg/ml |
| YC-StBSL1 | AGL1 | CL113 | Rifampicin<br>Spectinomycin | Rif - 50 µg/ml<br>Spec – 100 µg/ml |
| | | | | |
| YFP-StR2 | AGL1:pVIRG | pB7WGY2,0 | Rifampicin<br>Spectinomycin<br>Chloramphenicol | Rif - 50 µg/ml<br>Spec – 100 µg/ml<br>Chlor – 25 µg/ml |
| p19 | AGL1 | pJL3 | Kanamycin | Kan - 50 µg/ml |

## 2.6 – Yeast 2 Hybrid and cloning of interactor

### 2.6.1 - Yeast Two Hybrid library screen

This experiment used the Invitrogen Pro-Quest™ System (Invitrogen, Paisley, UK). The initial screen used the Forward-Two-Hybrid Library Screen as per the manufacturer's instructions. The potato library used was made from pooled, pathogen challenged resistant and susceptible potato cultivars (Bos *et al.,* 2010). The library was also generated by Invitrogen (Invitrogen, Paisley, UK). The bait protein used in the initial screen contained PiAVR2$^{N31}$. Pro-Quest™ indicates the use of sheared salmon sperm DNA when transforming the yeast; herring sperm DNA was used as an alternative. Transformed cells were plated out on synthetic complete media lacking Leucine (Leu) and Tryptophan (Trp). After 3 days colonies were picked from these plates to test interactions on the reporter gene assays. The reporter genes were *HIS3, LacZ* and *URA3*.

Plasmid was extracted from yeast colonies, using the Zymoprep protocol from Zymo Research (Zymo Research, Cambridge, UK), for the colonies that showed activation of at least two of the three reporter gene assays. These plasmids were then transformed into electro-competent DH10B *E. coli* cells. To distinguish between the bait and prey plasmids that were extracted, the transformed cells were plated out on both LB ampicillin and LB gentamicin. The individual bait and prey plasmids were then purified from the *E. coli* cells using the Qiagen QIAprep® Miniprep Spin protocol (Qiagen, Crawley, UK) with the following change. Once the cultures had grown, the cells were scraped off LB plates using 1 ml of sterile distilled water and then centrifuged for 4 min at 8,000 rpm. The plasmids were sequenced with the Prey and Bait F and Prey R primers shown in Table 2.6.1 and previously described in Armstrong *et al.,* (2005); Gilroy *et al.,* (2007).

**Table 2.6.1: Primers for Y2H**

| Primer Name | Plasmid it sequences | Primer Sequence |
|---|---|---|
| Prey F | pDEST22 | 5' TATAACGCGTTTGGAATCACT '3 |
| Prey R | pDEST22/pDEST32 | 5' AGCCGACAACCTTGATTGGAGAC '3 |
| Bait F | pDEST32 | 5' AACCGAAGTGCGCCAAGTGTCTG '3 |

## 2.6.2 – Specific Yeast Two Hybrid screens

To confirm that the interactions detected in the initial library screen were genuine; specific transformations were carried out using the small scale yeast transformation protocol from the Pro-Quest™ manual (Invitrogen, Paisley, UK). This small scale yeast transformation protocol was also used to determine the interaction of other genes of interest from the BR pathway. The full length of StBSL1, StBSL2a (formally StBSL3) and StBSL2b (formally StBSL2) were cloned into both bait and prey vectors to determine interaction with the PiAVR2 forms, and between the phosphatases themselves i.e. StBSL1-StBSL2a, StBSL1-StBSL2b etc. StR2 was also cloned into the bait and prey vectors to determine interaction with the PiAVR2 forms and the StBSLs. Finally StBSK2 and StBIN2 were cloned into the bait and prey vectors to determine interaction with the StBSLs.

**Table 2.6.2: Genes in Y2H vectors**

| Gene | Vector |
|---|---|
| *PiAVR2$^{N31}$* | pDEST32 |
| *PiAVR2$^{K31}$* | pDEST32 |
| *PiAVR2 C-terminal* | pDEST32 |
| *PiAVR2 N-terminal* | pDEST32 |
| *PiAVR2-like* | pDEST32 |
| *PiAVR2-like C-terminal* | pDEST32 |
| *PITG_08949* | pDEST32 |
| *StBSL1* | pDEST22/pDEST32 |
| *StBSL1 C-term* | pDEST22 |
| *StBSL2a* | pDEST22/pDEST32 |
| *StBSL2a C-term* | pDEST22 |
| *StBSL2b* | pDEST22/pDEST32 |
| *StBSK2* | pDEST22/pDEST32 |
| *StBIN2* | pDEST22/pDEST32 |
| *StR2* | pDEST22/pDEST32 |

## 2.7 - Virus Induced Gene Silencing (VIGS)

ESTs from *Nicotiana tabacum, Solanum lycopersicum* and *Solanum tuberosum* along with full length sequence information on *StBSL1* and *StBSL2a* (formerly *StBSL3)* were used to design primers to generate silencing constructs for *NbBSL1*, *2a* and *2b* in *N. benthamiana*. The protocol for this is described in Gilroy *et al*. (2007). Two silencing constructs were generated for *BSL1* (*5'BSL1* and *3'BSL1*), two constructs were generated for *BSL2a* (*5'BSL2a* and *3'BSL2a*), and one construct for *BSL2b* (*BSL2b*). For *BSL1* and *BSL2a,* the *5'BSL1* and *5'BSL2a* constructs were designed at the 5' end of the gene; all other constructs including the *BSL2b* construct were designed at the 3' end of the gene in the phosphatase domain. All primers for the VIGS constructs had restriction sites for *EcoRI* on the forward primer and *HpaI* on the reverse primer plus an extra 4 base pairs for digestion out of pGEM-T easy plasmid (Table 2.7.1). Pooled *N. benthamiana* cDNA was used as template for the amplification of the PCR product. The PCR product was ligated to the pGEM-T easy plasmid as per manufacuters instructions and sequenced to ensure amplification of the correct portion of DNA (Table 2.7.2). The *EcoRI* and *HpaI* restriction sites allowed digestion of the correct construct out of pGEM-T easy plasmid and ligation into the Tobacco Rattle Virus (TRV) RNA2 plasmid. The TRV RNA2 plasmid was also sequenced to determine if it contained the correct DNA construct (Table 2.7.2). Plasmids that contained the correct sequences were transformed into *A. tumefaciens* strain LBA4404. In these VIGS experiments a BAK1 construct previously published by Hesse *et al* was also used (Heese *et al*., 2007). Another VIGS construct for BRI1 was also used that had previously been designed by a visiting PhD student (Ana Confraria, University of Bristol, UK). This was previously generated in potato virus X (PVX) so for these experiments it was cloned out of PVX and recombined into TRV.

**Table 2.7.1: Primers for amplification of VIGS constructs**

| Primer Name | What it sequences | Primer Sequence |
|---|---|---|
| VIGS 5' BSL1 F | For 5' BSL1 VIGS construct | 5' TAAAGAATTCATGGGTTCAAAGCCAT '3 |
| VIGS 5' BSL1 R | For 5' BSL1 VIGS construct | 5' TTTTGTTAACTCACCGGCAGGTCTAAGT '3 |
| VIGS 3' BSL1 F | For 3' BSL1 VIGS construct | 5' ATTTGAATTCTGCATTGAGAGAATCCCACA '3 |
| VIGS 3' BSL1 R | For 3' BSL1 VIGS construct | 5' TTTAGTTAACACGATCAGGCCCAAATGTTA '3 |
| VIGS 5' BSL3 F | For 5' BSL2a VIGS construct | 5' TATTGAATTCGTAGTCCTGCTGTTGGGG '3 |
| VIGS 5' BSL3 R | For 5' BSL2a VIGS construct | 5' TTTTGTTAACTCTCCAATGGGAGTGATC '3 |
| VIGS 3' BSL3 F | For 3' BSL2a VIGS construct | 5' TATAGAATTCAGAGATGGAATCTGGGCTTG '3 |
| VIGS 3' BSL3 R | For 3' BSL2a VIGS construct | 5' AAAAGTTAACTCATTGTTGTTGCAAAATTCC '3 |
| VIGS BSL2 F | For BSL2b VIGS construct | 5' TTTTGAATTCCATCACCGTGCTGTGGTTAT '3 |
| VIGS BSL2 R | For BSL2b VIGS construct | 5' TTAAGTTAACACTCGCAAATATCCTTTCAGC '3 |
| BRI1TRVEcoRI | For BRI1 VIGS construct | 5' TTTTGAATTCTGCTGGAGTTGGAG '3 |
| BRI1TRVHpa1RI | For BRI1 VIGS construct | 5' TTAAGTTAACAATCATACCAGACAG '3 |

GAATTC = *EcoRI* restriction site; GTTAAC = *HpaI* restriction site

**Table 2.7.2: Primers for the sequencing of the VIGS plasmids**

| Primer Name | What it sequences | Primer Sequence |
|---|---|---|
| M13 F | Sequencing the pGEM-T vector | 5' CCCAGTCACGACGTTGTAAAACG '3 |
| M13 R | Sequencing the pGEM-T vector | 5' AGCGGATAACAATTTCACACAGG '3 |
| TRV250 | Sequencing the TRV vector | 5' GAGCATAATTATACTGATTT '3 |
| TRV300 | Sequencing the TRV vector | 5' CGAGAATGTCAATCTCGTAGG '3 |

The VIGS itself was performed in 2 week old *N. benthamiana*, on both wild-type and *NahG* transgenic lines. *A. tumefaciens* cultures were grown for 2 days at 27°C with 50 µg/ml kanamycin and rifampicin along with 6 mM $MgSO_4$ including a culture which contained the TRV RNA1 plasmid. All cultures were grown to an $OD_{600}$ of 1, all RNA2 cultures were mixed 1:1 with the TRV RNA1 giving a final $OD_{600}$ of 0.5 for each. A final concentration of 200 nM of acetosyringone was added to each culture and they were incubated at room temp in the dark for 3-4 h. The two oldest leaves of each plant were scored with a needle and the inoculum (RNA1 and RNA2) was infiltrated into the whole leaf. The plants were left for 2-3 weeks for silencing to spread systemically.

## 2.8 – RNA extractions

RNA extractions were done using the Qiagen RNeasy® Plant Mini Kit (Qiagen, Crawley, UK) following the protocol for either plant material or filamentous fungi. For plant extraction, frozen leaf material was ground in mortar and pestle using liquid nitrogen until a

fine powder was generated. 100 mg of leaf material was used for extraction following the manufacturer's instructions. The optional on column DNaseI treatment was used, again following the manufacturer's instructions.

For oomycete extraction germinating cysts were harvested and ground using a mortar and pestle frozen using liquid nitrogen. The RNA extraction was carried out following the manufacturer's instructions. DNA contamination was minimised using the TURBO DNA-free™ Kit from Applied Biosystems (Applied BioSystems, Paisley, UK) following the manufacturer's instructions.

## 2.9 – PCR-based methods

### 2.9.1 – General PCR method

For general PCR amplification Go Taq Flexi polymerase from Promega was used (Promega, Southampton, UK).

### 2.9.2 – Semi-quantitative Reverse Transcriptase PCR (RT-PCR)

Six isolates of *P. infestans* were inoculated on potato cv. binjte leaves as described in Section 2.11. RNA was extracted as described in Section 2.8. The quality and quantity of the RNA was determined using a Nanodrop® ND-1000 spectrophotometer (Labtech International, Lewes, UK). cDNA was synthesised using SuperScript™ II RT following the manufacturer's instructions (Invitrogen, Paisley, UK).

Primers were designed to distinguish between PiAVR2$^{N/K31}$ and PiAVR2-like (Table 2.9.1). Semi-quantitative RT-PCR was undertaken using Go Taq® Flexi polymerase (Promega,

Southampton, UK). The following PCR protocol was used: 92°C for 5 min, 40 cycles of 92°C for 40 s, 60°C for 40 s, 72°C for 40 s and a final incubation at 72°C for 10 min.

**Table 2.9.1: Diagnostic PiAVR2 primers**

| Primer Name | Amplifies | Primer Sequence |
|---|---|---|
| PiAVR2 F4 | Avirulent PiAVR2 | 5' ATGCGTCTCG CCTACATTTT '3 |
| PiAVR2 R4 | Avirulent PiAVR2 | 5' TGTCACCCTTAATTTCAAATGC '3 |
| avr2diagF1 | PiAVR2-like | 5' CCGCCCCAAGCCGCATG '3 |
| avr2diagR1 | PiAVR2-like | 5' TGTTACCCTTACTTTGTAAATAG '3 |

2.9.3 – qRT-PCR of PiAVR2_IR silenced line

PiAVR2_IR *P. infestans* isolates were generated as described in (Bos *et al.*, 2010) using the full length *PiAVR2* gene. RNA was extracted from germinating cysts following the Qiagen RNeasy® Plant Mini Kit following the protocol for filamentous fungi (Qiagen, Crawley, UK). The TURBO DNA-free™ Kit (Applied BioSystems, Paisley, UK) was used to remove any contaminating DNA. cDNA was synthesised using SuperScript™ II RT following the manufacturer's instructions (Invitrogen, Paisley, UK). The primers used are shown in Table 2.9.2 and amplify both PiAVR2 and PiAVR2-like; primers for the endogenous control Actin are also shown, all primers were previously optomised by Eleanor Gilroy. The qRT-PCRs were carried out using the Power SYBR® Green PCR Master Mix (Applied BioSystems, Paisley, UK) on the Chromo4 qRT-PCR machine (BIORAD, Hempstead, UK). The following PCR conditions were used: 1. 95°C for 15 min 2. 95°C for 15 s 3. 61°C for 1 min 4. read plate, repeat protocol from step two for 39 more cycles. After completion of the PCR the melting curve was analysed for each well.

**Table 2.9.2: PiAVR2 qRT-PCR primers**

| Primer Name | Primer Sequence | Concentration |
|---|---|---|
| Qrt7987Elli-for | 5' ACCCTGAAGAAGCTCAATCC '3 | 300 nM |
| Qrt7987Elli-rev | 5' CTTTTCCGTGACCTCTTTAGC '3 | 300 nM |
| ACTAF2 | 5' CATCAAGGAGAAGCTGACGTACA '3 | 300 nM |
| ACTAR2 | 5' GACGACTCGGCGGCAG '3 | 300 nM |

2.9.4 – qRT-PCR verification of VIGS

RNA was extracted as described in section 2.8.2, The cDNA was synthesised using SuperScript™ III First-Strand Synthesis SuperMix for qRT-PCR following the manufacturer's instructions (Invitrogen, Paisley, UK). This kit uses both oligo dT primers and random hexamers.

qRT-PCR primers were designed based on the *StBSL1* and *StBSL2a* (formerly *StBSL3*) full length sequence information and for *StBSL2b* (formerly *StBSL2*) based on *S. lycopersicum* and *S. tuberosum* EST data. Multiple primer pairs were designed based on the *StBSL* sequence information; however they were not specific enough for the qRT-PCR on the *N. benthamiana* cDNA. These primers are shown in Table 2.9.4, primer names used old naming BSL3 = BSL2a, BSL2 = BSL2b. These primer pairs were more specific for *S. tuberosum* cDNA.

qRT-PCR primers were designed for *NbBSL1*, *NbBSL2a* and *NbBSL2b* to determine the silencing levels in the VIGS plants. In order to generate sequence information from *N. benthamiana* to allow primer design, amplification of *NbBSLs* was needed. PCR amplification of the full length *NbBSL* genes failed when using the *StBSL* amplification primers (Table 2.1.2). The full length *NbBSL* sequences could not be amplified but sequence information was generated using a combination of the amplification and sequencing primers for each of the *StBSL* genes. A 1.5 kb section of *NbBSL1* was amplified using the StBSL1 F3 sequencing primer and StBSL1 R amplification primer (Table 2.1.2). A 1.8 kb section of *NbBSL2b* was amplified using the StBSL2 F amplification primer and StBSL2 R2 sequencing primer (Table 2.1.2). A 2.5 kb section of *NbBSL2a* was amplified using the StBSL3 5'Ra F2 sequencing primer and the StBSL3 R amplification primer (Table 2.1.2). This sequence information generated for the three *NbBSL* genes only had sections of overlap between all three. Between *NbBSL2a* and

*NbBSL2b* there was a 1.3 kb section of overlapping sequence and for *NbBSL1* and *NbBSL2a* there was a 1.5 kb section of overlap, but for *NbBSL1*, *NbBSL2a* and *NbBSL2b* there was only a 400 bp overlap. Although this limited the region where primer design could occur there was a large amount of difference between the *NbBSL1* and the *NBBSL2a* and *2b* genes. This sequence information was used to design multiple primer pairs for the *N. benthamiana* qRT-PCR. The primers were designed outside the areas used for silencing using the Primer3 software (http://frodo.wi.mit.edu/) following the Applied Biosystems guideline for qRT_PCR primer design. All primer pairs for use on *N. benthamiana* cDNA worked well but only one pair for each BSL gene was used to generate the graphs in the results chapters. These are listed in Table 2.9.3, the rest are listed in Table 2.9.4 with the primers designed based on the *S. tuberosum* sequence (primer names are using old naming BSL3 = BSL2a, BSL2 = BSL2b). The unpublished qRT-PCR primers designed by Ana Confraia were used to determine the silencing levels within the TRV::BRI1 samples and the primers used for the endogenous control gene 25s ribosomal RNA are also shown (Table 2.7.3). The qRT-PCR followed the methods described above in section 2.8.3.

**Table 2.9.3: VIGS qRT-PCR primers for silencing levels**

| Primer Name | Primer Sequence | Concentration |
|---|---|---|
| NbBSL1_F2 qRT-PCR | 5' CCATCTGGTGGGTTGAGC '3 | 300 nM |
| NbBSL1_R1 qRT-PCR | 5' GCTTCAGCAGCAAAATCCTT '3 | 300 nM |
| NbBSL3_F1 qRT-PCR | 5' GCAGCATCTAATATGCAAGAAGGA '3 | 300 nM |
| NbBSL3_R2 qRT-PCR | 5' GTGCAACAGGATTTCCCAAT '3 | 300 nM |
| NbBSL2_F1 qRT-PCR | 5' GAGTATAGCAGGAAGGTATGGGTTT '3 | 300 nM |
| NbBSL2_R1 qRT-PCR | 5' AGCCATCATTAACTACCTCAGGTT '3 | 300 nM |
| BRI1_F qRT-PCR | 5' GCCTTTGTTCAAGCAATCTG '3 | 300 nM |
| BRI1_R qRT-PCR | 5' CTCCATGGCACTCCTTAC '3 | 300 nM |
| Sl 25s_F | 5' CACGGACCAAGGAGTCTGACAT '3 | 300 nM |
| Sl 25s_R | 5' TCCCACCAATCAGCTTCCTTAC '3 | 300 nM |

**Table 2.9.4: *St* and *Nb* primer pairs for *BSL* genes**

| Primer Name | Primer Sequence |
|---|---|
| BSL1 qRT-PCR_F | 5' TGAGGGAAGCGACAATGA '3 |
| BSL1 qRT-PCR_R | 5' TGAAGGAACCATTCGTCTACTC '3 |
| qRTBSL1_EG_For: | 5' AGAAGGCGATAGACCGTCAG '3 |
| qRTBSL1_EG_Rev: | 5' AAGCAGCCCATAAGCATCTAC '3 |
| BSL1 5'qRT_for: | 5' CGGCTCCAACATATCGTTTA '3 |
| BSL1 5'qRT_rev: | 5' TGGGGCATCATCATCAGTAT '3 |
| BSL1 3'qRT_for: | 5' GCCCTCATCGAAAAGAAAAT '3 |
| BSL1 3'qRT_rev: | 5' TGGGATCAGACCATAGCAAA '3 |
| | |
| BSL3 qRT-PCR_F | 5' CGAATAATTCTGCCCCAACT '3 |
| BSL3 qRT-PCR_R | 5' ACCAAGAGCACCACCAGTCT '3 |
| qRTBSL3_EG_For: | 5' TGGATGTGGATTCAACTATGG '3 |
| qRTBSL3_EG_Rev: | 5' TGCTGTTGCTGAGTTTGTGA '3 |
| BSL3 5'qRT_for: | 5' GCACGAAGTGATAGAGAAAAAGG '3 |
| BSL3 5'qRT_rev: | 5' GAGCAGTAGCACCACCAAAA '3 |
| BSL3 3'qRT_for: | 5' GGTCTGACCCAACAGAAAATG '3 |
| BSL3 3'qRT_rev: | 5' GCCCAAAAGTAACCAATCCA '3 |
| | |
| NbBSL1_F1 qRT-PCR | 5' AAACAACTCAAATCTATTTAACTC '3 |
| NbBSL3_R1 qRT-PCR | 5' CCATCATTAACTGCCTCTGGAA '3 |
| NbBSL3_F2 qRT-PCR | 5' CAAGTGGTGAACAGGCATCT '3 |
| NbBSL3_R3 qRT-PCR | 5' CGTCGAATTATTTGAATCAGGTT '3 |
| NbBSL2_R2 qRT-PCR | 5' CCAGTAAAACTGAGCCATCATT '3 |

## 2.10 - Confocal microscopy

Confocal microscopy used either a Leica (Leica Microsystems, Germany) SP1 confocal laser scanning microscope (CLSM) mounted on a DMLFS microscope or an SP2 CLSM on a DM6000 microscope fitted with a FI/RH filter block and water dipping lenses (HCX APO L10x/0.30 W U-V-1, L20x/0.50 W U-V-1, L40x/0.80 W U-V-1 or L63x/0.90 W U-V-1). Images for GFP fluorescence were collected using excitation at 488 nm with emission collected at 500-530 nm using the L20x/0.50 W U-V-1 and L40x/0.80 W U-V-1 lenses. Images for YFP fluorescence were collected using excitation at 514 nm with emission collected at 530-575 nm using the L40x/0.80 W U-V-1 lens. Images for RFP fluorescence were collected using excitation at 561 nm and emission at 635-655 nm using the L40x/0.80 W U-V-1 lens. The auto-fluorescence signal from chlorophyll was collected simultaneously in the emission range of 650-700 nm. Co-localisation experiments using YFP and RFP were undertaken using sequential imaging. Unless otherwise stated,

images are presented as maximum intensity projections and were assembled and edited using Adobe® Photoshop® CS5.

2.10.1 – Vectors used for imaging

The following vectors were used in confocal imaging experiments (Table 2.10.1). The GFP, YFP and split YFP vectors have their Agrobacterium strain and antibiotics explained in Table 2.5.1; for the RFP vector the Agrobacterium strain was AGL1 and the antibiotics used for these cultures were: rifampicin (50 µg/ml) and spectinomycin (100 µg/ml)

**Table 2.10.1: Vectors used in confocal imaging**

| Vector name | Purpose | Gene in this vector |
|---|---|---|
| pB7FWG2,0 | GFP tag at C-term of gene | All PiAVR2 forms |
| pB7WGY2,0 | YFP tag at N-term of gene | StBSL3, StR2 |
| pK7RWG2,0 | RFP tag at C-term of gene | All PiAVR2 forms |
| CL112 | Split YFP - N-terminal section of YFP at the N-terminal of the gene | All PiAVR2 forms and StR2 |
| CL113 | Split YFP - C-terminal section of YFP at the N-terminal of the gene | St BSL1 |

**Table 2.10.2: Primers for confocal vectors**

| Primer Name | Primer Sequence |
|---|---|
| RTL2-P | 5' AAGGAAGTTCATTTCATTTGGAGAGGA '3 |
| RTL2-M | 5' CAACACATGAGCGAAACCCTATAAGAA '3 |

*A. tumefaciens* cultures were grown for 2 days, with shaking at 27°C in Luria-Bertani (LB) broth with the designated antibiotic (Table 2.5.1). Cultures were grown to a final $OD_{600}$ of 0.1 or 0.05 and infiltrated into *N. benthamiana* leaves. Leaves were attached, abaxial surface up, to microscope slides using double-sided adhesive tape (Banner, UK) for microscopic examination. Leaves were imaged at 2 and 3 dpi to determine the localisation of each of the proteins of interest.

## 2.11 – *P. infestans* infection of *N. benthamiana*

*P. infestans* isolate 88069 was used for plant infection assays. The 88069 isolate was cultured on Rye agar lacking antibiotics (Judelson and Roberts, 2002). Cultures were used at 12–14 days old for plant infection. The surface of the agar culture was covered with 5 ml sterile distilled water, the mycelia and sporangia scraped off into the water and poured into a sterile Falcon tube (Judelson and Roberts, 2002). The Sporangia concentration of the suspension was determined by use of a haemocytometer following standard microbiological techniques (Sambrook *et al*., 1989). A concentration of 250–500 sporangia per 10 µl droplet was used at each inoculation site.

### Growth of *P. infestans* on VIGS plants

Plants were used 2-3 weeks after infiltration with the VIGS constructs. Detached leaves were infected with *P. infestans* isolate 88069 as described above. The number of inoculation sites that formed sporulating lesions was compared to the total number of sites inoculated at 5, 6 and 7 days post infection (dpi) to generate a percentage.

### Growth of *P. infestans* on hormone treated plants

Wild type *N. benthamiana* were sprayed with 0.1% ethanol, 20 µM epi-brassinolide (EBL), 20 µM salicylic acid (SA) and a combination of 20 µM each SA and EBL. Plants were left for 2 days before inoculation with *P. infestans* isolate 88069. The spread of infection was monitored at 7 dpi.

### *Agrobacterium tumefaciens* Transient Assay

VIGS plants were infiltrated with Agrobacterium containing *Sto1* and *R2* plasmids on separate halves of the leaves (Table 2.4.1). At two dpi the leaves were detached and inoculated with *P. infestans* isolate 88069. The percentage of inoculation sites that formed

sporulating lesions was compared to the total number of sites inoculated. Leaves were photographed at 5-6 days post *P. infestans* inoculation. Trypan blue staining was performed as described in Gilroy *et al.* (2007).

## 2.12 – Fluorometry

*A. tumefaciens* cultures were grown for 2 days, with shaking at 27$^{o}$C in Luria-Bertani (LB) broth with the designated antibiotic (Table 2.5.1). Cultures used contained the CL112 plasmids with PiAVR2, PiAVR2-like and PITG_08949; these were mixed with the culture that contained the CL113_StBSL1 plasmid. Cultures were grown to a final $OD_{600}$ of 0.1 and infiltrated into *N. benthamiana* leaves. 1 cm diameter leaf discs were cut out at 2 dpi and floated on water abaxial surface up along with a control disc which had not been infiltrated. Quantification of fluorescence was performed using a SpectraMax M5 fluorometer (Molecular Devices). The YFP fluorescence was excited at 480 nm and measured at 520 nm.

## 2.13 – Statistical analysis

All statistical analysis was performed in Sigmaplot. Statistical analysis on all data, except the *BSL* qRT-PCR gene expression data, was performed using a one-way ANOVA. The Holm-Sidak method was used for fluorometry data, VIGS HR data, *BRI1* qRT-PCR data and *P. infestans* growth on VIGS plants. The Dunn's method was used to analyse *P. infestans* growth on hormone treated plants. Some of the data used in these anyalsis did not pass the Shapiro-Wilk test for normality as reported by Sigmaplot; a visual inspection of diagnostic residual plots indicated approximate normality and equality of variance. On that basis the Shapiro-Wilk warning was ignored. The t-test method was used to analyse the *BSL* qRT-PCR gene expression data on all VIGS plants.

# 3 – *PiAVR* and *R* gene recognition

## 3.1 - Introduction

Previous work identified two candidate RXLR–EER effectors from *P. infestans* that could be the avirulence protein detected by the host R2 protein (Gilroy *et al.*, 2011a). The presence of a dominant avirulence factor was initially identified by screening the F1 progeny of a cross between the *P. infestans* isolates 88029 (race 2.4.7; A1 mating type) and 88133 (race 1.3.7.10.11; A2 mating type) against 6 different potato lines that contained one dominant *R* gene in each. For example, the progeny that triggered an HR on the plant containing *R2* must have contained *PiAVR2*. This allowed a map-based cloning approach to position all six dominant *AVR* genes in linkage groups (van der Lee *et al.*, 2001). Seven amplified fragment length polymorphism (AFLP) markers were tightly linked with avirulence of F1 progeny on an R2 potato line which resulted in the positioning of the *PiAVR2* locus (van der Lee *et al.*, 2001). This led to a bacterial artificial chromosome (BAC) library being constructed from an individual member of the F1 progeny (T30-4) that contained all six avirulence genes to allow positional cloning of these *PiAVR* genes (Whisson *et al.*, 2001). Two of the seven markers that defined the *PiAVR2* locus (E + GA/M + ATs513 and E + TG/M + CTs338) were used to screen the BAC library. This led to identification of four positive BAC clones that assembled into two contigs. However these did not completely span the *PiAVR2* region (Figure 3.1.1) (Gilroy *et al.*, 2011a). The gap (of unknown size) was recently filled when sequencing of the *P. infestans* genome was completed (Figure 3.1.1) (Haas *et al.*, 2009). The genome sequence presented a region of 742 kb that contained *PiAVR2* (Gilroy *et al.*, 2011a). Within this 742 kb region are 3 predicted RXLR-dEER effector-encoding genes, *PITG_22870*, *PITG_08943* and *PITG_08949* (Figure 3.1.1). *PITG_22870* and *PITG_08943* are apparent gene duplications as they are identical and only 2 kb apart. *PITG_08949* is 34 kb from the gene

duplication (Gilroy *et al.*, 2011a). The PITG_08949 protein is highly conserved in the first 79 amino acids when aligned to PITG_22870 and PITG _08943 but then diverges from amino acid 80 until the end of the protein and is also 16 amino acids shorter. This is suggestive of a recent recombination event having occurred to generate PITG_08949 (Figure 3.1.2) (Gilroy *et al.*, 2011a).

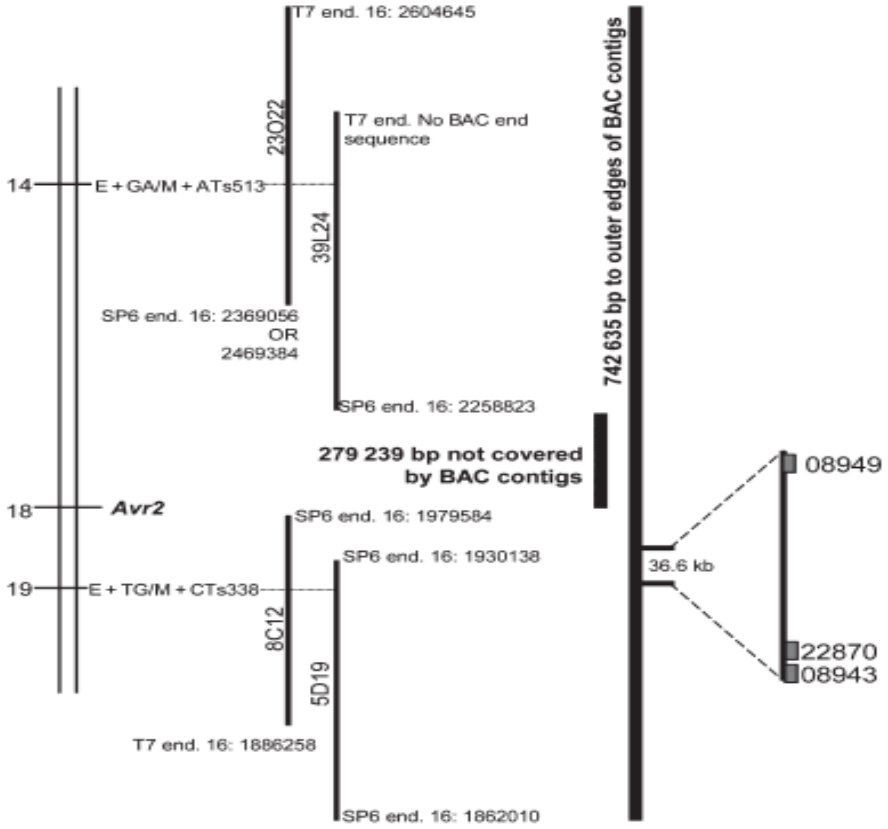


**Figure 3.1.1: Mining the genome for *PiAVR2***. Two AFLP genetic markers for *PiAVR2* were used to screen a BAC library made from genomic DNA from T30-4. Positive BAC clones were end-sequenced and contiged into two groups, however the gap of unknown size could not be solved until completion of the *P. infestans* genome sequencing project. Three RxLR-dEER containing candidate genes were found in the 36.6 kb region (*PITG_22870*, *PITG_08943* and *PITG_08949*). Figure adapted from Gilroy *et al* (2011a).

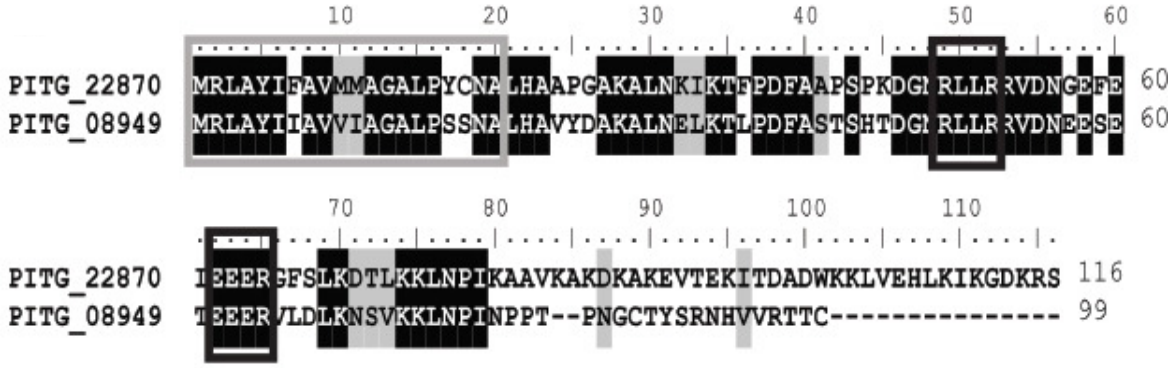


**Figure 3.1.2: Amino acid alignment of PITG_22870, and PITG_08949**. The grey box shows the signal peptide. All cloning was done after the signal peptide. The black boxes highlight the RxLR and EER motifs. These two proteins are very similar up until amino acid 79, they then diverge completely. PITG_08949 is 16 amino acids shorter. Figure adapted from Gilroy *et al* (2011a).

To determine which of the candidate RxLR-EER genes was *PiAVR2*, *PITG_22870* and *PITG_08949* were cloned into plant expression vector (pGRAB) and transiently expressed using *A. tumefaciens* infiltration into leaves. These genes were tested on 1512 c(16), an *R2* expressing cultivar, Bintje a susceptible potato cultivar lacking *R2* and, as a further control, *R3a* transgenic *Nicotiana benthamiana* plants (Figure 3.1.3).

As controls, *A. tumefaciens* containing empty pGRAB was infiltrated into each leaf and pGRAB containing alleles of another *P. infestans* effector, *PiAVR3a*$^{EM}$ and *PiAVR3a*$^{KI}$, as described in Armstrong *et al* (2005). Two inoculations of *PITG_22870* and *PITG_08949* were carried out on each leaf to show repetition, empty pGRAB vector was used as a negative control to show that the vector did not induce an HR on its own and *PiAVR3a*$^{EM}$ and *PiAVR3a*$^{KI}$ were used to show *R* gene specificity. The susceptible cultivar Bintje did not show any HRs, as expected (Figure 3.1.3). *PiAVR3a*$^{KI}$ is an allele of PiAVR3a that is recognised by R3a (Armstrong *et al*., 2005) which can be shown to generate an HR in the transgenic *R3a N. benthamiana* plants (Figure 3.1.3). In the *R2* expressing cultivar, the *PiAVR3a*$^{EM}$ and *PiAVR3a*$^{KI}$ infiltration sites show that R2 does not recognise these

effectors (Figure 3.1.3). The *R2* expressing leaf exhibits two HRs and both are at the infiltration sites of PITG_22870 but not at the PITG_08949 infiltration sites (Figure 3.1.3). PITG_22870 is not recognised on the *R3a* plants, showing that the formation of an HR is *R* gene-specific. It can be concluded from this work that PITG_22870 is likely to be *PiAVR2*.

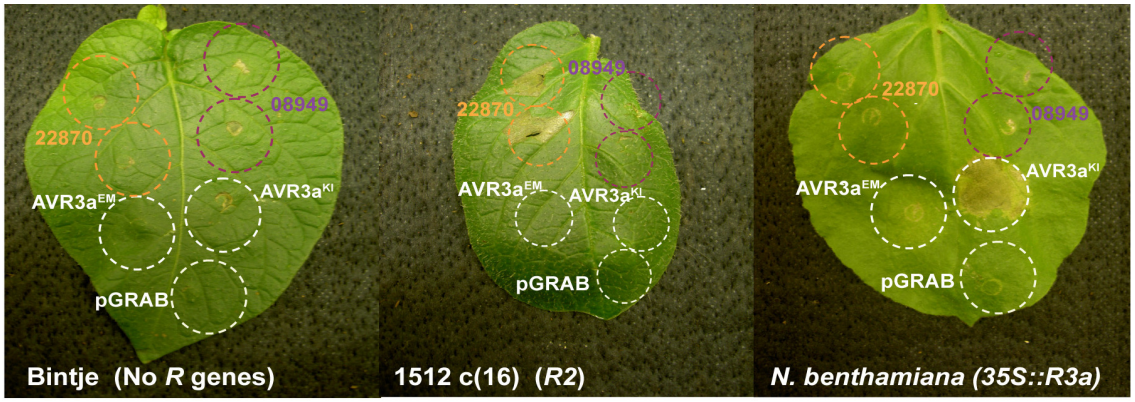


**Figure 3.1.3: PITG_22870 is *PiAVR2*.** Bintje is a susceptible cultivar of potato with no known *R* genes that recognize *P. infestans*, 1515 c(16) is a potato cultivar naturally expressing the *R2* gene and *N. benthamiana* transgenic plants constitutively express the potato *R3a* gene.
All constructs infiltrated on Bintje show no response, however PITG_22870 causes an HR on 1512 c(16) plants. PITG_08949 shows no response. PITG_22870 shows no response on *N. benthamiana* R3a transgenic plants with *PiAVR3a*$^{KI}$ used as a positive control giving an HR. Figure adapted from Gilroy *et al* (2011a).

## 3.2 – *PiAVR2* alleles

Since 2005, a particularly aggressive A2 genotype, known as 13_A2 or Blue13, has quickly dominated the UK *P. infestans* population and has been shown to overcome some previously effective forms of plant host resistances, including *R2* (David Cooke, the JHI, personal communication). Therefore, it was decided to look at the diversity of *PiAVR2* in a wide range of *P. infestans* isolates. This was done by David Cooke using multiple primer pairs to amplify *PiAVR2* from genomic DNA from 29 diverse *P. infestans* isolates (Table 3.2.1). The primer pairs were located in the coding sequence or just outside in the flanking

region (see Appendix 1 Fig. S1 for primer pair locations). Seventeen of these 29 isolates are avirulent on 1512 c(16) *R2* expressing plants while 12 are virulent (Table 3.2.1). From these 29 isolates good amplification of *PiAVR2* appeared from all 17 avirulent isolates but from only 3 of the 12 virulent isolates. From the 17 avirulent and 3 virulent isolates from which the gene did amplify only one amino acid polymorphism was discovered, N31K, which is located in the N-terminal half of PiAVR2 between the cleavage point of the signal peptide and the RXLR motif (Figure 3.2.1a). *PiAVR2*$^{K31}$ is more abundant in the 17 avirulent isolates with 10 isolates being homozygous and none being homozygous for *PiAVR2*$^{N31}$. This leaves 7 isolates that were heterozygous for *PiAVR2*$^{N31}$ and *PiAVR2*$^{K31}$. Both *PiAVR2*$^{N31}$ and *PiAVR2*$^{K31}$ are present in the 17 avirulent and 3 virulent isolates indicating that the absence of PiAVR2 may not be the cause of virulence.

| Genotype[a] | Isolate name | Origin | *R2*[b] virulence | Amplification with primers below: AVR2 F2 and R2[c] | AVR2 F1 and R1 | AVR2 F4 and R4 | SNP[d] within *PiAVR2* | Amplification with primers below: avr2 F7 and R7 | avr2 F6 and R6 | SNP[e] within *PiAVR2-like* |
|---|---|---|---|---|---|---|---|---|---|---|
| 3_A2 | 2006_4012F | UK | + | – | – | – | n/a | + | + | MI/TV |
| 3_A2 | 2006_4244E | UK | + | – | – | – | n/a | + | + | — |
| 13_A2 | 2006_3884B | UK | + | – | – | – | n/a | + | + | — |
| 13_A2 | 2006_3928A | UK | + | +/– | – | – | n/a | + | + | MI/TV |
| 13_A2 | 2006_3964A | UK | + | – | – | – | n/a | + | + | — |
| 13_A2 | 2006_4132B | UK | + | – | – | – | n/a | + | + | — |
| 5_A1 | 01/29 | UK | + | +/– | – | – | n/a | + | + | MI |
| 5_A1 | 1996_9_5_1 | UK | + | – | – | – | n/a | + | + | — |
| Misc | MP618 | Poland | + | +/– | – | – | n/a | + | + | MI/TV |
| 7_A1 | 2006_4168B | UK | + | + | + | + | K | + | + | MI |
| 7_A1 | 2006_4168C | UK | + | + | + | + | K | + | + | — |
| 17_A2 | 2006_4388D | UK | + | + | + | + | K/N | + | + | MI |
| 1_A1 | 2006_3984C | UK | – | + | + | + | K/N | + | + | TV |
| 2_A1 | 2006_3888A | UK | – | + | + | + | K | + | + | — |
| 2_A1 | 2006_4068B | UK | – | + | + | + | K | + | + | MI |
| 8_A1 | 2006_4256B | UK | – | + | + | + | K | + | + | MI |
| 8_A1 | SC_95 17_3_2 | UK | – | + | + | + | K | + | + | MI |
| 22_A2 | 2003_25_1_3 | UK | – | + | + | + | K | + | + | MI/TV |
| 22_A2 | 2003_25_3_1 | UK | – | + | + | + | K | + | + | MI/TV |
| Misc | 88069 | The Netherlands | – | + | + | + | K | + | + | MI |
| EC1 | EC1 | Ecuador | – | + | + | + | K | + | + | — |
| 4_A1 | 2006_4352E | UK | – | + | + | + | K | – | – | n/a |
| 6_A1 | 2006_4100A | UK | – | + | + | + | K/N | – | – | n/a |
| 6_A1 | 2006_3920A | UK | – | + | + | + | K/N | – | – | n/a |
| 10_A2 | 2006_4440C | UK | – | + | + | + | K | – | – | n/a |
| 10_A2 | 2006_3936C2 | UK | – | + | + | + | K | – | – | n/a |
| 15_A2 | 2004_7804B | UK | – | + | + | + | K/N | – | – | n/a |
| Misc | Ca65 | USA | – | + | + | + | K/N | – | – | n/a |
| Misc | T30-4 | n/a | – | + | + | + | K/N | – | – | n/a |

SNP, single nucleotide polymorphism; n/a, not applicable.
[a]*Phytophthora infestans* genotypes are based on defined simple-sequence repeat marker profiles that will be reported in detail elsewhere.
[b]'+' indicates ability to infect *R2* plants and '–' indicates the isolate triggers HR on *R2* plants.
[c]'+/–' indicates PCR amplification only when the annealing temperature was decreased.
[d]SNP results in amino acid polymorphism N31K in PiAVR2. K/N is heterozygous.
[e]Two SNPs result in amino acid polymorphisms M10T and I92V in PiAVR2-like. MI/TV is heterozygous
Protein alignments from the isolates above, indicating the N31K, M10T and I92V polymorphisms, are shown in Fig. S4.

**Table 3.2.1: Details of isolates and PCR product amplification with different primer sets used in this study.** Table adapted from Gilroy *et al* (2011a).

To investigate if this one SNP could account for the virulence phenotype, the two alleles, *PiAVR2*$^{N31}$ and *PiAVR2*$^{K31}$, were cloned and tested *in planta*. Both alleles were cloned minus the signal peptide, the N-terminus was cloned from the end of the signal peptide to the end of the EER and the C-terminus was cloned from after the EER to the end of the gene (Figure 3.2.1a). All *PiAVR2* constructs were co-infiltrated with the *R2* gene, using *A. tumefaciens,* into *N. benthamiana* plants. It was discovered that PiAVR2$^{N31}$ and PiAVR2$^{K31}$ were both recognised by R2 to a similar extent so the SNP responsible for the N31K substitution does not appear to explain virulence (Figure 3.2.1b & c). The PiAVR2 N-terminus was not recognised by R2. However the C-terminus gave a consistent, strong and quick HR (96% inoculations giving HRs) compared to the two full length forms (70%

inoculations giving HRs) (Figure 3.2.1b & c). Each of the genes was stable when expressed in *N. benthamiana* leaves, as each was tagged with GFP at their C-terminus and detected on a western blot (Figure 3.2.1d). PiAVR2$^{K31}$ appears to be less stable than PiAVR2$^{N31}$ in this western image. However, this is specific to this sample as other biological replicates of this western produced a band as strong as PiAVR2$^{N31}$. PITG_08949 is also included in this western to show that it is stable *in planta,* so the lack of recognition on 1512 c(16) R2 expressing plants is most likely not due to protein instability in plants (Figure 3.2.1d).

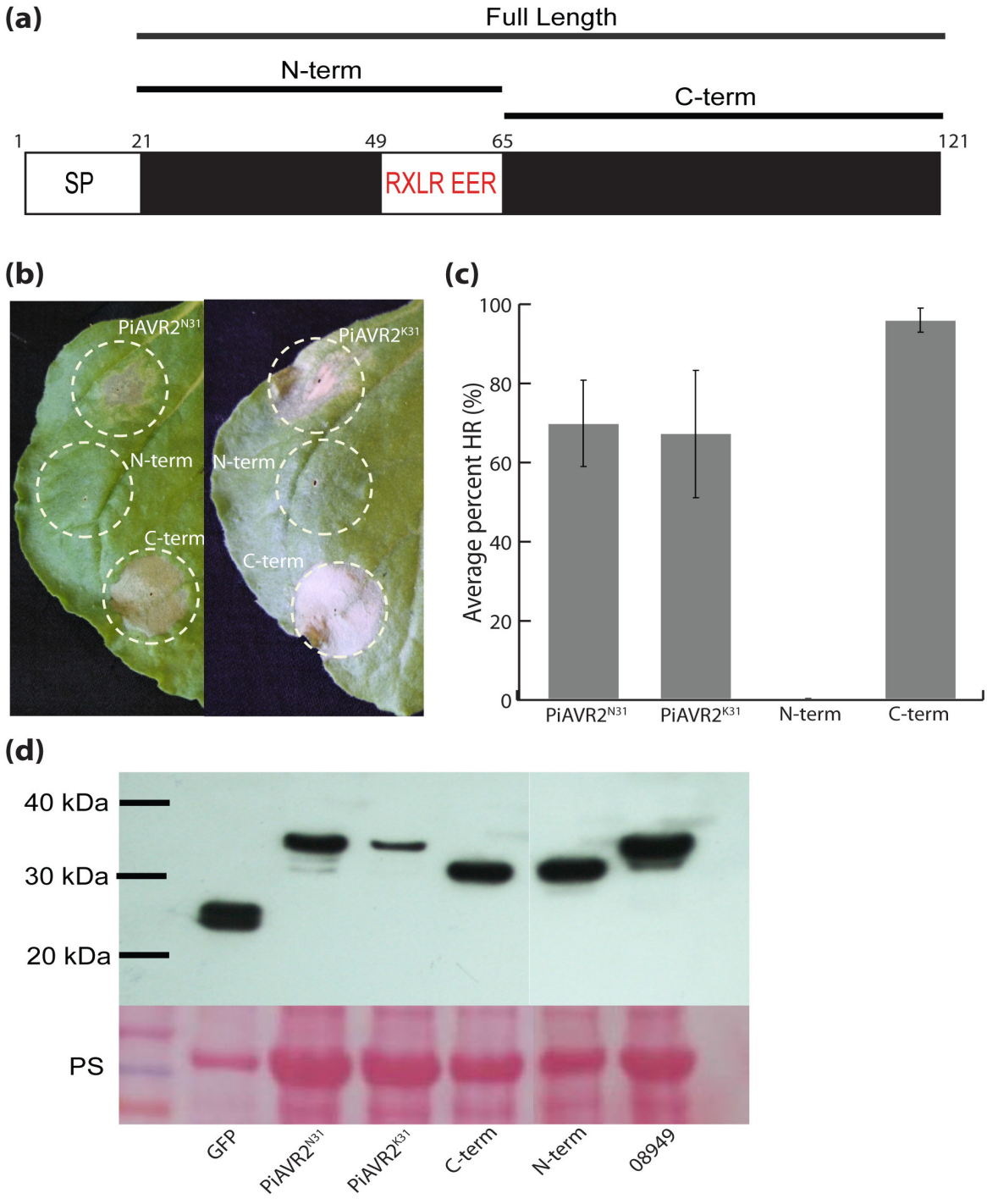


**Figure 3.2.1: Cloning, R2 recognition and stability of PiAVR2$^{N31}$ and PiAVR2$^{K31}$.** (a) Schematic of the cloned genes. Black bars indicate the products cloned for agro-expression. (b) *N. benthamiana* co-infiltrations of R2 with pGRAB PiAVR2$^{N/K31}$, N-terminus and C-terminus. (c) Graph displaying percentage of inoculation sites developing HRs as the mean of 3 biological replicates each involving 24 inoculation sites per construct combination. Error bars represent +/- standard error. (d) The best of four western blots of PiAVR2$^{N31}$, PiAVR2$^{K31}$, C-terminus, N-terminus and PITG_08949 is shown. All PiAVR2 constructs were translationally fused at the C-terminus to GFP to show stability *in planta* using anti-GFP antibody. The Ponceau stain (PS) shows the relative protein loading of each sample.

As the above proteins had been tagged with GFP to determine stability, they could also be used *in planta* to determine their localisation within a plant cell. Representative images of the localisation are shown in Figure 3.2.2. PiAVR2$^{N31}$ localises to the plasma membrane, cytoplasm and spherical objects within the cell which appear to be chloroplasts. This chloroplastic fluorescence is not auto-fluorescence as not all chloroplasts fluoresce. Thus it appears to be a genuine localisation. PiAVR2$^{K31}$, PiAVR2 N-term and 08949 localise to the plasma membrane and cytoplasm and PiAVR2 C-term only localises to the plasma membrane of the cells. There is no chloroplast localisation signal found in the PiAVR2$^{N31}$ protein.

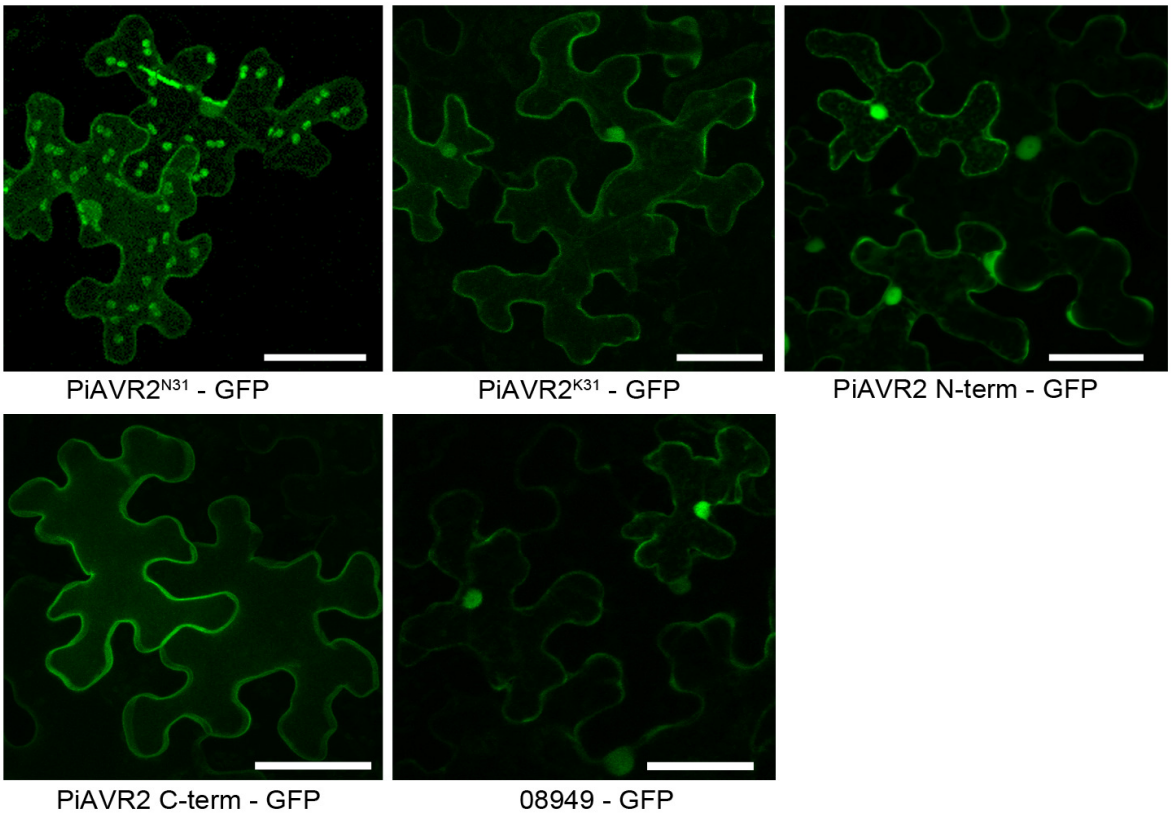


**Figure 3.2.2: Localisation of PiAVR2 forms.** PiAVR2 forms and PITG_08949 tagged at the C-terminus of the protein. Images taken using the Leica Confocal software. Scale bars are 50 µm.

## 3.3 – *PiAVR2-like* identification and characterisation

As mentioned in Section 3.2, 9 of the 12 virulent isolate's DNA failed to yield a *PiAVR2* PCR product. However, dropping the annealing temperature during these PCRs did give a weak band for 3 of the remaining 9 virulent isolates. This PCR product was re-sequenced (D. Cooke) and the sequence generated was similar to that of *PiAVR2*$^{N/K31}$ but with more SNPs (Figure 5a). There were a total of 25 SNPs in the nucleic acid sequence and this translates to 13 amino acid changes in the protein. Eight of these SNPs occur in the C-terminus. Two occured before the RxLR and three between the RxLR and EER motifs. The gene sequence was similar to *PiAVR2* but the area of the genome surrounding this gene was highly divergent. It could not be confirmed whether this form of *PiAVR2* had been PCR-amplified from the same locus identified in T30-4, therefore it was named *PiAVR2-like* (Gilroy *et al.*, 2011a). The fact that these areas were so different when comparing the 2006_3928A genome to T30-4 also led to difficulty in aligning the reads from the Illumina sequencing. In fact, the Illumina sequence reads that contained the *PiAVR2-like* sequence were contigged from unassembled reads only once the sequence was known from weak PCR products derived from virulent isolates. These are some problems that can arise when looking for divergent gene variants between isolates, and which can erroneously lead to the conclusion that a gene may be absent, rather than divergent. With the sequence of this gene now available it was clear why previous primers had failed to amplify, as there were too many SNPs at the C-terminus of the gene to allow binding of the *PiAVR2* primers and the genetic region surrounding *PiAVR2-like* was so different to T30-4 that the primers outwith the coding region would also not amplify the gene. With the sequence of *PiAVR2-like,* new primers (avr2 F6/R6 and F7/R7) were designed that were specific to this gene. The original screen of the 29 divergent isolates was then repeated (Table 3.2.1, Figure 3.3.1b). These new primers amplified *PiAVR2-like* from all 12 isolates that were virulent on R2 plants, and from 9 avirulent isolates (Figure

3.3.1b, Table 3.2.1). Figure 3.3.1b shows that there are 12 isolates that possess *PiAVR2*$^{N31}$ or *PiAVR2*$^{K31}$ and *PiAVR2-like* in their DNA, so how is virulence determined for these isolates?

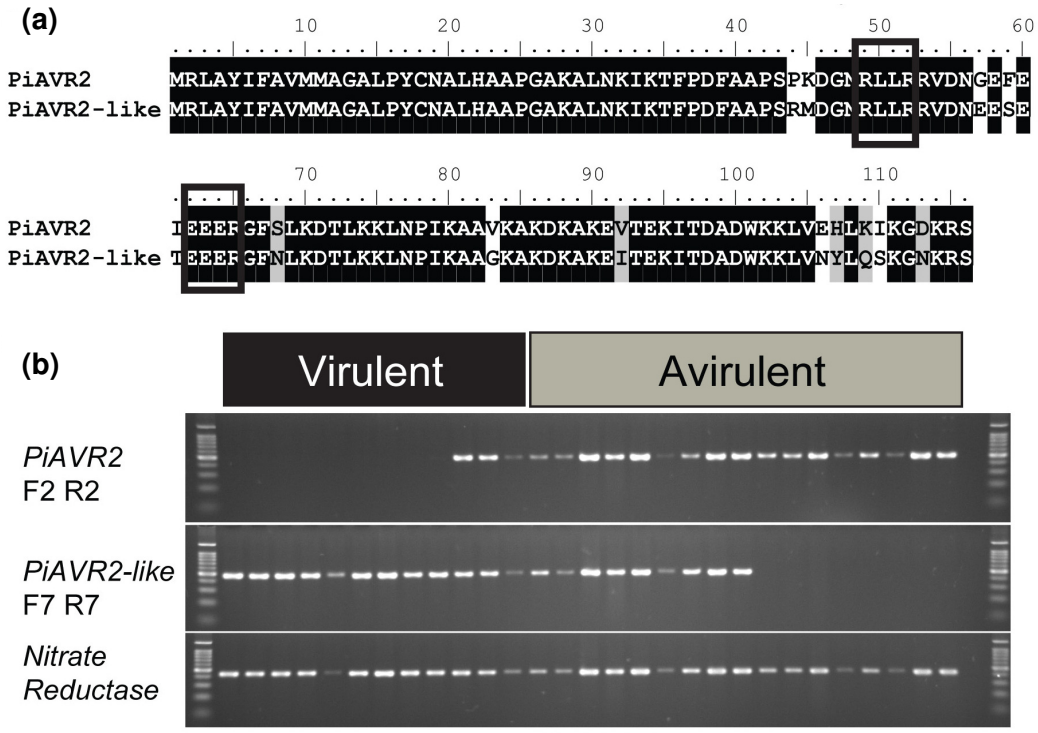


**Figure 3.3.1: Sequence and amplification of *PiAVR2-like*.** (a) This shows the protein alignment between PiAVR2 and PiAVR2-like. The conserved amino acids are highlighted in black the grey amino acids are a conservative change. Again the RxLR-EER motifs are highlighted by a black box. (b) A gel showing the PCR amplification of *PiAVR2* and *PiAVR2-like* from the DNA of *P. infestans* genotypes that are virulent or avirulent on R2 potato. *PiAVR2* F2 R2 are primers specific for *PiAVR2*. *PiAVR2-like* F7 R7 are primers specific for *PiAVR2-like*. *Nitrate Reductase* is the endogenous control gene, showing that all DNA samples provide a good template for this gene.

To investigate this newly discovered form of *PiAVR2*, the full length *PiAVR2-like* was cloned minus the signal peptide and just the C-terminus, as shown for *PiAVR2* in Figure 3.2.1a. This allowed co-infiltration with *R2* in *N. benthamiana* and infiltration on *R2* expressing potato plants to determine if PiAVR2-like evades recognition by R2. Figure

3.3.2a shows an *N. benthamiana* leaf with PiAVR2$^{K31}$ and PiAVR2 C-terminus co-expressed with R2, showing the presence of an HR, as positive controls. Below these infiltrations are PiAVR2-like and PiAVR2-like C-terminus co-expressed with R2 which did not induce an HR at either infiltration site. The results from multiple experiments show that PiAVR2 and PiAVR2 C-terminus are consistently recognised, whereas PiAVR2-like is not recognised by R2 and its C-terminus component is recognised only 20% of the time (Figure 3.3.2b). PiAVR2 only and *R* gene only were used as negative controls to show each protein expressed individually is not capable of producing an HR. When PiAVR2 and PiAVR2-like variants were infiltrated into R2 expressing potato plants similar results were observed (Figure 3.3.2c). There is some recognition of the PiAVR2-like protein but it is only between 5-10%, which could also be down to non-specific response to Agrobacterium expression as an empty vector control was not included. Again, the C-terminus of PiAVR2-like was recognised only 20% of the time in R2 potato. These results show that PiAVR2-like is able to evade recognition by the R2 protein. To confirm that the absence of an HR was not due to instability of PiAVR2-like proteins *in planta*, the genes were tagged with GFP at their C-terminus and detected with GFP antibody in a western blot (Figure 3.3.2d). This figure shows that PiAVR2-like and PiAVR2-like C-terminus are both stable when transiently expressed in *N. benthamiana* leaves. These results reveal that *PiAVR2-like* is the virulent form of *PiAVR2*. The presence of *PiAVR2-like* in the DNA of *P. infestans* isolates does not appear to be the sole explanation for virulence as it has been shown in Figure 3.3.1b that there are 9 avirulent isolates which contain *PiAVR2-like*.

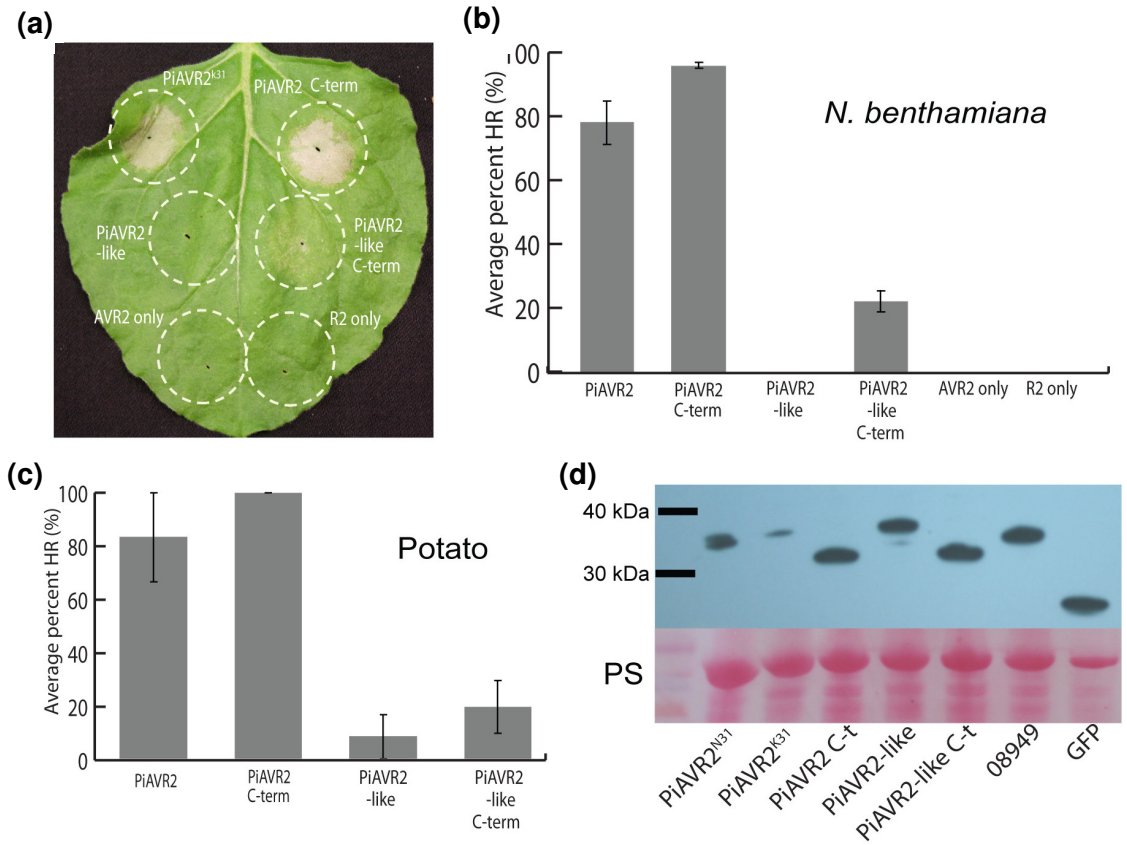


**Figure 3.3.2: Recognition of PiAVR2-like**. (a) *N. benthamiana* leaf showing agro expression of PiAVR2$^{K31}$, PiAVR2 C-terminus, PiAVR2-like, PiAVR2-like C-terminus all co-infiltrated with R2. *Agrobacterium* expressing PiAVR2 only and R2 only were included as negative controls. (b) A graph depicting the average percentage of inoculation sites that develop an HR on *N. benthamiana* leaves. This is the average of 3 biological replicates, involving 24 inoculation sites for each construct combination. Error bars represent +/- SE (c) A graph of the mean percentage of inoculation sites that develop an HR on R2 potato leaves. Best biological replicate is presented here with errors representing +/-SE across 24 inoculation sites for each construct. (d) Western blot to show the stability of each protein in *N. benthamiana.* The Ponceau stain at the bottom shows protein loading and transfer onto membrane before probing.

The localisations of PiAVR2-like and PiAVR2-like C-terminus were also determined since they were tagged with GFP to check their stability. PiAVR2-like appears to localise to the cytoplasm, plasma membrane and the chloroplasts (Figure 3.3.3), which is similar to the localisation seen for PiAVR2$^{N31}$ in Figure 3.2.2. This could be because the amino acid sequence of PiAVR2-like also has an asparagine (N) residue at position 31 (Figure 3.3.1). As with PiAVR2 C-terminus, PiAVR2-like C-terminus is also only localised to the plasma membrane (Figure 3.3.3).

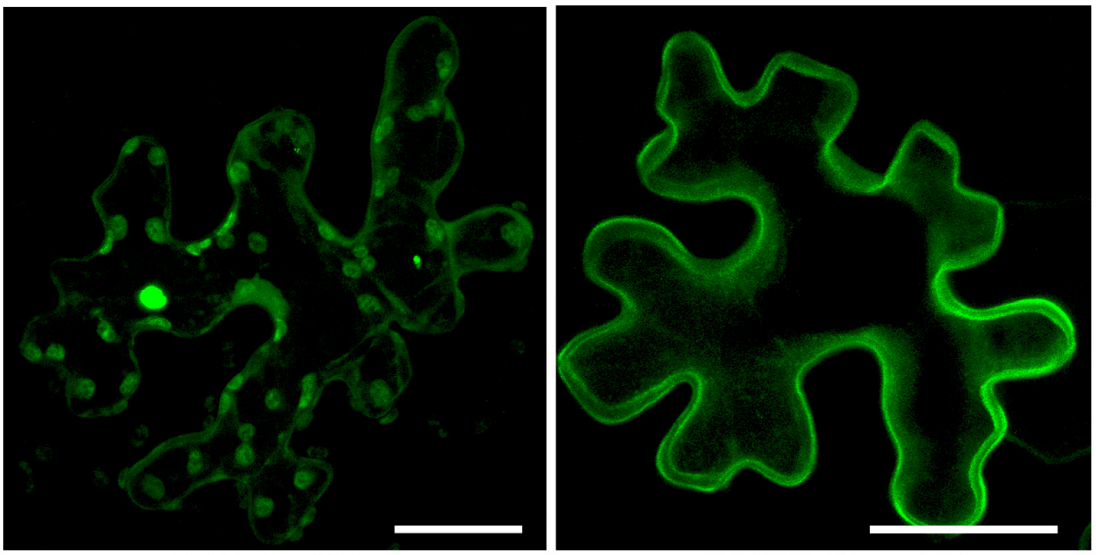


**Figure 3.3.3: Localisation of PiAVR2-like and PiAVR2-like C-terminus.** PiAVR2 forms tagged at the C-terminus of the protein with GFP. Images were taken using the Leica Confocal software. Scale bars are 50 µm.

## 3.4 – Expression Analysis

As the presence/absence of *PiAVR2*$^{N/K31}$ and *PiAVR2-like* does not fully explain the virulence/avirulence seen on the *R2*-expressing potato plants, another factor must exist to explain virulence. To test whether there was a difference in the expression of each of the genes, recognised versus unrecognised, a semi-quantitative RT-PCR on the cDNA synthesised from leaf material 24 hpi with each isolate was performed. Since the primer pairs used in Figure 3.3.1 were designed to amplify products from genomic DNA, specific primers were designed in the ORFs of both genes to distinguish between the transcripts of *PiAVR2* and *PiAVR2-like*, shown in Chapter 2 Table 2.9.1. As a positive control for the *PiAVR2* primers, the cDNA from the sequenced isolate T30-4 was included as the genome sequence of this isolates encodes only *PiAVR2*$^{N31}$ and *PiAVR2*$^{K31}$. As a positive control of the *PiAVR2-like* primers, virulent isolate 2006_3928A was utilised as the DNA of this

isolate only encodes *PiAVR2-like* (Figure 3.3.1b, Table 3.2.1). The cDNA at 24 hpi on leaf material was prepared from four *P. infestans* isolates that were shown to possess both *PiAVR2* and *PiAVR2-like* in their DNA, two of which are virulent on R2 expressing plants (2006_4168B and 2006_4168C) and two of which are avirulent (88069 and 2006_4256B) (Table 3.2.1). T30-4 shows no amplification of *PiAVR2-like* and 2006_3928A shows no amplification of *PiAVR2,* so these primers are specific as expected (Figure 3.4.1). Although the virulent isolates 2006_4168B and 2006_4168C encode both genes in their DNA, they only express the *PiAVR2-like* form (Figure 3.4.1). The avirulent isolates 88069 and 2006_4256B also contain both forms (*PiAVR2/PiAVR2-like*) in their DNA and appear to express both (Figure 3.4.1). This leads to the conclusion that the expression of *PiAVR2* is the key factor in avirulence. The *P. infestans* isolates that are virulent on *R2* potatoes, but encode both genes in their genome, only express *PiAVR2-like*.

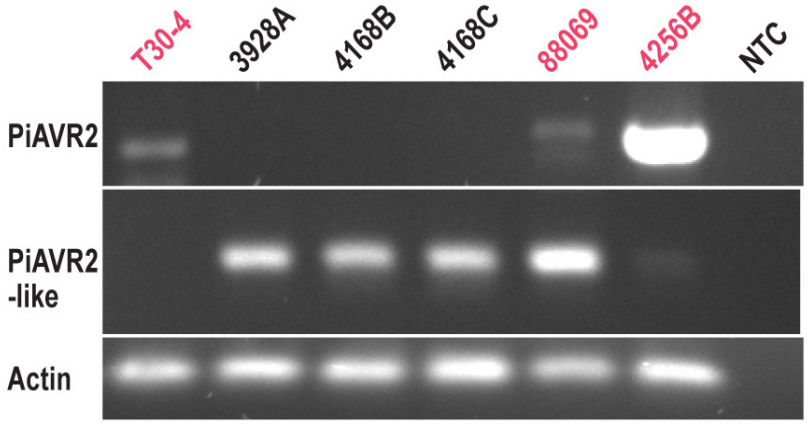


**Figure 3.4.1: Expression analysis of PiAVR2 and PiAVR2-like.** Semi-qRT-PCR was performed on cDNA synthesised from material harvested 24 hpi on *N. benthamiana* leaves. The top panel indicates the expression of PiAVR2 in *P. infestans* at 24hpi. The middle panel shows the expression of PiAVR2-like. Actin was used as an endogenous control. Red indicates avirulent isolates and black indicates virulent isolates on R2 expressing potato plants. This was performed 3 times with similar results.

## 3.5 – PiAVR2 silencing in *P. infestans*

To determine the importance of *PiAVR2* to *P. infestans* during an infection *PiAVR2* expression was silenced in isolate 88069, which is shown to express both forms of *PiAVR2* (Figure 3.4.1). Zhendong Tian and Steve Whisson designed and constructed an inverted repeat hairpin construct using the full length $PiAVR2^{N31}$. Protoplasts were transformed with the pSTORA plasmid as described by Bos *et al* (2010). The transformation generated sixteen 88069 transgenic lines, 53% of which were unable to grow on the susceptible cultivar Bintje when compared to untransformed 88069 (Figure 3.5.1a). To quantify the level of silencing in the lines shown in Figure 3.5.1a, qRT-PCR was undertaken using primers which amplify products from both *PiAVR2* and *PiAVR2-like*. cDNA was synthesised from RNA extracted from germinating cysts from each transgenic line that displayed significant loss of virulence and used for the qRT-PCR. This stage of the life cycle was chosen as it is the beginning of the biotrophic stage of the *P. infestans* life cycle when many RXLRs are known to be up-regulated in preparation for infection. The results in Figure 3.5.1b show the expression of *PiAVR2/PiAVR2-like* in the transformed lines relative to that detected in the control isolate 88069. This shows that for all lines there is at least an 80% reduction in *PiAVR2/PiAVR2-like* expression. In the case of AVR2_IR SW4 there is an extremely large reduction of 99.5% in expression. It remains to be determined if these silenced lines can be complemented *in planta* by expressing *PiAVR2* or *PiAVR2-like* via Agrobacterium infiltration into plant leaves.

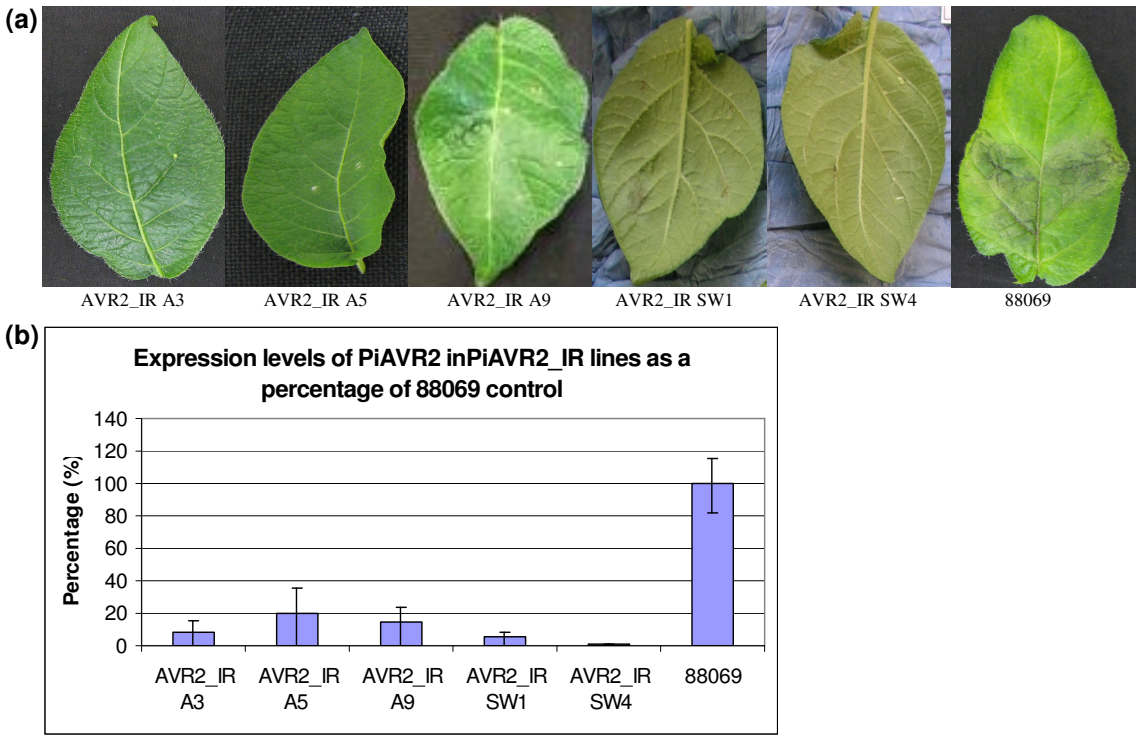


**Figure 3.5.1: PiAVR2 silencing in 88069. (a)** leaf images of 5 PiAVR2 transgenic lines and 88069 control. **(b)** qRT-PCR results of *PiAVR2* expression in the 5 PiAVR2 transgenic lines compared to 88069.

## 3.6 – SNP investigation of PiAVR2-like protein

The western blots shown previously in Figures 3.2.1 and 3.3.2 were undertaken to show the stability of the PiAVR2 forms, and in doing so another interesting observation was made. For some of the PiAVR2 forms, PiAVR2$^{N31}$, PiAVR2$^{K31}$ and PiAVR2 N-term, the bands of expected sizes were observed, but other bands were also seen. PiAVR2$^{N31}$ and PiAVR2$^{K31}$ show two extra bands present (Figure 3.6.1). One of the extra bands appears to be the same size as the C-terminus, ~31 kDa, while the second is ~34.5 kDa in size (Figure 3.6.1). For the PiAVR2 N-term the second band that is present on the western blot is ~27 kDa (Figure 3.6.1). These extra bands could suggest that there may be some cleavage of these proteins occurring in the plant. One of these cleavage sites may occur

within the N-terminus of the protein as there is a second band present in the N-terminus lane in Figure 3.6.1 and the 34.5 kDa band in the full length forms adds significance to this observation. The fact that there is a second smaller band at ~31 kDa in the full length form lanes, which appears to be the same size as the C-terminus, could also suggest that cleavage of the protein may occur within the RXLR region. Investigate of these extra bands by looking at the SNPs which lead to amino acid changes surrounding the RXLR region between PiAVR2$^{N/K31}$ and PiAVR2-like was undertaken (Figure 3.3.1). When a western blot was run using PiAVR2-like it was observed that there were also extra bands (Figure 3.6.1). This image is a little over-exposed but reveals a band in the PiAVR2-like lane that is the same size as the PiAVR2-like C-terminus. The western shown above in Figure 3.3.2 also shows a second band in the PiAVR2-like lane which is ~34.5 kDa, the western below in Figure 3.6.1 is slightly overexposed and it is possible that this band cannot be observed. It appears that there is still cleavage occurring in the PiAVR2-like form so the SNPs that occur between the virulent and avirulent forms do not appear to lead to a loss of cleavage.

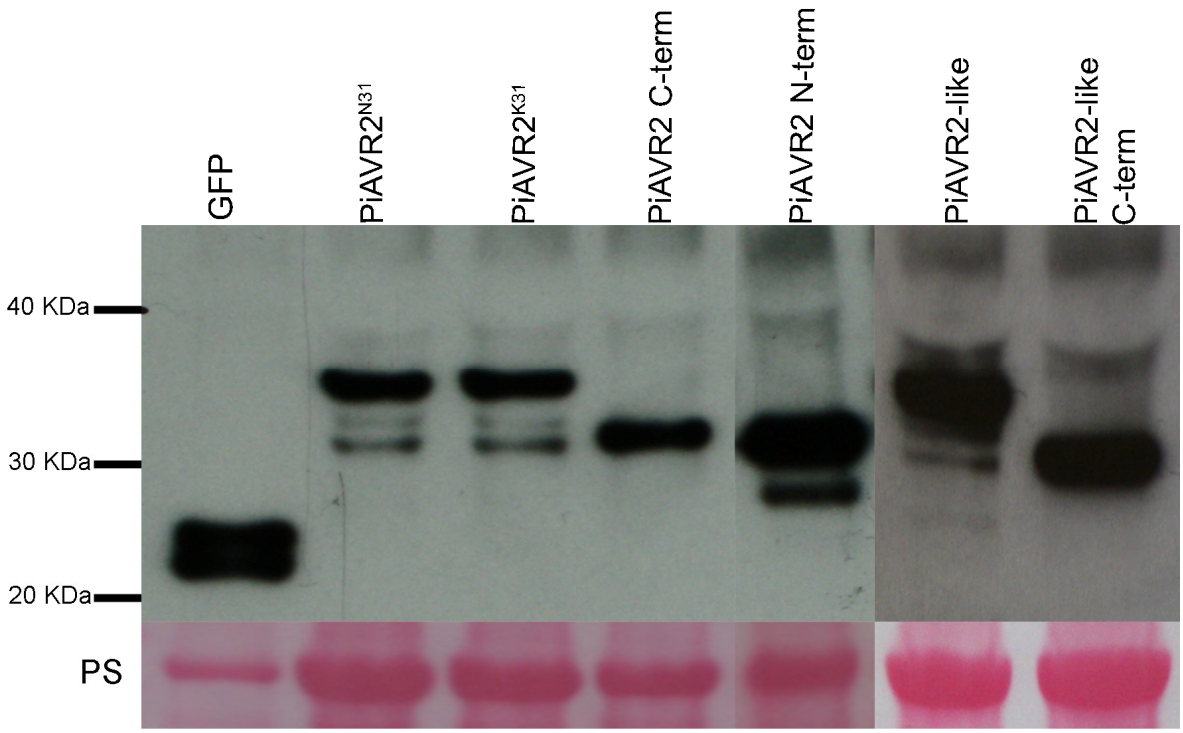


**Figure 3.6.1: Western Blot showing cleavage of PiAVR2 forms.** PiAVR2 forms on a western blot. The Ponceau stain shows relative loading of the proteins.

In Section 3.3 the identification of *PiAVR2-like* was described and shown that is not detected by transient expression of *R2* in *N. benthamiana* and the endogenous *R2* in potato. In the above western blots it was shown that the SNPs between PiAVR2-like and PiAVR2 were not responsible for a change in cleavage. However the ability of PiAVR2-like to evade recognition could be linked to the SNPs that have caused amino acid changes in PiAVR2-like when compared to PiAVR2. To further investigate this lack of recognition of PiAVR2-like, some SNPs were examined in more detail to investigate if these were determinants of virulence. Two different clones were made, one to investigate the SNPs around the RXLR and dEER, called PiAVR2 mutated dEER. This clone is PiAVR2 with the following amino acid changes F59S, I61T, S68N and V83G (Figure 3.6.2a). The second clone is called PiAVR2 V83G C-term and as the name suggests it is the C-terminus of PiAVR2 with the amino acid change V83G (Figure 3.6.1a). These genes

were all cloned and co-expressed with *R2* in *N. benthamiana*. It can be seen clearly that these SNPs are not responsible for the lack of recognition by R2, as both proteins are clearly recognised by R2 (Figure 3.6.2b and c). PiAVR2 and PiAVR2 C-terminus were used as positive controls, and PiAVR2-like and PiAVR2-like C-terminus were used as negative controls (Figure 3.6.2b and c).

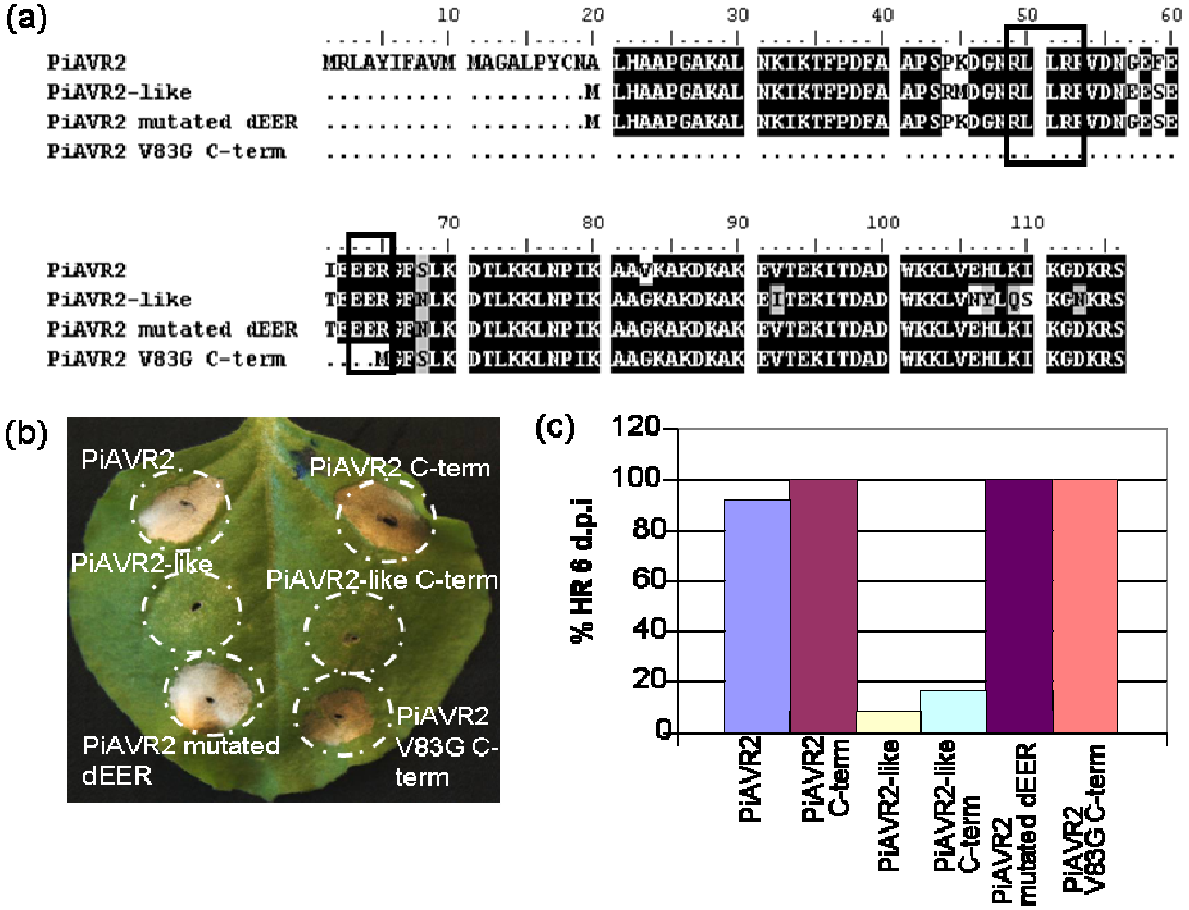


**Figure 3.6.2: Amino acid changes surrounding the EER region are not responsible for PiAVR2-like's ability to evade R2 recognition.** (a) An alignment of PiAVR2-like, PiAVR2, PiAVR2 mutated dEER and PiAVR2 V83G C-terminus. It shows the SNPs that were made in the two new clones, F59S, I61T, S68N and V83G. the RXLR and EER domains are marked (b) A leaf picture of the clones co-infiltrated with R2. (c) A graph showing the percentage HRs of each clone when co-expressed with *R2* at 6 dpi.

## 3.7 – *R2* orthologues

It was previously described that *R2* resides in a major late blight resistance locus on linkage group IV in potato which harbours a number of other LZ-NBS-LRR resistance genes including *Rpi-abpt* and *R2-like* from *Solanum demissum,* and *Rpi-blb3* from *Solanum bulbocastanum* (Lokossou *et al.*, 2009). All four Rpi proteins are highly homologous in the LRR domains, whereas the LZ and NBS domains are more polymorphic, with R2 being the most divergent (Lokossou *et al.*, 2009). Lokossou *et al.* (2009) demonstrated that these orthologues of R2 recognise full length PiAVR2. However, it could now be tested whether any of these R2 orthologues are different enough from R2 to allow recognition of PiAVR2-like. Co-infiltrations of each R2 orthologue with PiAVR2$^{K31}$ and PiAVR2-like were performed in *N. benthamiana* leaves. All three orthologues recognise PiAVR2$^{K31}$ to a similar level as R2 but none appear to recognise PiAVR2-like (Figure 3.7.1a and b). Agrobacterium expressing each *R* gene alone was used as a negative control to identify any possible auto-activation. The recognition spectrum of these *R* genes appears to be the same as *R2* and would therefore be no more useful than *R2* for breeding or engineering resistance to *P. infestans* genotypes that are homozygous for *PiAVR2-like*, such as genotype 13_A2.

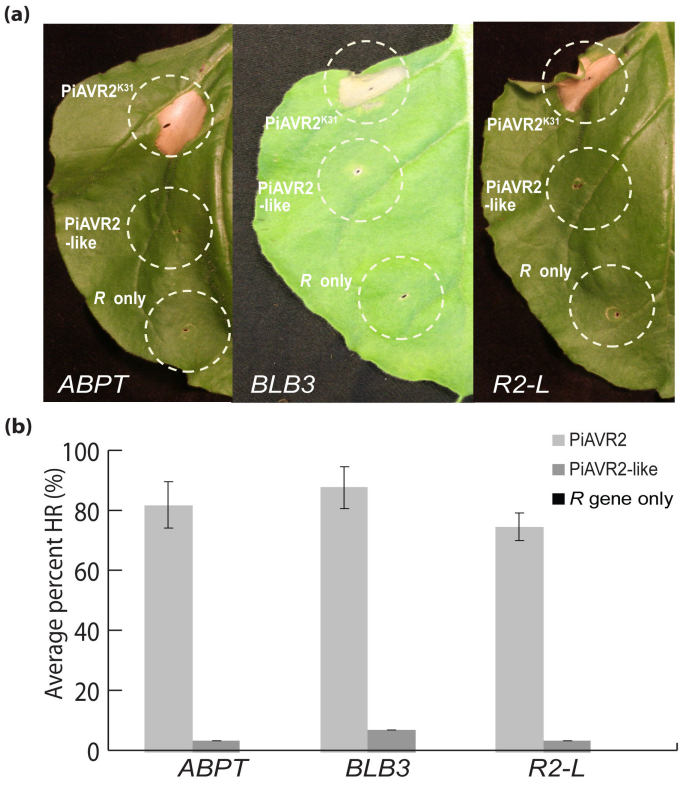


**Figure 3.7.1: R2 orthologues from potato linkage group IV.** (a) Leaf images of co-infiltrations into *N. benthamiana* leaves taken at 5 dpi. There were 3 biological reps with 24 infiltration sites in each rep. This shows recognition of PiAVR2$^{K31}$ by Rpi-abpt, Rpi-blb3 and R2-like, but all show weak recognition of PiAVR2-like. (b) Graph showing the percentage recognition for each of the *R* genes. The graph was generated from 3 reps each with 24 inoculation sites, HRs were counted at 5 dpi and the error bars represent +/- standard error.

Nicolas Champouret (Wageningen University, The Netherlands) provided six additional *R2*-like genes that were amplified from wild *Solanum* species (Champouret, 2010). These R2 orthologues share between 92.1% and 99.9% identity with R2, R2-like, Rpi-abpt and Rpi-blb3 at the amino acid level. The six new orthologues have been named *Rpi-edn1.1*, *Rpi-snk1.1*, *Rpi-snk1.2*, *Rpi-hjt1.1*, *Rpi-hjt1.2*, and *Rpi-hjt1.3*. *Rpi-edn1.1* was cloned from *S. edinense, Rpi-snk1.1* and *Rpi-snk1.2* were cloned from *S. schenckii* and *Rpi-hjt1.1*, *Rpi-hjt1.2*, and *Rpi-hjt1.3* were cloned from *S. hjertingii.* These new orthologues were tested

for their ability to recognise PiAVR2 and PiAVR2-like and their respective C-termini. This was done by co-infiltration of the *R* gene with the effector genes into *N. benthamiana* leaves. All of the new and old *R* genes are able to recognise PiAVR2-like C-terminus to varying degrees, some very efficiently (100%), and others weakly (10%-20%) (Figure 3.7.2). *Rpi-abpt, Rpi-edn1.1, Rpi-hjt1.2*, and *Rpi-hjt1.3* and *Rpi-snk1.2* are also able to recognise PiAVR2-like full length between 5% – 45% efficiency (Figure 3.7.2). Three of the new *R* genes (*Rpi-edn1.1, Rpi-hjt1.2* and *Rpi-hjt1.3*) auto-activate an HR at the concentrations used here (Figure 3.7.2). Unfortunately these are the *R* genes that weakly recognise PiAVR2-like. Consequently, there is no significant difference in the average HR induction by these three *R* genes between inoculation sites infiltrated with or without *PiAVR2-like*. All R2 orthologues are able to recognise PiAVR2 and PiAVR2 C-terminus as expected (Figure 3.7.2). Interestingly, none of the *R2* orthologues cloned thus far have provided more resistance to R2-breaking virulent isolates of *P. infestans* (Vivianne Vleewshouvers, Wageningen University, *personal communication*). This evidence suggests that cleavage of the effector proteins around the EER motif does not occur during or after translocation into host cells. If cleavage was occurring during a natural infection, *Rpi-edn1.1, Rpi-hjt1.2* and *Rpi-hjt1.3* that recognised PiAVR2-like C-terminus in more than 80% of the inoculation sites (Figure 3.4.2) may have provided adequate resistance to *PiAVR2-like* expressing isolates.

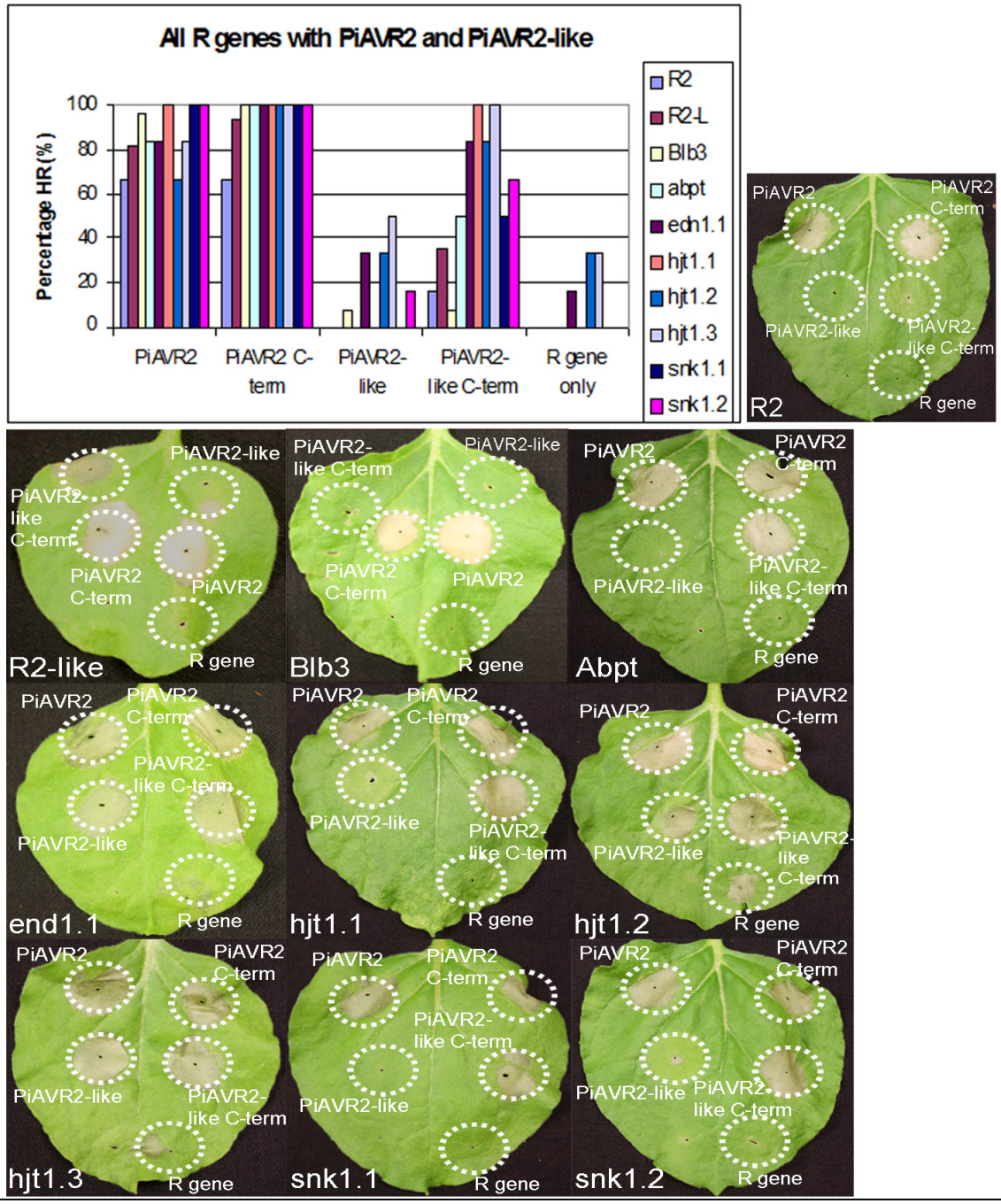


**Figure 3.7.2: Recognition spectrum of all 10 *R2* orthologoues**. Graph and leaf pictures of all 10 *R* genes co-infiltrated with PiAVR2, PiAVR2 C-terminus, PiAVR2-like, PiAVR2-like C-terminus into *N. benthamiana* leaves. Each R gene was infiltrated on its own as a negative control. Images and counting of the HRs was done at 5 dpi.

## 3.8 - Discussion

The identification of *PiAVR2* was delayed by the failure to identify BAC clones that completely spanned the mapped *AVR2* region. The genome sequence of T30-4 was critical in the completion of this region and a combination of this and the information from the BAC library led to the identification of three RXLR-dEER containing genes within the *AVR2* locus. The infiltration of these identified genes into 1512 c(16), an *R2*-expressing cultivar, showed a clear HR at the infiltration site of PITG_22870, thus identifying *PiAVR2*, while PITG_08949 reproducibly failed to trigger an HR (Figure 3.1.3).

Both *PITG_08949* and *PiAVR2* have the characteristic RXLR-dEER expression profile, which is up-regulation before infection and during the biotrophic phase (Figure 3.8.1a). Up-regulation before and during infection causes the accumulation of the encoded PiAVR2 protein at the haustoria (Figure 3.8.1b), which is consistent with other well characterised RXLR effectors such as *AVR3a* from *P. infestans* (Whisson *et al.*, 2007). There is also consistency between *PiAVR2* and *AVR3a* when these genes are silenced. It was shown in Figure 3.5.1a that transgenic isolates silenced for *PiAVR2* are unable to grow on the susceptible cultivar Bintje. This lack of growth was also seen when *AVR3a* was silenced (Bos *et al.*, 2010).

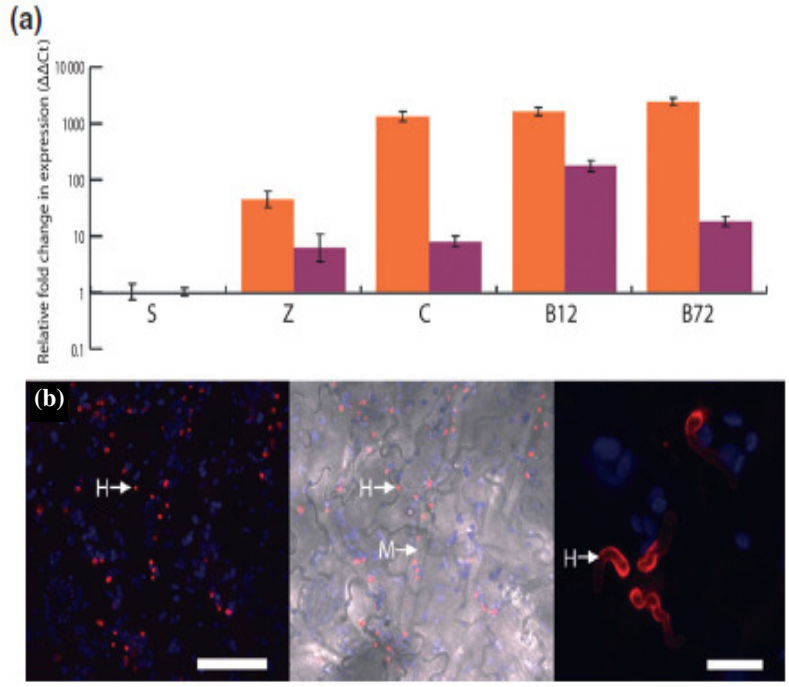


**Figure 3.8.1: PiAVR2 gene expression and protein accumulation.** (a) This shows the expression profile of PiAVR2 in orange, and PITG_08949 in purple. These are characteristic RXLR expression profiles. (b) A transgenic *P. infestans* isolate expressing PiAVR2::Tdtomato fusion. The fusion protein can be seen to accumulation at the haustoria (H). The middle panel shows the haustoria in relation to the mycelium (M), and the right panel shows a higher magnification of the haustorial accumulation. White bars are left panel 50 µm and right panel 10 µm. Gilroy *et al.,* 2011a.

It is believed that *P. infestans* RXLR effectors have a modular structure, whereby positive selection has acted on the C-terminal "effector" domain, resulting in high sequence variation across the family for interaction with a diverse set of targets in the host (Win *et al*., 2007;Dou *et al*., 2008). In contrast, the N-termini, which contain the signal peptide and the RXLR-dEER regions, appear to be relatively conserved, suggesting that they perform specific functions that constrain sequence evolution (Win *et al*., 2007; Dou *et al*., 2008). The high degree of sequence similarity between PiAVR2 and PITG_08949 over the first 79 amino acids (Figure 3.1.2) suggests that these two genes share a common ancestor. The complete sequence divergence after 79 amino acids, that produces two different C-termini, would most likely occur through a recombination event as the differences are not due to

frame shift mutations. The success of *P. infestans* as a pathogen is thought to be in part due to its complex and diverse set of RXLR effector genes that are undergoing relatively rapid evolution. This is thought to be achieved to some extent through recombination, and the sequences of *PiAVR2* and PITG_08949 provide a good example of this (Gilroy *et al.*, 2011a).

Interestingly, there appears to be a prevalence for *PiAVR2*$^{K31}$ in the population of *P. infestans* isolates which is similar to what has been observed for the *P. infestans* effector *AVR3a,* with *AVR3a*$^{EM}$ being more abundant in a diverse range of isolates than *AVR3a*$^{KI}$ (Armstrong *et al.*, 2005). For *AVR3a,* the reason for this bias could be due to *R3a* recognising *AVR3a*$^{KI}$*,* whereas *AVR3a*$^{EM}$ is able to evade recognition. This, however, is not the case for *PiAVR2* as both alleles, *PiAVR2*$^{N31}$ and *PiAVR2*$^{K31}$, are recognised by *R2*. The stronger recognition of the PiAVR2 C-term, Figure 3.1.3, which is shared between *PiAVR2*$^{N31}$ and *PiAVR2*$^{K31}$ also implies that this bias is not linked to evasion of *R2*-mediated recognition. The only phenotypic difference between the *PiAVR2*$^{N31}$ and *PiAVR2*$^{K31}$ so far has been the localisation of the corresponding proteins within plant cells. PiAVR2$^{K31}$ and PiAVR2$^{N31}$ localise to the plasma membrane and cytoplasm while PiAVR2$^{N31}$ also localises to chloroplasts. Perhaps the explanation for the prevalence of *PiAVR2*$^{K31}$ shall be explained by examination of the function of PiAVR2 (see later Chapters). The stronger recognition of the PiAVR2 C-term by R2 is an interesting observation when we consider that cleavage of both PiAVR2 and PiAVR2-like may occur when expressed *in planta* (Figure 3.6.1). An important question raised by this data is how appropriate is it to examine the recognition and function of only full length or C-termini of RXLRs, as some literature is based solely on one or the other and very rarely both.

PiAVR2$^{N31}$ and PiAVR2-like, both localise to chloroplasts, plasma membrane and cytoplasm. Chloroplast localisation is also seen for other pathogen effectors. For

example, HopI1 has a putative chloroplast-targeting sequence (Jelenska *et al.*, 2007). The chloroplast has a central role in plant defence, it is an important site for production of ROS, reactive nitrogen oxide intermediates (NOI) and plant hormones and it is also important for the formation of an HR (Coll *et al.*, 2011). It is interesting that PiAVR2$^{K31}$ does not share this chloroplast localisation even though there is only one amino acid difference with PiAVR2$^{N31}$. On the other hand, PiAVR2$^{N31}$ and PiAVR2-like do share chloroplastic localisation even though there are 13 amino acid differences between these proteins. The N31 amino acid is however conserved between PiAVR2$^{N31}$ and PiAVR2-like. Interestingly, Asparagine (N) is an uncharged amino acid whereas lysine (K) is basic implying that this non-conservative change at this key residue may determine chloroplast localisation.

A combination of weakly amplified PCR products and genome sequencing of the 2006_3928A isolate led to the identification of *PiAVR2-like* (David Cooke, the JHI, personal communication; Gilroy *et al.*, 2011a). During this identification process it was discovered that a 14.8 kb region that contains the *PiAVR2* paralogues is highly divergent in 2006_3928A compared to T30-4 (Gilroy *et al.*, 2011a). Cloning of this gene and co-expression with R2 in *N. benthamiana* revealed that PiAVR2-like is not recognised (Figure 3.3.2). The 13 amino acid changes between PiAVR2 and PiAVR2-like must play a role in the detection of these proteins by R2 and data in Figure 3.6.1 rules out 4 of the 13 changes in determining recognition by R2. It can be presumed that the key amino acid changes that determine recognition by R2 lie in the 5 amino acid polymorphisms at the end of the proteins but these have yet to be investigated.

It was shown in Figure 3.7.1 that the 4 characterised *R* genes *R2*, *R2-like, Rpi-abpt* and *Rpi-blb3* are all unable to recognise the full length PiAVR2-like. However, they are able to recognise PiAVR2-like C-term, although this is very weak for R2 and *Rpi-blb3* (between 10–18%), but stronger for R2-like and *Rpi-abpt* (between 35–50%) (Figure 3.7.2). The 6

new *R* genes found from other wild *Solanum* species, *Rpi-edn1.1*, *Rpi-snk1.1*, *Rpi-snk1.2*, *Rpi-hjt1.1*, *Rpi-hjt1.2*, and *Rpi-hjt1.3* have a similar recognition spectrum. They are all able to recognise PiAVR2-like C-term (Figure 3.7.2), and *Rpi-blb3, Rpi-edn1.1, Rpi-hjt1.2*, and *Rpi-hjt1.3* and *Rpi-snk1.2* all convey weak recognition to full-length PiAVR2-like in co-expression experiments. However, intriguingly, all 6 genes failed to provide resistance to isolates of *P. infestans* known to express *PiAVR2-like* (Vivianne Vleeshouwers, personal communication) which means new *R* genes that recognise PiAVR2-like are still needed.

In this study there were 12 *P. infestans* isolates that encoded both forms of *PiAVR2* and *PiAVR2-like* in their DNA (Figure 3.3.1) and that expression of these genes determined virulence on R2-expressing potato (Figure 3.4.1). Thus, any isolate of *P. infestans* that contains both forms will be virulent if only *PiAVR2-like* is transcribed, if PiAVR2 is transcribed then the isolate will be avirulent on R2-expressing plants. This has been further confirmed by transformation of the virulent isolate 2006_3928A with $PiAVR2^{K31}$ (Gilroy *et al.,* 2007). This isolate was then recognised by R2-expressing plants (Figure 3.8.2), demonstrating that the transcription of *PiAVR2* plays a critical role in the recognition of isolates. It appears that there are multiple factors that have led to the virulence of isolates on R2-expressing cultivars; the presence/absence of *PiAVR2*, differential expression of *PiAVR2* and *PiAVR2-like* and SNPs that occur between the two genes.

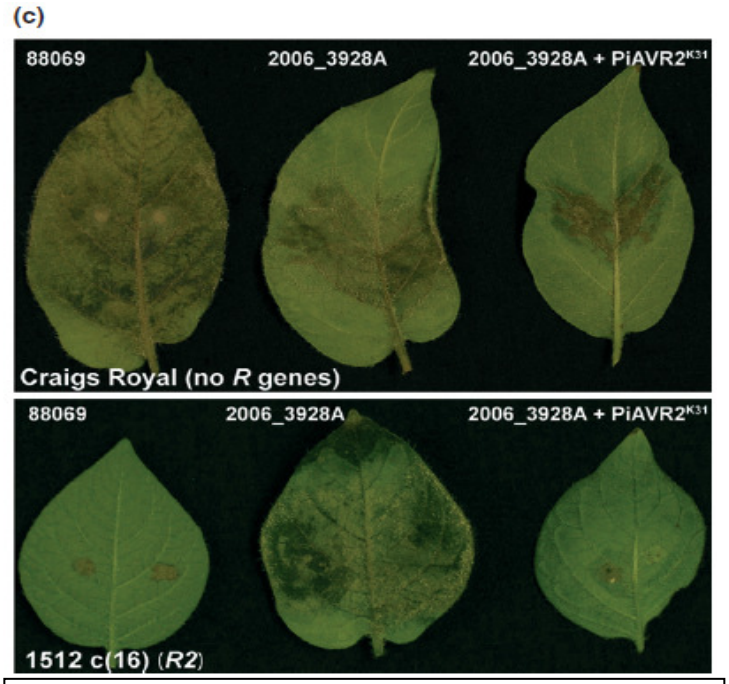


**Figure 3.8.2: Restoration of avirulence in a virulent isolate.** Top panel – a susceptible cultivar of potato, Craigs Royal, contains no R genes. Bottom panel – 1512 C(16) which is an *R2* expressing cultivar. Leaves were infected with 88069 (avirulent on R2), 2006_3928A (virulent on R2) and 2006_3928A transformed with *PiAVR2*$^{K31}$. Gilroy *et al.,* 2011a.

## Conclusions

Virulent and avirulent forms of *PiAVR2* were identified in many isolates of *P. infestans*. The initial identification of *PiAVR2* arose due to PiAVR2$^{N31}$ being recognised by the R2 containing cultivar 1512 c(16). The mechanism of virulence of *P. infestans* on *R2* plants was discovered by a combination of allele mining in the genomic DNA of 29 diverse isolates and semi qRT-PCR amplifications of the cDNA of 6 of the 29 isolates to determine expression of the *PiAVR2*/*PiAVR2-like* forms.

It has been shown that all isolates of *P. infestans* screened contained either the virulent form *PiAVR2-like* or avirulent form *PiAVR2* and when the expression of these genes are

reduced infection of susceptible plants is compromised. This evidence shows the importance of this effector to the pathogen. It has also been shown that the new *R2* orthologues do not have a greater spectrum of resistance than the existing four *R2*, *R2-like, Rpi-abpt* and *Rpi-blb3.* All 10 *R2-like* genes have been identified using allele mining of specific cultivars which were thought to contain the same linkage group IV. In order to find an *R* gene that is able to recognise PiAVR2-like different wild Solanum species could be screened which may provide another *R* gene, that is not related to the *R2* gene family that has the ability to recognise PiAVR2-like. An *R* gene which is not related to the *R2* gene family which has the ability to recognise PiAVR2 has already been discovered from *S. mochiquense* called *Mcq1* (Smilde et al., 2005). If an *R* gene which recognised *PiAVR2-like* could be found and used in combination with one of the *R2* genes or *Mcq1* this would provide greater durable resistance. This would also apply a large selection pressure for *P. infestans* isolates given the apparent importance of this effector.

# 4 – PiAVR2 targets the brassinosteroid signal transduction pathway

## 4.1 - Introduction

In Chapter 3 the avirulent and virulent forms of PiAVR2 were described and the means by which *P. infestans* achieves virulence on *R2*-expressing cultivars was revealed. It next seemed logical to ask: what is the host target and function of this important effector during a *P. infestans* infection? It was subsequently discovered that PiAVR2 is interacting with components of the brassinosteroid pathway. This pathway was introduced in Chapter 1, but more detail is warranted here.

The brassinosteroid (BR) pathway is complex. However, the roles of some of the most important proteins are well understood, particularly in *A. thaliana*. Nevertheless, there are still a significant number of proteins and signalling events in the pathway still to be uncovered and functionally characterized, even in *A. thaliana.* Unfortunately, the translation of information from the model plant *A. thaliana* to crop species has not been published in much detail. The focus of this chapter will be on some of the major components of the BR pathway in *A. thaliana* that are to be investigated in this work (refer to Figure 1.3.2 for a diagram of the pathway).

The first component of this pathway is the cell surface receptor BRASSINOSTEROID-INSENSITIVE 1 (BRI1), which contains an extracellular LRR domain and intracellular Ser/Thr kinase domain and is one of the best-studied plant receptor kinases (Oh *et al.*, 2012). This receptor is responsible for the perception of extracellular BR hormones and subsequent activation of the downstream signal transduction pathway. There are many studies showing that the loss of this receptor has a dramatic effect on the growth and

development of plants, leaving them severely stunted with small and curling leaves (Clouse *et al.*, 1996; Li and Chory, 1997). Three homologues of *BRI1* have been identified, called *BRI1-like* (*BRL1*, *BRL2* and *BRL3*). Of these BRL1 and BRL3 are also functional BR receptors (Cano-Delgado *et al.*, 2004). Both these receptor homologues can rescue the *bri1* mutant phenotype when they are expressed under the control of the *BRI1* promoter, while a triple mutant of *bri1*, *brl1* and *brl3* has an enhanced dwarfed phenotype (Cano-Delgado *et al.*, 2004). *BRI1* is expressed in all growing cells, although *BRL1* and *BRL3* are expressed in non-overlapping vascular tissue. All three play a key role in growth and development of plants (Cano-Delgado *et al.*, 2004).

BRASSINOSTEROID INSENSITIVE1-ASSOCIATED KINASE1 (BAK1) is the next key component of the BR pathway and a co-receptor of BRI1, but is also a co-receptor with the LRR-RLKs FLAGELLIN SENSING 2 (FLS2) and EF-TU RECEPTOR (EFR) during PTI. BAK1 (SERK3) belongs to a subclass of LRR-RLKs referred to as the SOMATIC-EMBRYOGENESIS RECEPTOR-LIKE KINASE (SERK) family, which consists of five closely-related members in *A. thaliana*. The binding of Brassinolide (BL), the most abundant BR hormone, causes BRI1 and BAK1 to heterodimerize and become activated by auto- and transphosphorylation (Wang *et al.*, 2008). When BAK1 is over-expressed, stems, leaves and petioles are elongated (Li *et al.*, 2002), indicating an increase in the BR signal transduction pathway. Loss of function mutants of BAK1 result in plants with a slight dwarf phenotype which have a reduced sensitivity to BL (Li *et al.*, 2002). When a dominant negative mutant of BAK1 is over-expressed a severe dwarf phenotype is observed, similar to *bri1* (Li et al., 2002). This leads to the conclusion that the slight phenotype seen by the loss of function mutant is due to redundant functions of other BAK1 family members. Intriguingly, SERK1 and BAK1-LIKE1/SERK4 (BKK1/SERK4) also interact with BRI1 as positive regulators of BR responses (Karlova *et al.*, 2006; He *et al.*, 2007; Albrecht *et al.*, 2012)

The phosphorylation of BR-SIGNALLING KINASE 1 (BSK1) by active BRI1 triggers BSK1 activation and its dissociation from the BRI1 receptor. BSK1 is the activator of BRI1 SUPPRESSOR 1 (BSU1) (Kim *et al.*, 2009). There are also family members of BSK1 called BSK2 and BSK3; these are thought to have redundant function within the pathway (Tang *et al.*, 2008).

BSU1 is a phosphatase in the BR pathway and is part of a family of genes that contains 3 other members named *BSU-like 1*, *2* and *3* (*BSL1*, *2* and *3*). This family of genes encode Ser/Thr Kelch-repeat containing phosphatases and are thought to function solely in the BR pathway. The BSU1-like family are positive regulators of the BR pathway. The *A. thaliana* literature is limited on this gene family. In this Chapter the focus will be on *BSL2* and *BSL3* as *BSL1* will be looked at in more detail in Chapter 5. It is thought that *BSL2* and *BSL3* are expressed throughout the plant but are more highly expressed in the younger parts of the plant (Mora-Garcia *et al.*, 2004). *BSL2* and *BSL3* have 88% nucleotide sequence identity making it difficult for micro-arrays to distinguish between them (Mora-Garcia *et al.*, 2004). RNAi lines of *BSL2* and *BLS3* were made to determine what effect the silencing of these two genes had on plant growth and development. An RNAi construct designed within a Kelch-repeat domain was generated that could knock down both *BSL2* and *BSL3*. The *BSL2* and *BSL3* genes showed 89% nucleotide sequence identity within the region where the construct was designed (Mora-Garcia *et al.*, 2004). This construct only had 59% and 70% identity to *BSU1* and *BSL1*, respectively (Mora-Garcia *et al.*, 2004). The RNAi plants showed dwarfism that resembles the *bri1* deficient phenotype, implying that these genes may be involved in the elongation process in plant development (Mora-Garcia *et al.*, 2004). To further investigate this family, *BSL2* and *BSL3* RNAi was performed on *bsu1* and *bsl1* double knock-out plants. This produced an extremely dwarfed plant with an abundance of stomata on the leaf epidermis, further

showing the link between this family and the growth and development of plants (Kim *et al.*, 2009; Kim *et al.*, 2012).

BR-INSENSITIVE 2 (BIN2) is dephosphorylated by BSU1. BIN2 is an AtGSK-like kinase, which phosphorylates transcription factors. This phosphorylation results in them being targeted for degradation. The dephosphorylation of BIN2 by BSU1 allows the accumulation of unphosphorylated transcription factors and, thereafter, the transcription of BR-responsive genes.

No studies of the *BSL* genes have been documented in the *Solanaceae*, which makes this work novel. However this also leads to difficulties. Not all the information generated in the model plant, *A. thaliana*, is easily transferable to other plant species. This could be due to differences occurring in gene evolution, differences in gene regulation or loss/gain of genes. There is also a challenge in that not all the tools used in *A. thaliana* research are available to other plant species. This Chapter will investigate the BR pathway in *Solanaceae* to determine if the key components from *A. thaliana* are intact and the role of this pathway during a *P. infestans* infection, looking specifically at *BSL2*, *BSL3*, *BRI1* and *BAK1*.

## 4.2 – A BR pathway protein is the host target of PiAVR2

To determine the host target of the avirulence protein PiAVR2 from *P. infestans* a Yeast Two Hybrid (Y2H) library screen was undertaken. The library was made from pooled, pathogen-challenged resistant and susceptible potato cultivars. Nine million colonies were screened in this experiment, but only 64 grew sufficiently to pick for the reporter gene assays. All 64 colonies grew on plates lacking leucine, tryptophan and histidine (LTH), five turned blue in the *LacZ* reporter gene assay and two grew on plates lacking leucine,

tryptophan and uracil (LTU) (Figure 4.2.1). These two samples that grew activated the *URA3* reporter gene (LTU plates) and also turned blue in the *LacZ* reporter gene assay. Plasmids from the five colonies positive on the *LacZ* reporter gene assay were sequenced. Colonies 35 and 51 were thought to be out-of-frame fragments and were not considered further. It was determined that colonies 3, 15 and 53 all contained 3' fragments from the same gene of around 1.2 Kb in length that encoded a complete phosphatase domain. The longest fragment was used to search the TAIR10 database using BLASTN default settings. The results indicated that this interacting phosphatase domain was most similar to members of the BSU1 family of kelch-repeat containing Ser/Thr phosphatases with the most similar sequence being AtBSL3. Therefore it will tentatively be refered to as StBSL3 C-terminus. A confirmation Y2H experiment showed that PiAVR2 interacts with a 400 amino acid fragment of StBSL3, as the transformed yeast grew on both the *HIS3* and *LacZ* reporter gene assays when compared to a negative control empty vector (Figure 4.2.2).

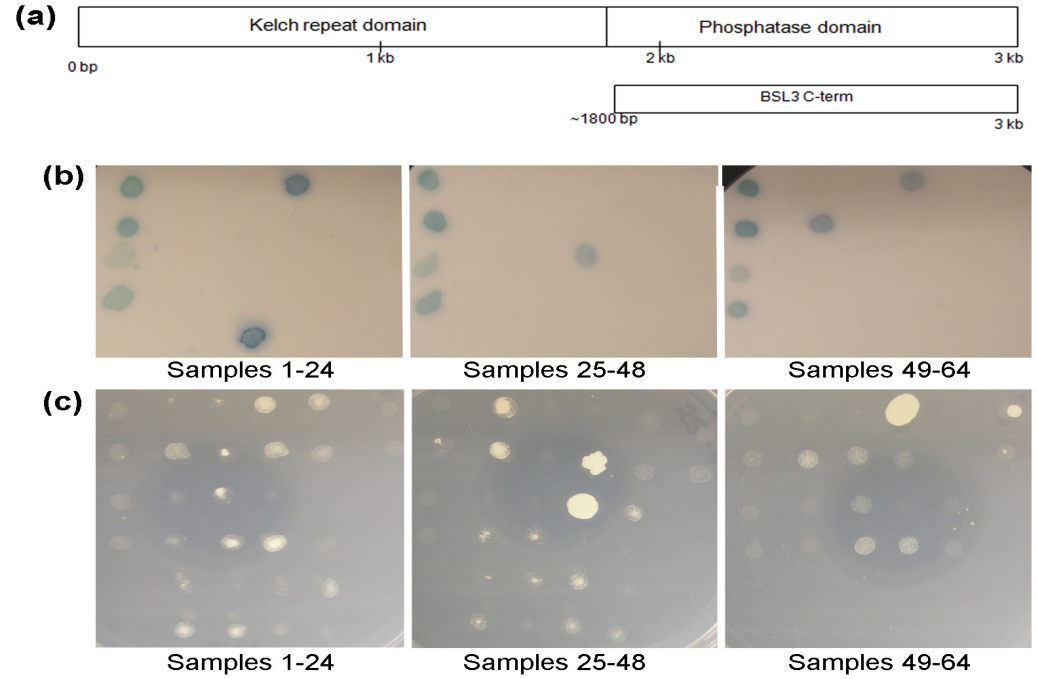


**Figure 4.2.1: Original Y2H reporter gene assay.** **(a)** Schematic of BSL domain structure with the BSL3 C-terminus shown in order to visualise the section found in the Y2H screen. **(b)** *LacZ* reporter gene assay showing blue colouration of positive colonies: numbers 3, 15, 35, 51 and 53. Positive controls are the four blue spots on the left of the membrane. The numbering of the colonies spotted is by rows. **(c)** The *URA3* reporter gene assay shows growth of colonies 35 and 51 on plates lacking LTU. The positive controls are spotted on to the left hand side of the plate but have not grown well. Again the numbering of the colonies is by row.

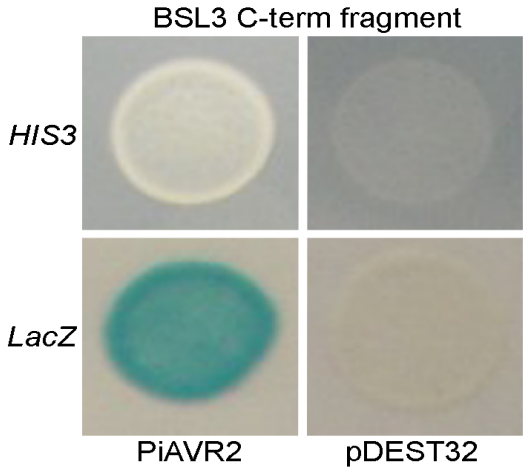


**Figure 4.2.2: Confirmation of Y2H library screen.** Protein fragment recovered from the library screen test with PiAVR2 in the first column, second column is empty pDEST32 as negative control. Top panel is the histidine reporter assay, bottom panel is the *LacZ* reporter gene.

## 4.3 – Confirmation of the host target of PiAVR2

The StBSL3 C-terminus was tested in a specific Y2H assay to determine if it could interact with any of the other PiAVR2 forms. These results show that all forms of PiAVR2 were able to interact in the yeast system with this StBSL3 C-terminus, as there is good growth on the *HIS3* reporter gene assay and the *LacZ* gene was activated to cause blue colouration of the yeast cells on X-gal substrate (Figure 4.3.1a). The closely related *P. infestans* gene PITG_08949, however, did not interact with StBSL3 C-terminus. The empty vector pDEST32 acts as a negative control and shows minimal growth on the histidine reporter assay.

Using the nucleotide sequence of the *StBSL3* C-terminus encoding fragment (C-term), a 5' RACE primer was designed. This primer and the RACE protocol generated enough sequence information to allow cloning of the entire coding sequence from *S. tuberosum*. The full length *StBSL3* is 3 kb in length and was placed in the Y2H vector pDEST22. With the full length *StBSL3* a specific screen was performed against all of the PiAVR2 forms. It was shown that interaction only occurs with the full length forms of PiAVR2: PiAVR2$^{N31}$, PiAVR2$^{K31}$, and PiAVR2-like, shown by the *LacZ* reporter gene causing the blue colouration (Figure 4.3.1b). It appears that this interaction is quite weak as the blue colouration is faint. There is no interaction with the C-termini of PiAVR2 or PiAVR2-like, shown by the lack of blue colouration and slightly reduced growth on the LTH plates. PITG_08949 again does not show any interaction with the full length StBSL3 protein, and the empty pDEST32 vector was included as a negative control (Figure 4.3.1b).

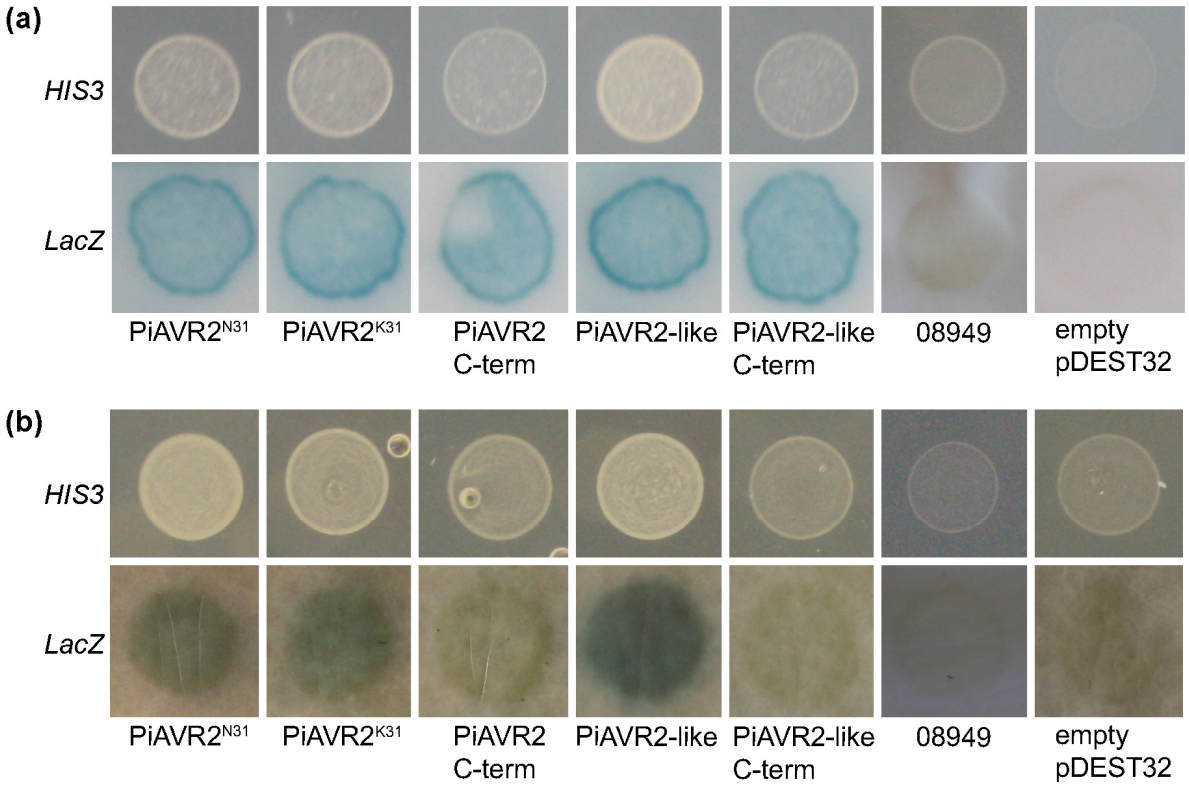


**Figure 4.3.1: Specific Y2H screens with PiAVR2 forms and StBSL3. (a)** StBSL3 C-term specific screen with all PiAVR2 forms and PITG_08949. Top panel shows the *HIS3* reporter gene and the bottom shows the *LacZ* reporter gene. **(b)** StBSL3 full length specific screen against all the PiAVR2 forms and PITG_08949. Top panel shows the *HIS3* reporter gene and the bottom shows the *LacZ* reporter gene.

*In planta* confirmation was sought using bimolecular fluorescence complementation (BiFC). However, after many repetitions, and using all available combinations of vectors, fluorescence was not observed. Instead co-localisation was performed using YFP_StBSL3 and PiAVR2_RFP to determine if, individually, the localisations were very different. The images below were taken by Tanya Bukharova at the JHI (Figure 4.3.2). These show that both PiAVR2 full length forms and StBSL3 localise to the cytoplasm and plasma membrane of cells, although the images of the PiAVR2 C-termini show that they localise primarily to the plasma membrane. An overlap in the RFP and YFP fluorescence for these proteins only occurs at the plasma membrane. The individual proteins appear to

localise to a similar region of the cells. However, it is difficult to draw any conclusions from the cytoplasmic localisation as to why the split YFP would not be working. There are so many proteins located in the cytoplasm, it could be that PiAVR2 and StBSL3 are genuinely not interacting or it could be that the folding of the large protein causes steric hindrance to prohibit interaction of the two YFP halves from occurring. It was predicted that an interaction *in planta* between PiAVR2 and StBSL3 would be seen, as another labratory has confirmed this interaction *in planta* using co-immunoprecipitation in *N. benthamiana* of PiAVR2 and StBSL3 (S. Kamoun, the Sainsbury Laboratory, personal communication).

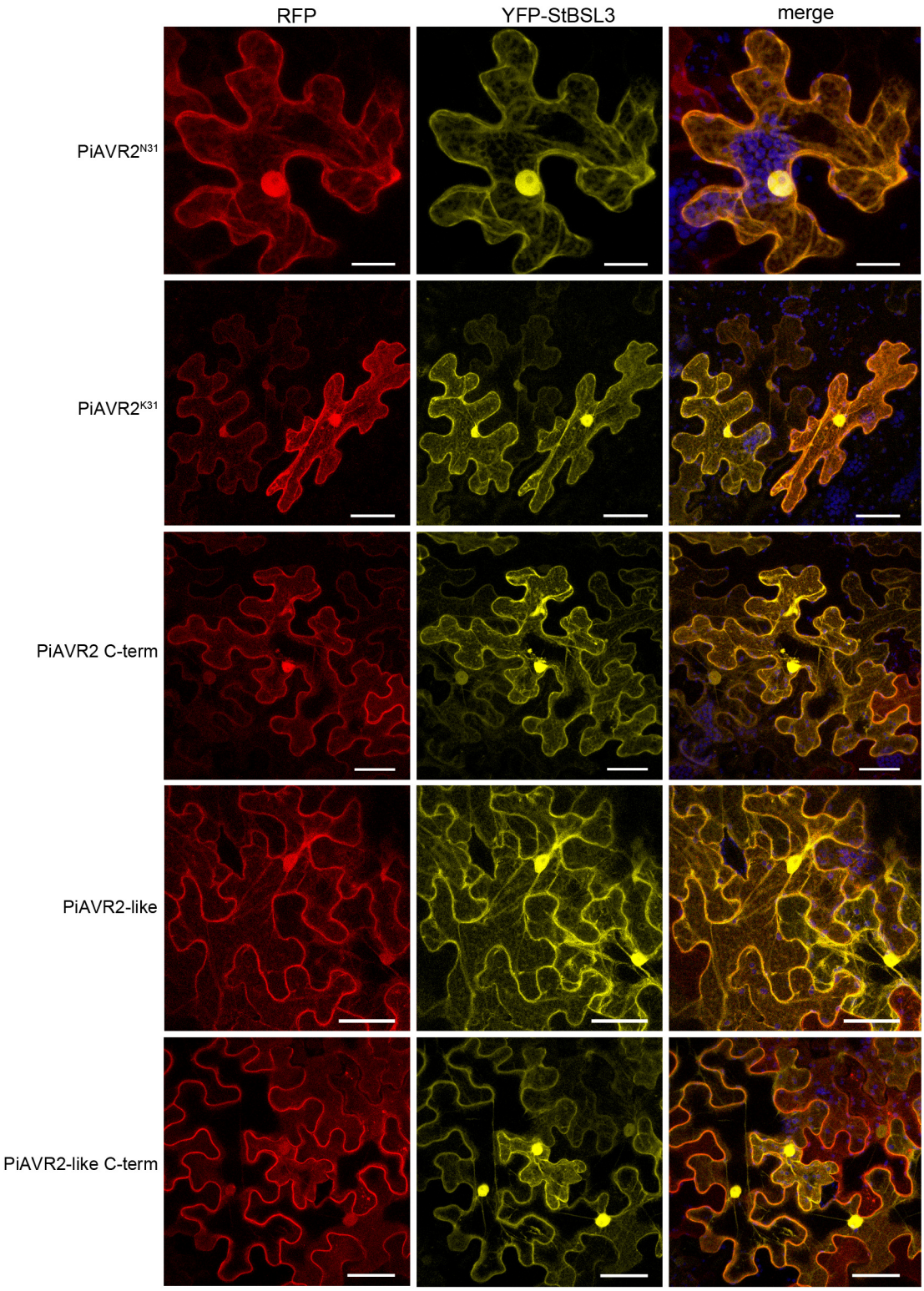


**Figure 4.3.2: Co-localisation of PiAVR2-RFP forms with YFP-BSL3.** Images were taken at 2 dpi with a final $OD_{600}$ of 0.1 using the Leica imaging software. The first row of images are PiAVR2 forms tagged at the C-terminus with RFP, the second row is StBSL3 tagged at the N-terminus with YFP and the final row is a merged image showing an overlap of fluorescence. The blue in the merged images are the chloroplast. Scale bars are 50 µm.

## 4.4 – The BSL family

The sole interactor of PiAVR2 discovered in the Y2H library screen appears to be StBSL3. As stated in the introduction, *AtBSL3* is part of a family made up of four genes with a high level of sequence similarity. This family was investigated in the *Solanaceae* to determine if it consisted of the same number of genes and to determine the level of similarity between the genes. As described in Section 4.3 *StBSL3* was cloned from *S. tuberosum* cDNA using primers that were designed as a result of a 5' RACE, and from sequencing the Y2H interactor fragment, *StBSL3 C-term.* In the case of *StBSL1* a full length EST (TC194541 TC187939) was found for the *Solanum lycopersicum BSL1* using The Gene Index Project database in April 2009. Primers were designed based on this EST and the equivalent gene was amplified from *S. tuberosum* cDNA. The sequence information for *StBSL1* and *StBSL3* was generated from the cloning of these two genes from *S. tuberosum* cDNA. There was no information available to design primers for the amplification of *StBSL2* or *StBSU1.* To generate sequence information on these genes Leighton Pritchard (the JHI) used *AtBSL2* and *AtBSU1* to search the *S. tuberosum* cv. *Phureja* genome (version 3.4) using BLASTX to find the the most similar sequence to each gene. BLASTX yielded a top result for *AtBSL2,* which was then used as a query to search the *A. thaliana* database using BLASTP. This yielded a reciprocal blast match for AtBSL2. This implies that the top result, now named *StBSL2,* is a putative orthologue of *AtBSL2.* The sequence information generated for *StBSL2* allowed the design of primers for the cloning of *StBSL2* from *S. tuberosum* cDNA. The same search process was carried out for *AtBSU1*: BLASTX on the *S. tuberosum* cv. *Phureja* genome (version 3.4) generating a top result with only 38% identity over 100% query coverage. The top result was used as a query for BLASTP on the *A. thaliana* database but there was no reciprocal blast match found for AtBSU1. The low level of sequence identity, at 38%, cast doubt on the direct transfer of functional annotation for this gene.

The EST databases of *S. tuberosum* and *S. lycopersicum* were also searched using the *AtBSU1* sequence but no matches were made. For *BSU1* the combination of the lack of a reciprocal blast match and no information being found in the EST databases excludes *BSU1* from further investigation in the *Solanaceae*. The three genes amplified from *S. tuberosum* cDNA, *StBSL1*, *StBSL2* and *StBSL3* were each queried against the *A. thaliana* TAIR10 database from the TAIR website using the BLASTN tool, to confirm sequence similarity. For this BLASTN search the nucleotide mismatch parameters were changed from the default of -3 to -1 (Table 4.4.1). For *StBSL1* the BLASTN top hit is *AtBSL1,* and percentage coverage is 100% while percentage identity of the alignment is 75%. This is a reasonable match when comparing sequences between species. The next five BLAST results for *StBSL1*, which are the remaining genes from the AtBSU1-family, show less than the 100% percentage coverage that was seen for *AtBSL1*. These BLASTN data imply that S*tBSL1* is putatively the orthologue of A*tBSL1*. The BLASTN top match for *StBSL2* is *AtBSL3* splice variant 1 with 79% identity over 95% query coverage while the top result for *StBSL3* is *AtBSL2* splice variant 1 with 78% identity over 94% query coverage (Table 4.4.1). Although the most similar sequences to *StBSL2* and *StBSL3* are convincing there is not much difference between the four most similar sequences shown below for either gene. This implies that they have such a high level of similarity that it is difficult to separate them at the nucleotide level. Another interesting observation is that the *AtBSU1* nucleotide sequence appears quite divergent to the *StBSLs* as it is always the 6$^{th}$ result and in the case of *StBSL2* and *StBSL3* the percentage coverage is quite poor at 50-54%.

| ***S.tuberosum* gene** | **Atg number** | ***A. thaliana* gene name** | **Bit score** | **E value** | **Percentage coverage** | **Percentage identities** |
|---|---|---|---|---|---|---|
| *StBSL1* | AT4G03080.1 | *BSL1* | 2065 | 0.0 | 100% | 75% |
| | AT1G08420.2 | *BSL2* | 787 | 0.0 | 71% | 70% |
| | AT1G08420.1 | *BSL2* | 787 | 0.0 | 80% | 68% |
| | AT2G27210.2 | *BSL3* | 752 | 0.0 | 73% | 69% |
| | AT2G27210.1 | *BSL3* | 752 | 0.0 | 81% | 68% |
| | AT1G03445.1 | *BSU1* | 518 | e-145 | 76% | 64% |
| | | | | | | |
| *StBSL2* | AT2G27210.1 | *BSL3* | 2608 | 0.0 | 95% | 79% |
| | AT1G08420.1 | *BSL2* | 2607 | 0.0 | 94% | 79% |
| | AT2G27210.2 | *BSL3* | 1719 | 0.0 | 95% | 79% |
| | AT1G08420.2 | *BSL2* | 1711 | 0.0 | 93% | 80% |
| | AT4G03080.1 | *BSL1* | 779 | 0.0 | 65% | 69% |
| | AT1G03445.1 | *BSU1* | 367 | e-100 | 54% | 60% |
| | | | | | | |
| *StBSL3* | AT1G08420.1 | *BSL2* | 2497 | 0.0 | 94% | 78% |
| | AT2G27210.1 | *BSL3* | 2453 | 0.0 | 95% | 78% |
| | AT1G08420.2 | *BSL2* | 2434 | 0.0 | 94% | 78% |
| | AT2G27210.2 | *BSL3* | 2390 | 0.0 | 95% | 77% |
| | AT4G03080.1 | *BSL1* | 665 | 0.0 | 70% | 67 % |
| | AT1G03445.1 | *BSU1* | 340 | 5e-92 | 50% | 61% |

**Table 4.4.1: BLASTN nucleotide mismatch -1 *StBSL* results.** The top six most similar sequences for each *StBSL* gene blast are shown along with their bit score, E value, percentage coverage and percentage identities. This data was generated using the TAIR blast tool searching the TAIR10 database.

The sequence similarity of these genes was also tested at the protein level as this is a better comparative measure for protein structure and function. BLASTX searches were conducted on the TAIR website, searching the TAIR10 database, using the default settings to determine how well the amino acid sequence between the species was conserved. This aids in determining if these genes from *S. tuberosum* are putative orthologues indicating functional conservation. The BLASTX results for StBSL1, StBSL2 and StBSL3 are shown below (Table 4.4.2).

| ***S.tuberosum* protein** | **Atg number** | ***A. thaliana* protein name** | **Bit score** | **E value** | **Percentage coverage** | **Percentage identities** |
|---|---|---|---|---|---|---|
| StBSL1 | AT4G03080.1 | BSL1 | 1346 | 0.0 | 100% | 76% |
| | AT1G08420.1 | BSL2 | 982 | 0.0 | 100% | 57% |
| | AT2G27210.1 | BSL3 | 980 | 0.0 | 100% | 57% |
| | AT1G08420.2 | BSL2 | 971 | 0.0 | 100% | 56% |
| | AT2G27210.2 | BSL3 | 969 | 0.0 | 100% | 56% |
| | AT1G03445.1 | BSU1 | 783 | 0.0 | 77% | 50% |
| | | | | | | |
| StBSL2 | AT2G27210.1 | BSL3 | 1604 | 0.0 | 100% | 80% |
| | AT2G27210.2 | BSL3 | 1589 | 0.0 | 100% | 79% |
| | AT1G08420.1 | BSL2 | 1585 | 0.0 | 100% | 79% |
| | AT1G08420.2 | BSL2 | 1570 | 0.0 | 100% | 78% |
| | AT4G03080.1 | BSL1 | 659 | 0.0 | 79% | 68% |
| | AT1G03445.1 | BSU1 | 466 | e-131 | 44% | 51% |
| | | | | | | |
| StBSL3 | AT2G27210.1 | BSL3 | 1590 | 0.0 | 100% | 79% |
| | AT2G27210.2 | BSL3 | 1575 | 0.0 | 100% | 79% |
| | AT1G08420.1 | BSL2 | 1570 | 0.0 | 100% | 78% |
| | AT1G08420.2 | BSL2 | 1555 | 0.0 | 100% | 77% |
| | AT4G03080.1 | BSL1 | 654 | 0.0 | 80% | 67% |
| | AT1G03445.1 | BSU1 | 459 | e-129 | 74% | 51% |

**Table 4.4.2: Results of BLASTX using the *StBSL* genes.** The top six most similar sequences for each *StBSL* gene using blastx are shown along with their bit score, E value, percentage coverage and percentage identities. This data was generated using the TAIR blast tool searching the TAIR10 database.

For the StBSL1 protein the top match is AtBSL1 protein with 76% identities over 100% of the query protein (Table 4.4.2). There is a drop to between 50%-57% identities over the next five similar sequences which are the rest of the AtBSU1-like family. There is consistency over the two tables (Tables 4.4.1 and 4.4.2), when StBSL1 is used as the query the most similar sequences in both BLASTN and BLASTX is AtBSL1. The BLAST outputs for StBSL2 and StBLS3 given in the tables do not allow for clear separation of these genes, an understanding of the biological function of these genes may help in determining their putative orthologues within *A. thaliana*. The best BLASTX result for

StBSL2 is AtBSL3 splice variant 1 (Table 4.4.2), and this is consistent with the best *StBSL2* BLASTN result (Table 4.4.1). The two best BLASTX results for StBSL2 are the splice variants of AtBSL3, with the splice variants of AtBSL2 being 3rd and 4th. There is only two percent difference between the top four results; this shows how closely related StBSL2 is to both AtBSL2 and AtBSL3. The results for the StBSL3 search are in exactly the same order as those for StBSL2, with AtBSL3 splice variant 1 being the top result, but the percentage identities are slightly reduced compared to the StBSL2 percentages (Table 4.4.2). This top result for StBSL3 is not consistent with the above BLASTN results for *StBSL3* which show *AtBSL2* splice variant 1 as the top result (Table 4.4.1). Overall these two BLAST outputs show is that AtBSL1 and StBSL1 are most similar to each other but there is not much sequence difference between BSL2 and BSL3 in either plant species.

In order to investigate the ancestral divergence and sequence similarity of these genes a phylogenetic tree was generated by aligning the protein sequences from each species and back-translating that alignment to the nucleotide sequences using T-COFFEE (Notredame *et al*., 2000). TOPALi v2.5 (Milne *et al*., 2009) was used to draw a maximum likelihood tree using the full length nucleotide sequence (100 bootstraps) and the tree was re-rooted in FigTree v1.3.1 (http://tree.bio.ed.ac.uk/software/figtree/). AtPP2AB'alpha was used as the outlier (Figure 4.4.1a). AtPP2AB'alpha is a PP2A phosphatase that is distantly related to the BSL sequences, but is also found in the BR signal transduction pathway. The tree and the Blast data above indicate that *StBSL2* and *StBSL3* are paralogues within *S.tuberosum.* These four genes from *A. thaliana* and *S. tuberosum* may result from independent divergence of these genes, from a common ancestral gene found in both *A. thaliana* and *S. tuberosum,* after speciation had occurred (Figure 4.4.1a). The reconstruction is not as clear regarding *AtBSL1* and *StBSL1.* The nucleotide sequences of *AtBSL1*, *StBSL1* and *AtBSU1* appear to have relatively noisy nucleotide alignments, consistent with more ancient divergence. This makes it difficult to resolve the order of

divergence and this uncertainty is shown by the low bootstrap values at these branch points (Figure 4.4.1a). A phylogenetic tree based on the protein alignment generated in T-COFFEE was constructed. Again a maximum likelihood tree using the full length protein sequence with 100 bootstraps was generated in TOPALi v2.5 and the tree re-rooted in FigTree. This again indicates that StBSL2/3 are clearly paralogues within *S. tuberosum* but the information is not available to determine if they are orthologues of *AtBSL2/3* (Figure 4.4.1b). The relationship between StBSL1, AtBSL1 and AtBSU1 is again uncertain, and the branching is not robust. What is clear from both nucleotide and protein trees is that there is significant sequence divergence of StBSL1 from StBSL2 and StBSL3. Since this tree depicts protein similarity this separation could imply a different function for StBSL1. Given the uncertainty over the AtBSL1, StBSL1 and AtBSU1 sequences, another phylogenetic tree was reconstructed using only the phosphatase domains, as it was believed that these regions of the proteins could have been under relatively little diversifying selection pressure. This tree is consistent with an orthologous relationship between StBSL1 and AtBSL1, although the bootstrap values for AtBSU1 are still so low that its position on the tree is uncertain (results not shown).

From the Blast results shown in Tables 4.4.1 and 4.4.2 and the phylogenetic trees in Figure 4.4.1 it can be concluded that *StBSL1* may be the putative orthologue of *AtBSL1*. It also appears that the two genes cloned from *S. tuberosum* cDNA both have a high level of sequence similarity, at the nucleotide and amino acid level, to two genes from *A. thaliana BSL2/3*. The branching of the two *S. tuberosum* genes on both trees implies that these are paralogues from *S. tuberosum* that arose after speciation, rather than putative orthologues of *AtBSL2* or *AtBSL3*. The discovery that the two genes amplified from *S. tuberosum* cDNA are paralogues results in them being re-named from here on. *StBSL3* will be known from now on as *StBSL2a* as it was the first discovered and *StBSL2* will be known from now on as *StBSL2b*.

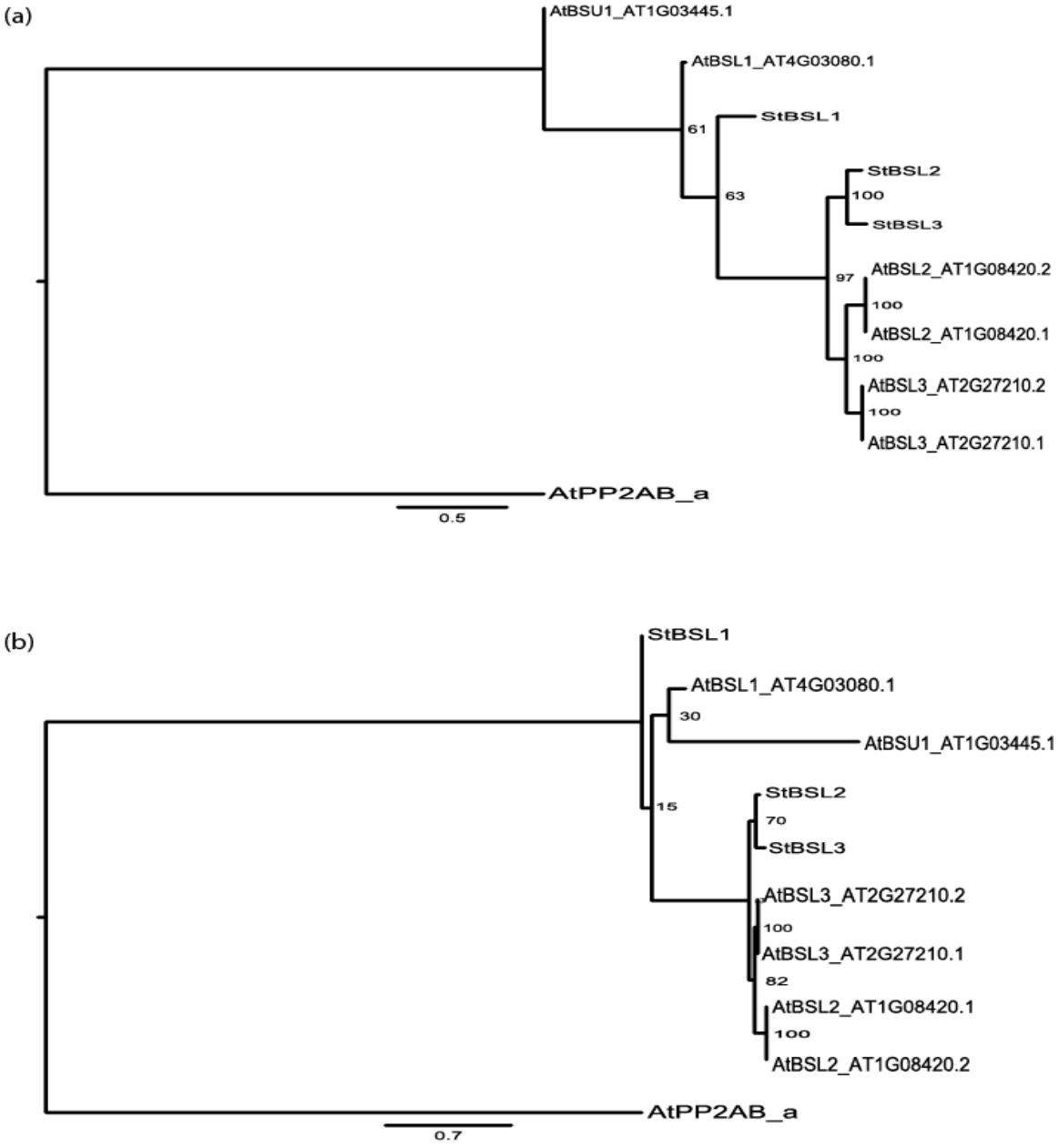


**Figure 4.4.1: Phylogenetic trees of all StBSLs with AtBSU1-family. (a)** a maximum likelihood tree based on backtranslated full length nucleotide sequences of *St* and *AtBSLs*, *AtBSU1* and *AtPP2AB'alpha*. The tree was generated in TOPALi using a bootstrapping of 100 and re-rooted in FigTree. **(b)** a maximum likelihood tree based on the full length protein alignment made from St and AtBSLs, AtBSU1 and AtPP2AB'alpha. The tree was generated in TOPALi using a bootstrapping of 100 and re-rooted in FigTree. From this protein alignment TOPALi generated this phylogenetic tree.

## 4.5 – StBSL2b is also a host target of PiAVR2

It was shown above that the *StBSL2a* and *StBSL2b* genes amplified from *S. tuberosum* cDNA are paralogues. It was also shown that *StBSL2a* and *StBSL2b* have very similar sequence identity to each other. With this information it seemed strange that StBSL2b was not recovered from of the Y2H library screen. Therefore, to determine whether StBSL2b could also physically interact with the PiAVR2 forms within the Y2H system, StBSL2b was co-transformed into yeast cells with each of the PiAVR2 forms. The results show that there is no growth of colonies on the *HIS3* reporter gene assay and no blue colouration of the colonies using the *LacZ* reporter gene for PiAVR2 C-term, PiAVR2-like C-term or PITG_08949 colonies (Figure 4.5.1). There is growth on the *HIS3* reporter gene assay and blue colouration on the *LacZ* assay for the full length PiAVR2 forms i.e. $PiAVR2^{N31}$, $PiAVR2^{K31}$ and PiAVR2-like (Figure 4.5.1). It appears that only the full length PiAVR2 forms can interact with StBSL2b (Figure 4.5.1). These results are consistent with what was seen for the StBSL2a full length protein (formerly StBSL3) (Figure 4.3.1b). This result implies that there is not only sequence similarity between StBSL2a and StBSL2b but they may also have similar functions *in planta* if they are both targets of PiAVR2.

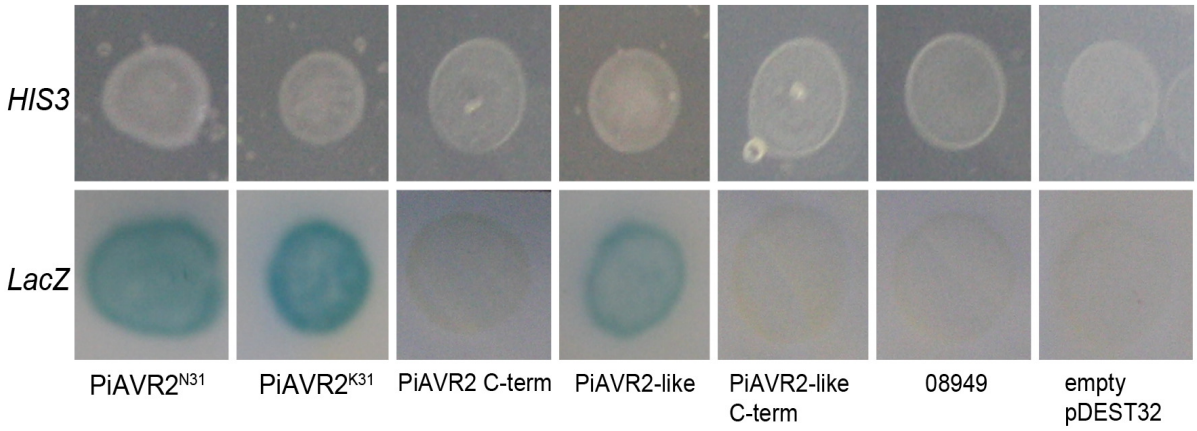


**Figure 4.5.1: StBSL2b with the PiAVR2 forms.** StBSL2b-specific screen with all PiAVR2 forms and PITG_08949. Top panel shows the *HIS3* reporter gene and the bottom shows the *LacZ* reporter gene.

## 4.6 – Function of *Solanaceae* BR signal transduction pathway

The *A. thaliana* literature contains a fairly detailed dissection of the BR pathway but this does not extend to the family members of key components, i.e. AtBSU1 and AtBSL1 are well described in comparison to AtBSL2 and 3. In *A. thaliana,* AtBSK1 is the phosphatase shown to interact with AtBSU1 and AtBSL1, while AtBIN2 is their substrate kinase. To determine if this pathway is the same as described in the *A. thaliana* literature the interactions of the StBSL family with the known BSU1-interacting components of the BR pathway, StBSK2 and StBIN2, were examined. Both *StBSK2* and *StBIN2* sequences were found by Leighton Pritchard (the JHI) using the *A. thaliana* sequences to search the *S. tuberosum* cv. *Phureja* genome database as described for *StBSL2b* in Section 4.4. This search provided sequence information that was used to design primers allowing the PCR amplification of these genes from *S. tuberosum* cDNA. *StBSK2* and *StBIN2* were recombined into the Y2H vectors to allow them to be tested against the BSL proteins. Each full length potato BSL (StBSL1, StBSL2a and StBSL2b) was tested to determine if it interacted with the activator StBSK2, and also with the substrate, StBIN2. The results

show the *HIS3* and *LacZ* reporter genes for the StBSK2 and StBSL interactions (Figure 4.6.1a). The *HIS3* and *LacZ* reporter genes show only weak growth and colouration, respectively, of the yeast colonies for the StBSK2-StBSL1 and StBSK2-StBSL2a interaction, but the positive result using the *LacZ* reporter gene implies there is interaction between these proteins (Figure 4.6.1a). The interaction of StBSK2-StBSL2b is much more visible than the other StBSK2-StBSLs (Figure 4. 6.1a). It does appear that StBSK2 is interacting with all StBSL proteins as the empty vector control does not show any auto-activation.

StBIN2 was also tested against the StBSLs (Figure 4. 6.1b). The growth of the colonies on the *HIS3* reporter gene assay shows that there is some interaction occurring for all the genes tested with BIN2 although the growth for StBIN2-StBSL1 is quite weak (Figure 4. 6.1b). The *LacZ* reporter gene assay also shows blue colouration of the colonies. The blue colour is quite weak for StBIN2-StBSL2b (Figure 4. 6.1b). There is also activation of both reporter genes, *HIS3* and *LacZ*, with the empty vector control (Figure 4. 6.1b). This means that no conclusions can be drawn from these results. The auto-activation could be due to the BIN2 protein interacting with a protein fragment that is generated in the empty vector from the ccdB gene. The StBIN2 protein was also tested against the StBSLs using the opposite vectors: the pDEST32_StBSLs co-transformed with the pDEST22_StBIN2. This combination saw reasonable growth on the histidine plate for StBSL1 and StBSL2b with StBIN2 but minimal to no growth for StBSL2a. There was also no blue colouration of the colonies observed using the LacZ assay (results not shown). This suggests that there may be no interaction between StBIN2 and the StBSLs in yeast. This needs further work for confirmation. However the StBSK2 – StBSLs interaction data is encouraging as it confirms the *A. thaliana* observations with the proteins from the *Solanaceae*.

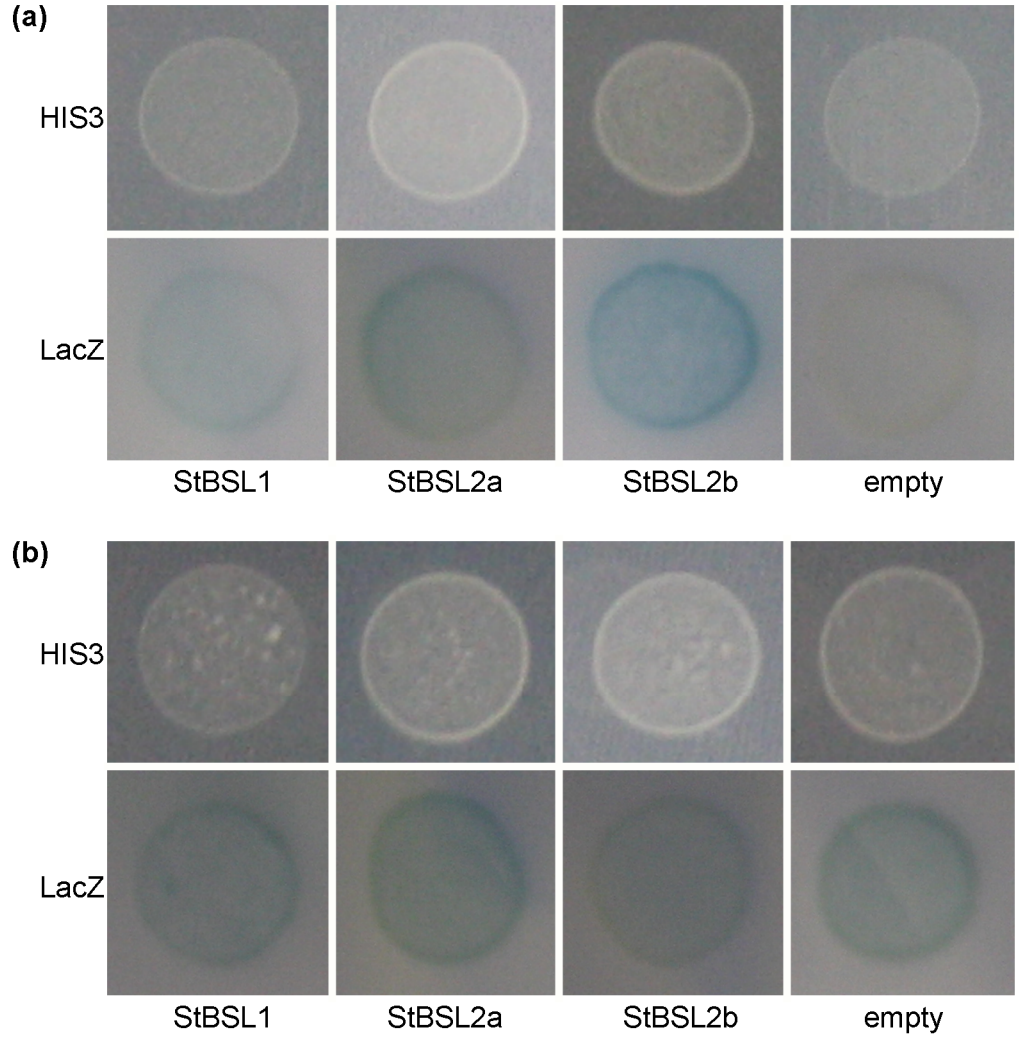


**Figure 4.6.1: Y2H screen investigating the BR pathway. (a)** Co-transformation of yeast cells with pDEST32_StBSK2 and the three StBSLs in the pDEST22 vector with the empty vector as a control. The *HIS3* and *LacZ* reporter genes are shown. **(b)** Co-transformation of yeast cells with pDEST32_StBIN2 and the three StBSLs in the pDEST22 vector with the empty vector as a control. The *HIS3* and *LacZ* reporter genes are shown.

To investigate potential interactions between StBSL proteins with each other they were also compared in a Y2H-specific interaction assay. pDEST32_StBSL1 was tested against pDEST22_StBSL2a and pDEST22_StBSL2b, pDEST32_StBSL2a was tested against pDEST22_StBSL1 and pDEST22_StBSL2b and finally pDEST32_StBSL2b was tested against pDEST22_StBSL1 and pDEST22_StBSL2a (Table 4.6.1). The results from

StBSL1 with StBSL2a and StBSL2b both showed activation of both the *HIS3* and *LacZ* reporter genes. However these results are inconclusive as StBSL1 with the empty vector control also showed similar activation levels indicating that pDEST32_StBSL1 auto-activates (Table 4.6.1). StBSL2a was tested in the bait plasmid against StBSL1 and StBSL2b in the prey plasmid. The results for StBSL1 showed some blue colouration on the *LacZ* reporter gene, although there is also auto-activation of the StBSL2a with its empty vector control therefore no conclusions can be drawn. However for StBSL2a with StBSL2b the results are clearer; there is definite growth of the colony using the histidine reporter assay and clear blue colouration of the colonies using the *LacZ* reporter gene (Table 4.6.1, Figure 4.6.2). Auto-activation of StBSL2a with its empty vector control, stated above, produces minimal blue colouration. Therefore, the StBSL2a-StBSL2b interaction appears to be genuine. The interaction between StBSL2b and StBSL1 showed minimal interaction using the *HIS3* reporter gene but no blue colouration of the colonies was seen on the *LacZ* reporter gene, which suggests no interaction. The reporter assays for the interaction between StBSL2b and StBSL2a show growth on the histidine assay and a clear blue on the LacZ reporter gene. It has been shown previously that bait empty vector – prey StBSL2a does not auto-activate (Figure 4.3.1b). However, the empty prey vector control with pDEST32_StBSL2b was missing from this experiment, so until auto-activation has been ruled out again no firm conclusions can be drawn (Table 4.6.1). It has been shown here that StBSL2a and StBSL2b appear to interact within the yeast system, what has not been tested is whether StBSL2a and StBSL2b dimerise with themselves. This will need further work.

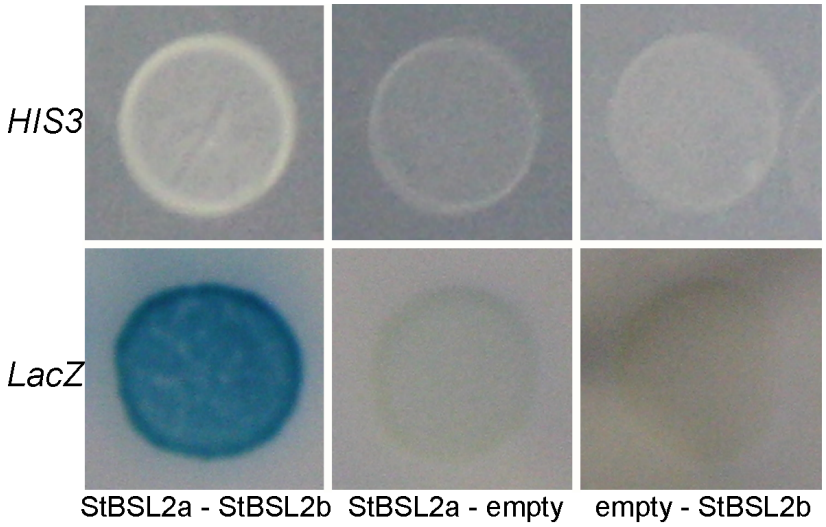


**Figure 4.6.2: Interaction between BSLs.** Interaction of pDEST32_StBSL2a – pDEST22_StBSL2b using the *HIS3* and *LacZ* reporter genes. pDEST32_StBSL2a – pDEST22_empty and pDEST32_empty – pDEST22_StBSL2b control transformations are also shown using the *HIS3* and *LacZ* reporter genes.

| pDEST32 (Bait) | pDEST22 (Prey) | *HIS3* reporter gene | *LacZ* reporter gene |
|---|---|---|---|
| StBSL1 | StBSL2a | + | + |
| StBSL1 | StBSL2b | + | + |
| StBSL1 | empty | + | + |
| | | | |
| StBSL2a | StBSL1 | + | + |
| StBSL2a | StBSL2b | +++ | +++ |
| StBSL2a | empty | + | + |
| | | | |
| StBSL2b | StBSL1 | + | - |
| StBSL2b | StBSL2a | ++ | ++ |
| StBSL2b | empty | N/A | N/A |
| | | | |
| empty | StBSL1 | - | - |
| empty | StBSL2a | - | - |
| empty | StBSL2b | - | - |

**Table 4.6.1: Y2H results for BSL – BSL interactions.** This table summarises the BSL – BSL interaction results. – means no growth and no blue colouration, + means minimal growth and minimal blue colouration, ++ means good growth and blue colouration, +++ means strong growth and colouration.

## 4.7 – Development of *P. infestans* infection after treatment with Brassinolide.

The BSL proteins are activators of the brassinosteroid signal transduction pathway. It was shown above that the activator of the StBSLs, StBSK2 is present in the *Solanaceae* and does interact with them in yeast. This information implies that the initial stages of the pathway may be similar in the *Solanaceae* as to *A. thaliana*, it also implies that the initial stages of the pathway are intact in the *Solanaceae.* The BR pathway has never been directly linked to defence against pathogen attack before.

In order to determine why an effector of *P. infestans* would target the BR pathway *N. benthamiana* plants were treated with BR hormone. Epi-brassinolide (EBL) was applied to the plants prior to their infection with the *P. infestans* isolate 88069. Two independent replicates of this experiment show that pre-treatment of the plants with EBL 24 hours before the inoculation of *P. infestans* isolate 88069 reduces the ability of the pathogen to infect (Figure 4.7.1). This is seen by the reduction in the lesion size on the leaves treated with EBL compared to the control, either water or 0.1% EtOH (Figure 4.7.1). SA treatment was used as a positive control as it is known that pre-treatment of plants with SA reduces the ability of biotrophic pathogens to infect. The combination of SA and EBL was also investigated to determine if a combined treatment would have a greater effect. However, it does not appear to (Figure 4.7.1). Pre-treatment with EBL activates the BR pathway and from these data it appears that this activation aids the plant in its defence against *P. infestans*. *P*. infestans growth on all hormone treated leaves is statistically significant compared to the leaves treated with 0.1% EtOH, $P < 0.05$ (top graph Figure 4.7.1) however in the second replicate, EBL treatment alone is not statistically significant while SA and the combined SA and EBL treatments are statistically significant compared to the $H_2O$ control treatment, $P < 0.05$ (bottom graph Figure 4.7.1). No other pathogens were tested, so it cannot be determined if this observation is specific to *P. infestans* or more general to other biotrophic and necrotrophic pathogens.

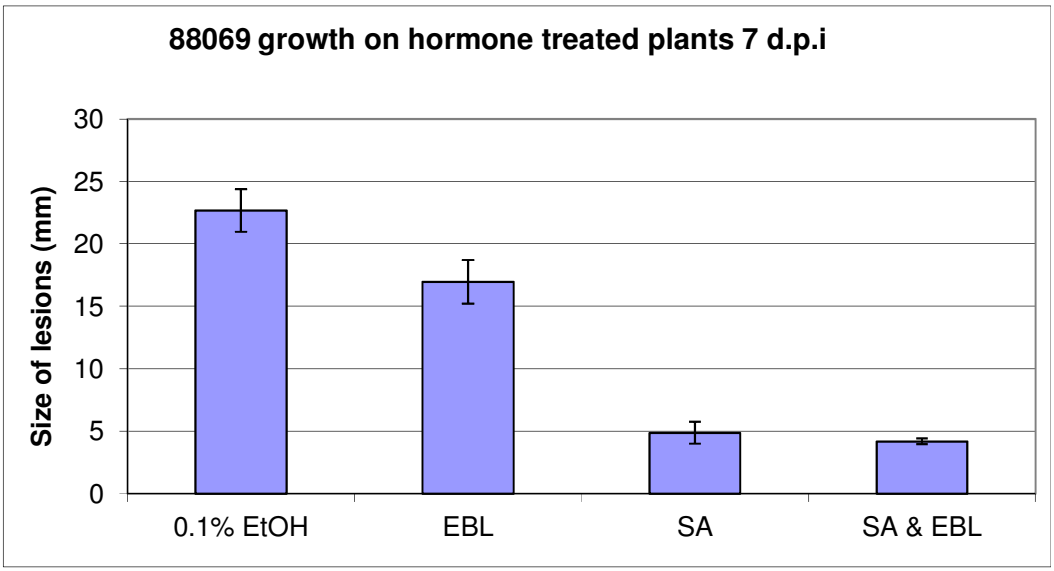


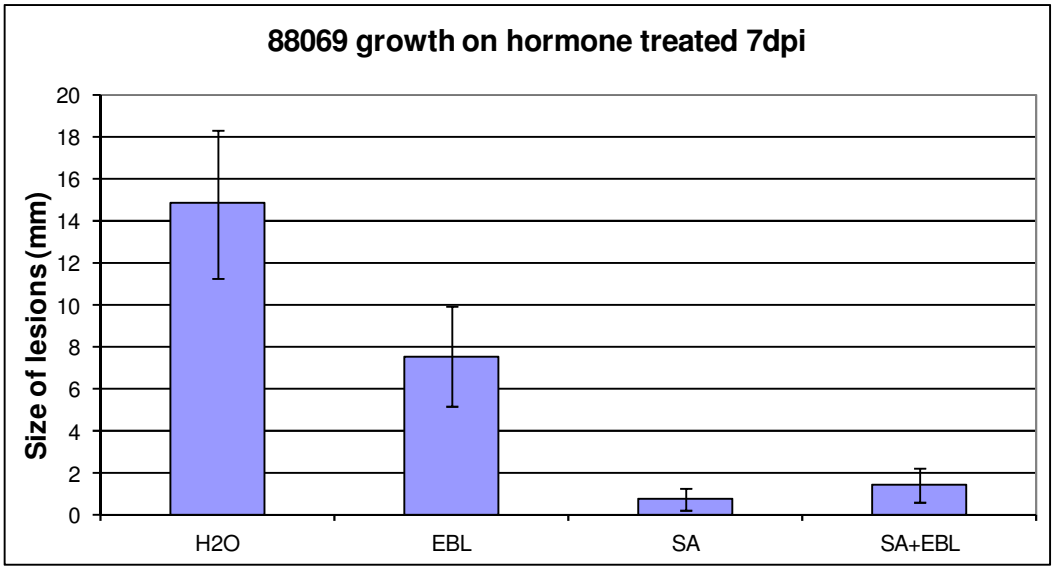


**Figure 4.7.1: Lesion size of 88069 infection on hormone treated leaves.** Each graph is a biological replicate; data collected 7 dpi for each experiment. Leaves sprayed 24 hpi with each hormone or mock treatment. 20 µM EBL and SA were used.

## 4.8 – Virus-Induced Gene Silencing of BR pathway genes

Virus-Induced Gene Silencing (VIGS) was used on members of the BR pathway to determine the effects this would have on the plant growth phenotype and whether they were similar to those already described in the *A. thaliana* literature. The VIGS was carried out on the *BSL* gene family along with *BRI1*, encoding the cell surface receptor, and

*BAK1,* encoding the co-receptor of BRI1 in *N. benthamiana*. The silencing of the *NbBSL1* gene will be described in more detail in Chapter 5. Primers were designed based on the potato full length sequence for *StBSL2a* and EST data for *StBSL2b* and products were amplified from *N. benthamiana* cDNA. Two tobacco rattle virus (TRV) based silencing constructs were generated for *NbBSL2a*: TRV::*5'BSL2a* and TRV::*3'BSL2a*. The TRV::*5'BSL2a* construct is located in the region encoding the Kelch-repeat domain, 150 bp from the start of the gene, while the TRV::*3'BSL2a* construct is located in the phosphatase-encoding domain between 2350 bp – 2670 bp (Figure 4.8.1a). The TRV::*BSL2b* construct is located on the edge of the phosphatase-encoding domain between 1760 bp – 2060 bp (Figure 4.8.1a). Only one silencing construct was used for each of *NbBRI1* and *NbBAK1*. The *NbBRI1* construct is located in the middle of the gene between 1874 bp – 2109 bp. The *NbBAK1* construct, also referred to as *NbSERK3*, was obtained from John Rathjen (The Australian National University) and previously described in Heese *et al*., (2007).

The dwarf phenotype of *bri1* and *bak1* deficient plants is well documented in the *A. thaliana*. This dwarf phenotype was also observed when *N. benthamiana* plants were infiltrated with the TRV::*BRI1* and TRV::*BAK1* constructs. It was observed that the plants were not only dwarfed but that the leaves were curled as well (Figure 4.8.1b). The silencing constructs for *NbBSL2a* and *NbBSL2b* generated stunted plants which had small underdeveloped petioles as well as curled leaves (Figure 4.8.1b). The phenotype shown for *bsl2a* and *bsl2b* silencing is consistent with the brassinosteroid-deficient phenotype shown in the *bri1* and *bak1* silenced plants. These phenotypes imply further that *NbBSL2a* and *NbBSL2b* genes play an important role in the brassinosteroid pathway.

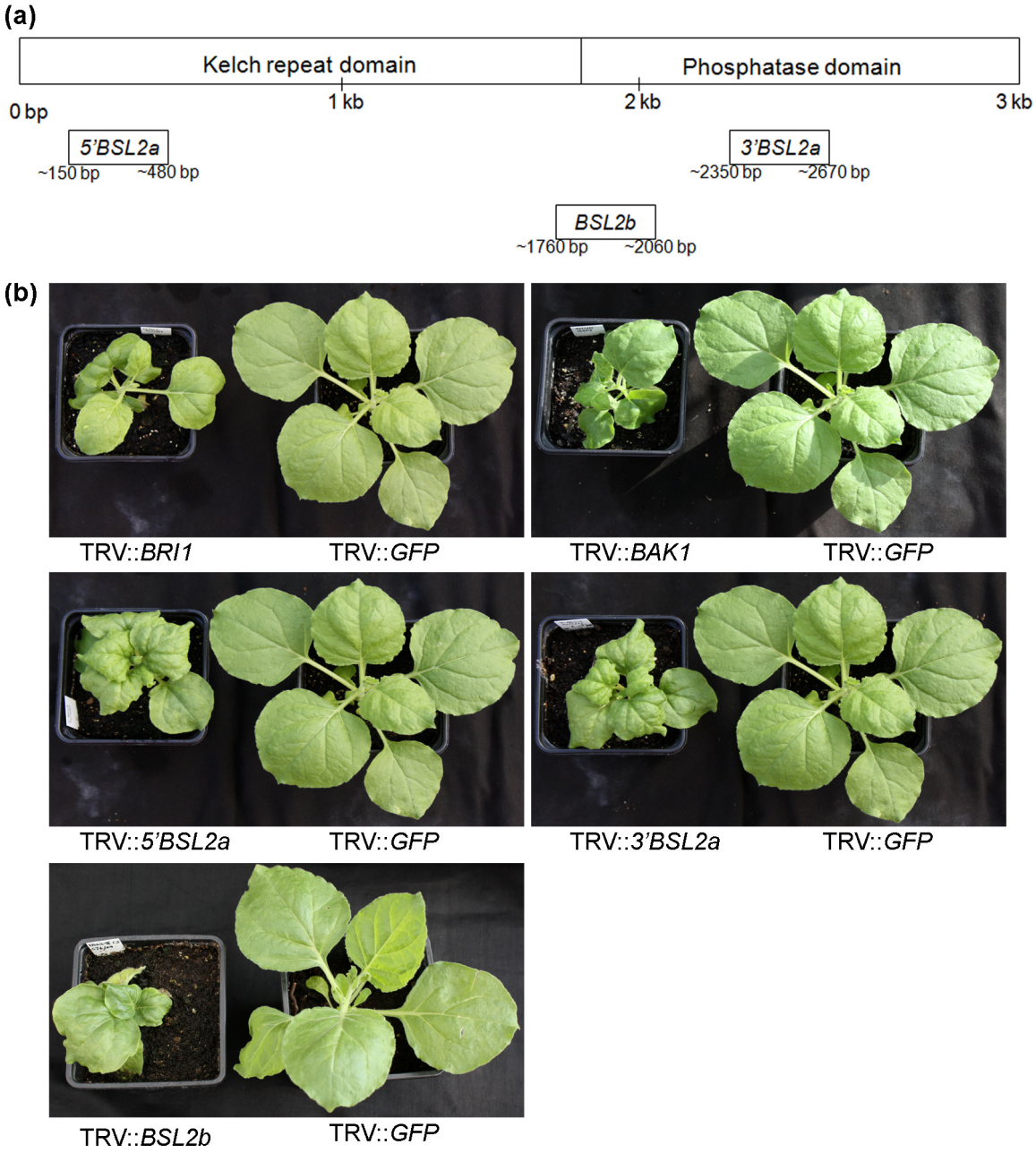


**Figure 4.8.1: Virus induced gene silencing constructs. (a)** Shows the positioning of the *BSL2a* and *BSL2b* silencing constructs relative to the whole gene. **(b)** Images of the phenotypes of the silencing constructs TRV::*BRI1*, TRV::*BAK1*, TRV::*5'BSL2a*, TRV::*3'BSL2a* and TRV::*BSL2b* compared to a TRV::*GFP* control plant on the right of each image.

To confirm the silencing levels of these plants and to determine that no off-target silencing of related genes was occurring, primers were designed using the *S. tuberosum* sequence information. After many attempts to optimise multiple primer pairs for each *BSL* gene *N.*

*benthamiana* sequence was needed to design primers that would efficiently amplify from the cDNA generated from the VIGS plants. Fragments of the *BSL* genes were amplified from *N. benthamiana* cDNA using internal sequencing primers from the *S. tuberosum* genes. These PCR products generated some sequence information from *N. benthamiana* for these genes allowing primers specific to *N. benthamiana* to be designed. When the sequence information from *N. benthamiana* was compared to *S. tuberosum* it was understandable why the primers based on the potato sequence failed, as there are many SNP differences between the species. The primers specific to *N. benthamiana* allowed qRT-PCR to be used to determine the level of silencing of each VIGS construct. The location of each qRT-PCR primer pair for each gene is shown in Figure 4.8.2a. It can be seen that the qRT-PCR primers are in the centre of the genes and not near any of the VIGS constructs. The graph of the *BSL* gene expression indicates that all three *BSL* genes have an increase of expression by 2 or 3 fold in the TRV::*BRI1* plants compared to the TRV::*GFP* plants (Figure 4.8.2b). The absence of BRI1 could be causing a disturbance in the signalling feedback loop associated with transcription of these genes. The TRV::*BAK1* plants have similar levels of *BSL* gene expression as the TRV::*GFP* plants, there is no statistical difference (Figure 4.8.2b). The *BSL* gene expression in the TRV::*5'BSL2a* and TRV::*3'BSL2a* is more complex. In either of the *NbBSL2a* silenced plants the expression of the *NbBSL2a* gene only undergoes minimal reduction. In the TRV::*5'BSL2a* plants the reduction in *NbBSL2a* expression is only 18% of the GFP control while the expression of the *NbBSL2b* gene has increased and the *NbBSL1* gene is reduced by 25%, there is no statistical difference (Figure 4.8.2b). This implies that either a very small knock down of this gene is causing a severe phenotype or that silencing is diminishing by the time of measurement, possibly due to restoration of expression in order for the plant to survive. In the TRV::*3'BSL2a* plants there is a different expression pattern of the three genes compared to the TRV::*5'BSL2a* plants. *NbBSL1* expression is increased, *NbBSL2b* expression is comparable to the TRV::*GFP* plants, there is no

statistical difference and the *NbBSL2a* expression is reduced by 55% in the TRV::*3'BSL2a* plants, this reduction is statistically significant, P = <0.001 (Figure 4.8.2b). The silencing levels of the *NbBSL2a* gene in the TRV::*5'BSL2a* and TRV::*3'BSL2a* plants are difficult to assess when compared to the phenotype generated. There are a few options, the one mentioned above is that it only takes a small drop in the silencing levels for a severe phenotype to occur or that, for the plant to survive by 3 weeks after inoculation, near normal levels of expression for these genes has been restored to allow plant development to occur. If this is the case then sampling at earlier time points may yield different results for the gene expression analysis. The TRV::*BSL2b* plants show reduction in *NbBSL2b and NbBSL2a* genes to varying levels, there is no statistical difference. The *NbBSL1* expression in the TRV::*BSL2b* plants is increased by 70% compared to the TRV::*GFP* plants, there is no statistical difference (Figure 4.8.2b). The *NbBSL2b* gene is reduced in expression by 45% and the *NbBSL2a* gene by 35% in the TRV::*BSL2b* plants compared to the TRV::*GFP* plants (Figure 4.8.2b). The down-regulation of both *NbBSL2b* and *NbBSL2a* in this background is not entirely unexpected – likely due to off-target silencing, as these genes are so similar at the nucleotide sequence level. However, the fact that both genes are silenced also yeilds extra tools to investigate the BR pathway and the role the *BSL* genes play within this pathway. The expression of *NbBSL1* is increased in the TRV::*3'BSL2a* and TRV::*BSL2b* plants similar to that observed in the TRV::*BRI1* plants. This again suggests that blocking the pathway prevents the feedback loop for detecting the transcription of these genes. The silencing of the *BRI1* gene was addressed using primers previously designed by Eleanor Gilroy, at the JHI. The silencing of this gene was only investigated in the TRV::*GFP* and TRV::*BRI1* plants. The data show that over three replicates the expression of *BRI1* in the TRV::*BRI1* plants is reduced by about 55% compared to the control plant TRV::*GFP* which is statistically significant, P<0.001 (Figure 4.8.2c). Again, this low level of silencing by 3 weeks after inoculation may reflect a restoration of expression levels.

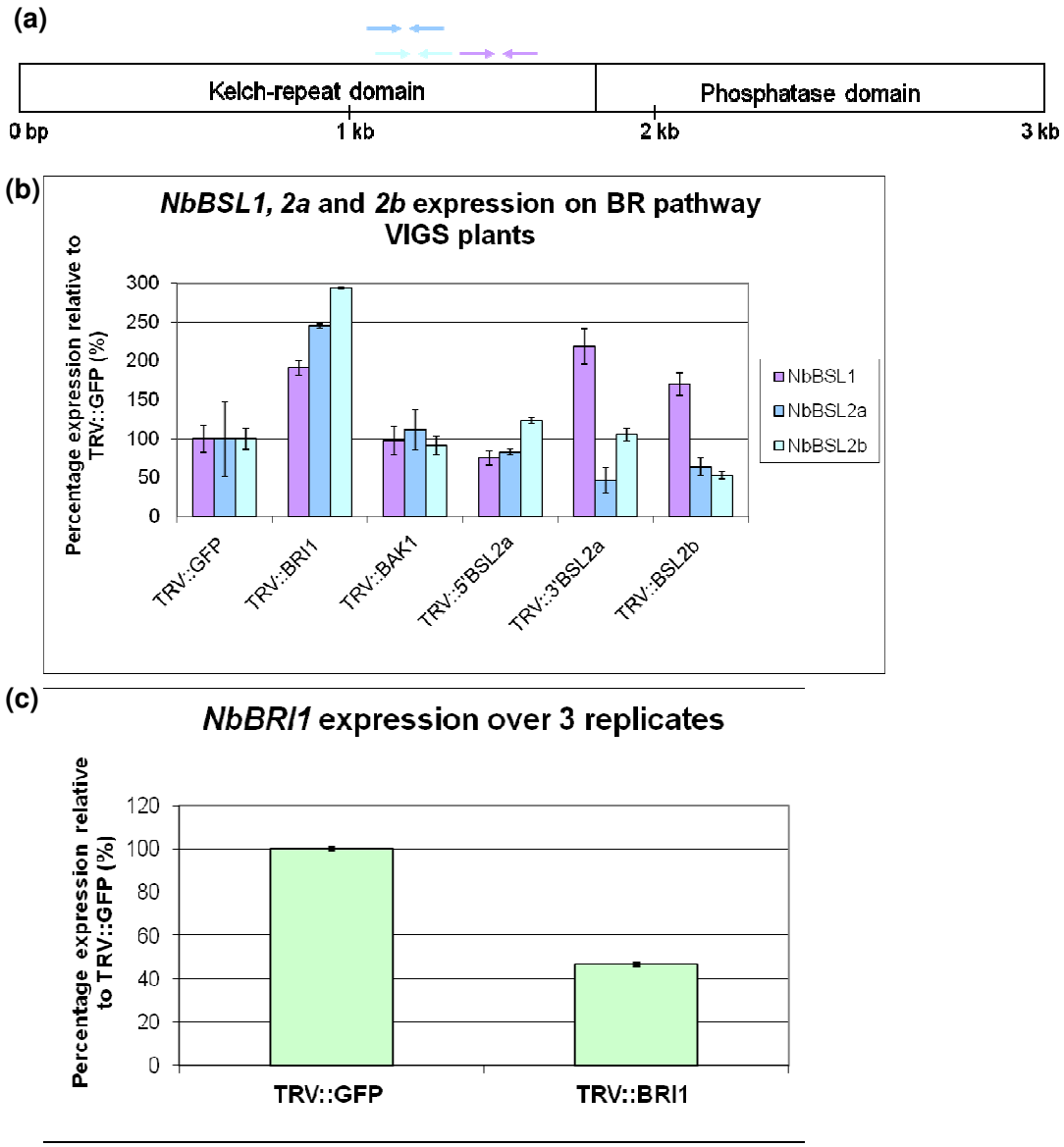


**Figure 4.8.2: qRT-PCR of *BSL1, 2a* and *2b* expression in BR pathway VIGS plants. (a)** a diagram of the positions of the qRT-PCR primer pairs within the *BSL* genes. Colour of arrows refers to colours in the graph, lilac = BSL1 primers, blue = BSL2a primers and turquoise = BSL2b primers. **(b)** qRT-PCR showing expression of *NbBSL1*, *NbBSL2a* and *NbBSL2b* in the TRV::*GFP*, TRV::*BRI1*, TRV::*BAK1*, TRV::*5'BSL2a,* TRV::*3'BSL2a*, and TRV::*BSL2b* plants. The *NbBSL1* expression is 3 biological replicates for TRV::*GFP*, TRV::*BAK1*, TRV::*3'BSL2a* and TRV::*BSL2b* but only one biological replicate for TRV::*BRI1* and TRV::*5'BSL2a*. *NbBSL2b* expression is a combination of 3 biological replicates for TRV::*GFP*, TRV::*BAK1*, TRV::*3'BSL2a* and TRV::*3'BSL3* but only one biological replicate for TRV::*BRI1* and TRV::*5'BSL1*. *NbBSL3* expression is a combination of 3 biological replicates for TRV::*GFP*, TRV::*BAK1*, TRV::*BSL2* and TRV::*BSL2b* but only only one biological replicate for TRV::*BRI1* and TRV::*5'BSL2a*. All data was normalized to 25S rRNA endogenous control. **(c)** qRT-PCR expression of NbBRI1 in the TRV::*GFP* and TRV::*BRI1* plants. The data in the graph is the combination of three biological replicates. All data was normalized to 25S rRNA endogenous control.

An interesting phenotype of the TRV::*5'BSL2a* and TRV::*3'BSL2a* is that approximately 3 weeks after the silencing construct has been infiltrated into the plants runaway senescence occurs in these leaves (Figure 4.8.3). This may be linked to the salicylic acid (SA) pathway. SA is an important signalling molecule in plant defence and is important in defence against biotrophic pathogens. Signal transduction from *R* gene-mediated resistance against biotrophs leads to the development of an HR (Dangl *et al*., 1996). SA is also involved in systemic acquired resistance (SAR), which involves the signalling from an infected area of the plant to non-infected areas. This triggers the defence responses in non-infected areas of the plant allowing it to resist the coming pathogen attack (Shah, 2003). The activation of the SA pathway leads to the accumulation of pathogenesis-related (*PR*) gene transcripts which are known to act in plant defence and are used as markers of resistance (Hammond-Kosack and Jones, 1996). Transgenic plants which contain the bacterial salicylate hydroxylase gene (*NahG*) prevent the accumulation of SA by degrading it to catechol, blocking the activation of SA defence responses (Shah, 2003). When transgenic *N. benthamiana NahG* plants are infiltrated with TRV::*3'BSL2a* these plants do not have such a stunted phenotype. Their petioles have recovered and look close to normal and the growth has recovered compared to the images seen in Figure 4.8.1. There is also reduced senescence in these plants as well as the recovery of the stunted growth phenotype (Figure 4.8.3). This could indicate that there is a role for SA in the BR signal transduction pathway.

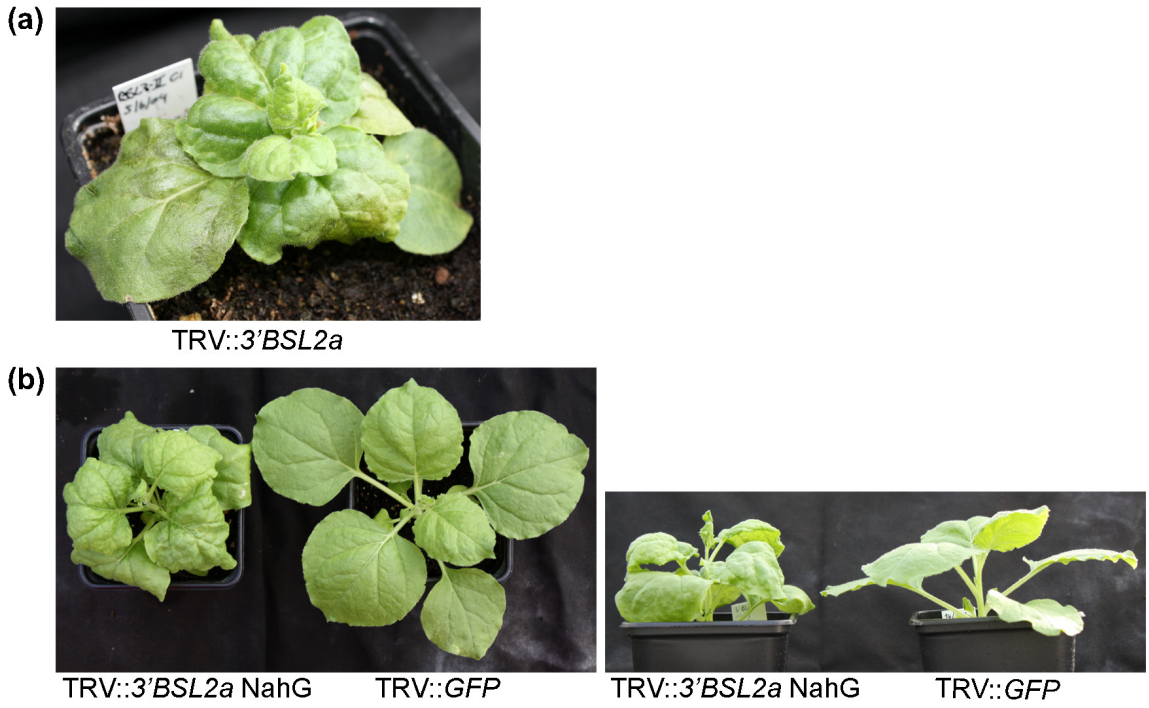


**Figure 4.8.3: TRV::*3'BSL2a* NahG transgenic *N. benthamiana*. (a)** TRV::*3'BSL2a* showing the beginning of senescence. **(b)** TRV::*3'BSL2*a infiltrated into transgenic NahG *N. benthamiana.*

## 4.9 – Pathogen assays on BR pathway VIGS plants

### 4.9.1 – Is susceptibility to *P. infestans* altered?

To determine if the silencing of the genes of interest from the BR pathway altered the ability of these plants to defend against pathogen attack, *P. infestans* was inoculated on to detached leaves. The isolate 88069 was inoculated on to leaves from TRV::*GFP*, TRV::*BRI1*, TRV::*BAK1*, TRV::*5'BSL2a*, TRV::*3'BSL2a* and TRV::*BSL2b* plants and the results analysed 6 dpi. TRV::*5'BSL2a*, TRV::*3'BSL2a* and TRV::*BSL2b* leaves show minimal growth of the pathogen compared to TRV::*GFP* leaves (Figure 4.9.1). Statistical analysis of these results reveals that this minimal growth is significantly different with a P value of <0.001. This minimal growth could be down to the silencing of these genes but it is also possible that since these plants have a tendency for early senescence, the low

percentage of sporulation observed could also be due to the fact that there is a lack of healthy tissue that *P. infestans* requires in its early biotrophic phase. The TRV::*BAK1* leaves appear to be more susceptible than the TRV::*GFP* leaves (Figure 4.9.1); this increase in infection is statistically significant with a P value of <0.05. The TRV::*BRI1* leaves have a similar level of infection to the TRV::*GFP* leaves (Figure 4.9.1). Statistical analysis was generated using a one way ANOVA on the Sigmaplot statistical software package using the Holm-Sidak method.

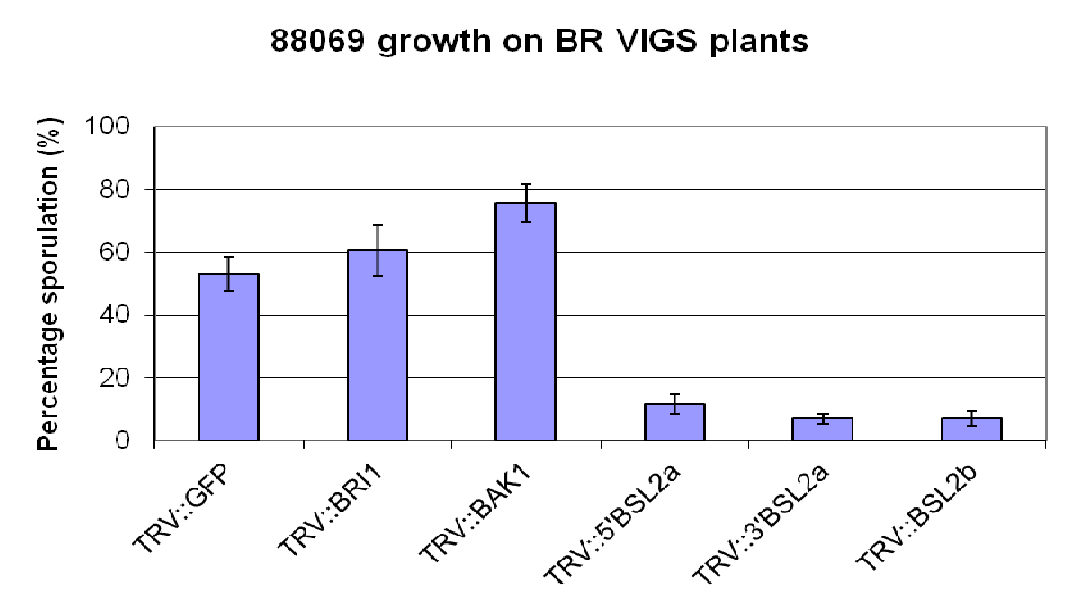


**Figure 4.9.1: 88069 growth on BR VIGS plants.** Percentage of total *P. infestans* (isolate 88069) inoculations sporulating on TRV::*GFP*, TRV::*BRI1*, TRV::*BAK1*, TRV::*5'BSL2a*, TRV::*3'BSL2a* and TRV::*BSL2b* plants. Data in graph is from 6 dpi.

4.9.2 – Cell death assay on VIGS plants

PiAVR2 was found to interact with StBSL2a in the yeast system. To determine if silencing of *NbBSL2a* has an affect on the ability of the plant to produce the PiAVR2/R2 HR a cell death assay was conducted on these plants. The rest of the BR pathway VIGS plants were also included in this experiment to determine if any observations about the formation of HR in these plants could be made. The four published *R2* orthologues, *R2*, *R2-like*, *Abpt* and *Blb3* were examined, as well as some control *R* genes, *R3a*, *Sto1* and *Rx*. R3a recognises the RXLR-dEER effector PiAVR3a from *P. infestans*, Sto1 recognises the effector PiIpio1 also from *P. infestans* and Rx recognises the coat protein of Potato Virus X (PVX) (Bendahmane *et al.*, 1999; Armstrong *et al.*, 2005; Vleeshouwers *et al.*, 2008).

The results indicate that the formation of the HRs for two of the three control *R* genes, *Sto1* and *Rx* do not appear to be affected by the silencing of these BR pathway genes (Figure 4.9.2). The percentages of *Sto1* and *Rx* HR development on all plants are not statistically significantly different to those seen on the TRV::*GFP* control plants. *R3a*, however, does appear to be affected by the silencing of *BRI1* and *BAK1* (Figure 4.9.2). There is a significant difference in the formation of the R3a/PiAVR3a$^{KI}$ HR between the TRV::*BRI1* and TRV::*BAK1* when compared to TRV::*GFP* with a P value of <0.001.

For the *R2* orthologues, *R2*, *R2-like*, *Blb3* and *Abpt* there is an approximate 25% reduction in the formation of the R2-mediated HR in the TRV::*BAK1*, TRV::*5'BSL2a* and TRV::*3'BSL2a* plants compared to the TRV::*GFP* control plants (Figure 4.9.2). The reduction in the *R2* orthologues on the TRV::*BAK1* and TRV::*3'BSL2a* plants have a P value of <0.001. As for the TRV::*5'BSL2a* plants the P value for the formation of the *R2* HR is <0.01, for the *R2-like* and *Blb3* it is <0.05 and for *Abpt* only <0.1. The *R2*, *R2-like* and *Blb3* HRs in the TRV::*5'BSL2a* background are statistically significantly different from TRV::*GFP,* although the *Abpt R* gene is only showing a trend. The formation of the *R2-*

mediated HR appears not to be significantly different in the TRV::*BRI1* and TRV::*BSL2b* plants when compared to TRV::*GFP*. However, the TRV::*BSL2b* plants do show a slight reduction, approximately 20%, with the *R2-like, Blb3* and *Abpt* genes. All statistical analysis was performed in Sigmaplot using the Holm-Sidak method in a one-way ANOVA. The data used in the statistical analysis for this experiment did not pass the Shapiro-Wilk test for normality as reported by Sigmaplot; a visual inspection of diagnostic residual plots indicated approximate normality and equality of variance. On that basis the Shapiro-Wilk warning was ignored.

These data suggests that silencing of the *BSL2a* and *BAK1* genes affects the ability of the *R2* orthologues to generate the HR when *PiAVR2* is present indicating that these genes could be essential for the recognition of PiAVR2 by the plant resistance gene *R2*. Unfortunately the investigation of this could not be taken any further in these plants due to the runaway senescence observed. A more detailed investigation of the R2/PiAVR2 recognition will be discussed in Chapter 5 using the *BSL1* gene.

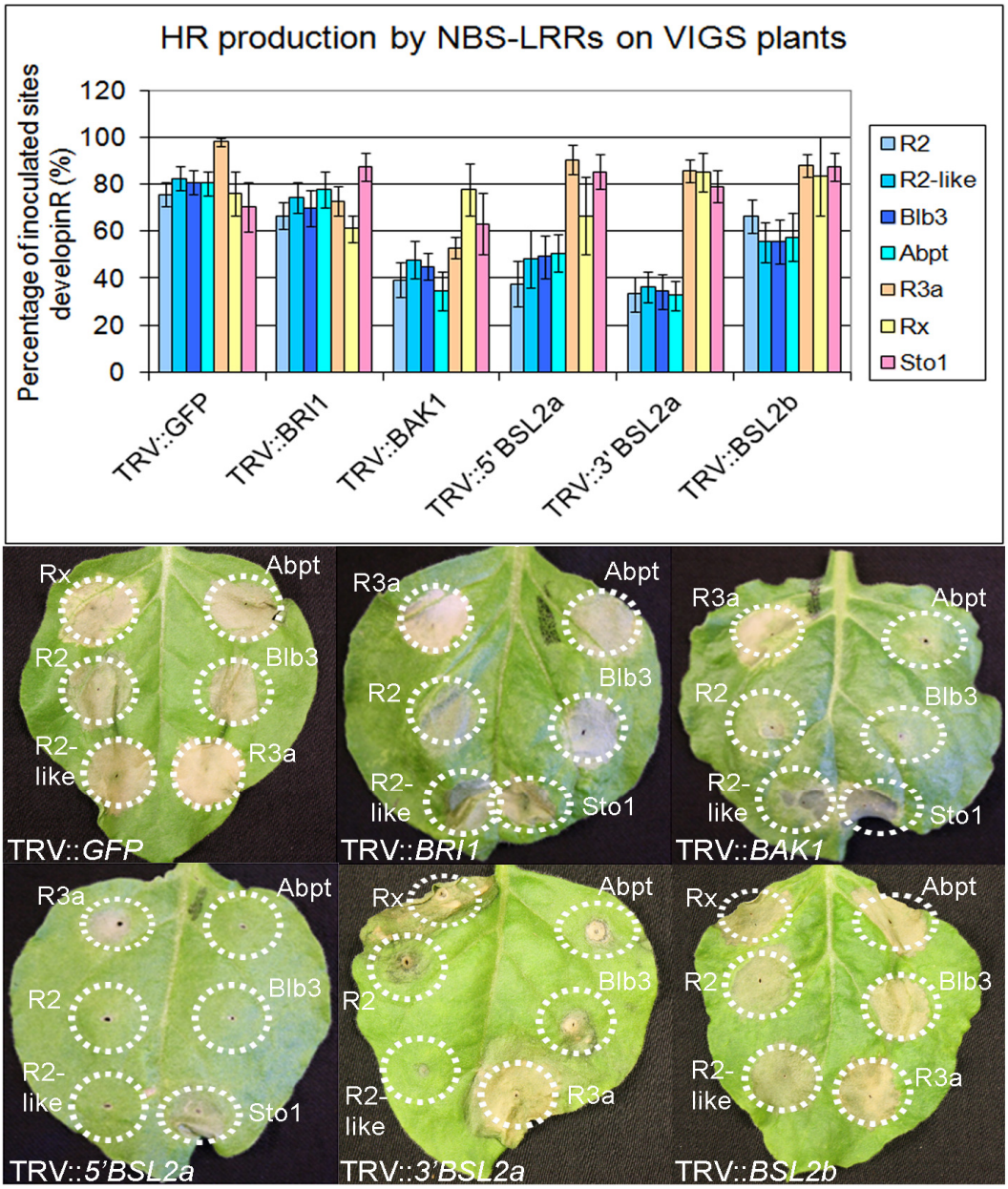


**Figure 4.9.2: Cell death assay on VIGS plants.** A graph showing the development of HRs from seven potato *R* genes. *R3a*, *Rx* and *Sto1* are the control *R* genes and *R2*, *R2-like*, *Abpt* and *Blb3* were being investigated for their ability to function on the TRV::*BRI1*, TRV::*BAK1*, TRV::*5'BSL2a*, TRV::*3'BSL2a* and TRV::*BSL2b* silenced plants. For the *R2* orthologues data from 8 biological replicates for TRV::*GFP*, 3 biological replicates for TRV::*BRI1*, 4 biological replicates for TRV::*BAK1*, 3 biological replicates for TRV:: *5'BSL2a,* 5 biological replicates for TRV::*3'BSL2a* and 4 biological replicates for TRV::*BSL2b*. The data for the control *R* genes on the TRV::*GFP* plants was collected from, *R3a*, 6 biological replicates, *Sto1*, from 4 and *Rx*, from 4. On the TRV::*BRI1* plants *R3a* was collected from 4 biological replicates, *Sto1* from 2 and *Rx* from 1. On the TRV::*BAK1* plants *R3a* was collected from 3 biological replicates, *Sto1* from 2 and *Rx* from 2. On the TRV::*5'BSL2a* plants *R3a* from 2, *Sto1* from 2 and *Rx* from 1 biological replicate. On the TRV::*3'BSL2a* plants *R3a* from 4, *Sto1* from 2 and *Rx* from 3 biological replicates. On the TRV::*BSL2b* plants *R3a* from 5, *Sto1* from 2 and *Rx* from 1 biological replicate. Examples of the TRV::*GFP*, TRV::*BRI1*, TRV::*BAK1*, TRV::*5'BSL2a*, TRV::*3'BSL2a* and TRV::*BSL2b* leaf images are below the graph. Pictures and HRs were taken/recorded 6 dpi.

## 4.10 - Discussion

Interaction of a pathogen effector protein with a component of the BR pathway is an interesting discovery and raises many important questions about the connection of this developmental pathway to defence. Understanding the mechanism by which PiAVR2 may manipulate the BSL family of phosphatases should provide a useful tool to understand this connection, and also to study the regulation of the BR pathway in the *Solanaceae*.

The interaction of PiAVR2 with StBSL2a (formerly StBSL3) is shown in Figure 4.2.1 and 4.3.1 using the *in vitro* yeast two hybrid system, but could not be confirmed *in planta* during this work. It has, however, been confirmed elsewhere (S. Kamoun, The Sainsbury Laboratory, UK), using co-IP in *N. benthamiana*, that StBSL2a is an interacting protein of PiAVR2 (Figure 4.10.1). This experiment was done with a FLAG_PiAVR2 C-terminus and StBSL2a_GFP co-infiltrated into *N. benthamiana* leaves. When an anti-FLAG pull down is performed and an anti-GFP antibody used to probe the products, it detects StBSL2a_GFP at ~150 KDa, thus confirming that StBSL2a is in complex with PiAVR2 C-terminus in the plant cell. Therefore, even though the *in planta* interaction of PiAVR2 was not confirmed here, confidence that this is a genuine interaction can be gained from complementary experiments in another lab. Nevertheless, the work described here has also shown that it is not only StBSL2a that can interact with PiAVR2 but also StBSL2b using the yeast system (Figure 4.5.1). The interaction between PiAVR2 and StBSL2b will have to be confirmed *in planta* using split YFP, co-IPs or fluorescence-lifetime imaging microscopy-fluorescence resonance energy transfer (FLIM-FRET). Both StBSL2a and StBSL2b have a very high degree of sequence similarity and therefore structural similarity, which could be responsible for both interacting with PiAVR2.

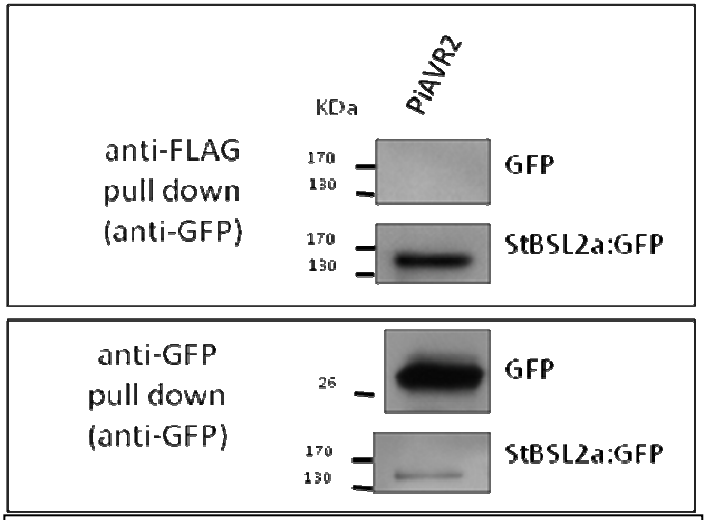


**Figure 4.10.1: Co-IP of PiAVR2 in *N. benthamiana*.** PiAVR2 was tagged with FLAG on the N-terminus of the protein. The top image is an anti-FLAG pull down with GFP antibody detecting GFP-StBSL2a. The bottom box shows an anti-GFP pull down with an anti-GFP antibody. Images of western blots provided by S. Kamoun, The Sainsbury Laboratory.

The complexity of the BSU1-family has been described in Section 4.4. The first thing that should be noted is that the family within *S. tuberosum* cv. *Phureja* appears to consist of three members while in *A. thaliana* it consists of four. *S. tuberosum* cv. *Phureja* appears to be missing the *BSU1* gene. It is unfortunate that AtBSU1 is the BSL family member with the best described function in the BR pathway in *A. thaliana*. It is therefore difficult to draw direct comparisons on the functions of the other *BSLs* in the *Solanaceae* when they have not been described in detail in the model system. What is clear from the analysis in Section 4.4 is that *StBSL1* can be distinguished from *StBSL2a* and *StBSL2b* using the nucleotide and amino acid sequences in the methods described in this work. *StBSL2a* and *StBSL2b* are homologues of *AtBSL2* or *AtBSL3* (Figure 4.4.1), but it is not possible to infer whether they are functional orthologues. It could be suggested that that the AtBSL2/3 and StBSL2a/b evolved independently, after speciation, from a common ancestor. The phylogenetic trees imply that the separation of AtBSL1, AtBSU1 and StBSL1 is difficult and

the bootstrap values do not imply robustness of the trees shown (Figure 4.4.1). It is possible that AtBSL1 and StBSL1 are putative orthologues from the Blast data shown (Tables 4.4.1 and 4.4.2).

This family of proteins is a very unusual one, as the combination of Kelch-repeat domains and a phosphatase domain does not appear to arise very often. There have only been reports of this combination of domains on phosphatases occurring in plants and protists but in no other prokaryotic or eukaryotic organism (Kutuzov and Andreeva, 2002). The name protein phosphatases with Kelch-like repeat domains (PPKLs) has been proposed and these proteins have been found in *P. falciparum* and in the BSU1 family in *A. thaliana* (Kutuzov and Andreeva, 2002). It was suggested that the protist enzymes are more similar to plant enzymes due to the endosymbiotic origin of protists. This means PPKLs could be specific to photosynthetic organisms and their non-photosynthetic descendents (Kutuzov and Andreeva, 2002).

The Y2H system was employed to try to confirm and extend the interactions observed between characterised components of the BR pathway from the model plant *A. thaliana* to *Solanum* species. BSK2 and BIN2 are known interactors of AtBSU1 and AtBSL1 (Kim *et al.*, 2009). The *Solanum* putative orthologues StBSK2 and StBIN2 were tested to determine if they could interact with all three StBSLs *in vitro*. The interaction of StBSK2 with the three StBSLs was shown in the *Solanaceae* expanding on the information available from *A. thaliana* (Figure 4.6.2a). These *Solanaceae* interactions will, of course, have to be confirmed *in planta*.

Auto-activation of some proteins with their empty vector controls within the yeast system means it is difficult to draw conclusions from some experiments. This was seen clearly for StBIN2, StBSL1 and StBSL2a in the bait vector. This could be due to a small protein

fragment from the ccdb gene forming and interacting with these proteins but it appears specific to the bait vector as these proteins do not show auto-activation in the prey vector. It means no conclusions can be drawn from the results of the *LacZ* assay when this combination is seen especially when the blue colour is of similar strength in the control as seen in the samples. In order for the findings of this Y2H work to be confirmed or dismissed these proteins will have to be tested *in planta* as Y2H is only an indicator of interaction and not necessarily a faithful indicator of what happens *in planta*. When these interactions have been tested in *A. thaliana* used bimolecular fluorescence complementation and co-immunoprecipitation assays were used (Kim *et al.*, 2009).

The *BSL2* silenced plants display quite striking developmental phenotypes. Stunted growth and curled leaves are obvious, and this phenotype is consistent with the dwarf phenotype seen in *A. thaliana* when RNAi was used to silence *BSL2/3* in a *bsu1/bsl1* knock-out line (Figure 4.5.1) (Kim *et al.*, 2009). The TRV::*BSL2b* VIGS plants show the down-regulation of both *NbBSL2a* and *NbBSL2b* (Figure 4.8.2b). The silencing constructs for *NbBSL2a* and *NbBSL2b* were designed to be gene-specific to avoid off-target silencing. However, given the sequence similarity upstream and downstream of the VIGS regions between these two genes, the occurrence of secondary silencing could be responsible for the results shown (Figure 4.8.2b). Both off target silencing and the effect of gene regulation should be investigated further in future work. It is interesting that the TRV::*5'BSL2a* plants showed such a small change in transcript when they show such a severe growth phenotype, runaway senescence and measurable reduction of the R2/PiAVR2 HR. If the reduction of the *NbBSL2a* gene is not the cause of these observations then: what is?

The TRV::*3'BSL2a* plants and TRV::*BSL2b* showed an increase in transcript levels of the *NbBSL1* gene. This is possibly due to preventing a regulatory feedback loop within these

plants (Figure 4.5.2b). In addition qRT-PCR data show the *BSL* expression of all three family members is increased by two to three-fold in the TRV::*BRI1* plants (Figure 4.8.2b). In the absence of the cell surface receptor the plants cannot sense and respond to the BL hormones that are being synthesised. In wild-type plants down-regulation of the expression of BR biosynthesis genes occurs through dephosphorylation of BZR1 when the BR signalling pathway is active, resulting in a negative feedback loop. Consequently, the production of BR continues and could cause the increased expression in downstream signalling components as the plant continues to activate this pathway. The data presented here point towards the possibility that up-regulation of the *BSLs* is coordinated with the transcription of BR biosynthesis genes. This could be confirmed by comparing the expression of the *BSLs* with *DWF4* and *CPD* after different treatments.

The links between the BR pathway and plant defence pathways activated by JA, SA and auxin, have long been suggested but are difficult to prove due to the complex nature of crosstalk between them. This work has reinforced some of the potential links. First of all, an effector protein from *P. infestans,* PiAVR2, targets a key regulatory step of the BR pathway through interaction with the BSLs. When expression of the host targets are reduced, albeit only slightly, there is still a striking effect on the growth and development of the plant and triggering of runaway senescence, which could be linked to the SA pathway (Figure 4.8.3). Another piece of evidence to suggest a link between the pathways is that when plants are pre-treated with EBL they have increased resistance to *P. infestans* (Figure 4.7.1). This implies that the pre-treatment with EBL may prime the plant and cause the activation of defence response components prior to infection. This assay should be expanded to other pathogens, such as bacterial and fungal infections, and also to pests like nematodes and aphids, to determine if it has the same affects on plant interactions with these organisms. Previous work has shown when potato plants were sprayed with BR and then infected with *P. infestans* there was a reduction in infection, which was linked

to an increase in ABA and ethylene levels but also the presence of phenolic and terpenoid substances (Krishna, 2003). Increased disease resistance has also been observed in cucumber and barley plants when they were pre-treated with BR (Krishna, 2003).

Another interesting discovery from this work, which provides another link between the BR and defence pathways, was the reduction in the R2/PiAVR2 HR observed in the *bak1* and *bsl2a/2b* silenced plants (Figure 4.9.2). This information suggests that these genes are important for the ability of R2 to recognise PiAVR2 and subsequently produce an HR. The same reduction in HR is not observed in the *bri1* silenced plants (Figure 4.9.2). It is known that BAK1 is also the co-receptor to other cell surface receptors. It is thus possible that the BSLs are linked to another receptor complex and it is signalling within this pathway which is monitored by R2. This will be investigated in more detail using the *BSL1* gene in Chapter 5.

A recent paper has also investigated the link between the BR pathway and stress and salt tolerance. This work investigated the different hormone pathways by the use of transgenic plants that either lack a key component or over-express a key component of each pathway (Divi *et al.*, 2010). It was found that feeding plants through the soil with 24-Epi-brassinolide increased stress tolerance in WT *A. thaliana* (Divi *et al.*, 2010). This work also showed that the redox-controlled transcriptional cofactor NONEXPRESSOR OF PATHOGENESIS-RELATED GENES 1 (NPR1) which is needed for SA-mediated systemic acquired resistance was important for mediating the stress tolerance controlled by the BR pathway and that endogenous abscisic acid (ABA) levels suppress the effect of the BR pathway in WT plants (Divi *et al.*, 2010). Another important finding in this report is that the *PR-1* gene, which is known to be up-regulated in defence responses, was found to be up-regulated in response to BR treatment in *npr1-1* transgenic plants along with the transcription factor *WRKY70* which may promote potential cross-talk between the BR and

SA pathways (Divi *et al.*, 2010). *GTS1*, *PDF1.2* and *RD22* were also up-regulated in WT plants treated with 24-Epi-brassinolide which connects the BR pathway to the SA, JA and ABA pathways (Divi *et al.*, 2010). This work shows that there are links between the BR pathway and plant defence pathways. Nevertheless, other papers have shown that pre-treatment with brassinosteroid does not always increase resistance to pathogens, so there is still debate in this area (Albrecht *et al.*, 2012; Belkhadir *et al.*, 2012).

Although this has been a challenging family to investigate, reasonable progress has been made in understanding these proteins, especially given that AtBSL2 and AtBSL3 are not described in detail in *A. thaliana*. There is still much work to be done to determine why the BR pathway and, more specifically, StBSL2a and StBSL2b are effector targets. Why would an effector from *P. infestans* target these proteins? This pathway has been linked to other hormone pathways and it is possible that it therefore links to the plant defence system. Nevertheless, the pathway is primarily reported to regulate the growth and development of the plant and not defence. However, evidence here shows that pre-treatment of *N. benthamiana* plants with Epi-BL results in plants being more resistant to *P. infestans* infection and similar results have also been seen by other groups, which implies that there could be a link to defence systems (Krishna, 2003). If an increase in BR treatment leads to increased defence it would seem reasonable to hypothesise that the pathogen could be inactivating this pathway.

## Conclusions

Host targets of PiAVR2 have been found within the brassinosteroid pathway, which regulates the growth and development of plants. These BSL proteins are known activators of this pathway but it is shown here that they are important also for the development of the R2/PiAVR2 HR; therefore, they appear also to be linked to plant-pathogen interactions.

The BR pathway is not well understood in crop plants and, as such, reconstruction of the pathway was commenced from what was known from the *A. thaliana* literature. Although many components of the pathway are conserved, it was discovered that the *BSU1* gene appears to be missing in the *S. tuberosum* cv. *Phureja* genome.

# 5 - BSL1 and indirect recognition by R2

## 5.1 – Introduction

The work described in Chapter 4 has revealed that the candidate host targets of the PiAVR2 effector are the StBSL2a and StBSL2b proteins from the brassinosteroid pathway. It was also shown that the reduction of expression of *StBSL2a/2b* led to a reduction in the R2/PiAVR2 HR. This interesting observation will be extended here to see if StBSL1 also plays a role in R2 recognition of PiAVR2.

The brassinosteroid pathway is complex, with many functionally characterised components, but there is still much to be discovered. An example of this complexity is that each gene in the pathway is usually part of a gene family. Some families are quite large, for example *BIN2.* This gene is part of a family of ten AtGSK-like kinases which fall into four subgroups. *BIN2* is found in subgroup II which contains three genes; a knock-out mutant of all genes in this subgroup has been generated (Kim *et al.*, 2009). Even though *BIN2* was no longer expressed, the accumulation of phosphorylated transcription factor, BES1, was still observed (Kim *et al.*, 2009). This suggests that some of the other AtGSK-like kinases function in the BR pathway. Indeed it has been shown that six of these ten AtGSK-like kinases can interact in a yeast-2-hybrid assay with the transcription factor (TF) BZR1 and, for 1 of these 6, this interaction has also been shown *in planta* using split YFP (Kim *et al.*, 2009).

The *BSU1*-family was introduced in Chapter 4 and, as explained previously, there are four members in total. Splice variants of these genes add to the complexity of this family. This Chapter will focus on *BSL1*. The *A. thaliana* literature for this gene is more developed than that of *BSL2* or *BSL3*. *BSU1* and *BSL1* have divergent sequences and expression profiles but a double knock-out of these genes has little phenotypic effect (Mora-Garcia *et*

*al.*, 2004). *BSU1* is expressed in young roots, shoots and flowers and in seedling plants but is absent in mature stems and leaves of *Arabidopsis thaliana*, while *BSL1* is expressed more highly in older tissues when compared to younger tissues (Mora-Garcia *et al.*, 2004). The cellular localisations of BSU1 and BSL1 are also different, as BSU1 localises to the nucleus and weakly in the plasma membrane while BSL1 is found to have plasma membrane and cytoplamic localisations (Kim *et al.*, 2009).

The *BSU1* and *BSL1* genes are long, usually between 2.5–3 kb in length, and encode Kelch-repeat domains at the N-terminus and a phosphatase domain at the C-terminus. Between the Kelch and phosphatase domains is a third domain thought to be a linker. It is thought that a Kelch-repeat domain will form a β-propeller structure which would consist of six β-sheets (Mora-Garcia *et al.*, 2004). The phosphatase domain has properties which are consistent with both PP1 and PP2A phosphatase families. However, it also has some differences (Mora-Garcia *et al.*, 2004). These include extensions to some loops that connect secondary structure elements. There are also some changes to normally conserved residues which are important for regulation. These changes make this group of phosphatases divergent from the PP1 and PP2A families (Mora-Garcia *et al.*, 2004). Despite these differences it is known that BSU1 and BSL1 are functional phosphatases as they are able to de-phosphorylate pTyr200 of BIN2 which is the crucial residue for its function as a kinase (Kim *et al.*, 2009).

It has been shown that both BSU1 and BSL1 can interact in the split YFP system with both BSK1, the activator of BSU1/BSL1, and BIN2, the substrate of these phosphatases (Kim *et al.*, 2009). This information supports the assumption that both proteins have overlapping functions in the BR pathway.

The differences between *BSU1* and *BSL1* in the *Solanaceae* will not be investigated because, as stated in Chapter 4, a putative orthologue of *BSU1* could not be found in the genome of *S. tuberosum*. This Chapter will therefore focus solely on *StBSL1* and investigate the role it may play in R2-mediated disease resistance, and why it is targeted by the *P. infestans* effector PiAVR2.

## 5.2 – Is StBSL1 a host target of PiAVR2?

The yeast-two-hybrid (Y2H) library screen performed with PiAVR2, described in Chapter 4 Section 4.2, yielded one candidate interactor. The interactor represented the C-terminal half of a Kelch-repeat containing Ser/Thr phosphatase called BSL2a. It was shown in Chapter 4 (Section 4.2 and 4.5) that full length StBSL2a and StBSL2b interacted with PiAVR2. Due to the similarities between the proteins in the StBSL-family and the fact that the StBSL2a and StBSL2b family members were shown to interact, StBSL1 was tested to determine whether it could also interacted with PiAVR2. Full length *StBSL1* was amplified from *S. tuberosum* cDNA using primers designed on a full length EST from the *Solanum lycopersicum BSL1.* The *S. tuberosum* gene was cloned into the Y2H vectors to determine if interaction with PiAVR2 could occur. A specific interaction Y2H assay was undertaken (Figure 5.2.1a). This figure shows that PiAVR2$^{N31}$, PiAVR2$^{K31}$, PiAVR2 C-term (amino acids 65 – 121), PiAVR2-like and PiAVR2-like C-term (amino acids 65 – 121) can all interact with the full length StBSL1 due to activation of the *HIS3* and *LacZ* reporter genes. The *LacZ* assay suggests that the C-termini of PiAVR2 and PiAVR2-like so not have such strong interactions as the full length forms of PiAVR2 and PiAVR2-like. PITG_08949, a closely related effector from *P. infestans* (described in Chapter 3), does not interact with StBSL1, so is used as a negative control in future experiments.

The BSL2a fragment recovered from of the original Y2H screen included some of the linker domain and the C-terminal phosphatase domain (1803-2988 bp). To determine if the same domains of StBSL1 could interact with the various forms of PiAVR2, the corresponding region of StBSL1 was cloned. It was found that the PiAVR2 forms do interact with the C-terminus of StBSL1 but that the control effector PITG_08949 does not (Figure 5.2.1b). This implies that it is the phosphatase domain of the BSL proteins that is interacting with PiAVR2.

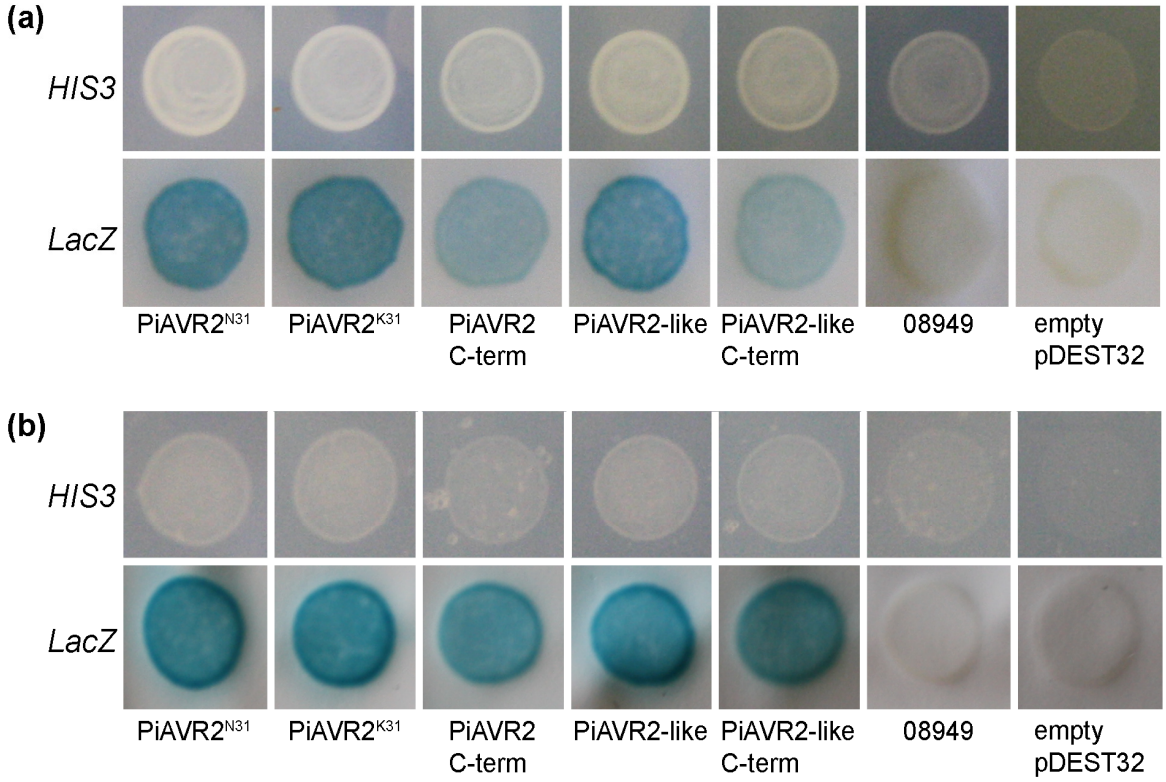


**Figure 5.2.1: StBSL1 Y2H.** **(a)** Specific Y2H assay to determine if interaction occurs between full length StBSL1 and the various forms of PiAVR2 and PITG_08949. **(b)** Specific Y2H assay to determine interaction between the C-termini of StBSL1 and the various PiAVR2 forms and PITG_08949. The top row in **(a)** and **(b)** is the histidine reporter assay, which shows growth of yeast co-transformants on a double dropout medium without histidine; bottom row is the LacZ reporter gene assay which depicts the activation of the LacZ reporter gene by blue colouration of yeast colonies.

## 5.3 – Genuine homologues

The sequence similarity at the nucleotide and protein level of *AtBSL1* and *StBSL1* was shown in Chapter 4 but an alignment of the amino acid sequences is shown below to visually illustrate the similarity between the BSL1 proteins from *A. thaliana, S. tuberosum* and *S. lycopersicum* (Figure 5.3.1). What this shows is that there is only one region where these three protein sequences differ greatly. This appears to occur at the linker domain between the Kelch repeat domain and the phosphatase domain, amino acids 375 to 465. The rest of the protein is highly conserved between the species.

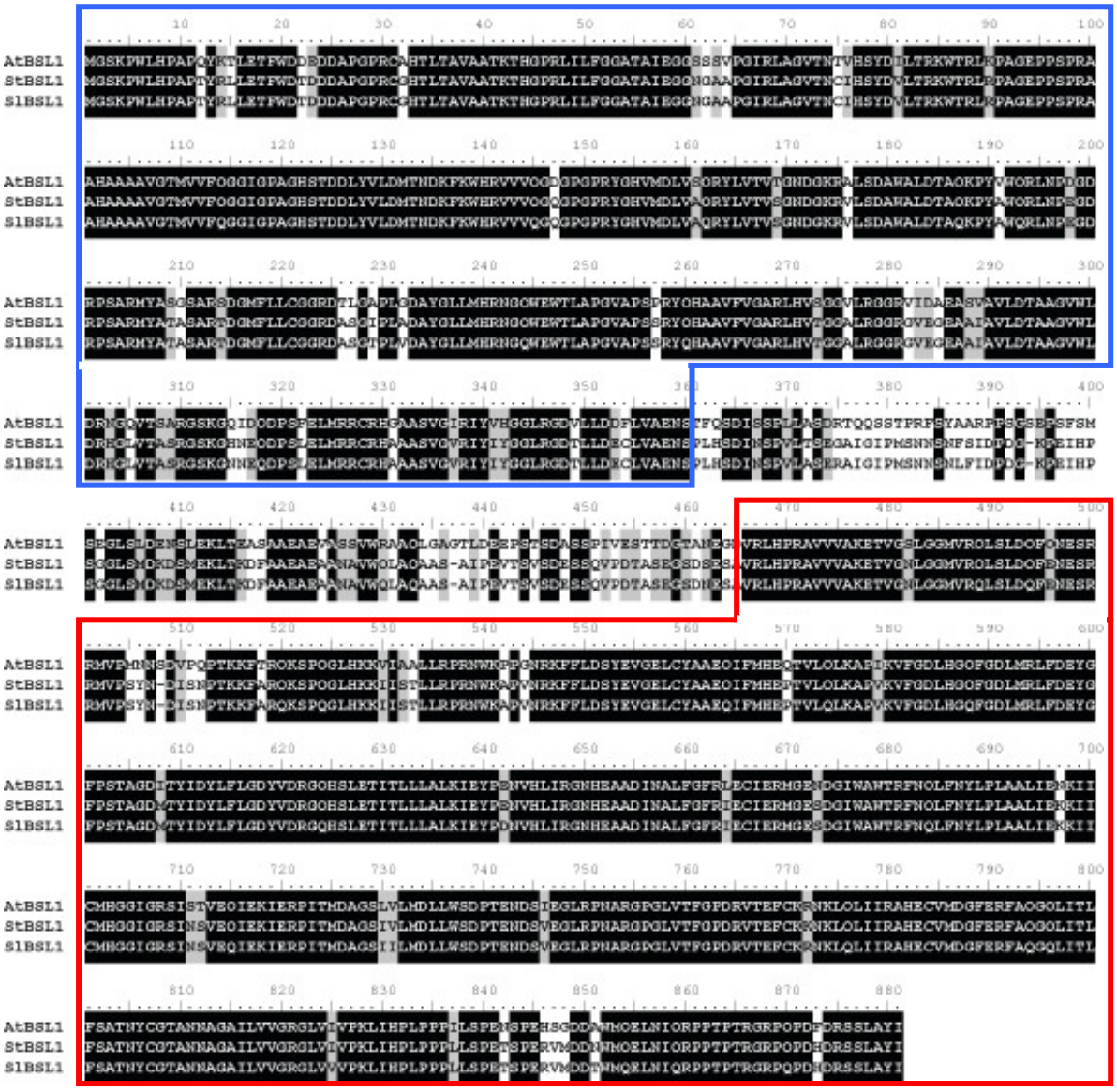


**Figure 5.3.1: BSL1 protein alignment.** Protein alignment of AtBSL1, StBSL1 and SlBSL1 showing amino acid sequence similarity between all three full length proteins. The blue box shows the Kelch-repeat domain and the red box shows the phosphatase domain. Alignment generated using Bioedit.

To further test that the three proteins shown above were orthologues of each other a phylogenetic tree was generated using the protein sequences of the *A. thaliana* BSU1 family members, StBSL1, and SlBSL1. AtPP2A B' alpha was used as the outlying phosphatase. The resulting tree illustrates that AtBSL2 and AtBSL3 are very closely related but StBSL1 and SlBSL1 group with AtBSL1 (Figure 5.3.2). Consequently, it can be

concluded that the protein being used in the Y2H experiments is the potato orthologue of AtBSL1. The potato and tomato proteins group together more closely than with *A. thaliana* BSL1 but this is expected as they are both members of the *Solanaceae*.

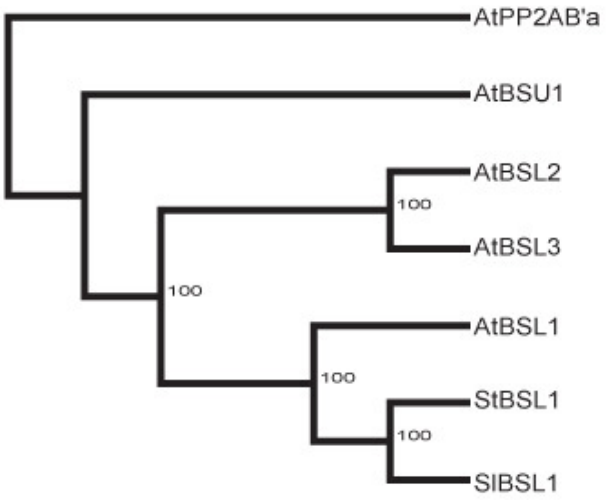


**Figure 5.3.2: Phylogenetic tree of the AtBSU family, StBSL1, SlBSL1 and AtPP2A B'alpha.** A Neighbour Joining Tree was generated in Topali. Numbers at each node represent the percentage bootstrapping value using 500 replicates.

## 5.4 – *in planta* confirmation of interaction

To confirm the interaction of the PiAVR2 forms with StBSL1, bimolecular fluorescence complementation (split YFP) experiments were carried out in *N. benthamiana* leaves. StBSL1 was tagged at the N-terminus of the protein with the C-terminal half of the YFP protein. The PiAVR2 forms and PITG_08949 were also tagged at the N-terminus of the protein but with the N-terminal of the YFP protein. PITG_08949 was again used as a negative control. The split YFP experiment confirmed the interaction of PiAVR2 with StBSL1 (Figure 5.4.1a). When each form of PiAVR2 is expressed with StBSL1 *in planta*

YFP fluorescence is present indicating that there is close enough proximity of the two proteins for the two halves of YFP to recombine. The same is not seen for the negative control PITG_08949. These data confirm that StBSL1 does appear to interact with all forms of PiAVR2 and PiAVR2-like (Figure 5.2.2a). This experiment also shows that the interaction occurs at either the plasma membrane and cytoplasm or in the endoplasmic reticulum (ER) (Figure 5.4.1a). The split-YFP interaction was quantified using a fluorometer. Leaf discs from infiltrated leaves were cut out and floated on water in a 24-well plate. Using the eGFP parameters on the fluorometer YN-PiAVR2$^{N31}$ – YC-StBSL1, YN-PiAVR2-like – YC-StBSL1 and YN-08949 – YC-StBSL1 were compared against un-infiltrated leaf discs. There is an increase in fluorescence when the PiAVR2 forms are present compared to PITG_08949 (Figure 5.4.1b). This increase in flouresence for PiAVR2$^{N31}$ and PiAVR2-like is statistically significant when compared to the flouresence emitted by PITG_08949 samples, $P < 0.05$. The stability of the proteins in these vectors was determined using western blots. The samples in the YN vector could be detected by an α-myc antibody and the YC-BSL1 could be detected by an α-HA antibody as these epitope tags are also found on these split YFP vectors. The PiAVR2 forms and PITG_08949 are stable in the YN split YFP vectors and StBSL1 is also stable in the YC split YFP vector (Figure 5.2.2c).

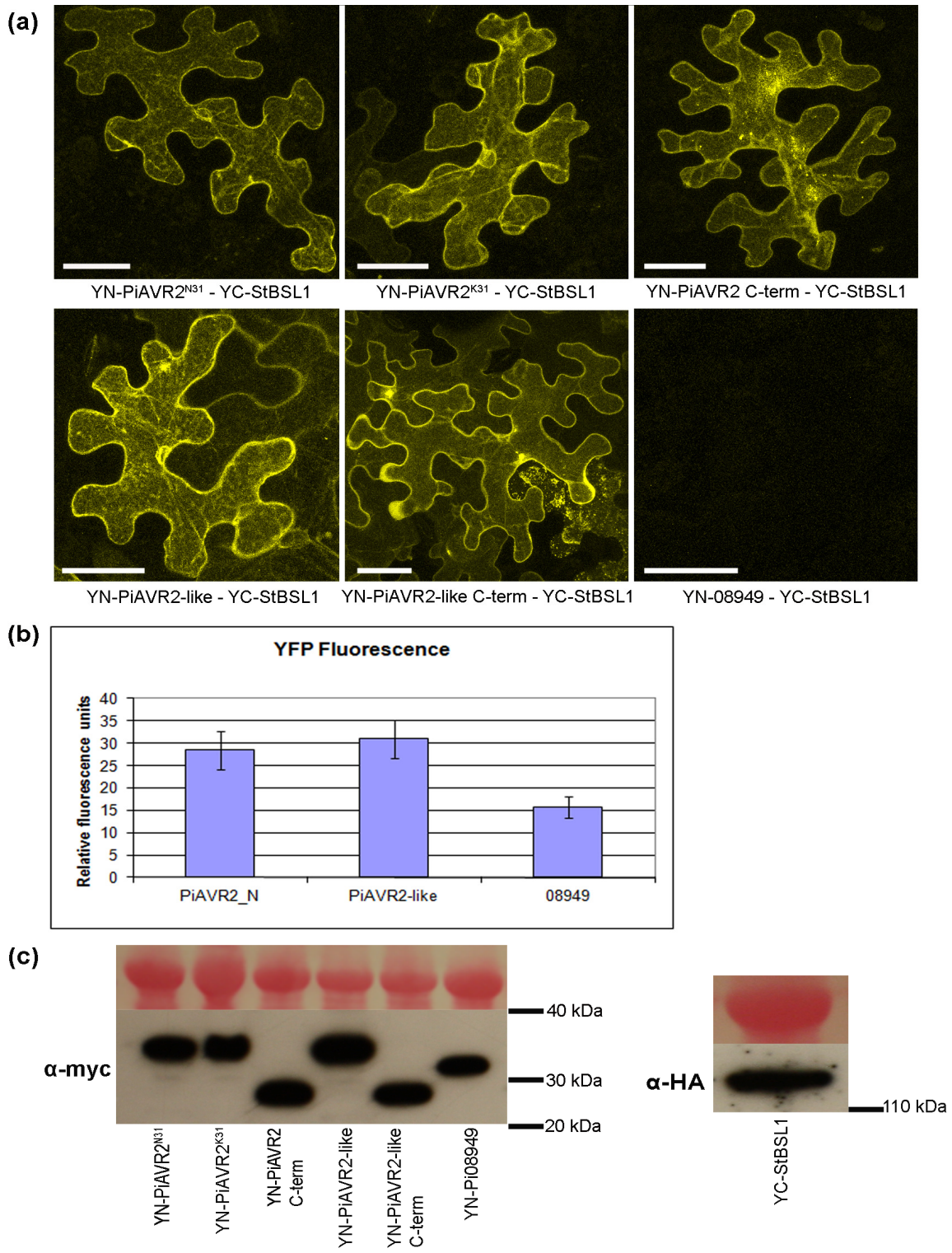


**Figure 5.4.1: *In planta* protein interaction confirmation. (a)** Split YFP between StBSL1 and all PiAVR2 forms and PITG_08949. The N-terminal half of the YFP protein is attached to the N-terminus of the PiAVR2 forms, the C-terminal half of the YFP protein is attached to the N-terminus of the StBSL1 protein. YN-08949 is a negative control. All images were taken at a gain of 615 and x40 magnification. Scale bars are 50 µm. **(b)** Fluorescence quantification. Graph of split YFP fluorescence YN-PiAVR2$^{N31}$ – YC-StBSL1, YN-PiAVR2-like – YC-StBSL1 and YN-08949 – YC-StBSL1. **(c)** Western blot showing the stability of each protein in the split YFP vectors. Ponceau stain shows protein loading on gel.

The interaction of BSL1 with PiAVR2 *in planta* has also been confirmed using co-immunoprecipitation in *N. benthamiana* (Figure 5.8.1) (S. Kamoun, The Sainsbury Laboratory, personal communication).

To further investigate the localisation of the PiAVR2 and StBSL1 interaction, the BiFC vectors were co-infiltrated with an RFP marker for the endoplasmic reticulum (ER). If the RFP and the YFP fluorescence have the same localisation then the interaction of PiAVR2 and StBSL1 occurs in the ER. This experiment was only conducted with PiAVR2$^{N31}$ and PiAVR2-like. Although the images suggest that the RFP and YFP fluorescence have similar localisations the YFP fluorescence is not sharp enough for it to be in the ER (Figure 5.4.2). The RFP images show sharp neat strands but the YFP images show these strands to be diffuse, implying that the YFP fluorescence is not in the ER itself but in the cytoplasm surrounding the ER strands. It can therefore be concluded that the interaction is occurring at the plasma membrane and in the cytoplasm.

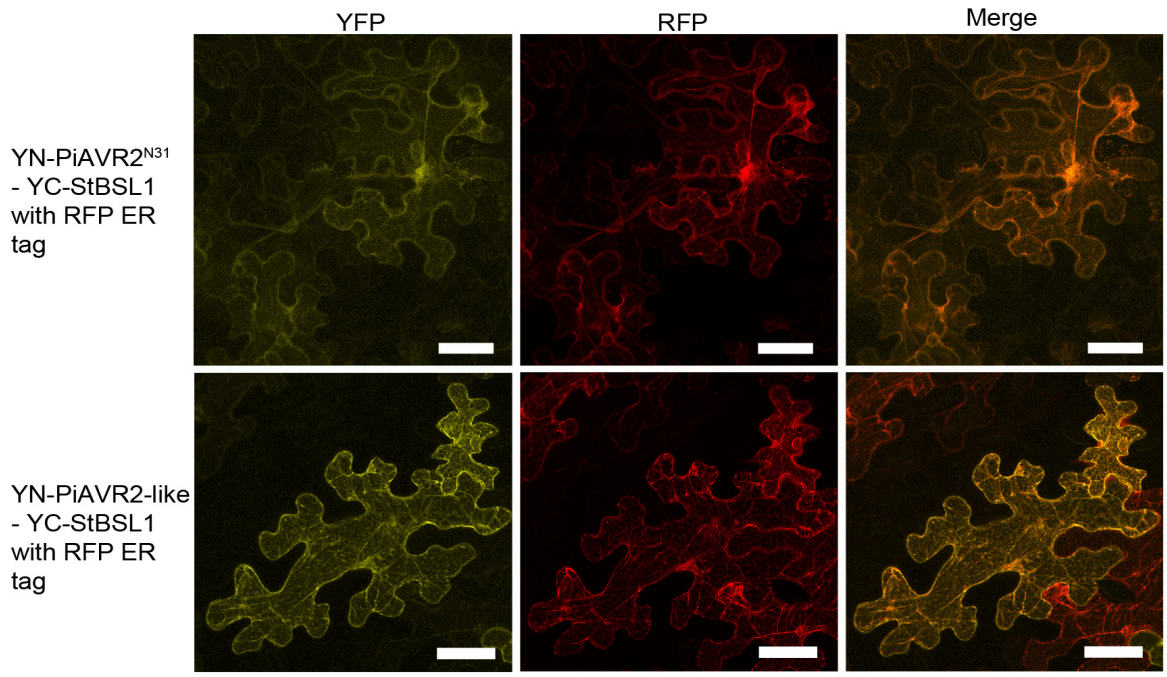


**Figure 5.4.2: Localisation of Split YFP comparison with RFP ER tag.** Split YFP StBSL1 – PiAVR2 with RFP ER tag. Top panel is YN-PiAVR2$^{N31}$ – YC-StBSL1 with the RFP ER tag. Bottom panel is YN-PiAVR2-like – YC-StBSL1 with the RFP ER tag. Scale bars are 50 µm.

## 5.5 – Virus Induced Gene Silencing of *BSL1*

The *BSL1* gene was silenced in *N. benthaminana* to determine what effect this had on the growth and development of the plant. The silencing was induced by VIGS using the TRV. Two different sections of the *NbBSL1* gene were amplified from *N. benthamiana* cDNA using primers designed from the *StBSL1* sequence. The first silencing construct, TRV::*5'BSL1,* is a 290 bp section at the 5' end of the gene. The second silencing construct, TRV::*3'BSL1,* is a 300 bp section situated in the phosphatase-encoding domain (Figure 5.5.1a). The plants expressing each of these silencing constructs give no developmental phenotypes when compared to the control TRV::*GFP* plant (Figure 5.5.1b). This is not entirely unexpected as the *BSL1* knock-out lines in *A. thaliana* also show no developmental phenotype. To test the silencing levels of these plants qRT-PCR was used. Primers were designed using sequence information generated from *NbBSL1*. This

sequence information was obtained by amplifying a 1.5 kb section of the *NbBSL1* gene from *N. benthamiana* cDNA using *StBSL1* internal sequencing primers. These *NbBSL1* primers were then used to screen TRV::*GFP*, TRV::*5'BSL1* and TRV::*3'BSL1* plants. The results show that there is an 80% reduction in the *NbBSL1* transcript in the TRV::*5'BSL1* and a 78% reduction in the TRV::*3'BSL1* plants when compared to control TRV::*GFP* plants (Figure 5.5.1c). The decrease in *NbBSL1* expression in the TRV::*3'BSL1* plants is statistically significant P = 0.003. The transcript level of the *NbBSL2a* and *NbBSL2b* genes were also measured as a control genes to assess off-target silencing in the TRV::*GFP*, TRV::*5'BSL1* and TRV::*3'BSL1* plants (Figure 5.5.1c). The primers used are described in Chapter 4, and were again designed based on *NbBSL2a* and *NbBSL2b* sequence information. A slight drop in the *NbBSL2a* and *NbBSL2b* transcript levels in the TRV::*5'BSL1* plants compared to TRV::*GFP* was observed. This drop is approximately 20% in the TRV::*5'BSL1* plants (Figure 5.5.1c). This drop in *NbBSL2a* and *NbBSL2b* expression could be caused by off-target silencing but could also be due to a change in gene regulation, caused by silencing *NbBSL1*, as the mode of regulation of this gene family is not clearly understood. The transcript level for the *NbBSL2a* and *NbBSL2b* in the TRV::*3'BSL1* plants is equivalent to that of the TRV::*GFP* control plants, there is no statistical difference. 25S transcript was used as the endogenous control gene for these experiments. Finally a phylogenetic tree was generated from an amino acid alignment, showing that StBSL2 is more closely related to AtBSL2 than AtBSL1 (Figure 5.5.1d).

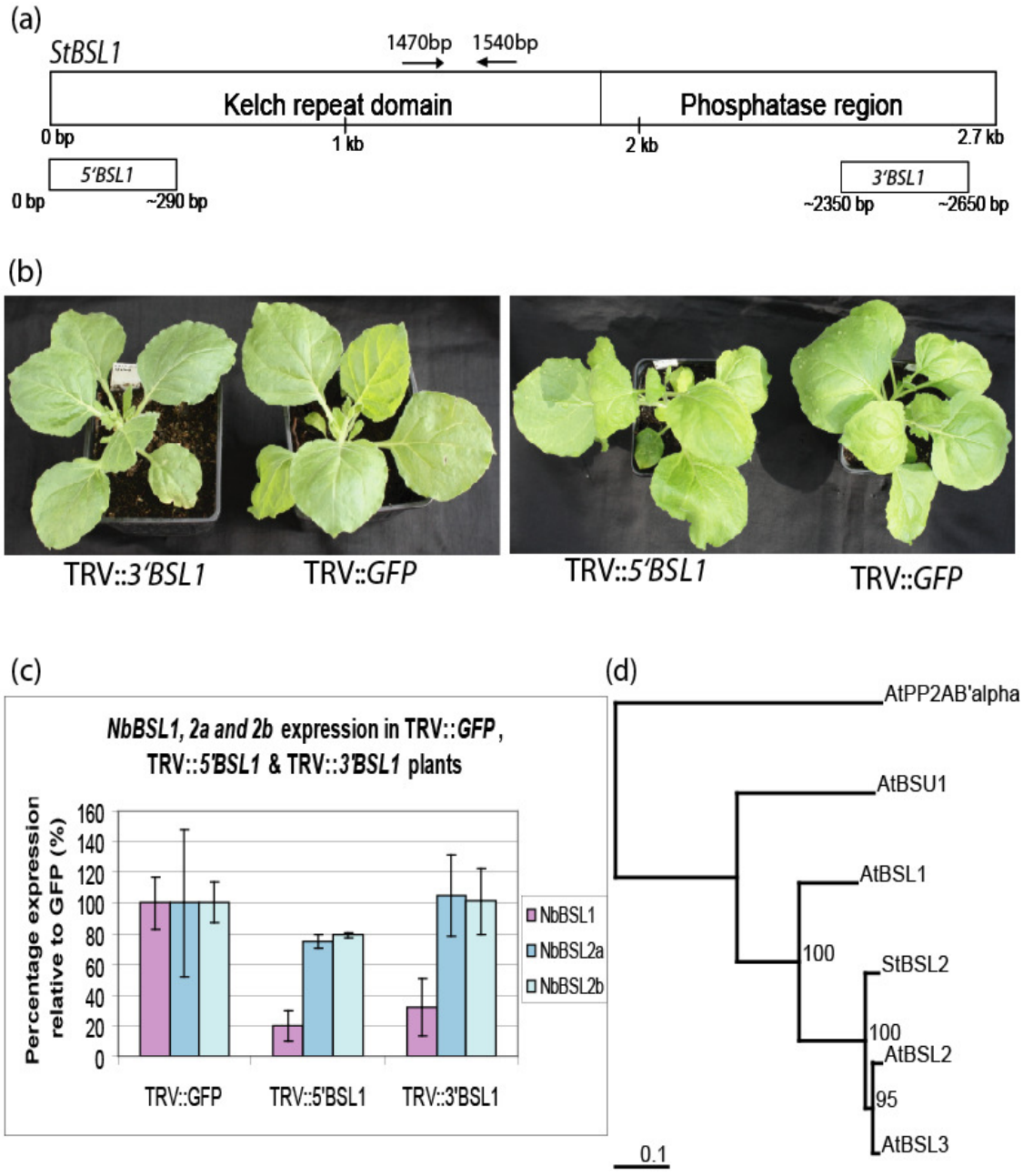


**Figure 5.5.1: *BSL1* silencing constructs. (a)** A diagram of *StBSL1* showing the positions of the two VIGS constructs. The two arrows at the top mark where the qRT-PCR primers for *NbBSL1* are positioned. **(b)** Pictures of the phenotypes of the TRV::*3'BSL1* and TRV::*5'BSL1* compared to the TRV::*GFP* control plants. **(c)** qRT-PCR showing expression of *NbBSL1, NbBSL2a* and *NbBSL2b* in the TRV::*GFP*, TRV::*5'BSL1* and TRV::*3'BSL1* plants. The *NbBSL1* expression is four biological replicates for TRV::*GFP* and TRV::*3'BSL1* but only one biological replicate for TRV::*5'BSL1*. *NbBSL2a* and *NbBSL2b* expression is a combination of three biological replicates for TRV::GFP and TRV::3'BSL1 but only one biological replicate for TRV::5'BSL1. All data were normalised to 25S rRNA endogenous control. **(d)** A Neighbour Joining Tree was generated in Topali. Numbers at each node represent the percentage bootstrapping value using 500 replicates. The tree was generated from an amino acid alignment of AtBSU1 family with StBSL2 and AtPP2A B'alpha as the outlier.

## 5.6 – Pathogen assays on *BSL1* VIGS plants

### 5.6.1 – Is susceptibility to *P. infestans* altered?

To determine if silencing of the *NbBSL1* gene has an affect on the ability of the plant to respond to a pathogen *P. infestans* isolate 88069 was used for infection assays. Leaves were harvested from TRV::*GFP*, TRV::*BAK1*, TRV::*5'BSL1* and TRV::*3'BSL1* plants and were examined six days post inoculation (Figure 5.6.1). This graph shows that there is no significant difference between the TRV::*GFP* plants and the *BSL1* silenced plants. The TRV::*BAK1* plants were used as a positive control as they show increased susceptibility to *P. infestans;* this increase in infection is statistically significant with a P value of <0.05. Statistical analysis was performed using the Holm-Sidak method in a one-way ANOVA on the Sigmaplot statistical software package. This could suggest that BSL1 is not the functional target of PiAVR2.

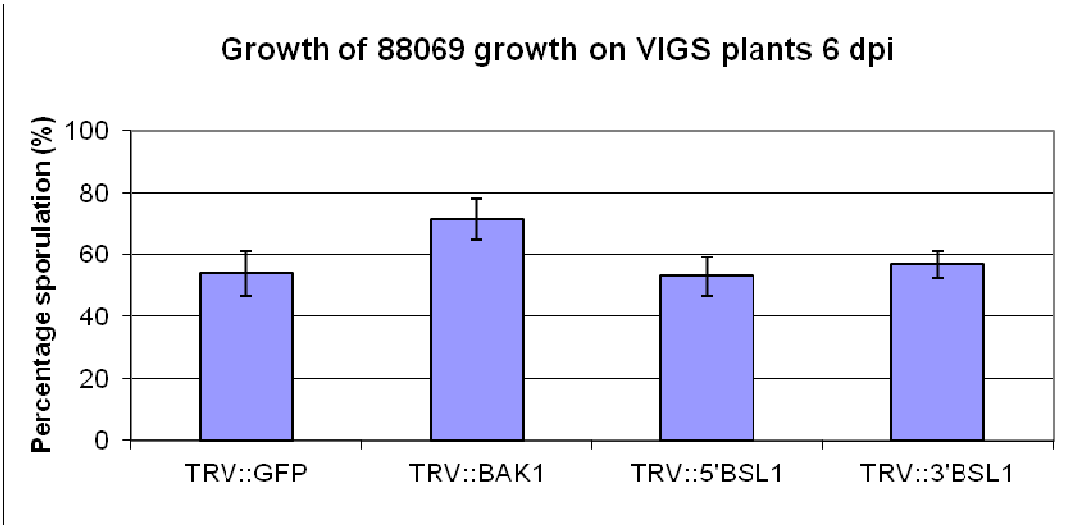


**Figure 5.6.1: *BSL1* infection assay.** Percentage of inoculated sites showing sporulation of *P. infestans* isolate 88069 on TRV::*GFP*, TRV::*BAK1*, TRV::*5'BSL1* and TRV::*3'BSL1*.

5.6.2 – R2-mediated cell death is specifically compromised following *BSL1* VIGS

It was shown in Chapter 4 Section 4.9.2 that the reduction in transcript of the *BAK1* and *BSL2a* genes had an effect on the formation of the R2/PiAVR2 HR. Since PiAVR2 is also able to interact with BSL1 an investigation of how the silencing of the *BSL1* gene would affect the formation of an HR when PiAVR2 was co-expressed in leaves with the *R2* orthologues, *R2*, *R2-like*, *Abpt* and *Blb3.* Three control potato *R* genes, *R3a, Sto1* and *Rx* were also used. R3a recognises the effector PiAVR3a$^{KI}$, Sto1 recognises the effector Pilpio1 (AvrBlb1) and Rx recognises the coat protein of Potato Virus X (PVX) (Bendahmane *et al.*, 1999; Armstrong *et al.*, 2005; Vleeshouwers *et al.*, 2008). These co-expression experiments were performed with TRV::*GFP*, TRV::*5'BSL1* and TRV::*3'BSL1* plants. When Rx, Sto1 and R3a are co-expressed with their cognate effectors they produce an HR on plants infected with any TRV construct (Figure 5.6.2). There is no statistical difference between the TRV::*GFP* control plants and the *BSL1* silenced plants for the control *R* genes using a one-way ANOVA on the Sigmaplot statistical software package. When the four *R2* orthologues are infiltrated into the leaves of the TRV::*GFP* control plants an HR is produced as expected (Figure 5.6.2). However, the ability of the *R2* orthologues to produce PiAVR2-induced HRs is significantly reduced on the *BSL1* silenced plants (Figure 5.6.2). Statistical analysis shows the four *R2* orthologues on the TRV::*3'BSL1* plants have a P value of <0.001 while on the TRV::*5'BSL1* plants they have a P value of <0.01 making the difference highly significant when compared to the TRV::*GFP* control plants. P values were generated using a one-way ANOVA on the Sigmaplot statistical software package using the Holm-Sidak method. The data used in the statistical analysis did not pass the Shapiro-Wilk test for normality as reported by Sigmaplot. A visual inspection of diagnostic residual plots indicated approximate normality and equality of variance. On that basis the Shapiro-Wilk warning was ignored. The data shown indicates that silencing of the *BSL1* gene compromised the ability of R2 to recognise PiAVR2 in a cell death assay (Figure 5.6.2).

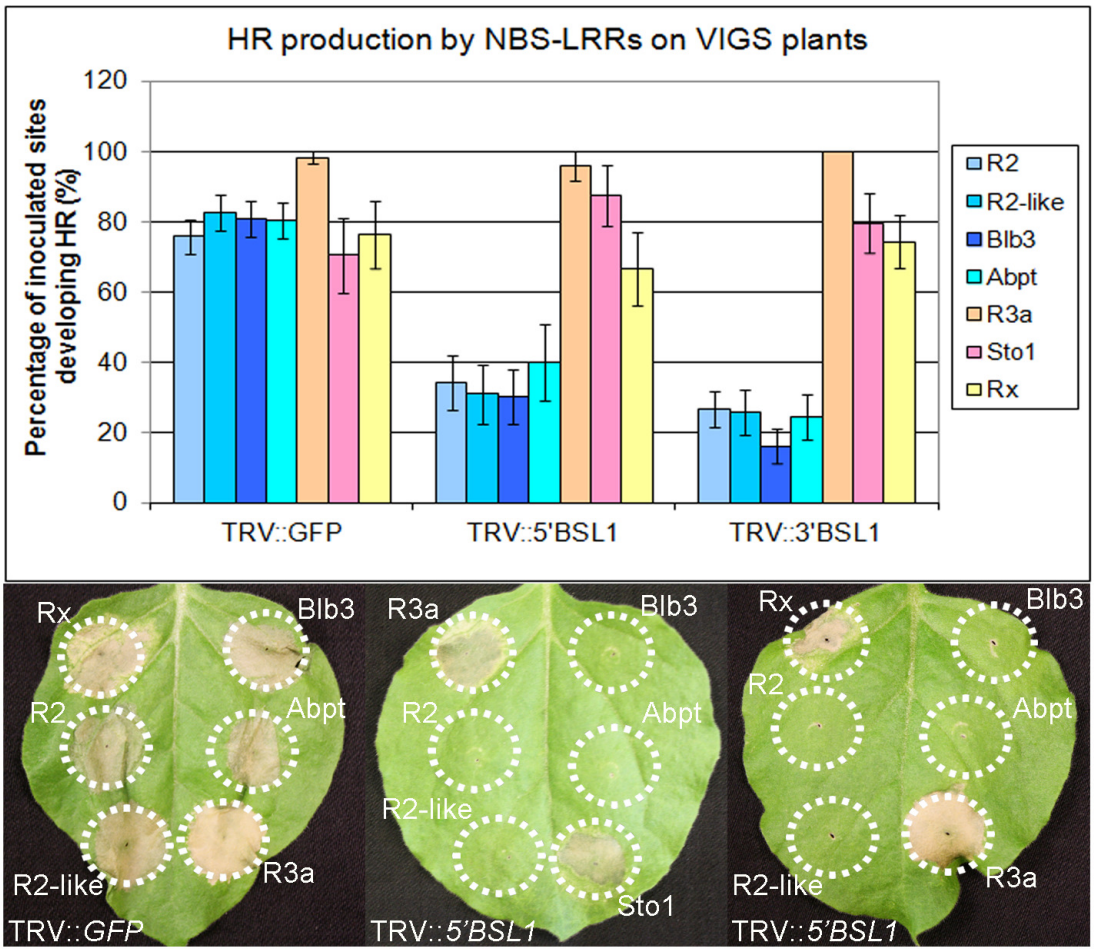


**Figure 5.6.2: Cell death on *BSL1* silenced plants.** A graph showing the development of HRs from seven potato *R* genes *R3a*, *Rx* and *Sto1* are the control *R* genes with *R2*, *R2-like*, *Abpt* and *Blb3* being investigated for their ability to function on the TRV::*5'BSL1* and TRV::*3'BSL1*. Examples of the TRV::*GFP*, TRV::*5'BSL1* and TRV::*3'BSL1* leaf images are below the graph in B. Four plants, three leaves per plant used in each biological replicate. For the *R2* orthologues data from eight biological replicates for TRV::*GFP*, three biological replicates for TRV::*5'BSL1* and seven biological replicates for TRV::*3'BSL1* were used. The data for the control *R* genes on the TRV::*GFP* plants was collected from, *R3a* six biological replicates, *Sto1* and *Rx*, from four biological replicates. On TRV::*5'BSL1* plants the data for *R3a*, *Sto1* and *Rx* was collected from two biological replicates. On TRV::*3'BSL1* plants data for *R3a* was collected from five biological replicates, *Sto1* from three biological replicates and *Rx* from four biological replicates. Pictures and HRs were taken 6 dpi.

5.6.3 – Silencing *BSL1* compromises R2-mediated disease resistance

The data in Figure 5.6.2 show that the ability of the *R2* gene to produce an HR is compromised by the silencing of *BSL1* expression. It was therefore examined whether silencing of *BSL1* expression affected the ability of R2 to stop the growth of an avirulent isolate of *P. infestans.* To investigate this, leaves from TRV::*GFP* and TRV::*3'BSL1* plants were infiltrated with Agrobacterium to transiently expressing *Sto1* on one half of the leaf and *R2* on the other half. *P. infestans* isolate 88069, which expresses both *PiIpio1* and *PiAVR2*, was then inoculated on the area of the leaf previously infiltrated with the resistance genes and left for infection to occur. Figure 5.6.3a shows that both resistance genes function as expected in the TRV::*GFP* plants by preventing the spread of *P. infestans* infection. Representative leaf images show no infection and the Trypan blue stained leaf shows that there is no growth of *P. infestans* (Figure 5.6.3b). However, on the TRV::*3'BSL1* plants the ability of Sto1 to prevent infection remains but the R2 response appears to be compromised, with a significant increase in infection occurring on the R2-infiltrated side of the leaves (Figure 5.6.3c). The leaf images show infection on the R2 infiltrated half of the leaf and the Trypan blue staining reveals the extent of *P. infestans* growth (Figure 5.6.3d). These results show that knocking down the expression of *BSL1* causes a reduction in R2 induced resistance. It can therefore be concluded that BSL1 is crucial for R2 recognition of PiAVR2 and, as a result, resistance to *P. infestans*.

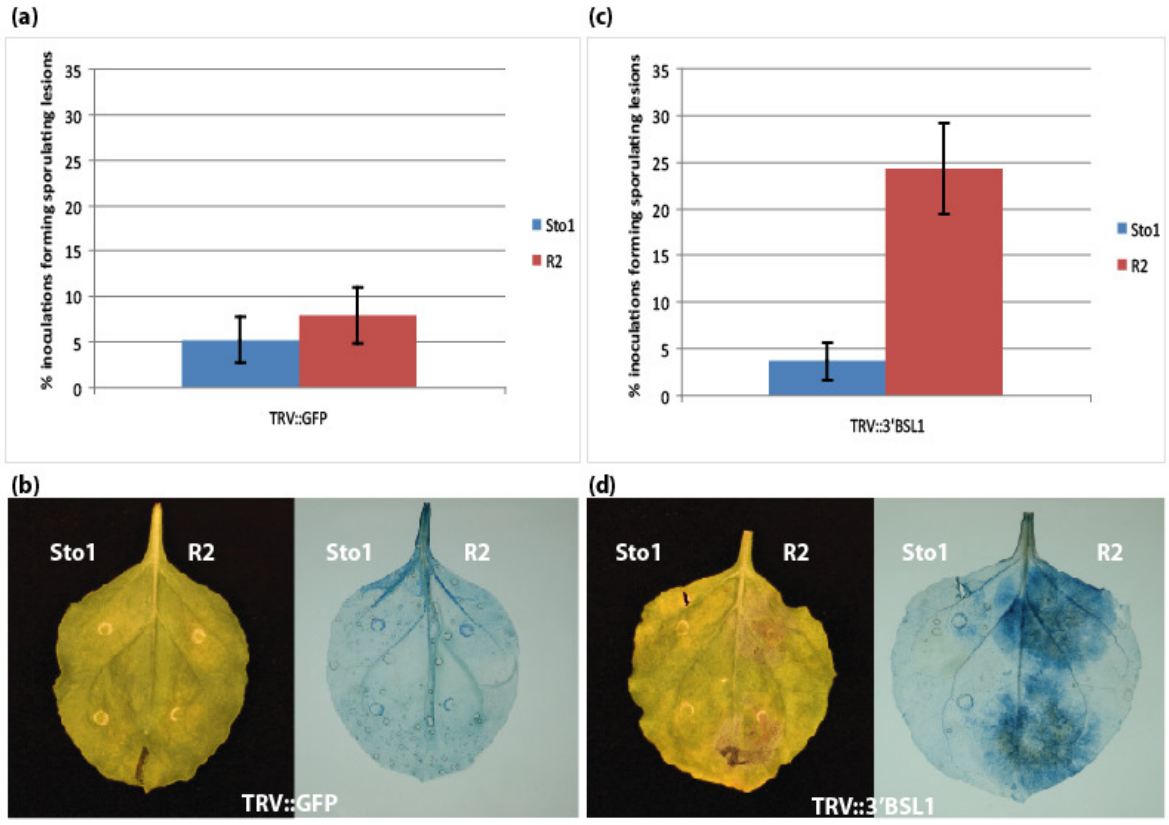


**Figure 5.6.3: *P. infestans* growth on *BSL1* silenced plants expressing resistance genes of interest. (a)** This shows the graph of *P. infestans* growth on TRV::*GFP* plants, representative images of this infection can be seen in **(b)**. **(c)** This shows a graph of *P. infestans* growth in the TRV::*3'BSL1* plants with representative images shown in **(d)**. The images are of the leaves under natural light and then the same leaf after it has undergone Trypan blue staining.

A reduction in *BSL1* expression affects the ability of resistance gene *R2* to provide resistance to *P. infestans*. To confirm this, it was necessary to demonstrate that R2 is stable in the TRV::*5'BSL1* and TRV::*3'BSL1* plants. A western blot was therefore carried out using a YFP_R2 construct. This construct contains the YFP protein fused at the N-terminus of the R2 protein. The construct was expressed in wild-type *N. benthamiana* leaves, TRV::*5'BSL1* and TRV::*3'BSL1* leaves and collected at 3 dpi. Two different concentrations of the construct were used to determine reproducibility. YFP_R2 appears stable in all backgrounds as there is a strong band in each lane of the expected size, (123 kDa), but not in the negative control lane which was un-infiltrated leaf material (Figure

5.6.4a). YFP_R2 was again infiltrated into the three backgrounds, wild-type *N. benthamiana* leaves, TRV::*5'BSL1* and TRV::*3'BSL1* leaves and this time imaged using the confocal microscope (Figure 5.6.4b). The images demonstrate that the uninfiltrated control, as expected, shows no fluorescence but there is fluorescence detected in wild-type *N. benthamiana*, TRV::*5'BSL1* and TRV::*3'BSL1* (Figure 5.6.4b). This does appear to be genuine YFP_R2 fluorescence in the TRV::*5'BSL1* and TRV::*3'BSL1* plants as the fluorescence is not seen in the nucleus of the cells as it would be if the YFP had been cleaved from the R2 protein. From these experiments it can be concluded that the R2 protein is stable in the TRV::*5'BSL1* and TRV::*3'BSL1* plants, which indicates that the loss of the recognition and resistance to *P. infestans* is due to the silencing of the *BSL1* gene.

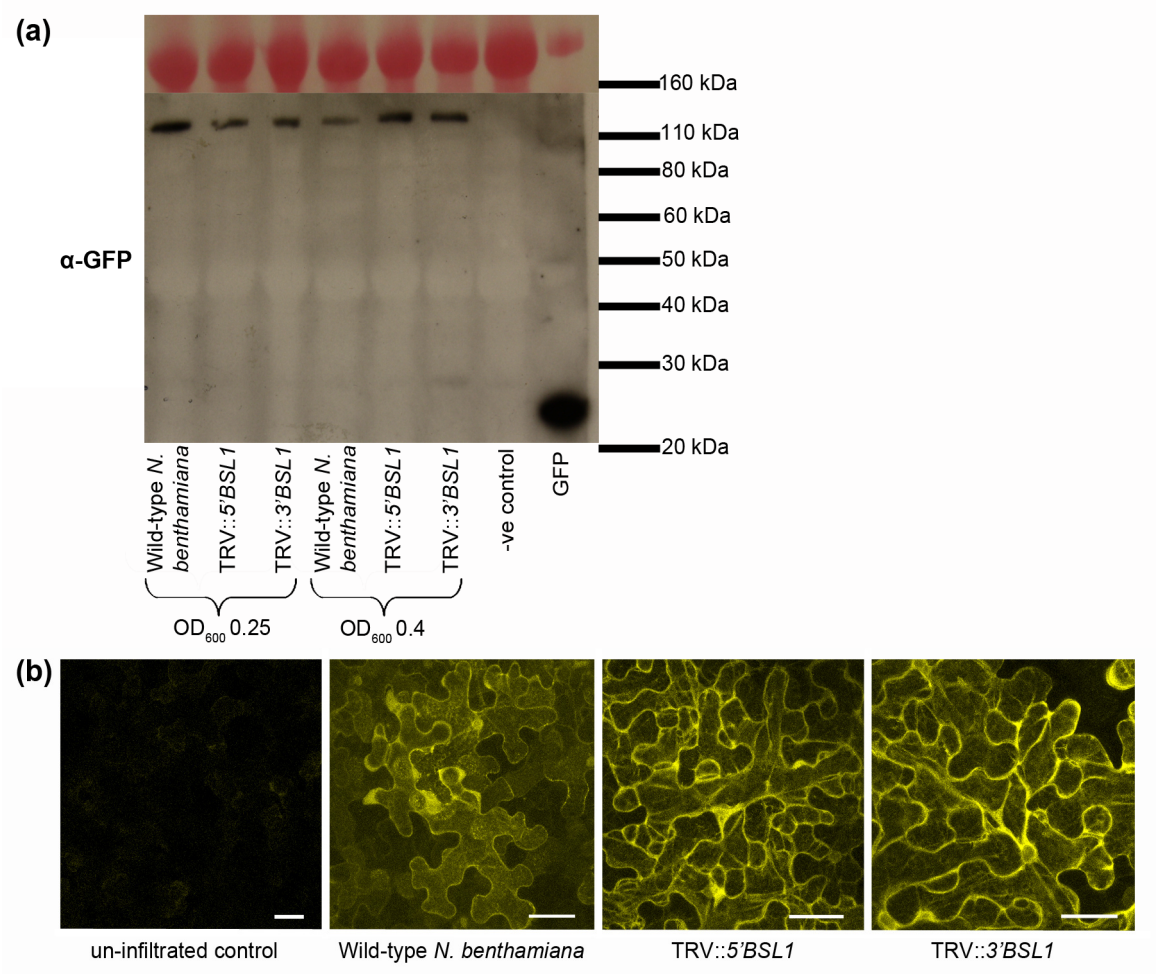


**Figure 5.6.4: YFP_R2 stability on BSL1 silenced plants. (a)** Western blot of YFP_R2 in wild-type *N. benthamiana*, TRV::*5'BSL1* and TRV::*3'BSL1* leaves. An α-GFP antibody was used to detect the YFP and the Ponceau stain shows the relative loading of the gel. **(b)** Confocal images showing the presence of YFP fluorescence in the three plant backgrounds. Gain was consistent across all images at 610 while the laser strength was also kept constant. Scale bars are 50 µm.

## 5.7 – Indirect recognition of R2 and PiAVR2

The data shown above indicates the importance of *BSL1* in the recognition of PiAVR2 by R2, but it is not known whether this is direct or indirect recognition. To begin to investigate this a specific Y2H interaction assay was carried out. In this assay direct interaction between R2 and PiAVR2, and R2 and StBSL1 were investigated using the *HIS3* and *LacZ* reporter gene assays. There only appears to be minimal growth on the histidine reporter

plate which is inconclusive of interaction. Therefore, there was no interaction between R2 and PiAVR2$^{N31}$, PiAVR2$^{K31}$, PiAVR2 C-term or PiAVR2-like (Figure 5.7.1a). There was also no interaction visualised between StBSL1 and R2 (Figure 5.7.1b).

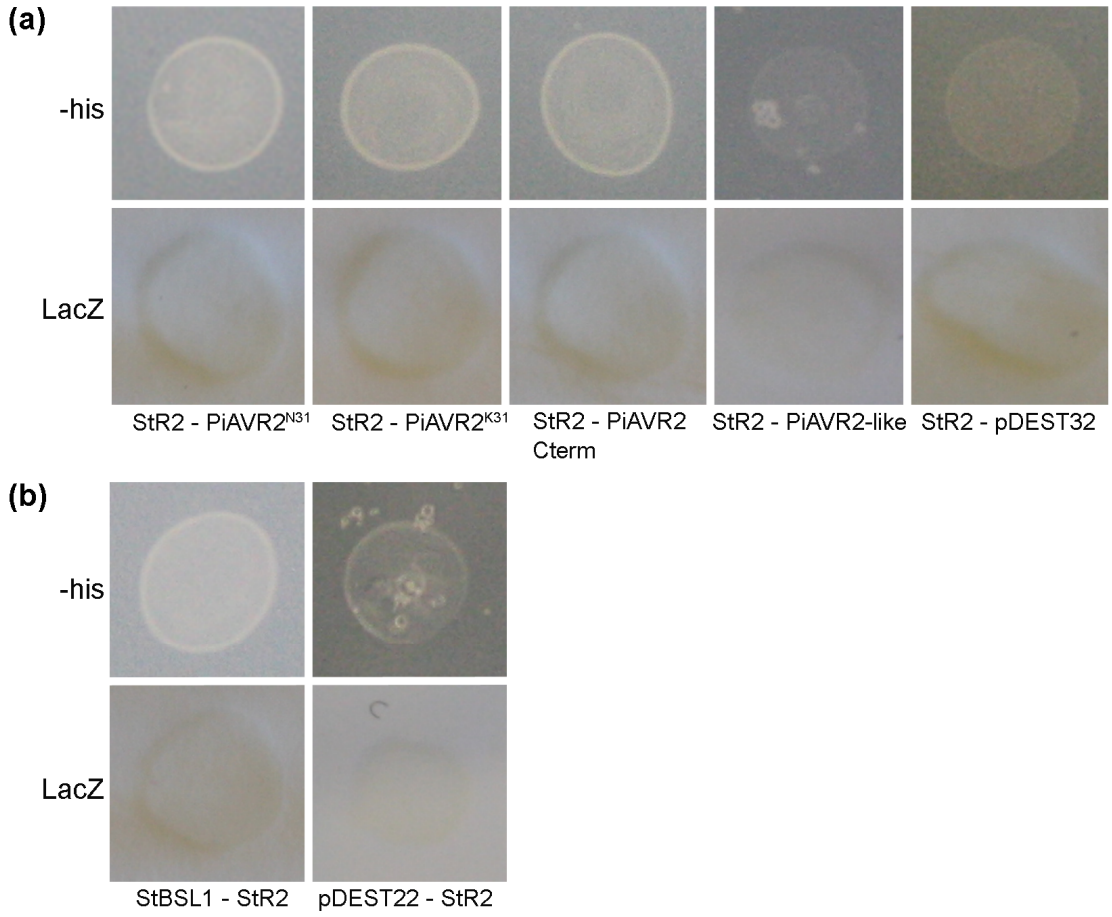


**Figure 5.7.1: Y2H assay investigating direct interaction of R2. (a)** A specific Y2H assay between StR2 and the three recognised forms of PiAVR2 and the unrecognised form PiAVR2-like with an empty vector control pDEST32. **(b)** A specific Y2H assay between StBSL1 and StR2 with an empty vector control pDEST22. The histidine reporter assay is on the top panel and the LacZ reporter assay on the lower panel for both **(a)** and **(b)**.

There are limitations with using the Y2H assay performed above but it does indicate that the interaction of R2 to the above tested proteins may not be direct and may therefore involve a third component in the complex. In order to investigate this, BiFC analysis was performed between R2 and StBSL1, with and without the expression of untagged PiAVR2$^{N31}$, PiAVR2 C-term and PiAVR2-like. R3a was used as a negative control for this experiment as it was not expected to interact with StBSL1 at any stage. It is clear that there is no interaction between R2 and StBSL1, which supports the data from the Y2H shown in Figure 5.7.1 (Figure 5.7.2a). However, when either PiAVR2$^{N31}$ or PiAVR2 C-term are introduced, fluorescence is clearly visible (Figure 5.7.2a). This fluorescence is not seen when the PiAVR2-like form is introduced with R2 and StBSL1. This implies that R2 and StBSL1 are only able to interact in the presence of the avirulent PiAVR2 (Figure 5.7.2a). The fluorescence for R2-StBSL1 interaction in the presence of PiAVR2$^{N31}$ appears to be mainly plasma membrane localised. However in the presence of PiAVR2 C-term the localisation appears more cytoplasmic. R3a does not interact with StBSL1, with or without any of the PiAVR2 forms, which was expected (Figure 5.7.2a). These data indicate that the recognition of PiAVR2 by R2 occurs via an indirect mechanism. The stability of the R2 protein in this vector was determined using western blot. The samples in the YN vector could be detected by an α-myc antibody. R2 and R3a are stable in the YN split YFP vector (Figure 5.7.2b).

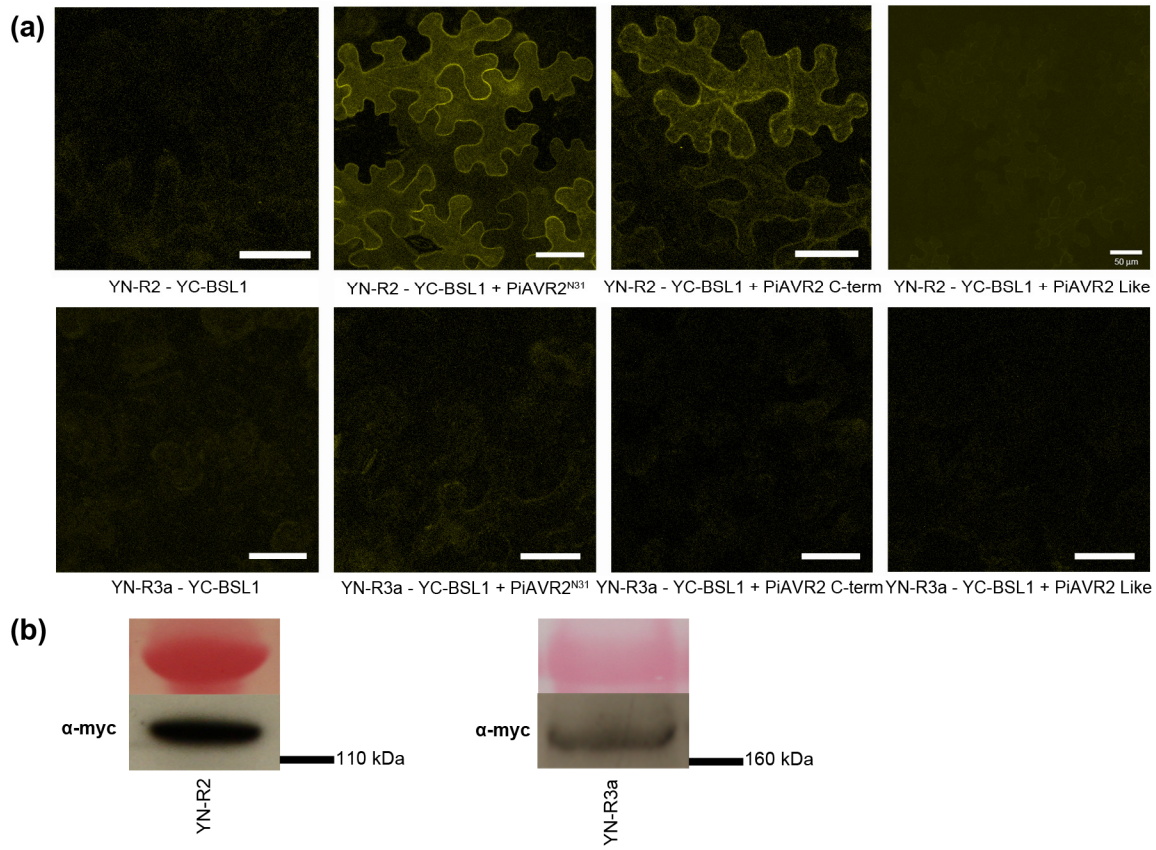


**Figure 5.7.2: Confocal microscopy investigating indirect interaction of R2 and StBSL1. (a)** Top panel is split YFP between YN-R2 and YC-StBSL1 -/+ PiAVR2$^{N31}$, PiAVR2 C-term and PiAVR2-like. Bottom panel is split YFP between YN-R3a and YC-StBSL1 -/+ PiAVR2$^{N31}$, PiAVR2 C-term and PiAVR2-like as controls. Scale bars are 50 µm. **(b)** Western blot showing the stability of the R2 and R3a proteins in the split YFP vectors. Ponceau stain shows protein loading on gel. R3a western was conducted by Stefan Engelhardt, University of Dundee.

## 5.8 – Discussion

It appears from the work so far that the function of PiAVR2 could be crucial to *P. infestans* as the variant form PiAVR2-like also interacts with the same target protein. This implies conserved function between the two forms of the effector, although one is able to evade recognition by the resistance gene. The fact that only one interactor, StBSL2a, was recovered from the Y2H screen with PiAVR2, suggests that this effector has a specific function. Of course the Y2H system can miss interactors if they are, for example,

membrane bound or nucleic acids. It is also interesting that the StBSL1 and StBSL2b proteins were not recovered from the Y2H screen since they appears to interact more strongly with PiAVR2 than StBSL2a. If genes are expressed at low levels these may be under-represented in the library which may cause them to be missed. This is a possible reason why StBSL1 and StBSL2b may not have been recovered from the initial Y2H screen. However, confidence can be found in the BSL1 interaction as another group have independently found PiAVR2 to specifically interact with the BSL family (S. Kamoun, The Sainsbury Laboratory); SlBSL1 co-immunoprecipitated with PiAVR2. The section of the StBSL proteins that interacts with PiAVR2 is in the C-terminus of the proteins and is most likely the phosphatase domain as the PiAVR2 forms interact with the C-termini of the StBSL1 and StBSL2a proteins (Figure 4.3.1 and Figure 5.2.1).

There is consistency between the data reported here from *Solanaceae* and the published data from *A. thaliana*. The localisation of the split YFP PiAVR2 – StBSL1 fluorescence is consistent with the plasma membrane and cytoplasmic localisation seen for the AtBSL1 (Mora-Garcia *et al.*, 2004). The data on phenotypic development are also consistent. When knock-out lines of AtBSL1, AtBSU1 and double knock-outs were generated in *A. thaliana* there was no developmental phenotype observed (Mora-Garcia *et al.*, 2004). The same lack of phenotype was also observed in the VIGS TRV::*5'BSL1* and TRV::*3'BSL1* plants generated in this work.

Although there are similarities between *A. thaliana* and *Solanaceae* species within the BSU1-family of the BR pathway, there are also some major differences. Using EST data the full length sequence for *SlBSL1* was established, allowing it to be amplified from *S. tuberosum*. However, the same was not true for *BSU1*. It was shown in Chapter 4 that no putative orthologue of the *BSU1* gene could be found in the potato genome and searching EST databases also yielded no similar matches for the *BSU1* gene, implying this gene is

not present in the *Solanaceae. AtBSU1* is the best described gene of this family in *A. thaliana*. The apparent absence of *BSU1* suggests that other members of this family could have the same function as *BSU1.* Unfortunately, the data to confirm this are not currently available. The function of *BSL1* in respect to the BR pathway has not been investigated in much detail in this work as its relationship to a *P. infestans* infection was of more interest at this stage. Therefore, no comparisons between the expression patterns of *AtBSL1* and *StBSL1* can be made at the moment. However, it does appear that BSL1 protein is needed for the function of the *R2* resistance gene which in itself is a significant discovery. It also provides more tools to further investigate the connections between the BR pathway and defence pathways.

One of the most significant findings of the work produced here could be the discovery of an interaction between R2 – StBSL1 in the presence of PiAVR2 (Figure 5.7.2). This is very exciting and has been confirmed, by others, using co-immunoprecipitation (co-IP) (Saunders *et al*., in preperation) (Figure 5.8.1). No interaction is observed between R2 – SlBSL1, and this is consistent with the results presented in this thesis (Figure 5.7.2). However, when PiAVR2$^{N31}$ is present, an interaction occurs between R2 and SlBSL1, as observed in this work (Figure 5.7.2). What can also be seen is that PiAVR2$^{N31}$ is not present when R2 co-immunoprecipitates with SlBSL1 (Figure 5.8.1). This implies that PiAVR2 may no longer be in complex with BSL1 when the R2 interaction occurs. This information leads to the hypothesis that the binding of PiAVR2$^{N/K31}$ to BSL1 causes a modification to occur, be it structural or biochemical, which triggers the binding and subsequent activation of R2 but perhaps also the dissociation of PiAVR2 from BSL1.

It has been shown that no interaction occurs between R2 and BSL1 when PiAVR2-like is present, Figure 5.7.2, and this is again confirmed by co-IP (Figure 5.8.1). These results for PiAVR2-like fit well with this effector being able to evade detection by R2. If there is no

modification of BSL1 by PiAVR2-like this could explain how it avoids recognition and subsequent activation of R2. It appears that the function of R2 orthologues require the presence of BSL1. Furthermore, an indirect interaction has been demonstrated and this is the first time it has been shown for a eukaryotic intracellular effector protein.

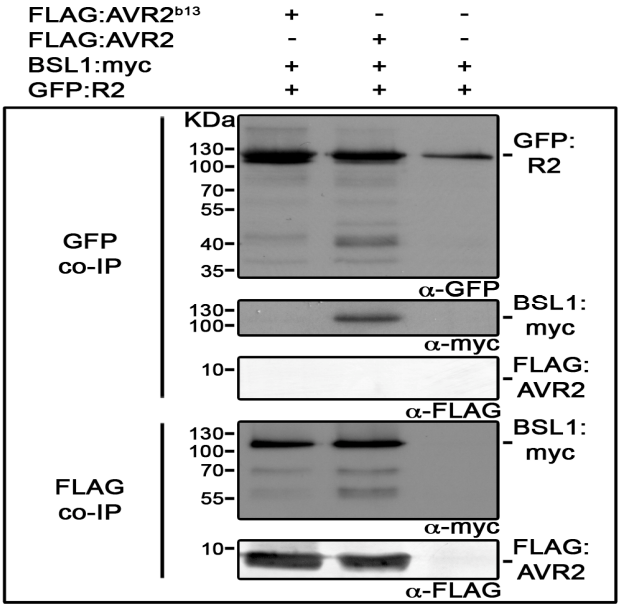


**Figure 5.8.1: Co-IP in *N. benthamiana*.** AVR2$^{b13}$ is PiAVR2-like. GFP co-IP is a pull down using R2, FLAG co-IP is a pull down using PiAVR2. Only one GFP shows interaction and this is with PiAVR2$^{N31}$, middle lane. AVR2 is not pulled down in complex. FLAG co-IP shows the PiAVR2 and PiAVR2-like C-termini interact with SlBSL1 (results from D. Saunders and S. Kamoun, The Sainsbury Laboratory).

From the data above a model for the indirect interaction has been devised (Figure 5.8.2). The first box shows that when PiAVR2 is absent there is no interaction occurring between R2 and BSL1. Upon introduction of PiAVR2$^{N/K31}$, panel two, a modification or conformational change may occur to BSL1. PiAVR2$^{N/K31}$ then dissociates allowing R2 to

interact. At present, the possible modification or conformational change is still unknown. The third panel shows the current working model of what may occur when PiAVR2-like is introduced. The interaction between PiAVR2-like and BSL1 still occurs but this interaction does not lead to a change in BSL1. Therefore, R2 is not recruited to the complex.

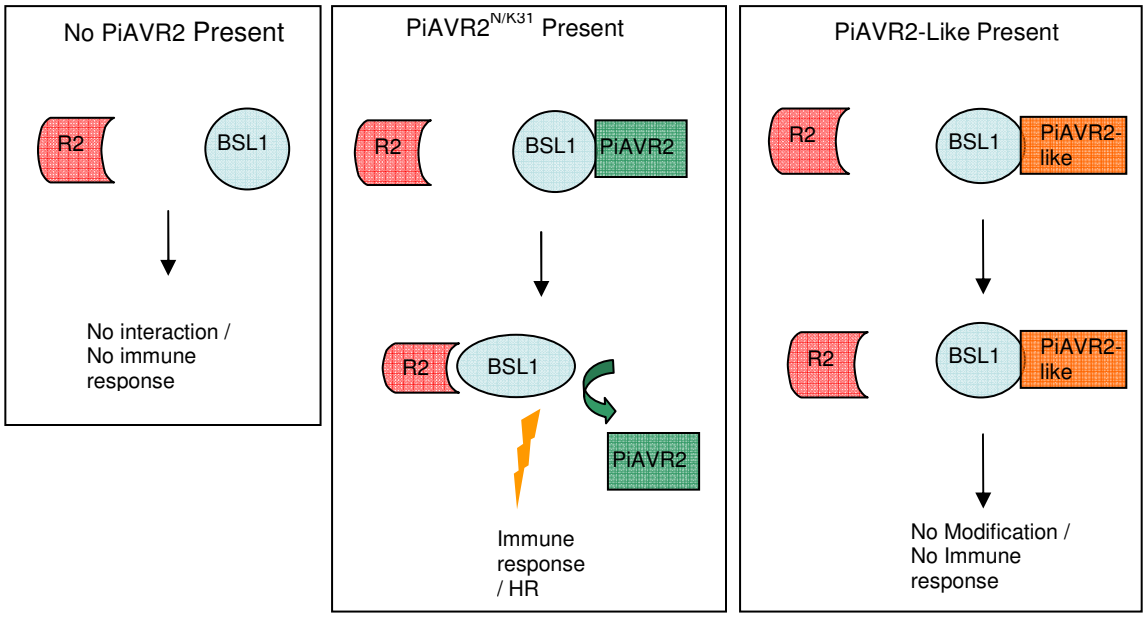


**Figure 5.8.2: Current model of the indirect interaction of R2.** Panel one indicates when no PiAVR2 is present. Panel two shows when PiAVR2$^{N/K31}$ is present and the third panel when PiAVR2-like is present.

## Conclusions

The main conclusions of this chapter are that PiAVR2 interacts with the Ser/Thr Kelch-repeat containing phosphatase, BSL1 from the brassinosteroid signal transduction pathway and that the loss of this gene compromises the ability of the resistance protein R2 to detect PiAVR2 and prevent the spread of infection. There is also some evidence that the interaction between R2 and PiAVR2 is indirect, utilising the BSL1 protein to mediate the signalling required for an HR to occur

# 6 – General Discussion and Future Work

In recent years there have been many published reports of effectors from plant pathogens interacting with host proteins (Jones and Dangl, 2006; Hein *et al.*, 2009). These interactions are thought to occur to aid and increase the efficiency of infection and to suppress the plant defence system. A great deal of progress has been made in understanding the plant defence system and in understanding how effector proteins from plant pathogens work.

The identification of the RXLR and LXLFLAK domains in oomycetes has led to the prediction of more than 700 intracellular effector proteins from *P. infestans* alone (Haas *et al.*, 2009). This number of effectors far exceeded expectations since other plant pathogens have been shown to suppress plant immunity and cause disease with 30 intracellular effectors or less. The challenge that researchers face is to identify the key effectors which are essential to the pathogen as there is expected to be functional redundancy within such a large repertoire of effectors. This is especially true for the effectors that belong to families; for example, *Avr3a* from *P. infestans* belongs to family 57 while Ipio1 belongs to family 53 (Haas *et al.*, 2009).

The effector recognition mechanisms of NB-LRR proteins during ETI have been of key interest in recent years with the confirmation of the gene-for-gene hypothesis and the development and confirmation of the guard hypothesis (Jones and Dangl, 2006; Van der Hoorn and Kamoun, 2008; Hein *et al.*, 2009). Plant hosts and their pathogens are essentially in a continuous arms race, each undergoing mutations in NB-LRRs and effector genes respectively to come out on top. The advantage pathogens have over their plant hosts is that their life cycle is much shorter, allowing more mutations to occur within the same period of time. Therefore, effectors that are essential to the pathogen have evolved

ways to remain functional but evade their hosts immune system (Jones and Dangl, 2006; Hein *et al.*, 2009).

## 6.1 – The use of effectors to identify durable resistance

Since the identification of the RXLR and LXLFLAK motifs and the increased availability of sequenced genomes the number of known and cloned *AVR* genes has risen. This has led to novel ways to investigate and develop durable resistance. Using *PiAVR2* as an example how knowledge of pathogen effectors can help understand and screen for novel resistances will be highlighted.

*PiAVR2*, cloned from the first *P. infestans* sequenced genome is recognised by *R2*, which encodes an NB-LRR protein. PiAVR2 has been screened by expression in wild *Solanum* species to identify a further nine *R2* orthologues that recognise it (Vleeshouwers *et al.*, 2011). Sequencing *PiAVR2* from isolates of *P. infestans* that overcome *R2*-based resistances has revealed the presence and expression of another form of *PiAVR2*, *PiAVR2-like*, which has been shown in this work to evade recognition by all *R2* orthologues. In addition, all isolates sequenced contained and expressed at least one form of *PiAVR2*, suggesting that this effector plays an important role in virulence. This was supported by the fact that silencing these genes in *P. infestans* resulted in lines that were unable to infect susceptible cultivars. It can be concluded that *P. infestans* uses multiple methods to evade recognition on R2-expressing cultivars; 1) the presence/absence of *PiAVR2*; 2) differential expression of *PiAVR2* and *PiAVR2-like;* and 3) SNPs that occur between the two genes.

*PiAVR2* (avirulent) and *PiAVR2-like* (virulent) can be used to search for a novel *R* gene which has the ability to recognise both effector forms. Based on our knowledge of

*PiAVR2*, durable resistance to *P. infestans* can be sought using several strategies. Screening effectors by transient expression in wild *Solanum* species may identify novel *R* genes from species that recognise both forms of PiAVR2. These new *R* genes could be further orthologues of *R2* or a completely unrelated *R* gene that has the ability to recognise both genes. Such *R* genes could be introgressed though breeding programmes or by the use of genetic engineering.

Another strategy to develop durable resistance is to engineer a new *R* gene from the existing *R2* orthologues by random mutagenesis (Vleeshouwers *et al.*, 2011). This would introduce SNPs into the existing genes to determine if the recognition of PiAVR2-like can be enhanced, whilst retaining recognition of PiAVR2. If this proved successful, these genes would have to be incorporated into cultivars by the use of genetic engineering.

Screening for natural resistance and random mutagenesis are currently being employed to find *R* genes which have the ability to recognise the virulent form of PiAVR3a, $AVR3a^{EM}$, results so far are encouraging (P. Birch, I. Hein. S. Chapman; The James Hutton Institute, personal communication). Random mutagenesis has also been shown to be successful in the case of the *R* gene, *Rx,* from *S. tuberosum* which recognises the coat protein of potato virus X (PVX) (Farnham and Baulcombe, 2006). If these methods are employed for *R2*, they will have one advantage over what is currently ongoing for *R3a*. The work presented in this thesis has gone some way to revealing the method of recognition of PiAVR2 by R2, through the latter guarding the BSL family. By contrast, any interactor that mediates the recognition of AVR3a by R3a remains elusive. Knowing the mediating interactor should aid in the investigation of new *R* genes for PiAVR2. The other benefit of knowing the host target that mediates resistance of R2 is that if another effector from a different pathogen was also to interact with the BSL family there is the possibility that i) one of the *R2*

orthologues would provide resistance or ii) that the mutated *R2* forms may also provide resistance to this other effector, and consequently to another pathogen.

If these approaches were able to generate new resistance genes that could be incorporated into the plant, it would be ideal if such *R* genes could be stacked. This would involve using combinations of *R* genes in cultivars in order to maintain durable resistance. The *R* genes that would be used would ideally recognise different *AVR* genes so that if a mutation occurred in one *AVR* gene it would not be enough to overcome the stacked resistance genes. This *R* gene stacking approach is currently being trialled in the genetically engineered cultivar Fortuna which was transformed with both *Rpi-blb1* and *Rpi-blb2 Rpi* genes (Vleeshouwers *et al.*, 2011). In Fortuna, both *R* genes used convey resistance to *P. infestans,* but additional *R* genes which recognise other pathogens can also be incorporated. This would mean that crops could have engineered resistance to multiple pathogens.

## 6.2 – How are AVR proteins recognised by the plant?

It has been well documented for bacterial effectors that the plant defence system primarily employs indirect recognition to detect secreted AVR proteins, often following the guard hypothesis (Dangl and Jones, 2001; Mackey *et al.*, 2002; Mackey *et al.*, 2003). In fact, some indirect recognition events originally thought to be key examples of the guard hypothesis are now considered to fit the decoy model better (Van der Hoorn and Kamoun, 2008). The guard hypothesis was originally thought to explain why Prf recognised AvrPto through its binding of Pto. AvrPto is a kinase inhibitor known to interact with the kinase domains of several defence-related kinases such as FLS2, EFR, BAK1 and Pto (Hogenhout *et al.*, 2009). Yet AvrPto contributes to virulence of *Pst* in tomato lacking Pto but not on plants lacking FLS2. Accordingly, Pto is now considered a decoy confined to

ETI signalling through Prf and that the virulence targets of AvrPto are the cell surface receptor-like kinases FLS2, EFR and BAK1 (Van der Hoorn and Kamoun, 2008). Thus, AvrPto binding to Pto would leave the actual targets, PRRs FLS2 and EFR, free to continue to act in PTI.

It also appears from the literature that recognition of fungal pathogens is primarily achieved by direct interaction i.e. the gene-for-gene hypothesis (Jones and Dangl, 2006). This is elegantly shown in the flax – flax rust system where the resistance genes L5, L6 and L7 directly bind to the effector AvrL567 to cause an immune response (Dodds *et al.*, 2006). The work in this thesis has shown for the first time that an intracellular eukaryotic effector protein (PiAVR2) is recognised *via* an indirect mechanism by the plant defence system. At this time, a distinction between whether PiAVR2 fits the guard or decoy hypotheses can not be made but future work should include an investigation into this. This work also shows that there is a distinction between the avirulent PiAVR2 and the virulent PiAVR2-like proteins, as PiAVR2 is able to trigger the interaction of StBSL1 with StR2 but PiAVR2-like does not, even though it has been shown that both effector forms interact with StBSL1. This implies that the interaction of the two effectors with the StBSL1 protein results in different effects on StBSL1. The mechanism for this difference is currently not known, but it is thought that the two proteins may cause a different conformational or biochemical change, one of which allows the binding of R2 and the other of which does not. This work has also shown that both forms of PiAVR2 also target the other BSL family members, BSL2a and BSL2b. The question remains as to how these other two proteins are linked to the recognition event that triggers the formation of the PiAVR2/R2 HR. It was shown that the silencing of *NbBSL1* and *NbBSL2a* genes significantly reduces the development of the PiAVR2/R2 HR. The role of the BSL2a/2b proteins in the R2 recognition event needs further investigation. It is also possible that one of the proteins in

this family is non functional in the plant and actually acts as a decoy for the other functional phosphatases. This will need further work to investigate in detail.

## 6.3 – Why target the BR signal transduction pathway?

The BR signal transduction pathway is the best described hormone pathway within plant cells and is primarily noted for its regulation of the growth and development of plants. The initial PiAVR2 interactor discovered was StBSL2a, although further work on mediating R2 resistance primarily focused on StBSL1. This was due to the fact that there was much more knowledge and information available from the model plant *A. thaliana* on this gene than the family members *BSL2* and *BSL3.* This lack of information led to these proteins being difficult to characterize experimentally, and the dwarf and early senescence phenotypes seen following the silencing of these genes made the plants difficult to study.

BSL proteins are reported to be activators of the BR pathway (Kim *et al*., 2009; Kim and Wang, 2010). There are several possible reasons for a pathogen to target this pathway: i) in order to prevent the growth of the plant cells, potentially providing the pathogen more free nutrients to feed from while in its biotrophic phase; ii) promoting an increase in the growth and development of the plants could reduce the amount of energy used in plant defence; iii) this pathway could be linked to other hormone pathways some of which may regulate defence responses; thus targeting this pathway could be a alternative route to alter these pathways.

The BSL family as a whole is not well understood and the information that PiAVR2 interacts with all members of this family leaves many unanswered questions. Why would a pathogen target this pathway? Is the effector only detected when binding to BSL1? How are the three *BSL* genes regulated? Is PiAVR2 genuinely targeting all three BSL proteins

during infection? What modifications are made to BSL1 that results in the defence response?

To try and make a reasonable attempt to understand these complex interactions a model has been designed. This model will need to be tested experimentally to determine how many of these proposed interactions actually occur (Figure 6.3.1). The model describes the interaction of PiAVR2 with all BSL proteins which has been experimentally shown *in vitro* for BSL1, BSL2a and BSL2b and *in vivo* for BSL1 and BSL2b. It also describes the indirect recognition of PiAVR2 by R2 via BSL1 which has also been experimentally demonstrated.

Information from Y2H has led to the knowledge that BSL2a and BSL2b may form a complex, as is shown within the model. The interaction of BSL2a and BSL2b with each other suggests that PiAVR2 may target/interact with both proteins at once. There is currently no experimental evidence showing that PiAVR2 interacts with both BSL2a and BSL2b while they are in complex, so this will need experimental verification. Another question that this model poses is: does R2 also recognise PiAVR2 due to its function and activity on BSL2a and BSL2b in the same manner as shown for BSL1? To investigate this question a similar approach as that taken with BSL1 should be used with BSL2a and BSL2b; i.e. the use of Co-IPs and bimolecular fluorescence complementation should indicate whether these two proteins are also guarded by R2.

Other issues to be resolved, relating to the BSLs, include whether BSL2a and BSL2b act upstream of BSL1 and/or do they interact directly with BSL1. This is an interesting question as the plants silenced for *BSL1* showed no developmental phenotype, whereas there was a severe phenotype observed with the *BSL2a* and *BSL2b* silenced plants. This implies that either BSL1 is not active within the pathway and is simply acting as a decoy to

trigger the plant defence system. Alternatively, BSL2a and BSL2b may regulate the function of BSL1 (and presumably additional downstream substrates, to provide the extreme silencing phenotype) so when *BSL2a/2b* are silenced BSL1 activity is also reduced. There is some experimental evidence to support this as removal, by VIGS, of either *BSL1, 2a* or *2b* affects the R2 HR. Thus they may be functionally linked, perhaps through enzymatic activity.

The reduction of the R2/PiAVR2 HR in the TRV::*BAK1* plants but not the TRV::*BRI1* plants indicates that this recognition phenotype may be influenced by signal transduction from an alternative receptor to BRI1, but one that is still in a complex with BAK1. Nevertheless, this signal transduction still employs BSL activity (Figure 6.3.1). It could be that this unknown pathway and its regulated genes are the intended targets of PiAVR2 effector.

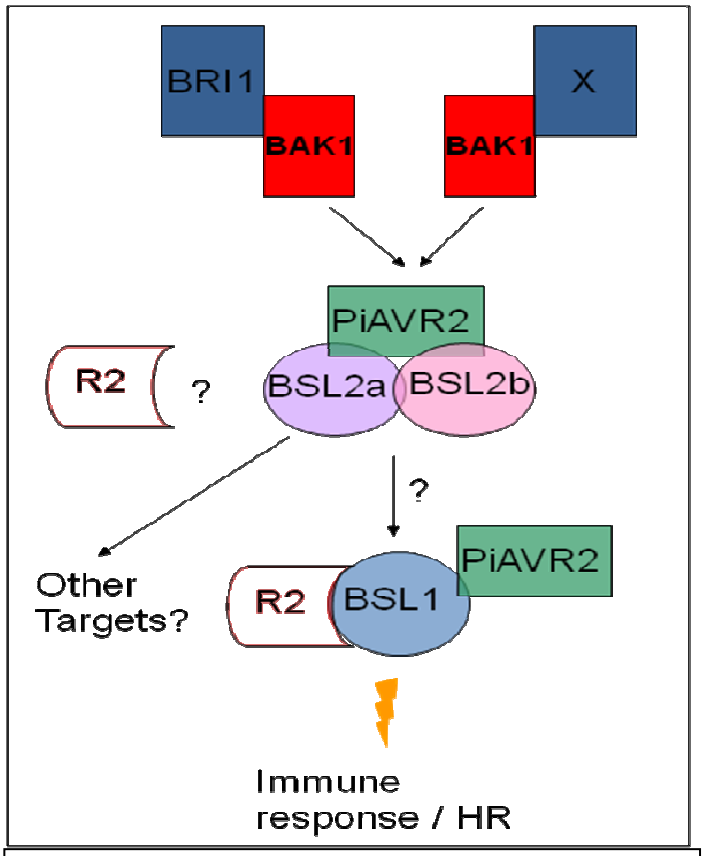


**Figure 6.3.1: A model proposing the complex interactions of the BSLs, R2, PiAVR2 and upstream receptor complexes.** An unknown cell surface receptor with BAK1 bound is shown. The ? between the BSL2a/BSL2b complex and both R2 and BSL1 indicates a hypothesised interaction while the arrow indicates a means of regulation. This model requires experimental verification.

## 6.4 – How is the BR signal transduction pathway linked to defence responses?

Plant processes are regulated by multiple hormone pathways, including salicylic acid (SA), jasmonates (JA), ethylene (ET), abscisic acid (ABA), auxin, gibberellic acid (GA), cytokinin (CK), brassinosteroids (BR) and peptide hormones. These pathways regulate different aspects within the plant, such as growth, development and defence, and there is some experimental evidence which suggests that all of these pathways are interconnected. The complex nature of these connections is still poorly understood. It is well documented that

SA, JA and ET regulate the plants responces to biotic stresses. However the link of the other hormones to defence is less well understood (Bari and Jones, 2009).

Within the BR pathway there are a few documented points which could allow cross-talk with defence pathways. The first is that of the BRI1 co-receptor BAK1. This is not only a co-receptor to BRI1 but has also been described in detail as an essential co-receptor to the PTI receptors FLS2 and EFR (Jones and Dangl, 2006). Some recent studies have examined the link between the BR pathway and PTI focusing on BAK1 (Albrecht *et al.*, 2012; Belkhadir *et al.*, 2012). Both studies conclude that the activation of the BR pathway has a negative effect on PTI shown by an increase in disease susceptibility on plants treated with Epi-BL or by the use of transgenic *A. thaliana* lines (Albrecht *et al.*, 2012; Belkhadir *et al.*, 2012). These results contradict other reports that treatment with BR increases the resistance of potato, tomato, rice and *N. benthamiana* plants to pathogen attack (Krishna, 2003; Nakashita *et al.*, 2003), and the results shown in this work in Chapter 4. However, the two recent studies do disagree on the significance of BAK1 in causing this negative effect. Albrecht *et al.* (2012) suggest that BAK1 is not the rate limiting step in the inhibition of PTI. Their study focused solely on early PTI responses (e.g. ROS production) with little experimental evidence of downstream responses such as MAPK responces (Albrecht *et al.*, 2012). Belkhadir *et al* (2012) conclude that the negative effect on PTI is caused by BAK1 being the co-receptor to both BRI1 and defence receptors like FLS2. The experimental replication in the publication appears limited, drawing into question the reproducibility of their findings (Belkhadir *et al.*, 2012). The fact that these two publications come to differing conclusions about the significance of BAK1 in the cross-talk between pathways shows the complex nature of this area of research.

Another protein found within the BR pathway that could provide a link to defence responses is BIN2. BIN2 has been shown to be targeted by beet curly top virus (BCTV)

protein C4 (Piroux *et al.*, 2007). It is thought that the binding of C4 to BIN2 activates BR signalling by inactivating BIN2, resulting in the activation of the transcription factors BZR1/2 (Piroux *et al.*, 2007). This shows that there are two stages within the BR pathway, at the level of either BSLs or the downstream BIN2, which are targeted by pathogenic proteins, supporting the importance of manipulating this pathway in aiding pathogen infection of their plant hosts. BIN2 also forms a link to another hormone pathway, Auxin. Auxin is an additional hormone that regulates the growth of plants. BIN2 was demonstrated to phosphorylate auxin response factor 2 (ARF2) which results in its inactivation and, therefore, a reduction of auxin responsive genes (Divi *et al.*, 2010). The fact that BIN2 has been documented to regulate both auxin and BR responsive genes and has been targeted by a pathogen protein again highlights the complex nature of the plant regulatory hormone pathways.

Another link between plant defence responses and the BR pathway is that genes involved in biosynthesis of ET (ACC synthase) and JA (OPR3) in *A. thaliana*, are induced by BR (Bari and Jones, 2009). It is not known whether the BR pathway is also regulated by the ET or JA pathways. All of this experimental evidence suggests that the BR pathway is involved in the regulation of plant defences. The specifics of its involvement remain unknown. A lot of work is needed in this area in the future to further understand these complex interactions. The fact that the *BSL* family is targeted by a pathogen effector may indicate that the *BSLs* be regulatory components in other hormone pathways which, as yet, have remained undiscovered.

## Conclusions

A number of strategies have been employed by *P. infestans* to evade recognition by R2. These approaches, in combination with preliminary *PiAVR2* silencing data in *P. infestans*, suggest that PiAVR2 is an important effector to this pathogen.

Recognition of PiAVR2 by R2 is mediated by its physical interaction with BSL1, revealing the first example of indirect recognition of an intracellular effector from a filamentous plant pathogen.

PiAVR2 clearly targets all members of the BSL family in *Solanaceae*. Whether this is to activate or inhibit the BR signal transduction pathway is unclear, but the research in this thesis establishes a strong case for further investigation of the role(s) this pathway may play in plant-pathogen interactions.

Finally, the effector PiAVR2 has provided a unique tool to study the BR pathway, whether it activates or inactivates it. Already, novel observations have been made concerning the relationships between BAK1, BRI1, and the BSLs.

## 6.5 - Future work

The work in this thesis has led to plenty of new questions and ideas. There were also some questions that were not fully answered during the work and these need further investigation. Below are some of the key questions and future experiments:

- To assess the virulence function of PiAVR2-like, work should be undertaken to determine which of the remaining un-investigated SNPs are key to the evasion of R2. In parallel to this, an error prone PCR approach should be undertaken on *R2* in order to generate a new *R2** gene that recognises both PiAVR2 and PiAVR2-like. This would then allow production of potato cultivars that would withstand *PiAVR2-like* expressing *P. infestans* isolates, and thus contribute to durable disease resistance.

- In order to understand the BR pathway within the *Solanaceae* and its links to other signal transduction pathways it will be necessary to (re)construct this pathway within the *Solanaceae,* then compare it to the described pathway in *A. thaliana.* It will also be important to determine the key modifications made to the BSL proteins that are required for their activation, and to determine if these modifications are mediated by the BSKs or if a signalling component from an alternative pathway is involved. The regulation of this family of proteins is also an interesting question. Do they have a feedback loop which allows them to regulate each other or do *BSL2a/2b* regulate *BSL1* as implied by the model (Figure 6.3.1)?

- It has been shown that PiAVR2 targets the BSLs but the specific modifications made to the BSLs, upon this interaction, remain unknown. This would be a key question to answer in future work. Related to this, it is important to investigate any differences between the BSL proteins, when PiAVR2 interacts with them as opposed to PiAVR2-like. The modifications made to the BSL proteins, by the two effectors, may also shed light on the effect this has on their function within the signalling pathways i.e. are they being activated or deactivated? It may also aid in determining why PiAVR2-like is not recognised by R2.

- The downstream effect of PiAVR2 activity on the BSLs is important to understand in order to determine the role of this effector in virulence. The modifications made to the signalling pathway in the presence of the effector could yield valuable information to determine whether this effector contributes to defence suppression, or whether it is involved in metabolic re-programming related to nutrient acquisition.

- A crucial question which may be answered when some of the above questions have been investigated is: does the BR pathway aid in plant defence?

# 7 – References

Albrecht C, Boutrot F, Segonzac C, Schwessinger B, Gimenez-Ibanez S, Chinchilla D, Rathjen JP, de Vries SC, and Zipfel C (2012) Brassinosteroids inhibit pathogen-associated molecular pattern-triggered immune signaling independent of the receptor kinase BAK1. *Proceedings of the National Academy of Sciences of the United States of America,* **109,** 303-308.

Allen RL, Bittner-Eddy PD, Grenville-Briggs LJ, Meitz JC, Rehmany AP, Rose LE, and Beynon JL (2004) Host-parasite coevolutionary conflict between *Arabidopsis* and downy mildew. *Science,* **306,** 1957-1960.

Armstrong MR, Whisson SC, Pritchard L, Bos JIB, Venter E, Avrova AO, Rehmany AP, Bohme U, Brooks K, Cherevach I, Hamlin N, White B, Fraser A, Lord A, Quail MA, Churcher C, Hall N, Berriman M, Huang S, Kamoun S, Beynon JL, and Birch PRJ (2005) An ancestral oomycete locus contains late blight avirulence gene Avr3a, encoding a protein that is recognized in the host cytoplasm. *Proceedings of the National Academy of Sciences of the United States of America,* **102,** 7766-7771.

Austin MJ, Muskett P, Kahn K, Feys BJ, Jones JDG, and Parker JE (2002) Regulatory role of SGT1 in early R gene-mediated plant defenses. *Science,* **295,** 2077-2080.

Avrova AO, Taleb N, Rokka VM, Heilbronn J, Campbell E, Hein I, Gilroy EM, Cardle L, Bradshaw JE, Stewart HE, Fakim YJ, Loake G, and Birch PRJ (2004) Potato oxysterol binding protein and cathepsin B are rapidly up-regulated in independent defence pathways that distinguish R gene-mediated and field resistances to *Phytophthora infestans*. *Molecular Plant Pathology,* **5,** 45-56.

Azevedo C, Sadanandom A, Kitagawa K, Freialdenhoven A, Shirasu K, and Schulze-Lefert P (2002) The RAR1 interactor SGT1, an essential component of R gene-triggered disease resistance. *Science,* **295,** 2073-2076.

Ballvora A, Ercolano MR, Weiss J, Meksem K, Bormann CA, Oberhagemann P, Salamini F, and Gebhardt C (2002) The *R1* gene for potato resistance to late blight (*Phytophthora infestans*) belongs to the leucine zipper/NBS/LRR class of plant resistance genes. *Plant Journal,* **30,** 361-371.

Bari R and Jones J (2009) Role of plant hormones in plant defence responses. *Plant Molecular Biology,* **69,** 473-488.

Belkhadir Y and Chory J (2006) Brassinosteroid signaling: A paradigm for steroid hormone signaling from the cell surface. *Science,* **314,** 1410-1411.

Belkhadir Y, Jaillais Y, Epple P, Balsemao-Pires E, Dangl JL, and Chory J (2012) Brassinosteroids modulate the efficiency of plant immune responses to microbe-associated molecular patterns. *Proceedings of the National Academy of Sciences of the United States of America,* **109,** 297-302.

Bendahmane A, Kanyuka K, and Baulcombe DC (1999) The *Rx* gene from potato controls separate virus resistance and cell death responses. *Plant Cell,* **11,** 781-791.

Bernoux M, Ellis JG, and Dodds PN (2011) New insights in plant immunity signaling activation. *Current Opinion in Plant Biology,* **14,** 512-518.

Bhattacharjee S, Hiller NL, Liolios K, Win J, Kanneganti TD, Young C, Kamoun S, and Haldar K (2006) The malarial host-targeting signal is conserved in the Irish potato famine pathogen. *PLoS Pathogen,* **2,** e50, doi:10.1371/journal.ppat.0020050.

Bos JI, Armstrong MR, Gilroy EM, Boevink PC, Hein I, Taylor RM, Tian Z, Engelhardt S, Vetukuri RR, Harrower B, Dixelius C, Bryan G, Sadanandom A, Whisson SC, Kamoun S, and Birch PR (2010) *Phytophthora infestans* effector AVR3a is essential for virulence and manipulates plant immunity by stabilizing host E3 ligase CMPG1. *Proceedings of the National Academy of Sciences of the United States of America,* **107,** 9909-9914.

Bos JI, Chaparro-Garcia A, Quesada-Ocampo LM, Gardener BB, and Kamoun S (2009) Distinct amino acids of the *Phytophthora infestans* effector AVR3a condition activation of R3a hypersensitivity and suppression of cell death. *Molecular Plant-Microbe Interactions,* **22,** 269-281.

Bos JI, Kanneganti TD, Young C, Cakir C, Huitema E, Win J, Armstrong MR, Birch PR, and Kamoun S (2006) The C-terminal half of *Phytophthora infestans* RXLR effector AVR3a is sufficient to trigger R3a-mediated hypersensitivity and suppress INF1-induced cell death in *Nicotiana benthamiana*. *Plant Journal,* **48,** 165-176.

Bradshaw JE, Pande B, Bryan GJ, Hackett CA, McLean K, Stewart HE, and Waugh R (2004) Interval mapping of quantitative trait loci for resistance to late blight [*Phytophthora infestans (Mont.) de Bary*], height and maturity in a tetraploid population of potato (*Solanum tuberosum* subsp *tuberosum*). *Genetics,* **168,** 983-995.

Brunner F, Rosahl S, Lee J, Rudd JJ, Geiler C, Kauppinen S, Rasmussen G, Scheel D, and Nurnberger T (2002) Pep-13, a plant defense-inducing pathogen-associated pattern from *Phytophthora* transglutaminases. *Embo Journal,* **21,** 6681-6688.

Champouret N. Functional genomics of *Phytophthora infestans* effectors and *Solanum* resistance genes (2010) Wageningen University, Wageningen, NL, ISBN 978-90-8585-658-0

Chang JH, Rathjen JP, Bernal AJ, Staskawicz BJ, and Michelmore RW (2000) avrPto enhances growth and necrosis caused by *Pseudomonas syringae* pv. *tomato* in tomato lines lacking either Pto or Prf. *Molecular Plant-Microbe Interactions,* **13,** 568-571.

Chinchilla D, Zipfel C, Robatzek S, Kemmerling B, Nurnberger T, Jones JDG, Felix G, and Boller T (2007) A flagellin-induced complex of the receptor FLS2 and BAK1 initiates plant defence. *Nature,* **448,** 497-500.

Clouse SD, Langford M, and McMorris TC (1996) A brassinosteroid-insensitive mutant in *Arabidopsis thaliana* exhibits multiple defects in growth and development. *Plant Physiology,* **111,** 671-678.

Coll N, Epple P, and Dangl J (2011) Programmed cell death in the plant immune system. *Cell Death and Differentiation,* **18,** 1247-1256.

Dangl JL, Dietrich RA, and Richberg MH (1996) Death don't have no mercy: cell death programs in plant-microbe interactions. *The Plant Cell,* **8,** 1793-1807.

Dangl JL and Jones JDG (2001) Plant pathogens and integrated defence responses to infection. *Nature,* **411,** 826-833.

de Koning-Ward TF, Gilson PR, Boddey JA, Rug M, Smith BJ, Papenfuss AT, Sanders PR, Lundie RJ, Maier AG, Cowman AF, and Crabb BS (2009) A newly discovered protein export machine in malaria parasites. *Nature,* **459,** 945-949.

Divi UK, Rahman T, and Krishna P (2010) Brassinosteroid-mediated stress tolerance in *Arabidopsis* shows interactions with abscisic acid, ethylene and salicylic acid pathways. *Bmc Plant Biology,* **10**, 151-165.

Dodds PN, Lawrence GJ, Catanzariti AM, Teh T, Wang CI, Ayliffe MA, Kobe B, and Ellis JG (2006) Direct protein interaction underlies gene-for-gene specificity and coevolution of the fax resistance genes and flax rust avirulence genes. *Proceedings of the National Academy of Sciences of the United States of America,* **103,** 8888-8893.

Dong SM, Qutob D, Tedman-Jones J, Kuflu K, Wang YC, Tyler BM, and Gijzen M (2009) The *Phytophthora sojae* avirulence locus *Avr3c* encodes a multi-copy RXLR effector with sequence polymorphisms among pathogen strains. *Plos One,* **4**, e5556, doi:10.1371/journal.pone.0005556.

Dong S, Yin W, Kong G, Yang X, Qutob D, Chen Q, Kale SD, Sui Y, Zhang Z, Dou D, Zheng X, Gijzen M, Tyler BM, and Wang Y (2011) *Phytophthora sojae* avirulence effector Avr3b is a secreted NADH and ADP-ribose pyrophosphorylase that modulates plant immunity. *Plos Pathogens,* **7,** e1002353, doi:10.1371/journal.ppat.1002353.

Dou D, Kale S, Wang X, Jiang R, Bruce N, Arredondo F, Zhang X, and Tyler B (2008) RXLR-mediated entry of *Phytophthora sojae* effector Avr1b into soybean cells does not require pathogen-encoded machinery. *Plant Cell,* **20,** 1930-1947.

Eitas TK and Dangl JL (2010) NB-LRR proteins: pairs, pieces, perception, partners, and pathways. *Current Opinion in Plant Biology,* **13,** 472-477.

Ellis C and Turner JG (2001) The *Arabidopsis* mutant *cev1* has constitutively active jasmonate and ethylene signal pathways and enhanced resistance to pathogens. *Plant Cell,* **13,** 1025-1033.

Farnham G and Baulcombe DC (2006) Artificial evolution extends the spectrum of viruses that are targeted by a disease-resistance gene from potato. *Proceedings of the National Academy of Sciences of the United States of America,* **103,** 18828-18833.

Felix G and Boller T (2003) Molecular sensing of bacteria in plants - The highly conserved RNA-binding motif RNP-1 of bacterial cold shock proteins is recognized as an elicitor signal in tobacco. *Journal of Biological Chemistry,* **278,** 6201-6208.

Felix G, Duran JD, Volko S, and Boller T (1999) Plants have a sensitive perception system for the most conserved domain of bacterial flagellin. *The Plant Journal,* **18,** 265-276.

Fellbrich G, Romanski A, Varet A, Blume B, Brunner F, Engelhardt S, Felix G, Kemmerling B, Krzymowska M, and Nurnberger T (2002) NPP1, a *Phytophthora*-associated trigger of plant defense in parsley and *Arabidopsis*. *Plant Journal,* **32,** 375-390.

Fischer K, Marti T, Rick B, Johnson D, Benting J, Baumeister S, Helmbrecht C, Lanzer M, and Lingelbach K (1998) Characterization and cloning of the gene encoding the vacuolar membrane protein EXP-2 from *Plasmodium falciparum*. *Molecular and Biochemical Parasitology,* **92,** 47-57.

Flor HH (1971) Current status of gene-for-gene concept. *Annual Review of Phytopathology,* **9,** 275-296.

Fry W (2008) *Phytophthora infestans:* the plant (and *R* gene) destroyer. *Molecular Plant Pathology,* **9,** 385-402.

Fu ZQ, Guo M, Jeong Br, Tian F, Elthon TE, Cerny RL, Staiger D, and Alfano JR (2007) A type III effector ADP-ribosylates RNA-binding proteins and quells plant immunity. *Nature,* **447,** 284-288.

Gampala SS, Kim TW, He JX, Tang WQ, Deng ZP, Bai MY, Guan SH, Lalonde S, Sun Y, Gendron JM, Chen HJ, Shibagaki N, Ferl RJ, Ehrhardt D, Chong K, Burlingame AL, and Wang ZY (2007) An essential role for 14-3-3 proteins in Brassinosteroid signal transduction in *Arabidopsis*. *Developmental Cell,* **13,** 177-189.

Gaulin E, Drame N, Lafitte C, Torto-Alalibo T, Martinez Y, meline-Torregrosa C, Khatib M, Mazarguil H, Villalba-Mateos F, Kamoun S, Mazars C, Dumas B, Bottin A, Esquerre-Tugaye MT, and Rickauer M (2006) Cellulose binding domains of a *Phytophthora* cell wall protein are novel pathogen-associated molecular patterns. *Plant Cell,* **18,** 1766-1777.

Gilroy EM, Hein I, van der Hoorn R, Boevink PC, Venter E, McLellan H, Kaffarnik F, Hrubikova K, Shaw J, Holeva M, Lopez EC, Borras-Hidalgo O, Pritchard L, Loake GJ, Lacomme C, and Birch PR (2007) Involvement of cathepsin B in the plant disease resistance hypersensitive response. *The Plant Journal,* **52,** 1-13.

Gilroy EM, Breen S, Whisson SC, Squires J, Hein I, Kaczmarek M, Turnbull D, Boevink PC, Lokossou A, Cano LM, Morales J, Avrova AO, Pritchard L, Randall E, Lees A, Govers F, van West P, Kamoun S, Vleeshouwers VG, Cooke DE, and Birch PR (2011a) Presence/absence, differential expression and sequence polymorphisms between *PiAVR2* and *PiAVR2-like* in *Phytophthora infestans* determine virulence on *R2* plants. *New Phytologist,* **191,** 763-776.

Gilroy EM, Taylor RM, Hein I, Boevink P, Sadanandom A, and Birch PR (2011b) CMPG1-dependent cell death follows perception of diverse pathogen elicitors at the host plasma membrane and is suppressed by *Phytophthora infestans* RXLR effector AVR3a. *New Phytologist,* **190,** 653-666.

Gohre V and Robatzek S (2008) Breaking the barriers: microbial effector molecules subvert plant immunity. *Annual Review of Phytopathology,* **46,** 189-215.

Gonzalez-Lamothe R, Tsitsigiannis DI, Ludwig AA, Panicot M, Shirasu K, and Jones JDG (2006) The U-Box protein CMPG1 is required for efficient activation of defense mechanisms triggered by multiple resistance genes in tobacco and tomato. *Plant Cell,* **18,** 1067-1083.

Gornhardt B, Rouhara I, and Schmelzer E (2000) Cyst germination proteins of the potato pathogen *Phytophthora infestans* share homology with human mucins. *Molecular Plant-Microbe Interactions,* **13,** 32-42.

Grenville-Briggs L and West Pv (2005). The biotrophic stages of Oomycete-plant interactions. In Allen,I.L. (Ed.), *Advances in Applied Microbiology*, Academic Press, pp. 217-243.

Grouffaud S, van West P, Avrova AO, Birch PR, and Whisson SC (2008) *Plasmodium falciparum* and *Hyaloperonospora parasitica* effector translocation motifs are functional in *Phytophthora infestans*. *Microbiology,* **154,** 3743-3751.

Grove MD, Spencer GF, Rohwedder WK, Mandava N, Worley JF, Warthen JD, Steffens GL, Flippenanderson JL, and Cook JC (1979) Brassinolide, a plant growth-promoting steroid isolated from brassica-napus pollen. *Nature,* **281,** 216-217.

Haas BJ, Kamoun S, Zody MC, Jiang RHY, Handsaker RE, Cano LM, Grabherr M, Kodira CD, Raffaele S, Torto-Alalibo T, Bozkurt TO, Ah-Fong AMV, Alvarado L, Anderson VL, Armstrong MR, Avrova A, Baxter L, Beynon J, Boevink PC, Bollmann SR, Bos JIB, Bulone V, Cai GH, Cakir C, Carrington JC, Chawner M, Conti L, Costanzo S, Ewan R, Fahlgren N,

Fischbach MA, Fugelstad J, Gilroy EM, Gnerre S, Green PJ, Grenville-Briggs LJ, Griffith J, Grunwald NJ, Horn K, Horner NR, Hu CH, Huitema E, Jeong DH, Jones AME, Jones JDG, Jones RW, Karlsson EK, Kunjeti SG, Lamour K, Liu ZY, Ma LJ, MacLean D, Chibucos MC, McDonald H, McWalters J, Meijer HJG, Morgan W, Morris PF, Munro CA, O'Neill K, Ospina-Giraldo M, Pinzon A, Pritchard L, Ramsahoye B, Ren QH, Restrepo S, Roy S, Sadanandom A, Savidor A, Schornack S, Schwartz DC, Schumann UD, Schwessinger B, Seyer L, Sharpe T, Silvar C, Song J, Studholme DJ, Sykes S, Thines M, van de Vondervoort PJI, Phuntumart V, Wawra S, Weide R, Win J, Young C, Zhou SG, Fry W, Meyers BC, van West P, Ristaino J, Govers F, Birch PRJ, Whisson SC, Judelson HS, and Nusbaum C (2009) Genome sequence and analysis of the Irish potato famine pathogen *Phytophthora infestans*. *Nature,* **461,** 393-398.

Hammond-Kosack KE and Jones JDG (1996) Resistance gene-dependent plant defense responses. *Plant Cell,* **8,** 1773-1791.

Hansen J, Colon L, Cooke D, Lassen P, Nielsen B, Cookes L, Andrivon D, and Lees A (2007) Eucablight - collating and analysing pathogenicity and resistance data on a European scale. *Bulletin OEPP,* **37,** 383-390.

Haverkort A, Boonekamp P, Hutten R, Jacobsen E, Lotz L, Kessel G, Visser R, Vossen E, der Vossen E, and van der Vossen E (2008) Societal costs of late blight in potato and prospects of durable resistance through cisgenic modification. *Potato Research,* **51,** 47-57.

He K, Gou X, Yuan T, Lin H, Asami T, Yoshida S, Russell SD, and Li J (2007) BAK1 and BKK1 regulate Brassinosteroid-dependent growth and Brassinosteroid independent cell-death pathways. *Current Biology,* **17,** 1109-1115.

Heese A, Hann DR, Gimenez-Ibanez S, Jones AM, He K, Li J, Schroeder JI, Peck SC, and Rathjen JP (2007) The receptor-like kinase SERK3/BAK1 is a central regulator of innate immunity in plants. *Proceedings of the National Academy of Sciences of the United States of America,* **104,** 12217-12222.

Hein I, Gilroy EM, Armstrong MR, and Birch PR (2009) The zig-zag-zig in Oomycete–plant interactions. *Molecular Plant Pathology,* **10,** 547-562.

Hein I, McLean K, Chalhoub B, and Bryan GJ (2007) Generation and screening of a BAC library from a diploid potato clone to unravel durable late blight resistance on linkage group IV. *International Journal of Plant Genomics,* **2007,** 51421-51426.

Hogenhout SA, Van der Hoorn RA, Terauchi R, and Kamoun S (2009) Emerging concepts in effector biology of plant-associated organisms. *Molecular Plant-Microbe Interactions,* **22,** 115-122.

Hothorn M, Belkhadir Y, Dreux M, Dabi T, Noel JP, Wilson IA and Chory J (2011) Structural basis of steroid hormone perception by the receptor kinase BRI1. *Nature,* **474**, 467–471.

Hulbert SH, Webb CA, Smith SM, and Sun Q (2001) Resistance gene complexes: Evolution and utilization. *Annual Review of Phytopathology,* **39,** 285-312.

Ingle RA, Carstens M, and Denby KJ (2006) PAMP recognition and the plant-pathogen arms race. *BioEssays,* **28,** 880-889.

Jaillais Y and Chory J (2010) Unraveling the paradoxes of plant hormone signaling integration. *Nature Structural & Molecular Biology,* **17,** 642-645.

Jelenska J, Yao N, Vinatzer BA, Wright CM, Brodsky JL, and Greenberg JT (2007) A J domain virulence effector of *Pseudomonas syringae* remodels host chloroplasts and suppresses defenses. *Current Biology,* **17,** 499-508.

Jia Y, McAdams AS, Bryan GT, Hershey HP, and Valent B (2000) Direct interaction of resistance gene and avirulence gene products confers rice blast resistance. *EMBO,* **19,** 4004-4014.

Jones JDG and Dangl JL (2006) The plant immune system. *Nature,* **444,** 323-329.

Judelson HS (1997) Expression and inheritance of sexual preference and selfing potential in *Phytophthora infestans*. *Fungal Genetics and Biology,* **21,** 188-197.

Judelson HS and Roberts S (2002) Novel protein kinase induced during sporangial cleavage in the Oomycete *Phytophthora infestans*. *Eukaryotic Cell,* **1,** 687-695.

Kale SD, Gu BA, Capelluto DGS, Dou DL, Feldman E, Rumore A, Arredondo FD, Hanlon R, Fudal I, Rouxel T, Lawrence CB, Shan WX, and Tyler BM (2010) External lipid PI3P mediates entry of eukaryotic pathogen effectors into plant and animal host cells. *Cell,* **142,** 284-295.

Kamoun S (2003) Molecular genetics of pathogenic Oomycetes. *Eukaryotic Cell,* **2,** 191-199.

Kamoun S, vanWest P, deJong AJ, deGroot KE, Vleeshouwers VGAA, and Govers F (1997) A gene encoding a protein elicitor of *Phytophthora infestans* is down-regulated during infection of potato. *Molecular Plant-Microbe Interactions,* **10,** 13-20.

Kanzaki H, Saitoh H, Takahashi Y, Berberich T, Ito A, Kamoun S, and Terauchi R (2008) NbLRK1, a lectin-like receptor kinase protein of *Nicotiana benthamiana*, interacts with *Phytophthora infestans* INF1 elicitin and mediates INF1-induced cell death. *Planta,* **228,** 977-987.

Karlova R, Boeren S, Russinova E, Aker J, Vervoort J, and de Vries S (2006) The *Arabidopsis* somatic embryogenesis receptor-like kinase1 protein complex includes Brassinosteroid-insensitive1. *Plant Cell,* **18,** 626-638.

Kim T, Guan S, Sun Y, Deng Z, Tang W, Shang J, Sun Y, Burlingame A, and Wang Z (2009) Brassinosteroid signal transduction from cell-surface receptor kinases to nuclear transcription factors. *Nature Cell Biology,* **11,** 1254-1260.

Kim TW and Wang ZY (2010) Brassinosteroid signal transduction from receptor kinases to transcription factors. *The Annual Review of Plant Biology*, **61**, 681-704.

Kim TW, Guan S, Burlingame AL and Wang ZY (2011) The CDG1 kinase mediates Brassinosteroid signal transduction from BRI1 receptor kinase to BSU1 phosphatase and GSK3-like kinase BIN2. *Molecular Cell,* **43**, 561–571.

Kim TW, Michniewicz M, Bergmann DC, and Wang ZY (2012) Brassinosteroid regulates stomatal development by GSK3-mediated inhibition of a MAPK pathway. *Nature,* **482,** 419-422.

Kinoshita T, Cano-Delgado AC, Seto H, Hiranuma S, Fujioka S, Yoshida S, and Chory J (2005) Binding of brassinosteroids to the extracellular domain of plant receptor kinase BRI1. *Nature,* **433,** 167-171.

Krasileva KV, Dahlbeck D, and Staskawicz BJ (2010) Activation of an *Arabidopsis* resistance protein is specified by the in planta association of its leucine-rich repeat domain with the cognate Oomycete effector. *Plant Cell,* **22,** 2444-2458.

Krishna P (2003) Brassinosteroid-mediated stress responses. *Journal of Plant Growth Regulation,* **22,** 289-297.

Kutuzov MA and Andreeva AV (2002) Protein Ser/Thr phosphatases with kelch-like repeat domains. *Cellular Signalling,* **14,** 745-750.

Li J, Wen JQ, Lease KA, Doke JT, Tax FE, and Walker JC (2002) BAK1, an *Arabidopsis* LRR receptor-like protein kinase, interacts with BRI1 and modulates brassinosteroid signaling. *Cell,* **110,** 213-222.

Li JM, Nagpal P, Vitart V, McMorris TC, and Chory J (1996) A role for Brassinosteroids in light-dependent development of *Arabidopsis*. *Science,* **272,** 398-401.

Li JM and Nam KH (2002) Regulation of Brassinosteroid signaling by a GSK3/SHAGGY-like kinase. *Science,* **295,** 1299-1301.

Li XY, Lin HQ, Zhang WG, Zou Y, Zhang J, Tang XY, and Zhou JM (2005) Flagellin induces innate immunity in nonhost interactions that is suppressed by *Pseudomonas syringae* effectors. *Proceedings of the National Academy of Sciences of the United States of America,* **102,** 12990-12995.

Liu ZY, Bos JIB, Armstrong M, Whisson SC, da Cunha L, Torto-Alalibo T, Win J, Avrova AO, Wright F, Birch PRJ, and Kamoun S (2005) Patterns of diversifying selection in the phytotoxin-like scr74 gene family of *Phytophthora infestans*. *Molecular Biology and Evolution,* **22,** 659-672.

Lokossou AA, Park TH, van Arkel G, Arens M, Ruyter-Spira C, Morales J, Whisson SC, Birch PRJ, Visser RGF, Jacobsen E, and van der Vossen EAG (2009) Exploiting knowledge of *R/Avr g*enes to rapidly clone a new LZ-NBS-LRR family of late blight resistance genes from potato linkage group IV. *Molecular Plant-Microbe Interactions,* **22,** 630-641.

Lopez-Estrano C, Bhattacharjee S, Harrison T, and Haldar K (2003) Cooperative domains define a unique host cell-targeting signal in *Plasmodium falciparum*-infected erythrocytes. *Proceedings of the National Academy of Sciences of the United States of America,* **100,** 12402-12407.

Lorrain S, Vailleau F, Balaque C, and Roby D (2003) Lesion mimic mutants: keys for deciphering cell death and defense pathways in plants? *Trends in Plant Science,* **8,** 263-271.

Mackey D, Belkhadir Y, Alonso JM, Ecker JR, and Dangl JL (2003) *Arabidopsis* RIN4 is a target of the type III virulence effector AvrRpt2 and modulates RPS2-mediated resistance. *Cell,* **112,** 379-389.

Mackey D, Holt III BF, Wiig A, and Dangl JL (2002) RIN4 Interacts with *Pseudomonas syringae* type III effector molecules and is required for RPM1-mediated resistance in *Arabidopsis*. *Cell,* **108,** 743-754.

Mateos FV, Rickauer M, and EsquerreTugaye MT (1997) Cloning and characterization of a cDNA encoding an elicitor of *Phytophthora parasitica* var. *nicotianae* that shows cellulose-binding and lectin-like activities. *Molecular Plant-Microbe Interactions,* **10,** 1045-1053.

McLellan H, Gilroy EM, Yun B, Birch PR, and Loake GJ (2009) Functional redundancy in the *Arabidopsis* Cathepsin B gene family contributes to basal defence, the hypersensitive response and senescence. *New Phytologist,* **183,** 408-418.

Milne I, Lindner D, Bayer M, Husmeier D, McGuire G, Marshall DF, and Wright F (2009) TOPALi v2: a rich graphical interface for evolutionary analyses of multiple alignments on HPC clusters and multi-core desktops. *Bioinformatics,* **25,** 126-127.

Mora-Garcia S, Vert G, Yin Y, Cano-Delgado A, Cheong H, and Chory J (2004) Nuclear protein phosphatases with Kelch-repeat domains modulate the response to Brassinosteroids in *Arabidopsis*. *Genes & Development,* **18,** 448-460.

Nakashita H, Yasuda M, Nitta T, Asami T, Fujioka S, Arai Y, Sekimata K, Takatsuto S, Yamaguchi I, and Yoshida S (2003) Brassinosteroid functions in a broad range of disease resistance in tobacco and rice. *Plant Journal,* **33,** 887-898.

Notredame C, Higgins DG, and Heringa J (2000) T-Coffee: A novel method for fast and accurate multiple sequence alignment. *Journal of Molecular Biology,* **302,** 205-217.

Oh MH, Wang X, Clouse SD, and Huber SC (2012) Deactivation of the *Arabidopsis* BRASSINOSTEROID INSENSITIVE 1 (BRI1) receptor kinase by autophosphorylation within the glycine-rich loop. *Proceedings of the National Academy of Sciences of the United States of America,* **109,** 327-332.

Oh SK, Young C, Lee M, Oliva R, Bozkurt TO, Cano LM, Win J, Bos JI, Liu HY, van Damme M, Morgan W, Choi D, Van der Vossen EA, Vleeshouwers VG, and Kamoun S (2009) In planta expression screens of *Phytophthora infestans* RXLR effectors reveal diverse phenotypes, including activation of the *Solanum bulbocastanum* disease resistance protein Rpi-blb2. *Plant Cell,* **21,** 2928-2947.

Orsomando G, Lorenzi M, Raffaelli N, la Rizza M, Mezzetti B, and Ruggieri S (2001) Phytotoxic protein PcF, purification, characterization, and cDNA sequencing of a novel hydroxyproline-containing factor secreted by the strawberry pathogen *Phytophthora cactorum. Journal of Biological Chemistry,* **276,** 21578-21584.

Piroux N, Saunders K, Page A, and Stanley J (2007) Geminivirus pathogenicity protein C4 interacts with *Arabidopsis thaliana* shaggy-related protein kinase AtSK eta, a component of the Brassinosteroid signalling pathway. *Virology,* **362,** 428-440.

Qutob D, Tedman-Jones J, Dong S, Kuflu K, Pham H, Wang Y, Dou D, Kale SD, Arredondo FD, Tyler BM, and Gijzen M (2009) Copy number variation and transcriptional polymorphisms of *Phytophthora sojae* RXLR effector genes *Avr1a* and *Avr3a*. *Plos One,* **4,** e5556. doi:10.1371/journal.pone.0005556.

Rehmany AP, Gordon A, Rose LE, Allen RL, Armstrong MR, Whisson SC, Kamoun S, Tyler BM, Birch PRJ, and Beynon JL (2005) Differential recognition of highly divergent downy mildew avirulence gene alleles by *RPP1* resistance genes from two *Arabidopsis* lines. *The Plant Cell,* **17,** 1839-1850.

Robatzek S, Chinchilla D, and Boller T (2006) Ligand-induced endocytosis of the pattern recognition receptor FLS2 in *Arabidopsis*. *Genes & Development,* **20,** 537-542.

Rooney HCE, van 't Klooster JW, van der Hoorn RAL, Joosten MHAJ, Jones JDG, and De Wit PJGM (2005) *Cladosporium* Avr2 inhibits tomato Rcr3 protease required for Cf-2-dependent disease resistance. *Science,* **308,** 1783-1786.

Rose JKC, Ham KS, Darvill AG, and Albersheim P (2002) Molecular cloning and characterization of glucanase inhibitor proteins: Coevolution of a counterdefense mechanism by plant pathogens. *Plant Cell,* **14,** 1329-1345.

Roux M, Schwessinger B, Albrecht C, Chinchilla D, Jones A, Holton N, Malinovsky FG, Toer M, de Vries S, and Zipfel C (2011) The *Arabidopsis* leucine-rich repeat receptor-like kinases BAK1/SERK3 and BKK1/SERK4 are required for innate immunity to hemibiotrophic and biotrophic pathogens. *Plant Cell,* **23,** 2440-2455.

Sambrook J, Fritsch EF, and Maniatis T (1989) Molecular cloning - A laboratory manual *2nd Edition.* Cold Spring Harbor Labouratory Press, Cold Spring Harbor, New York, USA.

Schornack S, van Damme M, Bozkurt TO, Cano LM, Smoker M, Thines M, Gualin E, Kamoun S and Huitema E (2010) Ancient class of translocated oomycete effectors targets the host nucleus. *Proceedings of the National Academy of Sciences of the United States of America,***107,** 17421-17426.

Shabab M, Shindo T, Gu C, Kaschani F, Pansuriya T, Chintha R, Harzen A, Colby T, Kamoun S, and Van der Hoorn RA (2008) Fungal effector protein AVR2 targets diversifying defense-related Cys proteases of tomato. *Plant Cell,* **20,** 1169-1183.

Shah J (2003) The salicylic acid loop in plant defense. *Current Opinion in Plant Biology,* **6,** 365-371.

Shan L, He P, Li J, Heese A, Peck SC, Nuernberger T, Martin GB, and Sheen J (2008) Bacterial effectors target the common signaling partner BAK1 to disrupt multiple MAMP receptor-signaling complexes and impede plant immunity. *Cell Host & Microbe,* **4,** 17-27.

Shan W, Cao M, Leung D, and Tyler BM (2004) The *Avr1b* locus of *Phytophthora sojae* encodes an elicitor and a regulator required for avirulence on soybean plants carrying resistance gene *Rps1b*. *Molecular Plant-Microbe Interactions,* **17,** 394-403.

She J, Han Z, Kim TW, Wang J, Cheng W, Chang J, Shi S, Wang J, Yang M, Wang ZY and Chai J (2011) Structural insight into brassinosteroid perception by BRI1. *Nature,* **474**, 472–476.

Smilde WD, Brigneti G, Jagger L, Perkins S, and Jones JDG (2005) *Solanum mochiquense* chromosome IX carries a novel late blight resistance gene *Rpi-moc1*. *Theoretical and Applied Genetics,* **110,** 252-258.

Szekeres M, Nemeth K, KonczKalman Z, Mathur J, Kauschmann A, Altmann T, Redei GP, Nagy F, Schell J, and Koncz C (1996) Brassinosteroids rescue the deficiency of CYP90, a cytochrome P450, controlling cell elongation and de-etiolation in *Arabidopsis*. *Cell,* **85,** 171-182.

Tang WQ, Kim TW, Oses-Prieto JA, Sun Y, Deng ZP, Zhu SW, Wang RJ, Burlingame AL, and Wang ZY (2008) BSKs mediate signal transduction from the receptor kinase BRI1 in *Arabidopsis*. *Science,* **321,** 557-560.

Tang W, Yuan M, Wang R, Yang Y, Wang C, Oses-Prieto JA, Kim TW, Zhou HW, Deng Z, Gampala SS, Gendron JM, Jonassen EM, Lillo C, DeLong A, Burlingame AL, Sun Y, and Wang ZY (2011) PP2A activates Brassinosteroid-responsive gene expression and plant growth by dephosphorylating BZR1. *Nature Cell Biology,* **13,** 124-131.

Tian MY, Benedetti B, and Kamoun S (2005) A second kazal-like protease inhibitor from *Phytophthora infestans* inhibits and interacts with the apoplastic pathogenesis-related protease P69B of tomato. *Plant Physiology,* **138,** 1785-1793.

Tian MY, Huitema E, da Cunha L, Torto-Alalibo T, and Kamoun S (2004) A Kazal-like extracellular serine protease inhibitor from *Phytophthora infestans* targets the tomato pathogenesis-related protease P69B. *Journal of Biological Chemistry,* **279,** 26370-26377.

Tian M, Win J, Song J, van der Hoorn R, van der Knaap E, and Kamoun S (2007) A *Phytophthora infestans* cystatin-like protein targets a novel tomato papain-like apoplastic protease. *Plant Physiology,* **143,** 364-377.

Tor M, Gordon P, Cuzick A, Eulgem T, Sinapidou E, Mert-Turk F, Can C, Dangl JL, and Holub EB (2002) *Arabidopsis* SGT1b is required for defense signaling conferred by several downy mildew resistance genes. *Plant Cell,* **14,** 993-1003.

Tornero P, Merritt P, Sadanandom A, Shirasu K, Innes RW, and Dangl JL (2002) RAR1 and NDR1 contribute quantitatively to disease resistance in *Arabidopsis*, and their relative contributions are dependent on the *R* gene assayed. *Plant Cell,* **14,** 1005-1015.

Torres MA and Dangl JL (2005) Functions of the respiratory burst oxidase in biotic interactions, abiotic stress and development. *Current Opinion in Plant Biology,* **8,** 397-403.

Twining S, Clarke J, Cook S, Ellis S, Gladders P, Ritchie F, and Wynn S. Pesticide availability for potatoes following revision of Directive 91/414/EEC: Impact assessments and identification of research priorities. 2009. Potato Council Ltd.

Umemoto N, Kakitani M, Iwamatsu A, Yoshikawa M, Yamaoka N, and Ishida I (1997) The structure and function of a soybean beta-glucan-elicitor-binding protein. *Proceedings of the National Academy of Sciences of the United States of America,* **94,** 1029-1034.

van der Hoorn RAL and Kamoun S (2008) From guard to decoy: A new model for perception of plant pathogen effectors. *The Plant Cell,* **20,** 2009-2017.

van der Lee T, Robold A, Testa A, van't Klooster JW, and Govers F (2001) Mapping of avirulence genes in *Phytophthora infestans* with amplified fragment length polymorphism markers selected by bulked segregant analysis. *Genetics,* **157,** 949-956.

van der Vossen EAG, Gros J, Sikkema A, Muskens M, Wouters D, Wolters P, Pereira A, and Allefs S (2005) The *Rpi-blb2* gene from *Solanum bulbocastanum* is an *Mi-1* gene homolog conferring broad-spectrum late blight resistance in potato. *Plant Journal,* **44,** 208-222.

van Poppel P, Guo J, Vondervoort P, Jung M, Birch P, Whisson S, and Covers F (2008) The *Phytophthora infestans* avirulence gene *Avr4* encodes an RXLR-dEER effector. *Molecular Plant-Microbe Interactions,* **21,** 1460-1470.

Vleeshouwers VG, Raffaele S, Vossen JH, Champouret N, Oliva R, Segretin ME, Rietman H, Cano LM, Lokossou A, Kessel G, Pel MA, and Kamoun S (2011). Understanding and exploiting late blight resistance in the age of effectors. *The Annual Review of Plant Biology*, **49**, 507-531

Vleeshouwers VG, Rietman H, Krenek P, Champouret N, Young C, Oh SK, Wang M, Bouwmeester K, Vosman B, Visser RG, Jacobsen E, Govers F, Kamoun S, and Van der Vossen EA (2008) Effector genomics accelerates discovery and functional profiling of potato disease resistance and *Phytophthora infestans* avirulence genes. *Plos One,* **3,** e2875. doi:10.1371/journal.pone.0002875.

Wang Q, Han C, Ferreira AO, Yu X, Ye W, Tripathy S, Kale SD, Gu B, Sheng Y, Sui Y, Wang X, Zhang Z, Cheng B, Dong S, Shan W, Zheng X, Dou D, Tyler BM, and Wang Y (2011) Transcriptional programming and functional interactions within the *Phytophthora sojae* RXLR effector repertoire. *Plant Cell,* **23,** 2064-2086.

Wang XF, Kota U, He K, Blackburn K, Li J, Goshe MB, Huber SC, and Clouse SD (2008) Sequential transphosphorylation of the BRI1/BAK1 receptor kinase complex impacts early events in Brassinosteroid signaling. *Developmental Cell,* **15,** 220-235.

Wang XL and Chory J (2006) Brassinosteroids regulate dissociation of BKI1, a negative regulator of BRI1 signaling, from the plasma membrane. *Science,* **313,** 1118-1122.

Wang ZY, Nakano T, Gendron J, He JX, Chen M, Vafeados D, Yang YL, Fujioka S, Yoshida S, Asami T, and Chory J (2002) Nuclear-localized BZR1 mediates Brassinosteroid-induced growth and feedback suppression of Brassinosteroid biosynthesis. *Developmental Cell,* **2,** 505-513.

Wawra S, Bain J, Durward E, de Bruijn I, Minor KL, Matena A, Loebach L, Whisson SC, Bayer P, Porter AJ, Birch PR, Secombes CJ, and van West P (2012) Host-targeting protein 1 (SpHtp1) from the oomycete *Saprolegnia parasitica* translocates specifically into fish cells in a tyrosine-O-sulphate-dependent manner. *Proceedings of the National Academy of Sciences of the United States of America,* **109,** 2096-2101.

Whisson SC, Boevink PC, Moleleki L, Avrova AO, Morales JG, Gilroy EM, Armstrong MR, Grouffaud S, van WP, Chapman S, Hein I, Toth IK, Pritchard L, and Birch PR (2007) A translocation signal for delivery of Oomycete effector proteins into host plant cells. *Nature,* **450,** 115-118.

Whisson SC, van der Lee T, Bryan GJ, Waugh R, Govers F, and Birch PR (2001) Physical mapping across an avirulence locus of *Phytophthora infestans* using a highly representative, large-insert bacterial artificial chromosome library. *Molecular Genetics and Genomics,* **266,** 289-295.

Win J, Morgan W, Bos J, Krasileva KV, Cano LM, Chaparro-Garcia A, Ammar R, Staskawicz BJ, and Kamoun S (2007) Adaptive evolution has targeted the C-terminal domain of the RXLR effectors of plant pathogenic Oomycetes. *Plant Cell,* **19,** 2349-2369.

Yin YH, Vafeados D, Tao Y, Yoshida S, Asami T, and Chory J (2005) A new class of transcription factors mediates Brassinosteroid-regulated gene expression in *Arabidopsis*. *Cell,* **120,** 249-259.

Yin YH, Wang ZY, Mora-Garcia S, Li JM, Yoshida S, Asami T, and Chory J (2002) BES1 accumulates in the nucleus in response to Brassinosteroids to regulate gene expression and promote stem elongation. *Cell,* **109,** 181-191.

Zenk SF, Stabat D, Hodgkinson JL, Veenendaal AKJ, Johnson S, and Blocker AJ (2007) Identification of minor inner-membrane components of the *Shigella* type III secretion system 'needle complex'. *Microbiology,* **153,** 2405-2415.

# Presence/absence, differential expression and sequence polymorphisms between *PiAVR2* and *PiAVR2-like* in *Phytophthora infestans* determine virulence on *R2* plants

Eleanor M. Gilroy[1], Susan Breen[1,2], Stephen C. Whisson[1], Julie Squires[1], Ingo Hein[3], Maciej Kaczmarek[1], Dionne Turnbull[1], Petra C. Boevink[1], Anoma Lokossou[4], Liliana M. Cano[5], Juan Morales[1,6], Anna O. Avrova[1], Leighton Pritchard[1], Eva Randall[1], Alison Lees[1], Francine Govers[7,8], Pieter van West[9], Sophien Kamoun[5], Vivianne G. A. A. Vleeshouwers[4], David E. L. Cooke[1] and Paul R. J. Birch[1,2]

[1]Plant Pathology, James Hutton Institute, Invergowrie, Dundee DD2 5DA, UK; [2]Division of Plant Sciences, College of Life Sciences, University of Dundee at JHI, Invergowrie, Dundee DD2 5DA, UK; [3]Genetics Programmes, James Hutton Institute, Invergowrie, Dundee DD2 5DA, UK; [4]Wageningen UR Plant Breeding, Wageningen University, Wageningen, the Netherlands; [5]The Sainsbury Laboratory, John Innes Centre, Colney, Norwich NR4 7UH, UK; [6]Universidad Nacional de Colombia sede Medellín, Campus El Volador, Departamento de Ciencias Agronómicas, Medellin, Colombia; [7]Laboratory of Phytopathology, Wageningen University, Wageningen, the Netherlands; [8]Centre for BioSystems Genomics, Wageningen University, Wageningen, the Netherlands; [9]Aberdeen Oomycete Laboratory, College of Life Sciences and Medicine, Institute of Medical Sciences, University of Aberdeen, Foresterhill, Aberdeen AB25 2ZD, UK

Author for correspondence:
*Paul R. J. Birch*
*Tel: +44 (0)1382 562731*
*Email: pbirch@scri.ac.uk*

Received: *15 January 2011*
Accepted: *9 March 2011*

*New Phytologist* (2011) **191**: 763–776
**doi**: 10.1111/j.1469-8137.2011.03736.x

**Key words:** durable disease resistance, effector-triggered immunity, gene-for-gene, hypersensitive response, potato blight.

## Summary

- A detailed molecular understanding of how oomycete plant pathogens evade disease resistance is essential to inform the deployment of durable resistance (*R*) genes.
- Map-based cloning, transient expression *in planta*, pathogen transformation and DNA sequence variation across diverse isolates were used to identify and characterize *PiAVR2* from potato late blight pathogen *Phytophthora infestans*.
- PiAVR2 is an RXLR-EER effector that is up-regulated during infection, accumulates at the site of haustoria formation, and is recognized inside host cells by potato protein R2. Expression of *PiAVR2* in a virulent *P. infestans* isolate conveys a gain-of-avirulence phenotype, indicating that this is a dominant gene triggering *R2*-dependent disease resistance. *PiAVR2* presence/absence polymorphisms and differential transcription explain virulence on *R2* plants. Isolates infecting *R2* plants express *PiAVR2-like*, which evades recognition by *R2*. PiAVR2 and PiAVR2-like differ in 13 amino acids, eight of which are in the C-terminal effector domain; one or more of these determines recognition by R2. Nevertheless, few polymorphisms were observed within each gene in pathogen isolates, suggesting limited selection pressure for change within *PiAVR2* and *PiAVR2-like*.
- Our results direct a search for *R* genes recognizing *PiAVR2-like*, which, deployed with *R2*, may exert strong selection pressure against the *P. infestans* population.

## Introduction

Oomycetes comprise a major group of eukaryotic microbial pathogens that cause devastating diseases on dicotyledonous plants (Kamoun, 2003). One notorious representative is *Phytophthora infestans*, the cause of late blight, the most significant global disease of potato. The genetic flexibility of *Phytophthora* (Brasier, 1992) and the coevolution of *P. infestans* populations in Central and South America with wild *Solanum* species have yielded a remarkable source of

genetic diversity in populations of this pathogen. *P. infestans* thus possesses an alarming, and demonstrated, adaptibility, able to respond rapidly to selection pressures within agricultural systems, resulting in global late blight epidemics (Fry, 2008). Breeding efforts to control this disease by introgression of resistance from wild *Solanum* species have had limited success, probably because of the genetic diversity within pathogen populations (Hein *et al.*, 2009a). Indeed, the genome sequence of *P. infestans* reveals striking potential for genetic change (Haas *et al.*, 2009). A major scientific goal is thus to develop a detailed understanding of how disease resistance to *P. infestans* has been overcome to date. Such knowledge is critical to combating this and other economically important oomycete plant pathogens.

Inducible disease resistance in plants is based on detection of two distinct classes of pathogen molecules. Recognition of secreted or surface-exposed pathogen/microbe-associated molecular patterns (PAMP/MAMPs) by pattern recognition receptors (PRRs) in the host leads to broadly effective PAMP (or, more generally, Pattern)-triggered immunity (PTI). Pathogens deploy effector proteins that suppress this response (effector-triggered susceptibility; ETS). Effectors are a second class of molecules that can be detected by plants, often by nucleotide-binding leucine-rich repeat (NB-LRR) resistance (R) proteins. When detected, effectors are termed avirulence (AVR) proteins, and the consequent disease resistance is referred to as effector-triggered immunity (ETI), or the hypersensitive response (HR) (Jones & Dangl, 2006; Chisholm *et al.*, 2006).

In recent years, a number of *AVR* genes have been identified from oomycete plant pathogens. These include *AVR3a* (Armstrong *et al.*, 2005), *AVR4* (Van Poppel *et al.*, 2008), *AVR-blb1* (Vleeshouwers *et al.*, 2008; Champouret *et al.*, 2009) and *AVR-blb2* (Oh *et al.*, 2009) from *P. infestans*; *Avr1b* (Shan *et al.*, 2004), *Avr3c* (Dong *et al.*, 2010), *Avr3a*, *Avr1a* (Qutob *et al.*, 2009) and *Avr4/6* (Dou *et al.*, 2008) from the soybean pathogen *P. sojae*; and *ATR13* (Allen *et al.*, 2004) and *ATR1* (Rehmany *et al.*, 2005) from the *Arabidopsis thaliana* pathogen *Hyaloperonospora arabidopsidis.* All are members of the extensive, diverse RXLR class of effectors (Birch *et al.*, 2006, 2008, 2009; Kamoun, 2006, 2007; Hein *et al.*, 2009b; Schornack *et al.*, 2009). These effectors are so named for the amino acid motif, RXLR (Arg-any amino acid-Leu-Arg), often closely followed by the motif EER (Glu-Glu-Arg), which is required for their entry into living plant cells (Whisson *et al.*, 2007; Dou *et al.*, 2008).

Each of these effectors has enhanced our understanding of how oomycete plant pathogens can evade ETI and thus overcome disease resistance. Single nucleotide polymorphisms (SNPs) within allelic forms may give rise to proteins with amino acid changes that evade recognition. This has been well documented for *AVR3a* from *P. infestans*; only two alleles reported within the pathogen population encode proteins differing in two amino acids (K80E and I103M) which dictate recognition by R3a (Armstrong *et al.*, 2005; Bos *et al.*, 2006). As AVR3a is an essential pathogenicity determinant (Bos *et al.*, 2010), deployment of an *R* gene that targets the virulent form, $AVR3a^{EM}$, in combination with *R3a*, which targets the avirulent form, $AVR3a^{KI}$, would potentially impose strong selection pressure on the pathogen population. In addition to *AVR3a*, SNPs that encode alternative, virulent alleles have been reported for *ATR1* and *ATR13* from *H. arabidopsidis* (Allen *et al.*, 2004; Rehmany *et al.*, 2005) and *Avr1b* and *Avr3c* from *P. sojae* (Shan *et al.*, 2004; Dong *et al.*, 2009). In addition to amino acid polymorphisms, which can retain the virulence function of the effector (Bos *et al.*, 2010), virulence on plants containing some *R* genes has been achieved by loss of a functional *AVR* gene. Frame-shift mutations, resulting in truncated versions of *AVR4*, have been reported in *P. infestans* isolates that infect potato expressing *R4* (Van Poppel *et al.*, 2008). Moreover, differential gene expression, sometimes associated with gene deletion or gene copy number variation, has been reported for *Avr1b* (Shan *et al.*, 2004), *Avr1a* and *Avr3a* (Qutob *et al.*, 2009) from *P. sojae*. Presumably, loss of an effector gene, or of its expression, may be compensated for by functional redundancy in the effector complement (Birch *et al.*, 2008).

In theory, durable disease resistance may be achieved with an R protein, or a judicious combination of R proteins, that target all of the effectors (or effector forms deriving from alleles) contributing to an essential pathogenicity function, as hypothesized earlier for *AVR3a* from *P. infestans*. This is apparently the case for the resistance protein Rpi-blb2 from *Solanum bulbocastanum*, which recognizes multiple members of a closely related *P. infestans* RXLR effector family, of which there are seven paralogues within the genome sequence of clone T30-4 (Oh *et al.*, 2009). *Rpi-blb2* has so far proven durable.

Here, we report the map-based cloning of *PiAVR2* from *P. infestans*. This gene (PITG_22870) from *P. infestans* clone T30-4 was previously shown to trigger *R2*-dependent cell death (Lokossou *et al.*, 2009). Transformation of a virulent isolate with *PiAVR2* conferred a gain-of-avirulence phenotype when inoculated on to the *R2* potato differential, indicating that it is a dominant gene specifying *R2*-mediated recognition and disease resistance. We show that, whereas all avirulent isolates possess *PiAVR2*, virulent isolates lack either *PiAVR2* or its expression. By contrast, virulent isolates express a divergent form, *PiAVR2-like*, which is not recognized by *R2* or *R2*-like orthologues from wild *Solanum* species. Remarkably, while there is little sequence diversity within either *PiAVR2* or *PiAVR2-like* in the sampled *P. infestans* populations, the predicted PiAVR2 and PiAVR2-like polypeptides differ from each other by 13 amino acids in the mature protein. Given that each form, though markedly divergent, nevertheless appears to be

highly conserved in diverse *P. infestans* isolates, and that all isolates tested possess one or other, or both forms, we propose a strategy for durable late blight disease resistance.

## Materials and Methods

### Plant and microbial strains and growth conditions

Potato plants and *P. infestans* isolates and transgenic strains were maintained, and infection assays performed, as described in Whisson *et al.* (2007). *Nicotiana benthamiana* and potato genotypes were grown as in Bos *et al.* (2010). *Escherichia coli* strain DH10B and *Agrobacterium tumefaciens* strain AGL1 were used for cloning. Agrobacterium strains for transient expression of potato *R2* and its orthologues *R2-like*, *BLB3* and *ABPT* are described in Lokossou *et al.* (2009). All *A. tumefaciens* cultures were grown at 27°C at 200 rpm for 2–3 d in LB (Luria Bertani broth), spun at 4000 rpm and the pellet resuspended in sterile 10 mM 2-(N-morpholine)-ethanesulphonic acid (MES) and 10 mM $MgCl_2$ buffer with 200 μM acetosyringone, to $OD_{600}$ = 0.5 for each construct.

### Map-based cloning of *PiAVR2*

Amplified fragment length polymorphism (AFLP) markers E + GA/M + ATs513 and E + TG/M + CTs338, which span the *Avr2* locus of *P. infestans* (Van der Lee *et al.*, 2001; Fig. 1a), were used to screen the pooled bacterial artificial chromosome (BAC) library of *P. infestans* T30-4 as described previously (Whisson *et al.*, 2001). BAC clones identified with E + GA/M + ATs513 (23O22 and 39L24) and with E + TG/M + CTs338 (8C12 and 5D19) were end-sequenced using SP6 and T7 primers as described (Whisson *et al.*, 2001), and these sequences were positioned on the genome sequence of T30-4 (Haas *et al.*, 2009), in supercontig 1.16 using BlastN. The region delimited by the outer BAC sequences was screened for annotated RXLR-EER coding sequences, revealing PITG_22870, PITG_08943 and PITG_08949.

### Transient expression of *P. infestans* genes in plants to assess *R* gene responses

PITG_08949 and PITG_22870 (*PiAVR2*) sequences were initially amplified from genomic DNA of *P. infestans* isolate 88069 using *Asc*1-For and *Bam*H1-Rev primers (Supporting Information, Table S1) and cloned into vector pGRAB using these restriction sites and transformed into *A. tumefaciens* strain AGL1 cells by electroporation as described in Bos *et al.* (2010). Positive transformants were subsequently grown in LB supplemented with rifampicin and kanamycin for transient expression in potato and *N. benthamiana*. For gateway cloning® (Invitrogen), PITG_22870 and PITG_08949 were amplified from sequences encoding from the cleavage site of the signal peptide (SP) to the stop codon from genomic DNA of *P. infestans* isolate T30-4 with gene-specific primers (Table S1). The N-terminus-encoding region of $PiAVR2^{N31}$ was cloned from the SP cleavage site to the last amino acid in the EER motif. The C-terminus-encoding region of *PiAVR2* was cloned from the first amino acid after the EER motif to the stop codon (see Table S1 for PCR primers). AttB recombination sites were added by a second PCR using the AttB1/AttB2 to all sequences and recombined into pDNR221 using BP clonase® (Invitrogen). *Piavr2* DNA encoding from the SP

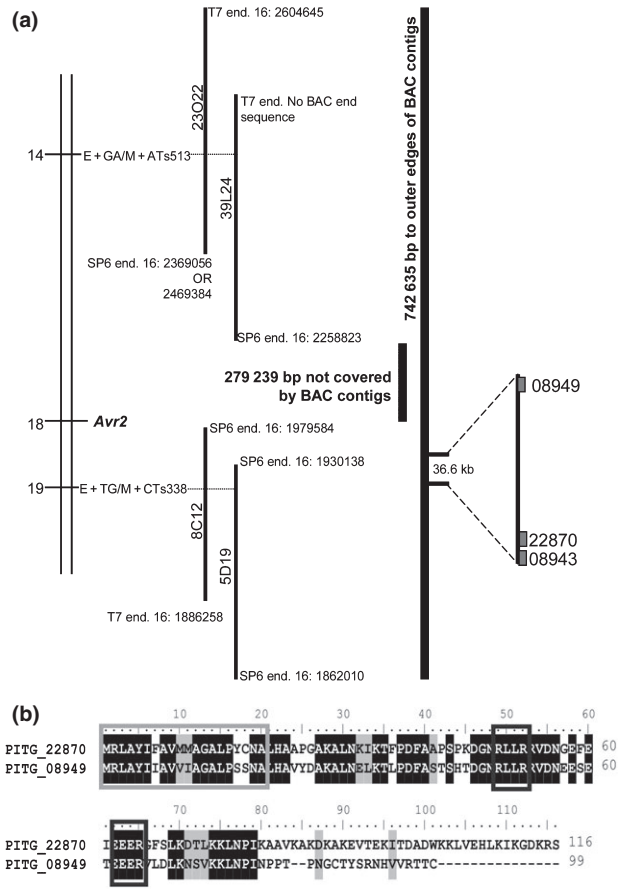


**Fig. 1** Identification of *PiAVR2* candidates by map-based cloning. (a) Genetic interval (left) showing amplified fragment length polymorphism markers flanking the *AVR2* locus. Bacterial artificial chromosome (BAC) clones containing these markers were end-sequenced and the DNA sequences positioned in supercontig 1.16 of the *Phytophthora infestans* T30-4 genome sequence, spanning a region of 742.6 kb. Within a 36.6 kb region of this (right), three candidate RXLR-dEER effector genes were identified: PITG_08949, PITG_08943 and PITG_22870. This diagram is not drawn to scale. (b) Alignment of the predicted protein sequences of PITG_22870 and PITG_08949 revealed considerable similarity over the first 79 amino acids, and subsequent divergence, as a result of a likely DNA recombination event (Supporting Information, Fig. S2). The pale box represents the signal peptide and the dark boxes indicate the RLLR and EER motifs.

cleavage site to the stop codon (357 bp), and the C-terminus-encoding region from the first amino acid after the EER motif until the stop codon, or without the stop (222 bp), was synthesized and delivered in pUC57 (Genscript, Piscataway, USA).

LR clonase® (Invitrogen) was used to recombine DNA sequences into pMDC32 plant expression vector (Curtis & Grossniklaus, 2003), transformed into *E. coli* by electroporation, sequenced, and plasmids with confirmed inserts were transformed into *A. tumefaciens* strain AGL1, pSoup, pVirG cells by electroporation. Positive transformants were subsequently grown for 2 d at 27°C in LB supplemented with rifampicin, chloroamphenicol, tetracycline and kanamycin for transient expression in potato and *N. benthamiana*. For plant inoculations, all *A. tumefaciens* cultures were resuspended to $OD_{600}$ = 0.5. Cultures carrying RXLRs were mixed 1 : 1 with one of the cultures carrying *R2* or an *R2* orthologue so the final $OD_{600}$ of each is 0.25. Cultures not mixed with either an RXLR or an *R* gene construct were diluted with an equal volume of buffer to a final $OD_{600}$ = 0.25. Cultures were infiltrated with a 1 ml syringe without a needle through the abaxial leaf surface superficially wounded with a needle. Three to four leaves on at least four plants were used for each biological replicate. HRs were recorded and photographed between 2 and 5 d postinfiltration depending on the expression vector and plant species. An individual inoculation was counted as positive if > 50% of the inoculated area developed a clear HR. Data graphs present the mean percentage of total inoculations per plant developing a clear HR with error bars representing ± standard error (SE) of combined data from at least three biological replicates. Co-bombardment assays with *GUS* were performed and assayed as described in Armstrong *et al.* (2005) using pGRAB::*PiAVR2*.

## Gene expression analyses

Standard RT-PCR to examine gene expression in a number of isolates at 48 h postinoculation (hpi) on potato was performed using primers diagnostic for expression of *PiAVR2* (AVR2F4 and AVR2R4) and *PiAVR2-like* (avr2diagF1 and avr2diagR1) (Fig. S1) at an annealing temperature of 61°C for 30 cycles. Quantitative gene expression analyses of RXLR genes were performed as described in Whisson *et al.* (2007), with Power SYBR® Green (Applied Biosystems, Warrington, UK), using a Chromo4® Real-Time Detector (Bio-Rad). *ActA* was used as an endogenous control gene as described previously (Bos *et al.*, 2010). General *PiAVR2* and *PiAVR2-like* expression was quantified using qRT-PCRfwd and qRT-PCRrev primers (Fig. S1). PITG_08949 expression was quantified using For 5′-AGGAATCTGAG-ACCGAGGAA-3′ and Rev 5′-GGGGGTTAATGGGAT-TGAG-3′. Data are presented as fold change relative to normalized expression in sporangia growth stage of each individual *P. infestans* isolate, calculated by the ΔΔCt method with error bars representing ± SE.

## Presence/absence and sequence diversity in *P. infestans* isolates

*PiAVR2* and *PiAVR2-like* were PCR-amplified from *P. infestans* isolates detailed in Table 1. Primers AVR2F1 and AVR2R1 (Fig. S1) were designed against PITG_22870 and amplified the predicted size product (541 bp) from *PiAVR2*. However, they repeatedly failed to generate PCR products from nine isolates (Fig. 2c; Table 1). The reverse primer AVR2R1 also proved unsuitable for initiating DNA sequencing of the PCR products as a result of a 1 bp indel adjacent to the primer (Fig. S1). Additional primer pairs AVR2F2/AVR2R2 and AVR2F4/AVR2R4 were designed (Fig. S1) to amplify this region from the nine isolates that failed previously and to provide improved sequencing primers. Both pairs amplified the expected product sizes (480 and 340 bp, respectively) from isolates that yielded products with the primer pair AVR2F1/R1 but neither amplified products from the nine isolates that failed previously. The primer pair AVR2F2/R2 proved optimal for PCR and sequencing of *PiAVR2* and was used in all subsequent work. The use of the primer pair AVR2F2/R2 at a lower annealing temperature of 58°C generated weak PCR products from three isolates (01/29, MP618 and 06_3928A; Table 1). The sequences of these products differed from PITG_22870 and PITG_08943 at 25 bases, revealing *PiAVR2-like* (Fig. S1). Primer pairs specific for the *PiAVR2-like* sequence (avr2F6/avr2R6 and avr2F7/avr2R7 (Fig. S1) amplified PCR products of the predicted size (392 and 472 bp, respectively) from the nine isolates that had failed to amplify *PiAVR2* but also from 12 isolates from which *PiAVR2* was also amplified. Primers NitRedF (5′-GGACCGCTGGGCCACTTCAC-3′)/NitRedR (5′-CGCTGGCTTGCAGGCGTACT-3′) were used as control reactions to amplify a 435 bp region from the nitrate reductase gene (GenBank accession U14405; PITG_13012).

All PCR reactions were carried out with the same reagents in a 20 μl reaction volume using a Primus $96^{plus}$ Thermalcycler (MWG-Biotech, Ebersberg, Germany). Each reaction contained 1 × GoTaq® Flexi buffer, 20 μg BSA, 1.5 mM $MgCl_2$, 100 μM dNTPs, 0.8 unit of Taq polymerase (GoTaq® DNA polymerase; Promega), 0.2 μM of primers and *c.* 20 ng of template DNA. Amplification conditions consisted of one cycle of 94°C for 1 min, 30 cycles of 95°C for 30 s, 60°C for primer pairs AVR2F1/R2, F2/R2 and F4/R4, 58°C for primer pairs avr2F6/R6 and F7/R7, and 55°C for the primer pair NitRedF/R for 30 s, 72°C for 30 s and a final cycle of 72°C for 5 min.

### Isolate 06_3928A genome sequence and alignment to T30-4 genome

For the genomic DNA extraction, *Phytophthora infestans* strain 06_3928A was cultured in rye sucrose agar (RSA) plates at 18°C for 12 d. Plugs with mycelium of *P. infestans* strain 06_3928A were transferred to modified plich medium (Kamoun *et al.*, 1993), grown for another 2 wk at 18°C and then harvested for genomic DNA isolation using Omniprep kit (G-Biosciences, Maryland Heights, MO, USA; catalogue number 786-136) with minor modifications. For sequencing, the flow cells were prepared according to the manufacturer's instructions using the Illumina pair read cluster generation kit, PE-203-4001. Sequencing reactions were performed mostly on 2G GAs (Illumina Inc., Chesterford Research Park, Essex, UK). The reference genome sequence of the *P. infestans* strain T30-4, annotation and gene/exon locations was downloaded from http://www.broad.mit.edu (GenBank project accession number AATU01000000). The generated raw reads with abnormal lengths and reads containing Ns were removed from the datasets. Filtered reads were use to align to the reference genome strain T30-4. Alignments were obtained with BWA software v0.5.7 (Li & Durbin, 2010) using as parameters a seed length (*l*) of 38 and a maximum of mismatches (*M*) of 3.

**Table 1** Details of isolates used in this study and details of PCR product amplification with primers sets (shown in Supporting Information, Fig. S1) specific to each of *PiAVR2* or *PiAVR2-like*

| | | | | Amplification with primers below | | | | Amplification with primers below | | |
|---|---|---|---|---|---|---|---|---|---|---|
| Genotype[a] | Isolate name | Origin | *R2*[b] virulence | AVR2 F2 and R2[c] | AVR2 F1 and R1 | AVR2 F4 and R4 | SNP[d] within *PiAVR2* | avr2 F7 and R7 | avr2 F6 and R6 | SNP[e] within *PiAVR2-like* |
| 3_A2 | 2006_4012F | UK | + | – | – | – | n/a | + | + | MI/TV |
| 3_A2 | 2006_4244E | UK | + | – | – | – | n/a | + | + | — |
| 13_A2 | 2006_3884B | UK | + | – | – | – | n/a | + | + | — |
| 13_A2 | 2006_3928A | UK | + | +/– | – | – | n/a | + | + | MI/TV |
| 13_A2 | 2006_3964A | UK | + | – | – | – | n/a | + | + | — |
| 13_A2 | 2006_4132B | UK | + | – | – | – | n/a | + | + | — |
| 5_A1 | 01/29 | UK | + | +/– | – | – | n/a | + | + | MI |
| 5_A1 | 1996_9_5_1 | UK | + | – | – | – | n/a | + | + | — |
| Misc | MP618 | Poland | + | +/– | – | – | n/a | + | + | MI/TV |
| 7_A1 | 2006_4168B | UK | + | + | + | + | K | + | + | MI |
| 7_A1 | 2006_4168C | UK | + | + | + | + | K | + | + | — |
| 17_A2 | 2006_4388D | UK | + | + | + | + | K/N | + | + | MI |
| 1_A1 | 2006_3984C | UK | – | + | + | + | K/N | + | + | TV |
| 2_A1 | 2006_3888A | UK | – | + | + | + | K | + | + | — |
| 2_A1 | 2006_4068B | UK | – | + | + | + | K | + | + | MI |
| 8_A1 | 2006_4256B | UK | – | + | + | + | K | + | + | MI |
| 8_A1 | SC_95 17_3_2 | UK | – | + | + | + | K | + | + | MI |
| 22_A2 | 2003_25_1_3 | UK | – | + | + | + | K | + | + | MI/TV |
| 22_A2 | 2003_25_3_1 | UK | – | + | + | + | K | + | + | MI/TV |
| Misc | 88069 | The Netherlands | – | + | + | + | K | + | + | MI |
| EC1 | EC1 | Ecuador | – | + | + | + | K | + | + | — |
| 4_A1 | 2006_4352E | UK | – | + | + | + | K | – | – | n/a |
| 6_A1 | 2006_4100A | UK | – | + | + | + | K/N | – | – | n/a |
| 6_A1 | 2006_3920A | UK | – | + | + | + | K/N | – | – | n/a |
| 10_A2 | 2006_4440C | UK | – | + | + | + | K | – | – | n/a |
| 10_A2 | 2006_3936C2 | UK | – | + | + | + | K | – | – | n/a |
| 15_A2 | 2004_7804B | UK | – | + | + | + | K/N | – | – | n/a |
| Misc | Ca65 | USA | – | + | + | + | K/N | – | – | n/a |
| Misc | T30-4 | n/a | – | + | + | + | K/N | – | – | n/a |

SNP, single nucleotide polymorphism; n/a, not applicable.
[a]*Phytophthora infestans* genotypes are based on defined simple-sequence repeat marker profiles that will be reported in detail elsewhere.
[b]'+' indicates ability to infect *R2* plants and '–' indicates the isolate triggers HR on *R2* plants.
[c]'+/–' indicates PCR amplification only when the annealing temperature was decreased.
[d]SNP results in amino acid polymorphism N31K in PiAVR2. K/N is heterozygous.
[e]Two SNPs result in amino acid polymorphisms M10T and I92V in PiAVR2-like. MI/TV is heterozygous
Protein alignments from the isolates above, indicating the N31K, M10T and I92V polymorphisms, are shown in Fig. S4.

### Western analyses of protein stability

*PiAVR2*, *PiAVR2-like* and PITG_08949 sequences were cloned into pDNR221 using almost identical primers as described earlier except with one nucleotide of TAA stop codon changed to make a sense codon AAA. LR clonase® (Invitrogen) was used to recombine correct sequences into pB7FWG2.0 (Karimi *et al.*, 2002) C-terminal GFP-tagged plant expression vector, transformed into *E. coli* by electroporation, sequenced, and plasmids with confirmed inserts were transformed into *A. tumefaciens* strain AGL1, pSoup, pVirG cells by electroporation. Positive transformants were grown for 2 d at 27°C in LB supplemented with rifampicin, chloroamphenicol, and spectinomycin. For transient expression in *N. benthamiana*, the conditions described earlier were used. A final $OD_{600}$ = 0.25 of pB7FWG2.0 containing cultures was achieved by mixing with an $OD_{600}$ = 0.2 pJL3-p19 containing culture in a 2 : 1 ratio. Whole leaves were infiltrated with culture to allow 1 $cm^2$ leaf discs to be cut out at 3 dpi for the protein extraction protocol. Leaf discs of *c.* 100 mg were ground in liquid $N_2$, 200 μl extraction buffer was added (20 mM HEPES, 13% sucrose, 1 mM EDTA, 1 mM DTT, proteinase inhibitor cocktail tablet, 0.1% Triton – the DTT (dithiothreitol), Triton and proteinase inhibitor cocktail tablet were added fresh each time) and left to thaw on ice. Twenty microlitres of the whole lysate was mixed with 20 μl sodium dodecyl sulphate loading buffer. Samples were boiled for 5 min at 95°C, loaded on to a 12% Bis-Tris NuPAGE® Novex® Mini gel (Invitrogen) and run at 200 V, 120 mA and 25 W for 1 h, then membrane-blotted for 1 h at 130 V. Four per cent% milk powder was used to block the membrane. The primary antibody was monoclonal mouse GFP antibody (Sigma-Aldrich) at 1 : 10 000 dilution. The membrane was washed with PBS-T 0.1% before addition of secondary goat antimouse immunoglobulin (Ig) horseradish peroxidise antibody (Sigma-Aldrich) at 1 : 2000 dilution. ECL-Plus Western Blotting Detection Reagents (Amersham) were used for detection, according to the manufacturer's instructions.

### *P. infestans* transformations

For expression of $PiAVR2^{K31}$ in *P. infestans* isolate 06_3928A, the gene was cloned from genomic DNA of isolate 88069 using primers shown in Fig. S1. The *Cla*I and *Sac*I restriction sites generated were used to clone $PiAVR2^{K31}$ into *P. infestans* expression pTOR, and transformation of isolate 06_3928A was carried out as previously described (Bos *et al.*, 2010). To generate a *P. infestans* strain expressing PiAVR2::Tdtomato, *PiAVR2* was amplified from isolate 88069 using an alternative reverse primer (Fig. S1) altering the stop codon to a sense codon, and cloned into pTOR::Tdtomato (based on pTOR::mRFP described in Whisson *et al.*, 2007; but with the fluorescent protein gene *Tdtomato* in place of *mRFP*) using *Cla*I and *Sac*I restriction sites. This was transformed into isolate 88069 as described in Bos *et al.* (2010). Isolate 06_3928A and this genotype expressing $PiAVR2^{K31}$ and isolate 88069 were inoculated on to potato cv Craigs Royal and R2 differential 1512 c(16) as described previously (Bos *et al.*, 2010) and lesions were observed 1 wk later. Inoculation of the 88069 strain expressing $PiAVR2^{K31}$*::Tdtomato* on to *N. benthamiana*, and confocal microscopy were conducted as described in Whisson *et al.* (2007), but to image Tdtomato, it was excited with the 561 nm laser line, and the emissions were collected between 570 and 600 nm.

## Results

### Map-based cloning of *PiAVR2* gene candidates

Previously, $F_1$ progeny of a cross between *P. infestans* parental isolates 80029 (race 2.4.7; A1 mating type) and 88133 (race1.3.7.10.11; A2 mating type) were found to segregate for six dominant *Avr* genes, allowing these to be positioned within a genetic linkage map (Van der Lee *et al.*, 1997, 2001). To facilitate positional cloning of *AVR* genes, a BAC library was constructed from T30-4, an $F_1$ individual from this cross that contains all six segregating avirulence genes (*AVR1*, *AVR2*, *AVR3*, *AVR4*, *AVR10* and *AVR11*) (Whisson *et al.*, 2001). The BAC library was screened with AFLP markers E + GA/M + ATs513 and E + TG/M + CTs338 (Fig. 1a), defining the *AVR2* map location. Four positive BAC clones that contained either one or other of the two markers were assembled into two contigs that did not completely span the *AVR2*-containing region (Fig. 1a). BAC end-sequencing allowed the contigs to be anchored to supercontig 1.16 of the *P. infestans* isolate T30-4 genome sequence (http://www.broad.mit.edu/annotation/genome/phytophthora_infestans/Home.html; Haas *et al.*, 2009). Sequences at the outer ends of the BAC contigs indicated that the cloned fragments spanned 742.6 kb, within which was a 36.6 kb region containing three predicted RXLR-dEER effector-encoding genes (PITG_08943, PITG_08949 and PITG_22870) (Fig. 1a). Two of these (PITG_08943 and PITG_22870) are identical, apparently duplicated copies 2 kb apart. We confirmed that this is a genuine duplication in the T30-4 genome using PCR primers AVR2F10 and AVR2R10 (Fig. S1), which amplified between the duplicated gene copies to generate a PCR product of the expected 2.2 kb size (results not shown). As they are identical in T30-4, we refer only to PITG_22870 in the following. The third gene (PITG_08949) encodes a predicted protein that is similar across the first 79 amino acids, but which diverges considerably at the C-terminus (Fig. 1b), probably as a result of a DNA recombination event (Fig. S2).

## PITG_22870 triggers R2-dependent HR

Transcripts of RXLR effector genes accumulate predominantly during the early, biotrophic stage of *P. infestans* infection (Whisson *et al.*, 2007; Haas *et al.*, 2009). Real-time qRT-PCR was used to investigate transcript accumulation of PITG_22870 and PITG_08949 during potato infection by isolate 88069, which is avirulent on *R2* plants and possesses gene sequences that are identical to those in T30-4. Transcripts of both genes accumulated significantly in preinfection stages and during the biotrophic phase (1–3 d postinoculation), showing the characteristic expression (Whisson *et al.*, 2007) of RXLR effector genes (Fig. 2a).

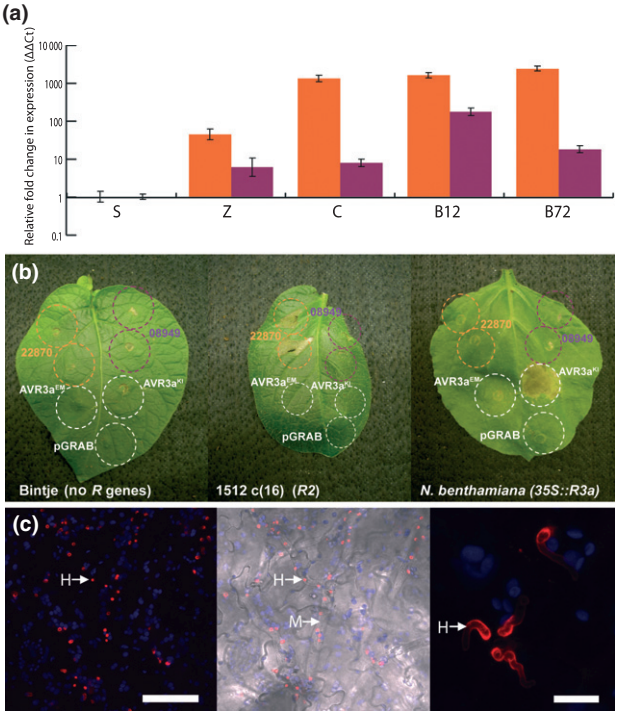


**Fig. 2** PITG_22870 is *PiAVR2*. (a) qRT-PCR showed that, relative to the control gene *ActA*, the expression of both PITG_22870 (orange) and PITG_08949 (purple) was up-regulated in *Phytophthora infestans* isolate 88069 in zoospores (Z), germinating cysts (C), and 12 and 72 h postinoculation of susceptible cv Bintje (B12 and B72), relative to expression in sporangia (S), which was given a value of 1. Error bars indicate ± SD for three biological replicates. (b) Whereas expression of PITG_22870 (orange), PITG_08943 (purple) and, as controls, $AVR3a^{EM}$, $AVR3a^{KI}$ and empty pGRAB vector (all white) yielded no response in cv Bintje (left), $AVR3a^{KI}$ alone caused a hypersensitive response (HR) in transgenic *Nicotiana benthamiana* expressing *R3a* (right), and only PITG_22870 triggered an HR in the *R2* potato differential 1512 c(16) (middle). (c) A *P. infestans* transformant expressing *PiAVR2* (PITG_22870)::*Tdtomato* fusion. The left panel shows the accumulation of the fusion protein in haustoria (H), which can be seen in relation to mycelium (M) in the middle panel. The right panel shows a higher magnification of haustorial accumulation of PiAVR2::Tdtomato fluorescence (H). White bars, 50 μm (left panel); 10 μm (right).

To test whether PITG_22870 and PITG_08949 are potentially *PiAVR2*, each was expressed, minus SP-encoding sequences, in potato cv Bintje, which lacks known late blight *R* genes; in the potato *R2* differential 1512 c(16); and, as a further control, in transgenic *N. benthamiana* expressing *R3a*. PITG_08949 failed to elicit an HR in any of these plants, whereas $AVR3a^{KI}$ elicited an HR, as expected (Armstrong *et al.*, 2005), only in *N. benthamiana* expressing *R3a*. PITG_22870 elicited an HR exclusively in the *R2* potato differential (Fig. 2b). Both PITG_22870 and PITG_08949, fused at the C-terminus to GFP, are stable when expressed in *N. benthamiana* (see Fig. 4).

To verify R2-dependent recognition of PITG_22870, the full-length construct (minus SP) was expressed, via co-bombardment with *GUS* as a marker of cell vitality, in cv Bintje and the *R2* differential clone 1512 c(16). Whereas no difference in GUS activity was seen following co-bombardment with PITG_22870 in Bintje, a considerable reduction in GUS activity, consistent with triggering the HR, was seen following co-bombardment with PITG_22870 exclusively on the *R2* differential (Fig. S3). Independently, both PITG_22870 and PITG_08949 were coexpressed in *N. benthamiana* with the *R2* gene, or with the orthologous genes *Blb3*, *ABPT* and *R2-like*, each of which provides a similar spectrum of resistance to *P. infestans* isolates. HR was observed with each *R2* orthologue only when coexpressed with PITG_22870 (Lokossou *et al.*, 2009). Taking these results together, PITG_22870 was tentatively renamed *PiAVR2*.

Previously, effector AVR3a was shown to accumulate at the site of haustorium formation during the biotrophic phase of late blight infection (Whisson *et al.*, 2007). Similar localization patterns have been observed for AVR4 and AVR-blb1 (Van Poppel, 2009). To investigate whether this was also the case for PiAVR2, isolate 88069 was transformed to express PiAVR2, translationally fused at its C-terminus to the fluorescent protein Tdtomato. Confocal microscopy revealed that PiAVR2 exclusively accumulated at haustoria during infection (Fig. 2c), a property consistent with a potential virulence role during biotrophy.

## Presence/absence and sequence polymorphisms in *PiAVR2*

To investigate polymorphisms that may explain *P. infestans* virulence on *R2* potato plants, three PCR primer pairs, one located in 3′ and 5′-flanking regions (primers AVR2F1 and R1), one spanning flanking and coding regions (AVR2F2 and R2; Fig. S1) and one set located within the coding region (AVR2F4 and R4; Fig. S1), were used to amplify *PiAVR2* from a diverse collection of 29 *P. infestans* isolates, 12 of which are virulent on *R2* plants and 17 of which are avirulent. Strikingly, no PCR amplification was observed with any of the three primer sets from nine of the 12 viru-

lent isolates, suggesting that *PiAVR2*, and its flanking regions, are either absent or highly divergent in these genomes. In the case of primer set AVR2F2/R2, lowering the annealing temperature resulted in weak PCR amplification products of the expected size from three of the nine virulent isolates that showed no amplification with AVR2F1/R1 and AVR2F4/R4 primers (Table 1). By contrast, all three primer sets amplified PCR products of the expected size from the remaining three virulent isolates and from all 17 avirulent isolates (Table 1).

The strong PCR amplification products generated with the AVR2F2/R2 PCR primer set from 20 of the tested isolates were sequenced. Only a single amino acid polymorphism, N31K, was observed in the predicted mature protein sequences derived from these *PiAVR2* genes. Seven isolates were heterozygous for $PiAVR2^{N31}$ and $PiAVR2^{K31}$, and 13 isolates were homozygous for $PiAVR2^{K31}$ (Table 1; Fig. S4). Both $PiAVR2^{N31}$ and $PiAVR2^{K31}$ sequences were represented within the three virulent and 17 avirulent isolates, indicating that this polymorphism is unlikely to specify differential recognition by R2. The *PiAVR2* sequence was PCR-amplified using the AVR2F2/R2 primer set and sequenced from a further 30 European and North American isolates of undetermined virulence on *R2* plants. Again, only the single N31K polymorphism was observed; 20 of these isolates were heterozygous for $PiAVR2^{N31}$ and $PiAVR2^{K31}$, and 10 isolates were homozygous for *PiAVR2*$^{K31}$ (Table S2). Intriguingly, out of the 50 tested isolates containing this gene, no $PiAVR2^{N31}$ homozygotes were observed.

## The C-terminal effector domain of PiAVR2 is recognized by R2

To test whether the N31K polymorphism in PiAVR2 proteins determined recognition by R2, each form, minus SP-encoding sequences, was coexpressed with *R2* in *N. benthamiana*. *R2* was also coexpressed with the N-terminal half (from the cleavage site of the SP to the end of the EER motif) or C-terminal half (from the first amino acid after the EER motif to the stop codon) coding regions of $PiAVR2^{N31}$ (the sequence within the assembled genome of avirulent clone T30-4; Haas *et al.*, 2009) (Fig. 3a). We found that R2-dependent HR occurred, to a similar extent, with both $PiAVR2^{N31}$ and $PiAVR2^{K31}$ full-length (minus SP-encoding) sequences (Fig. 3b,c). Given the presence of the $PiAVR2^{N31}$ and/or $PiAVR2^{K31}$ forms in three isolates that can infect *R2* plants, additional factors are needed to explain the virulence of these isolates. In agreement with this, no recognition of the N-terminus-encoding half of $PiAVR2^{N31}$ was observed, whereas a stronger and faster HR was observed with the C-terminus-encoding half alone (Fig. 3b,c). Western analyses with each *PiAVR2*-derived construct, fused at the C-terminus to *GFP*, revealed that

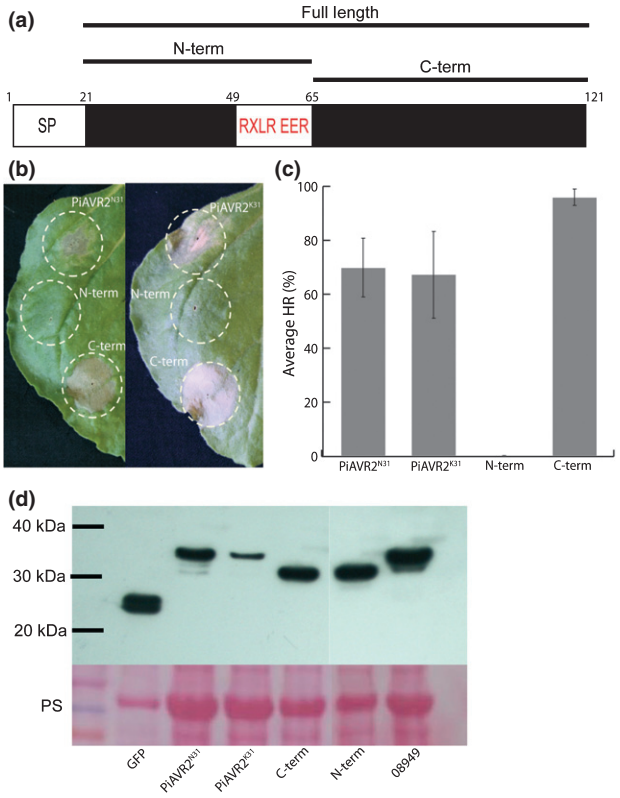


**Fig. 3** Resistance protein R2 recognizes the C-terminus of PiAVR2. (a) Schematic of portions of *PiAVR2* that were cloned and coexpressed with *R2*. (b) Coexpression of *R2* with full length of $PiAVR2^{N31}$ or $PiAVR2^{K31}$ (both minus SP), or the N-terminal or C-terminal coding portions of $PiAVR2^{N31}$, as indicated, in *Nicotiana benthamiana*. (c) Percentage of inoculation sites developing hypersensitive response (HR) following coexpression of *R2* with full length (minus SP) of $PiAVR2^{N31}$ or $PiAVR2^{K31}$, or the N-terminal or C-terminal coding portions of $PiAVR2^{N31}$, as indicated, in *N. benthamiana*. These results are the averages of three independent experiments each involving 24 inoculation sites per construct combination. Error bars indicate ± SE. (d) Western hybridization of green fluorescent protein (GFP) antibody to protein extracted 3 d postinoculation of plants expressing free *GFP*, full length (minus SP) of $PiAVR2^{N31}$ or $PiAVR2^{K31}$*::GFP*, the N-terminal or C-terminal coding portions of $PiAVR2^{N31}$, or PITG_08949, all translationally fused at the C-terminus to GFP, in *N. benthamiana*. Ponceau stain (PS) and size markers (kDa) are indicated.

each fusion protein was detectable following agroinfiltration and expression in *N. benthamiana*, albeit $PiAVR2^{K31}$ was apparently less stable than $PiAVR2^{N31}$ (Fig. 3d; see also Fig. 4g). These results indicate that, similar to $AVR3a^{KI}$ (Bos *et al.*, 2006), recognition of PiAVR2 is not dependent on the N-terminal half of the protein.

## An alternative form, PiAVR2-like, evades recognition by R2

No PCR product was obtained using primer sets AVR2F1/R1 or AVR2F4/R4 from nine of the *P. infestans* isolates that are virulent on *R2* potato, suggesting that

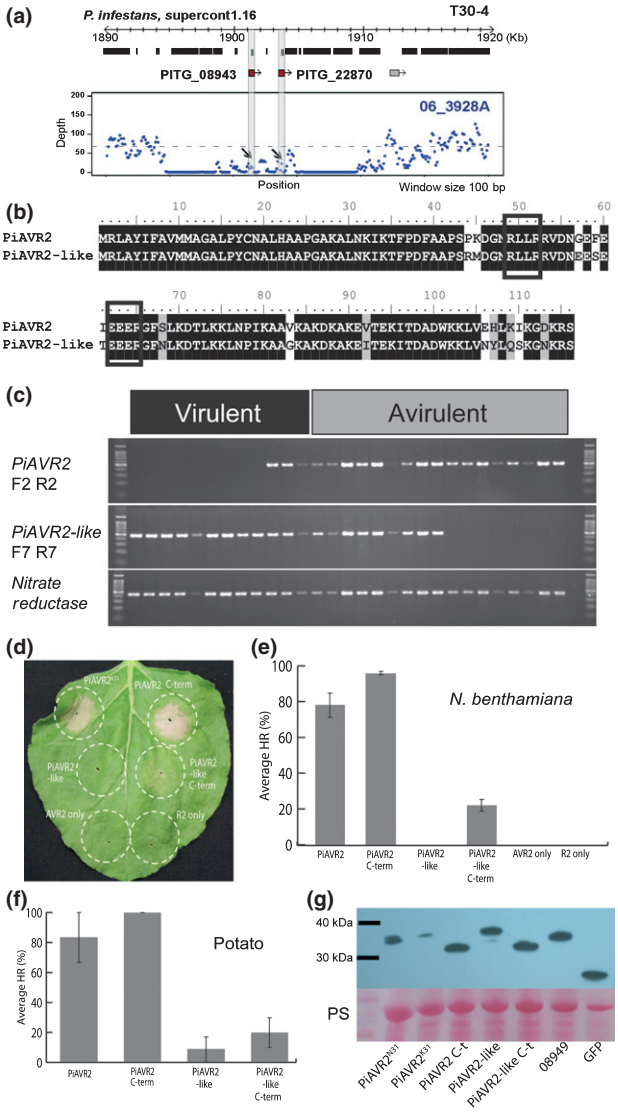


**Fig. 4** PiAVR2-like evades detection by R2. (a) Plot of sequencing depth of coverage of Illumina reads from isolate 06_3928A aligned to the region of supercontig 1.16 from isolate T30-4 containing the two *PiAVR2* paralogues (in red): PITG_22870 and PITG_08943. Arrows indicate regions where sequence reads from 06_3928A are aligned to *PiAVR2* genes highlighted within grey vertical bars. The horizontal dashed line indicates the average coverage of the 06_3928A genome. Note the *c.* 14.8 kb subregion (from 1894.9 to 1909.7 kb) that shows reduced coverage in reads from isolate 06_3928A, indicating high sequence divergence in this isolate (dark square, repeat; red square, RXLR effector; grey square, gene). (b) Protein alignment of PiAVR2 and PiAVR2-like, revealing 13 amino acid polymorphisms between the two mature proteins. The RLLR and EER motifs (dark boxes) is indicated. (c) Presence/absence polymorphisms between *PiAVR2* (PCR amplified with AVR2F2/R2 primers, annealing temperature 60°C) and *PiAVR2-like* (PCR amplified with AVR2F7/R7 primers, annealing temperature 58°C) across 12 virulent and 17 avirulent *Phytophthora infestans* isolates (arranged in the order shown, from top to bottom, in Table 1). PCR amplification of the control gene *nitrate reductase* is indicated. (d) Whereas the full-length (minus SP-coding) and C-terminus coding regions of *PiAVR2* trigger HR when coexpressed with *R2* in *Nicotiana benthamiana*, the equivalent regions of *PiAVR2-like* do not. Expression of *PiAVR2* and *R2* alone are indicated as controls. (e) Average percentage HR for 24 inoculation sites replicated in three experiments following expression of *PiAVR2* or *R2* alone, or coexpression of each construct combination in *N. benthamiana* (as in d) as indicated. Error bars indicate ± SE. (f) Average percentage HR across 24 inoculation sites for full-length (minus SP-coding) and C-terminus coding regions of *PiAVR2*, or equivalent regions of *PiAVR2-like* following expression in the *R2* differential 1512 c(16). (g) Western hybridization of green fluorescent protein (GFP) antibody to protein extracted 3 d postinoculation of plants expressing free *GFP*, full length (minus SP) of *PiAVR2*$^{N31}$*::GFP* or *PiAVR2*$^{K31}$*::GFP*, the C-terminal coding portion of *PiAVR2* (PiAVR2 C-t) fused to *GFP*, full-length (minus SP) *PiAVR2-like::GFP*, the C-terminal portion of *PiAVR2-like* (Piavr2 C-t) fused to *GFP*, or PITG_08949::*GFP*, in *N. benthamiana*. Ponceau stain (PS) and size markers (kDa) are indicated.

*PiAVR2*, if present, is divergent at the DNA sequence level. Nevertheless, three of these isolates yielded a weak PCR product with the AVR2F2/R2 primer set when the annealing temperature was lowered (Table 1). One of these isolates, 06_3928A, is a representative of the 13_A2 genotype that is currently prevalent in western Europe (Cooke *et al.*, 2009; Fry *et al.*, 2009). The genome of this isolate has recently been sequenced using Illumina technology and will be reported elsewhere. Alignment of 06_3928A reads against the genomic region of T30-4, including the two *PiAVR2* paralogues, PITG_22870 and PITG_08943, revealed that a subregion of 14.8 kb is highly divergent in this strain (Fig. 4a). Within the 14.8 kb subregion, very few reads could be aligned to the *PiAVR2* coding sequence, suggesting the gene is divergent in the 06_3928A strain. The weak AVR2F2/R2 PCR products from the three *P. infestans* isolates were thus sequenced. They revealed a gene sequence that was conserved between the three isolates and which showed striking similarity to *PiAVR2*; 25 SNPs were observed between the coding regions (Fig. S1), resulting in 13 amino acid polymorphisms between the mature proteins (Fig. 4b). The combined assembly of the aligned and unaligned sequence reads from 06_3928A corresponding to the *PiAVR2* gene confirmed the presence of the variant form (termed *PiAVR2-like*) within the 06_3928A genome. *PiAVR2-like* was absent from both assembled and unassembled reads of the T30-4 genome.

PCR primers (avr2F6/R6 and avr2F7/R7; Fig. S1) designed specifically to amplify this sequence variant yielded amplification products from all 12 isolates that are virulent on *R2*, and from nine of the 17 avirulent isolates (Fig. 4c; Table 1). PCR products were sequenced from 13 isolates that represent distinct *P. infestans* genotypes, as defined by simple sequence repeat markers (Lees *et al.*, 2006). Only two polymorphisms in the predicted proteins were observed, M10T and I92V (Table 1; Fig. S4). The first is within the predicted signal peptide, which is cleaved from the mature protein during secretion, and is thus unlikely to

affect recognition by R2. In the case of the I92V polymorphism, the Val residue is shared with the recognized PiAVR2 protein. If *PiAVR2-like* evades recognition by R2, the presence of the allele encoding a protein with the $Val^{92}$ residue in virulent isolates indicates that this polymorphism is unlikely to specify recognition by R2 (Fig. S4; Table 1). Although a number of isolates contain both *PiAVR2* and *PiAVR2-like*, all avirulent isolates contain the recognized *PiAVR2* sequence, and all virulent isolates contain *PiAVR2-like*. This prompted us to test whether *PiAVR2-like* is recognized by R2.

Regions encoding the full length (minus SP) and C-terminal halves (from the first amino acid after the EER motif to the stop codon) of *PiAVR2* and *PiAVR2-like* were independently coexpressed with *R2* in *N. benthamiana*. Whereas both *PiAVR2* constructs triggered *R2*-dependent HR, full-length *PiAVR2-like* did not, and the C-terminal portion very rarely triggered an HR (Fig. 4d,e). Moreover, expression of each construct in the potato *R2* differential, 1512 c(16), again revealed an HR with *PiAVR2*, but an HR was infrequently observed with only the C-terminal half of *PiAVR2-like* (Fig. 4f). As before for PiAVR2, western analysis of all forms translationally fused at the C-terminus to GFP indicated that PiAVR2-like was stable on expression in *N. benthamiana* (Fig. 4g).

## *R2* orthologues from wild *Solanum* species show a similar spectrum of recognition

Previously, three *R2* orthologues from wild *Solanum* species, *BLB3*, *ABPT* and *R2-like*, were all shown to possess the same spectrum of resistance and to respond with a strong HR when coexpressed with *PiAVR2* (Lokossou *et al.*, 2009). We coexpressed the full-length (minus SP) forms of $PiAVR2^{N31}$, $PiAVR2^{K31}$ or *PiAVR2-like* with each of these *R2* orthologues in *N. benthamiana*. As expected, whereas both $PiAVR2^{N31}$ and $PiAVR2^{K31}$ triggered a clear HR with each, there was seldom a response to *PiAVR2-like* (Fig. 5). Thus, none of these *R* genes is expected to extend resistance to additional *P. infestans* isolates, such as 06_3928A, a representative of the prevalent genotype 13_A2.

## Virulence on *R2* plants is associated with presence or expression of only *PiAVR2-like*

Whereas *PiAVR2* is present in all avirulent isolates, *PiAVR2-like* is present in all virulent isolates. Nevertheless, nine of the avirulent isolates, and three of the tested virulent isolates, possess both forms (Table 1). A possible explanation for the phenotypic differences in this class of isolate is differential expression of *PiAVR2* and *PiAVR2-like*. To investigate this, PCR primers specific to the coding regions of *PiAVR2* (F4/R4; Fig. S1) and *PiAVR2-like* (Fig. S1) were used to amplify the corresponding fragments from

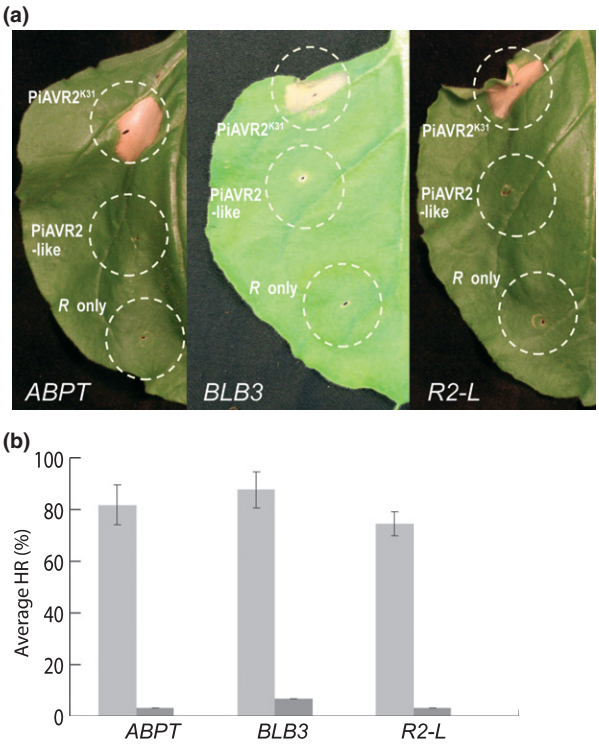


**Fig. 5** Resistance genes *ABPT*, *BLB3* and *R2-like* show similar specificity to *R2*. (a) Panels showing coexpression of full-length (minus SP-coding) regions of $PiAVR2^{K31}$ or *PiAVR2-like* with *ABPT* (left), *BLB3* (middle) or *R2-like* (right) in *Nicotiana benthamiana*. Expression of the relevant *R* gene alone is shown in each panel. (b) Average percentage hypersensitive response (HR) for 24 inoculation sites replicated in three experiments following coexpression of $PiAVR2^{N31}$ or $PiAVR2^{K31}$ (combined in the graph as PiAVR2, as both forms were recognized to a similar degree; light grey bars), or *PiAVR2-like* (mid-grey bars) with *ABPT* (left), *BLB3* (middle) or *R2-like* (right) in *N. benthamiana*. (*R* gene only, black bars) Error bars indicate ± SE.

cDNA prepared 2 d after leaf inoculation. The following isolates were tested: T30-4 (which possesses only *PiAVR2*); 06_3928A (which possesses only *PiAVR2-like*); 06_4168B and 06_4168C (which are virulent but possess both forms); and 88069 and 06_4256B (which are avirulent but possess both forms) (Table 1). As expected, expression of only *PiAVR2* was detected in T30-4, and of only *PiAVR2-like* in 06_3928A. In addition, expression of both *PiAVR2* and *PiAVR2-like* was detected in the avirulent isolates 88069 and 06_4256B. However, in the virulent isolates 06_4168B and 06_4168C, expression of only *PiAVR2-like* was detected (Fig. 6a). Thus, both presence/absence and expression polymorphisms of *PiAVR2* and *PiAVR2-like* explain virulence on *R2* potato. qRT-PCR primers which amplify both forms (Fig. S1) were used to show that the corresponding *PiAVR2* and *PiAVR2-like* genes show the expected biotrophic pattern of transcript accumulation early in infection in T30-4 and 06_3928A, respectively (Fig. 6b).

### *PiAVR2* is a dominant gene triggering *R2*-dependent resistance

To investigate whether R2-dependent recognition of *PiAVR2* confers disease resistance, isolate 06_3928A, which is virulent on *R2* potato plants and contains only the *PiAVR2-like* variant, was transformed to express the $PiAVR2^{K31}$ allele cloned from the avirulent isolate 88069. Isolate 88069 and both transformed and untransformed 06_3928A strains infected cv Craigs Royal, which lacks *R2*. By contrast, the 06_3928A strain transformed to express *PiAVR2* elicited a clear HR on the *R2* differential 1512 c(16), whereas untransformed 06_3928A was able to infect this plant (Fig. 6c). *PiAVR2* is thus a dominant gene that triggers *R2*-dependent HR and disease resistance.

## Discussion

A map-based cloning strategy was used to identify an RXLR-EER effector gene, *PiAVR2,* from the *P. infestans* T30-4 genome sequence (Fig. 1). Coexpression of *PiAVR2* with the potato resistance gene *R2* results in a clear HR (Figs 3, 4). Moreover, transformation of a virulent isolate of the pathogen to express *PiAVR2* resulted in R2-mediated HR (Fig. 6), indicating that this is a dominant gene responsible for triggering R2-dependent disease resistance. Expression in plants of either full-length PiAVR2 protein minus the signal peptide, or of its C-terminal effector domain (from the amino acid following the EER motif to the stop codon) resulted in R2-dependent HR (Figs 3, 4), indicating that, as shown for other RXLR effectors (Birch *et al.*, 2008; Schornack *et al.*, 2009), recognition occurs within the host cell. Again consistent with other RXLR effector genes, such as *AVR3a* from *P. infestans* (Armstrong *et al.*, 2005; Whisson *et al.*, 2007), *PiAVR2* transcripts accumulate during biotrophy and encode a protein that accumulates at haustoria (Fig. 2), which form an intimate association with the host cell during this stage of infection.

PCR amplification and sequencing of *PiAVR2* from a diverse set of *P. infestans* isolates revealed that this gene was present in all avirulent isolates and was highly conserved (Fig. 4). Only a single amino acid polymorphism, N31K, was observed between the signal peptide and the RLLR-EER motifs in the predicted proteins. Of 50 isolates containing this gene, 27 were heterozygous for the $PiAVR2^{N31}$ and $PiAVR2^{K31}$ alleles, and 23 were homozygous for the $PiAVR2^{K31}$ allele (Table 1; Table S2). The strong bias towards the $PiAVR2^{K31}$ allele is reminiscent of the bias towards $AVR3a^{EM}$, rather than the $AVR3a^{KI}$ allele, across a similar number of diverse *P. infestans* isolates (Armstrong

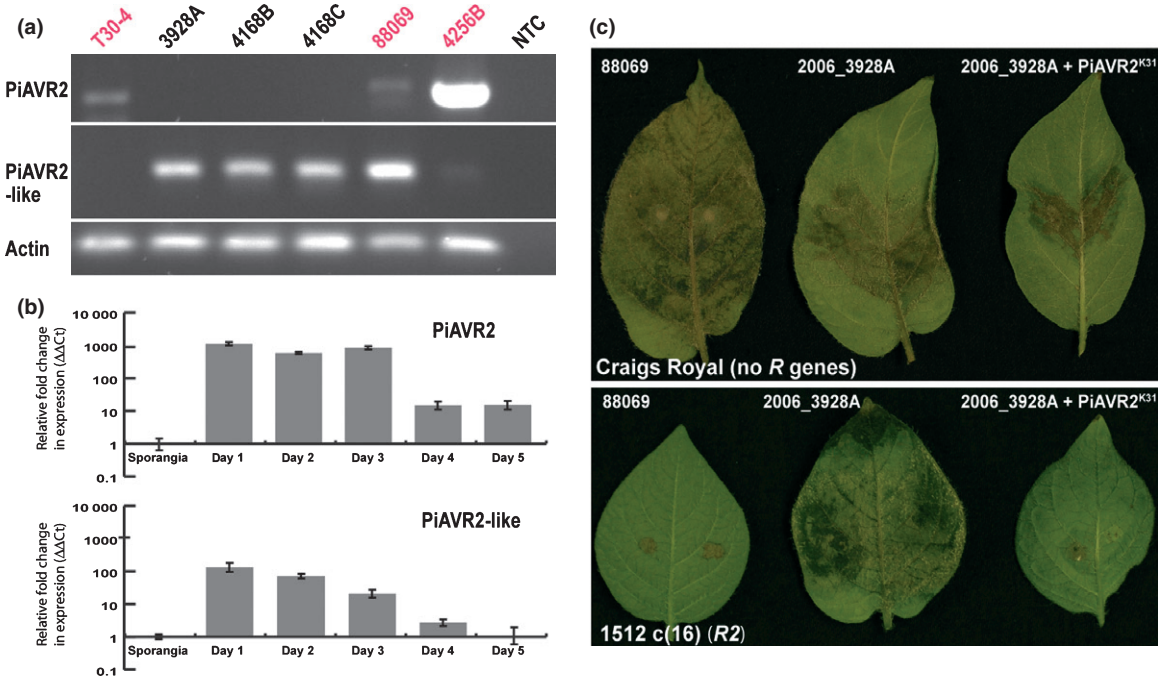


**Fig. 6** *PiAVR2* is a dominant gene specifying *R2*-dependent disease resistance. (a) RT-PCR showing expression of *PiAVR2* (upper panel), *PiAVR2-like* (middle panel) and control gene *ActA* (lower panel) in isolates T30-4, 06_3928A, 06_4168B, 06_4168C, 88069 and 06_4256B, 24 h postinoculation of potato cv Bintje. Isolates in red are avirulent and those in black are virulent on *R2* plants. (b) qRT-PCR showing up-regulation, relative to the control gene *ActA*, of *PiAVR2* in T30-4 (upper graph) and *PiAVR2-like* in 06_3928A (lower graph) during the first 5 d of potato cv Bintje infection, relative to that within sporangia (given a value of 1). (c) Infection of leaves from cv Craigs Royal (upper panel; CR), which lacks *R2*, and the *R2* potato differential 1512 c(16) (lower panel; R2), 6 d after inoculation with isolates 88069 (avirulent on *R2*), 06_3928A (virulent on *R2*) and 06_3928A transformed to express $PiAVR2^{K31}$.

*et al.*, 2005). However, whereas *AVR3a*$^{EM}$ evades recognition by the potato resistance gene *R3a*, both the *PiAVR2*$^{N31}$ and *PiAVR2*$^{K31}$ alleles are recognized equally by *R2*. Indeed, the strong recognition of the C-terminal effector domain, which is conserved between the proteins encoded by these alleles, indicates that any genotypic bias in pathogen populations is not associated with evasion of *R2*-mediated recognition.

## Gene duplication and recombination to create a new RXLR-EER effector

*PiAVR2* was apparent as two identical, adjacent copies (PITG_08943 and PITG_22870) within the genome of *P. infestans* isolate T30-4, the consequence of a recent duplication event. Approx. 30 kb away is a related gene, PITG_08949, which is up-regulated before and during biotrophy, a hallmark of RXLR effector genes. The predicted protein sequences of PiAVR2 and PITG_08949 are highly similar across the first 79 amino acids, strongly suggestive of a common ancestry. After this they diverge significantly, providing distinct C-termini of 37 and 20 amino acids, respectively. These differences are not the result of frameshift mutations, but rather are likely the result of a DNA recombination event (Fig. S2).

The N-terminal signal peptide and RXLR-EER domains of RXLR effectors can be regarded as a functional unit required for secretion and delivery to their site of action within the host cell. It is therefore reasonable to expect greater sequence diversity in response to selection pressure on the C-terminal 'effector' domains which, in addition to their proposed roles in manipulating host defences, must evade detection by R proteins. Indeed, positive selection has been detected mainly in the C-terminal portions of RXLR genes (Win *et al.*, 2007). Regarding the N-terminal and C-terminal regions of these effectors as functionally distinct modules, a likely mechanism by which the latter could evolve distinct virulence specificities is through recombination, and this appears to be the case to generate either *PiAVR2* or PITG_08949, the latter of which evades detection by R2 (Fig. 2). Further work is needed to determine the potential host targets of PiAVR2 and PITG_08949 and to investigate whether they play distinct, or related, roles in promoting *P. infestans* disease development.

## Virulence on *R2* plants

Copy number variation has been a feature of avirulence loci in *P. infestans* and *P. sojae* and has contributed to phenotypic variation (Jiang *et al.*, 2006; Qutob *et al.*, 2009; Dong *et al.*, 2009). This is well documented particularly for *PsAvr1a* and *PsAvr3a*, with some avirulent *P. sojae* isolates containing multiple copies and some virulent isolates revealing complete deletion of recognized forms (Qutob *et al.*, 2009). Both PCR and genome sequencing suggest that *PiAVR2* is deleted from the genomes of many virulent isolates. Alignment of sequence reads from the virulent isolate 06_3928A against the genome sequence of the avirulent clone T30-4 revealed that a 14.8 kb subregion, including *PiAVR2* paralogues, is highly divergent (Fig. 4a). In addition, for both *PsAvr1a* and *PsAvr3a*, transcriptional differences have contributed to virulence on plants containing the associated *R* genes (Qutob *et al.*, 2009). It is apparent that not only sequence but also transcriptional variation has occurred in *PiAVR2*, as no expression was detected in two virulent isolates that contain this gene (Fig. 6a).

In addition to *PiAVR2,* and by using the genomic and PCR sequencing data, we discovered a divergent form, *PiAVR2-like,* which is present in the genomes of all tested virulent isolates. The predicted protein of this sequence differs from PiAVR2 in 13 amino acids, eight of which reside in the C-terminal effector domain. As this domain alone, from PiAVR2, is detected by R2, one or more of these polymorphisms must specify the evasion of R2-mediated HR by PiAVR2-like.

We found that nine of the 12 virulent isolates tested lacked *PiAVR2* but possessed *Piavr2*. By contrast, eight of the 17 avirulent isolates tested possessed *PiAVR2* but lacked *PiAVR2-like*. The remaining three virulent and nine avirulent isolates contain both forms. Testing two of these three virulent isolates revealed that *PiAVR2-like* was expressed whereas *PiAVR2* was not. Therefore, not only does a combination of presence/absence polymorphisms and transcriptional silencing explain virulence on *R2* plants, but the data may also suggest functional complementarity between *PiAVR2* and *PiAVR2-like*, as absence or silencing of one form coincides with presence or expression of the other. It will thus be interesting to determine whether these sequences share a common function in pathogenicity. We noted that, of the two avirulent isolates tested that possess *PiAVR2* and *PiAVR2-like*, both forms were expressed during infection, albeit to different levels (Fig. 6a), indicating that expression of one does not preclude expression of the other. However, critically, every isolate investigated in this study expresses one form or the other, or both, and it will thus be important to determine whether, like *AVR3a* (Bos *et al.*, 2010), these sequences provide an essential role during infection.

## Proposed strategy for durable disease resistance

Although both *PiAVR2* and *PiAVR2-like* differ from each other by 25 nucleotides (13 amino acids), within each sequence we observed little variation. A single nonsynonymous change, N31K, was observed in the PiAVR2 protein sequences from 50 isolates, and only two polymorphisms, M10T and I92V, were observed in the PiAVR2 protein

from 13 isolates, one of which is in the signal peptide and therefore cleaved from the mature protein (Table 1; Fig. S4). Whereas *R2*, and related sequences from wild *Solanum* species, *BLB3*, *ABPT* and *R2-like*, all recognize *PiAVR2*, none of these resistances extends specificity to *PiAVR2-like*. Given the apparent conservation of each effector sequence, and the ubiquitous presence of either or both forms, we propose that a search for *R* genes that detect *PiAVR2-like* is a high priority. Deployed in combination, *R2* and an *R* gene that recognizes *PiAVR2-like* may provide effective and durable late blight resistances for the European potato industry, given that the pathogen genotypes studied here are representative of the wider European population. This study highlights the importance of understanding the molecular basis not only of recognition, which leads to disease resistance, but also of how the pathogen, at the molecular level, is equipped to evade such recognition. Armed with such knowledge, we propose that the targeted search for specific resistances, and their judicious deployment, can be carefully directed to control this versatile and economically devastating pathogen.

## Acknowledgements

We thank the Biotechnology and Biological Sciences Research Council and Rural and the Scottish Government Environmental Research and Analysis Directorate for funding this research. J.M. was funded by an EU Alβan programme PhD studentship awarded to SCRI.

## References

**Allen RL, Bittner-Eddy PD, Grenville-Briggs LJ, Meitz JC, Rehmany AP, Rose LE, Beynon JL. 2004**. Host-parasite coevolutionary conflict between Arabidopsis and Downy Mildew. *Science* **306**: 1957–1960.

**Armstrong MR, Whisson SC, Pritchard L, Bos JI, Venter E, Avrova AO, Rehmany AP, Böhme U, Brooks K, Cherevach I *et al.* 2005**. An ancestral oomycete locus contains late blight avirulence gene *Avr3a*, encoding a protein that is recognized in the host cytoplasm. *Proceedings of the National Academy of Sciences, USA* **102**: 7766–7771.

**Birch PRJ, Armstrong MR, Bos JI, Boevink P, Gilroy EM, Taylor RM, Wawra S, Pritchard L, Conti L, Ewan R *et al.* 2009**. Towards understanding the virulence functions of RXLR effectors of the oomycete plant pathogen *Phytophthora infestans*. *Journal of Experimental Botany* **60**: 1133–1140.

**Birch PRJ, Boevink PC, Gilroy EM, Hein I, Pritchard L, Whisson SC. 2008**. Oomycete RXLR effectors: delivery, functional redundancy and durable disease resistance. *Current Opinion in Plant Biology* **11**: 373–379.

**Birch PRJ, Rehmany AP, Pritchard L, Kamoun S, Beynon JL. 2006**. Trafficking arms: oomycete effectors enter host plant cells. *Trends in Microbiology* **14**: 8–11.

**Bos JI, Armstrong MR, Gilroy EM, Boevink PC, Hein I, Taylor RM, Zhendong T, Engelhardt S, Vetukuri RR, Harrower B *et al.* 2010**. *Phytophthora infestans* effector AVR3a is essential for virulence and manipulates plant immunity by stabilizing host E3 ligase CMPG1. *Proceedings of the National Academy of Sciences, USA* **107**: 9909–9914.

**Bos JI, Kanneganti TD, Young C, Cakir C, Huitema E, Win J, Armstrong MR, Birch PRJ, Kamoun S. 2006**. The C-terminal half of *Phytophthora infestans* RXLR effector AVR3a is sufficient to trigger R3a-mediated hypersensitivity and suppress INF1-induced cell death in *Nicotiana benthamiana*. *Plant Journal* **48**: 165–176.

**Brasier CM. 1992**. Evolutionary biology of *Phytophthora:* part I: genetic system, sexuality and the generation of variation. *Annual Review of Phytopathology*, **30**: 153–170.

**Champouret N, Bouwmeester K, Rietman H, van der Lee T, Maliepaard C, Heupink A, van de Vondervoort PJ, Jacobsen E, Visser RG, van der Vossen EA *et al.* 2009**. *Phytophthora infestans* isolates lacking class I *ipiO* variants are virulent on *Rpi-blb1* potato. *Molecular Plant-Microbe Interactions* **22**: 1535–1545.

**Chisholm ST, Coaker G, Day B, Staskawicz BJ. 2006**. Host–microbe interactions: shaping the evolution of the plant immune response. *Cell* **124**: 803–814.

**Cooke DEL, Lees AK, Hansen JG, Lassen P, Andersson B, Bakonyi J. 2009**. From a European to a global database of *P. infestans* genetic diversity: examining the nature and significance of population change. Proceedings of the third International Late Blight Conference, Beijing, China. 03–06 April 2008. *Acta Horticulture* **834**: 19–26.

**Curtis MD, Grossniklaus U. 2003**. A gateway cloning vector set for high-throughput functional analysis of genes in planta. *Plant Physiology* **133**: 462–469.

**Dong S, Qutob D, Tedman-Jones J, Kuflu K, Wang Y, Tyler BM, Gijzen M. 2009**. The *Phytophthora sojae* avirulence locus *Avr3c* encodes a multi-copy RXLR effector with sequence polymorphisms among pathogen strains. *PLoS ONE* **4**: e5556.

**Dou D, Kale SD, Liu T, Tang Q, Wang X, Arredondo FD, Basnayake S, Whisson S, Drenth A, Maclean D, Tyler BM. 2010**. Different domains of *Phytophthora sojae* effector Avr4/6 are recognised by soybean resistance genes Rps4 and Rps6. *Molecular Plant-Microbe Interactions* **23**: 425–435.

**Dou D, Kale SD, Wang X, Jiang RH, Bruce NA, Arredondo FD, Zhang X, Tyler BM. 2008**. RXLR-mediated entry of *Phytophthora sojae* effector Avr1b into soybean cells does not require pathogen-encoded machinery. *Plant Cell* **20**: 1930–1947.

**Fry W. 2008**. *Phytophthora infestans*: the plant (and *R* gene) destroyer. *Molecular Plant Pathology* **9**: 385–402.

**Fry WF, Grünwald NJ, Cooke DEL, McLeod A, Forbes GA, Cao K. 2009**. Population genetics and population diversity of *Phytophthora infestans*. In: Lamour K, Kamoun S, eds. *Oomycete genetics and genomics: diversity, interactions and research tools*. Hoboken, NJ, USA: Wiley Blackwell, 139–164.

**Haas BJ, Kamoun S, Zody MC, Jiang RH, Handsaker RE, Cano LM, Grabherr M, Kodira CD, Raffaele S, Torto-Alalibo T *et al.* 2009**. Genome sequence and analysis of the Irish potato famine pathogen *Phytophthora infestans*. *Nature* **461**: 393–398.

**Hein I, Birch PRJ, Danan S, Lefebvre V, Odeny DA, Genhardt C, Trognitz F, Bryan G. 2009a**. Progress in mapping and cloning qualitative and quantitative resistance against *Phytophthora infestans* in potato and its wild relatives. *Potato Research* **52**: 215–227.

**Hein I, Gilroy EM, Armstrong MR, Birch PRJ. 2009b**. The zig-zag-zig in oomycete-plant interactions. *Molecular Plant Pathology* **10**: 547–562.

**Jiang RH, Weide R, van de Vondervoort PJ, Govers F. 2006**. Amplification generates modular diversity at an avirulence locus in the pathogen *Phytophthora*. *Genome Research* **16**: 827–840.

**Jones JD, Dangl JL. 2006**. The plant immune system. *Nature* **444**: 323–329.

**Kamoun S. 2003**. Molecular genetics of pathogenic oomycetes. *Eukaryotic Cell* **2**: 191–199.

**Kamoun S. 2006**. A catalogue of the effector secretome of plant pathogenic Oomycetes. *Annual Review of Phytopathology* **44**: 41–60.

**Kamoun S. 2007**. Groovy times: filamentous pathogen effectors revealed. *Current Opinion in Plant Biology* **10**: 358–365.

**Kamoun S, Klucher KM, Cof\fey MD, Tyler BM. 1993**. A gene encoding a host-specific elicitor protein of *Phytophthora parasitica*. *Molecular Plant-Microbe Interactions* **6**: 573.

**Karimi M, Inzé D, Depicker A. 2002**. Gateway vectors for Agrobacterium-mediated plant transformation. *Trends in Plant Science* **7**: 193–195.

**Lees AK, Wattier R, Shaw DS, Sullivan L, Williams NA, Cooke DEL. 2006**. Novel microsatellite markers for the analysis of *Phytophthora infestans* populations. *Plant Pathology* **55**: 311–319.

**Li H, Durbin R. 2010**. Fast and accurate long-read alignment with Burrows-Wheeler transform. *Bioinformatics* **26**: 589.

**Lokossou AA, Park TH, van Arkel G, Arens M, Ruyter-Spira C, Morales J, Whisson SC, Birch PRJ, Visser RG, Jacobsen E *et al.* 2009**. Exploiting knowledge of R/Avr genes to rapidly clone a new LZ-NBS-LRR family of late blight resistance genes from potato linkage group IV. *Molecular Plant-Microbe Interactions* **22**: 630–641.

**Oh S-K, Young C, Lee M, Oliva R, Bozkurt TO, Cano LM, Win J, Bos JIB, Liu H-Y, van Damme M *et al.* 2009**. *In planta* expression screens of *Phytophthora infestans* RXLR effectors reveal diverse phenotypes, including activation of the *Solanum bulbocastanum* disease resistance protein Rpi-blb2. *Plant Cell* **21**: 2928–2947.

**Qutob D, Tedman-Jones J, Dong S, Kuflu K, Wang Y, Dou D, Kale S, Arredondo FD, Tyler BM, Gijzen M. 2009**. Copy number variation and transcriptional polymorphisms of *Phytopthora sojae* RXLR effector genes *Avr1a* and *Avr3a*. *PLoS ONE* **4**: e5066.

**Rehmany AP, Gordon A, Rose LE, Allen RL, Armstrong MR, Whisson SC, Kamoun S, Tyler BM, Birch PRJ, Beynon JL. 2005**. Differential recognition of highly divergent downy mildew avirulence gene alleles by *RPP1* resistance genes from two Arabidopsis lines. *Plant Cell*, **17**: 1839–1850.

**Schornack S, Huitema E, Cano LM, Bozkurt TO, Oliva R, Van Damme M, Schwizer S, Raffaele S, Chaparro-Garcia A, Farrer R *et al.* 2009**. Ten things to know about oomycete effectors. *Molecular Plant Pathology* **10**: 795–803.

**Shan W, Cao M, Leung D, Tyler BM. 2004**. The *Avr1b* locus of *Phytophthora sojae* encodes an elicitor and a regulator required for avirulence on soybean plants carrying resistance gene *Rps1b*. *Molecular Plant-Microbe Interactions* **17**: 394–403.

**Van der Lee T, De Witte I, Drenth A, Alfonso C, Govers F. 1997**. AFLP linkage map of the oomycete *Phytophthora infestans*. *Fungal Genetics and Biology* **21**: 278–291.

**Van der Lee T, Robold A, Testa A, van't Klooster JW, Govers F. 2001**. Mapping of avirulence genes in *Phytophthora infestans* with amplified fragment length polymorphism markers selected by bulked segregant analysis. *Genetics* **157**: 949–956.

**Van Poppel PMJA. 2009**. *The Phytophthora infestans avirulence gene PiAvr4 and its potato counterpart R4*. PhD thesis, University of Wageningen, Wageningen, the Netherlands.

**Van Poppel PMJA, Guo J, van de Vandervoort PJI, Jung MWJ, Birch PRJ, Whisson SC, Govers F. 2008**. The *Phytophthora infestans* avirulence gene *Avr4* encodes an RxLR-dEER effector. *Molecular Plant-Microbe Interactions* **21**: 1460–1470.

**Vleeshouwers VG, Rietman H, Krenek P, Champouret N, Young C, Oh SK, Wang M, Bouwmeester K, Vosman B, Visser RG *et al.* 2008**. Effector genomics accelerates discovery and functional profiling of potato disease resistance and *Phytophthora infestans* avirulence genes. *PLoS ONE*, **3**: e2875.

**Whisson SC, Boevink PC, Moleleki L, Avrova AO, Morales JG, Gilroy EM, Armstrong MR, Grouffaud S, van West P, Chapman S *et al.* 2007**. A translocation signal for delivery of oomycete effector proteins into host plant cells. *Nature* **450**: 115–118.

**Whisson SC, van der Lee T, Bryan GJ, Waugh R, Govers F, Birch PRJ. 2001**. Physical mapping across an avirulence locus of *Phytophthora infestans* using a highly representative, large-insert bacterial artificial chromosome library. *Molecular Genetics and Genomics* **266**: 289–295.

**Win J, Morgan W, Bos J, Krasileva KV, Cano LM, Chaparro-Garcia A, Ammar R, Staskawicz BJ, Kamoun S. 2007**. Adaptive evolution has targeted the C-terminal domain of the RXLR effectors of plant pathogenic Oomycetes. *Plant Cell* **19**: 2349–2369.

## Supporting Information

Additional supporting information may be found in the online version of this article.

**Fig. S1** Locations of PCR primers on the *PiAVR2* and *PiAVR2-like* gene sequences.

**Fig. S2** DNA sequence alignment of PITG_22870 and PITG_08949, showing the location of a likely recombination event.

**Fig. S3** Co-bombardment reveals *R2*-mediated recognition of *PiAVR2*.

**Fig. S4** Protein sequence alignments of PiAVR2 and PiAVR2-like from isolates virulence tested on *R2* plants.

**Table S1** PCR primers for cloning *PiAVR2* and *PiAVR2-like* regions for transient expression

**Table S2** *PiAVR2* genotypes of 30 *Phytophthora infestans* isolates of unknown virulence on *R2* plants

Please note: Wiley-Blackwell are not responsible for the content or functionality of any supporting information supplied by the authors. Any queries (other than missing material) should be directed to the *New Phytologist* Central Office.

**Table S1** PCR primers for cloning *PiAVR2* and *Piavr2* regions for transient agrobacterium-mediated expression or co-bombardment in potato or *Nicotiana benthamiana*.

| Vector | Gene | Primer | Primer Sequence |
|---|---|---|---|
| pGRAB | PiAVR2 (-SP) | AscI For | 5'-AAGGGGCGCGCCATGCTGCATGCAGCTCCAGGTGC-3' |
| | | BamHI Rev | 5'-AAGGGGATCCTTAACTCCTCTTGTCACC-3' |
| pDNR221 | PiAVR2 (-SP) | PiAVR2 For | 5'-AAAGCAGGCTTCACCATGCTGCATGCAGCTCCAGGTG-3' |
| | | PiAVR2 Rev | 5'-GAAAGCTGGGTCTTAACTCCTCTTGTCACCCTTAAT-3' |
| | PiAVR2 C-term | PiAVR2 Ct For | 5'-AAAGCAGGCTTCACCATGGGATTCAGTCTGAAGGATAC-3' |
| | | PiAVR2 Rev | 5'-GAAAGCTGGGTCTTAACTCCTCTTGTCACCCTTAAT-3' |
| | PiAVR2 N-term | PiAVR2 For | 5'-AAAGCAGGCTTCACCATGCTGCATGCAGCTCCAGGTG-3' |
| | | PiAVR2 Nt Rev | 5'-GAAAGCTGGGTCTTAACTCTCTTCCTCGATCTCAAA-3' |
| pGRAB | PITG_08949 (-SP) | AscI For | 5'-AAGGGGCGCGCCATGTTGCATGCCGTCTATGATGC-3' |
| | | BamHI Rev | 5'-AAGGGGATCCTTAACATGTTGTACGTACAAC-3' |
| pDNR221 | PITG_08949 (-SP) | For | 5'-AAAGCAGGCTTCACCATGTTGCATGCCGTC-3' |
| | | Rev | 5'-GAAAGCTGGGTCTTATTTAATGGGATTGAG-3' |
| pDNR221 | AttB sites | AttB1 For | 5'-GGGGACAAGTTTGTACAAAAAAGCAGGCTTCACC-3' |
| | | AttB2 Rev | 5'-GGGGACCACTTTGTACAAGAAAGCTGGG-3' |

Table S2 Additional data on 30 *P. infestans* isolates (of unknown virulence on *R2* plants) for which *PiAVR2* was amplified using PCR primer pair AVR2F2/R2.

| Genotype[a] | Isolate Name | Country of Origin | SNP within *PiAVR2* |
|---|---|---|---|
| 12_A1 | 2006_4320F | UK | K |
| 2_A1 | 2006_3960A | UK | K |
| 20_A1 | 2006_4024E | UK | K |
| 21_A1 | 2004_10477B | UK | K |
| 5g_A1 | 07_5866C | UK | K |
| 8_2a_A1 | 2006_4232E | UK | K |
| misc | 07_5738G | UK | K |
| misc | 08_6446F | UK | K |
| 1_A1 | 2006_4304A | UK | K/N |
| 16_A2 | 2006_3992G | UK | K/N |
| 17_A2 | 2006_4388E | UK | K/N |
| 17_A2 | 2006_4388G | UK | K/N |
| 18_A1 | 06_4332 (SS8_01) | UK | K/N |
| 18_A1 | 06_4332 (SS8_07) | UK | K/N |
| misc | 07_5054A | UK | K/N |
| misc | 07_5726D | UK | K/N |
| misc | 07_5726E | UK | K/N |
| misc | 07_5738B | UK | K/N |
| misc | 07_5738E | UK | K/N |
| misc | 07_5974A | UK | K/N |
| misc | 08_6394B | UK | K/N |
| misc | 08_6446D | UK | K/N |
| misc | 2006_3996A | UK | K/N |
| misc | 07_By9B | Germany | K/N |
| misc | 550 | Mexico | K/N |
| misc | MP_622 | Poland | K |
| misc | NL80029 | Netherlands | K/N |
| misc | NL88133 | Netherlands | K/N |
| misc | SE_03058 | Sweden | K |
| misc | SE_03087 | Sweden | K/N |

[a]misc represents a selection of miscellaneous genotypes

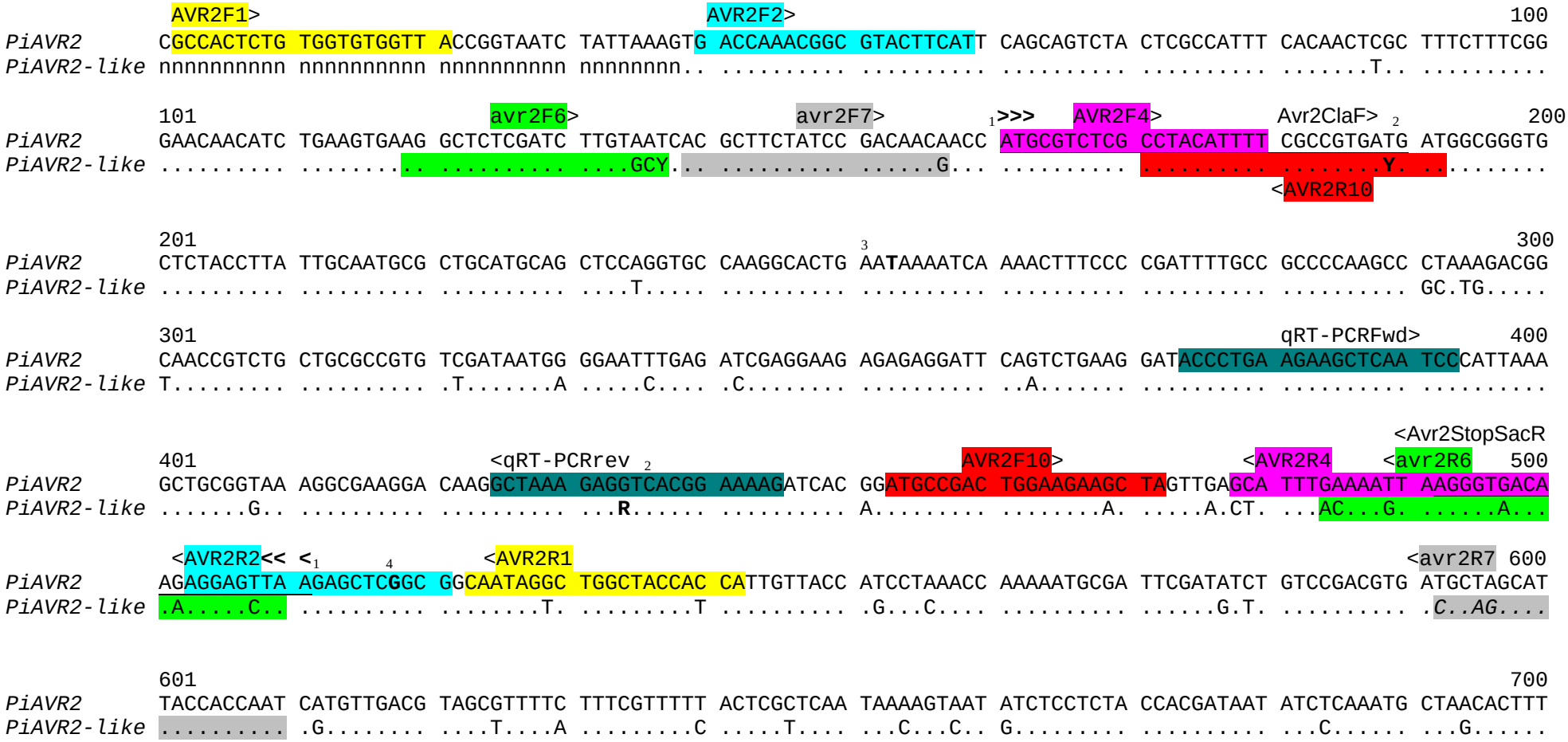


[1] >>> and <<< mark translation start and stop, respectively, of the coding sequence
[2] polymorphic within *PiAVR2-like* from 06_3928A
[3] polymorphic within *PiAVR2* from T30-4
[4] site of single bp deletion in PITG_08943 that distinguishes it from PITG_22870
Orientation of primers is denoted by > or <
The following primers were used as diagnostics for expression of recognized *PiAVR2* (AVR2F4 and AVR2R4), and the unrecognised *PiAVR2-like* (avr2diagF1 5'-CCGCCCCAAGCCGCATG-3' and avr2diagR1 5'-TGTTACCCTTACTTTGTAAATAG-3').
Primers for cloning *PiAVR2* for transformation and expression in isolate 06_3928A (Avr2ClaF and Avr2StopSacR) were, respectively, 5'- GGAAATCGATACC ATGCGTCTCG CCTACATTTT CGCCGTGA-3' and 5'- GGAACCGCGGTTAACTCCTCTTGTCACCCT-3' (locations underlined in figure). For fusion to Tdtomato (transformed into isolate 88069), the alternative reverse primer Avr2NoStopClaR was used: 5'-GGAAATCGATACTCCTCTTGTCACCCTTAA-3'. Underlined regions are indicated in the Figure.

**Figure S1** Location of PCR primers used in this study shown on sequences representative of the *PiAVR2* and *PiAVR2-like* genes.

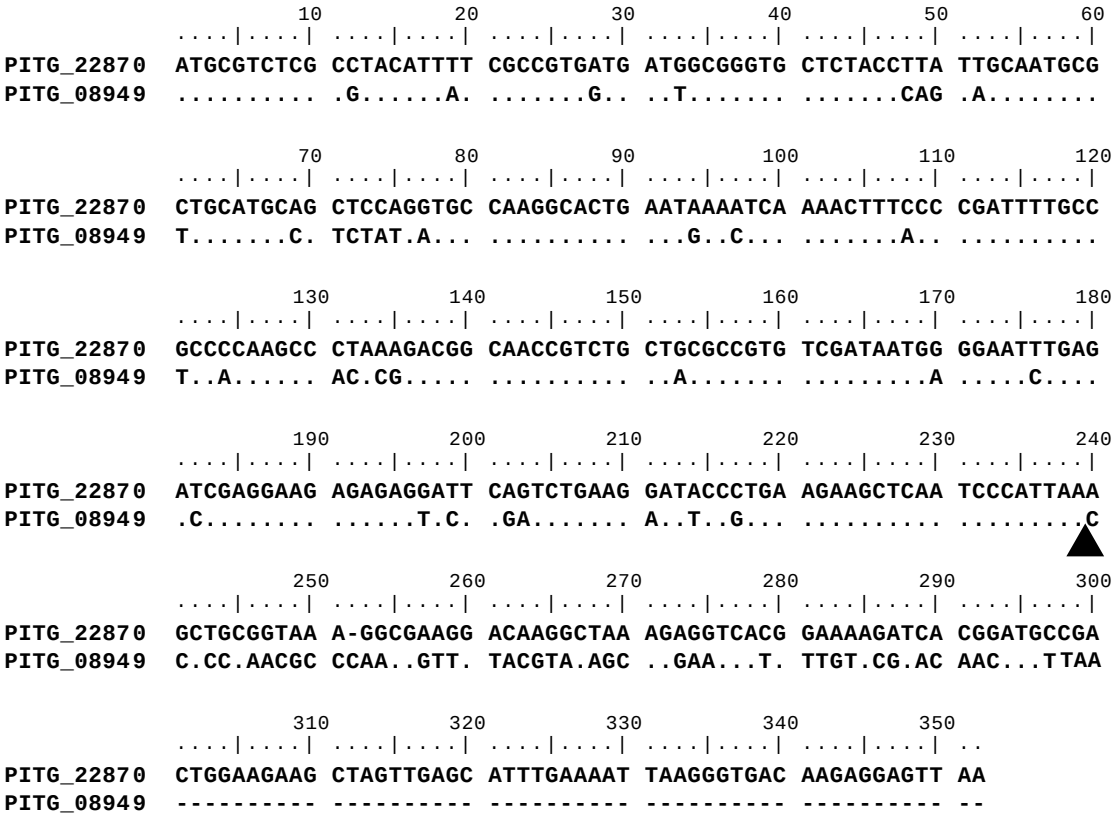


**Figure S2** DNA alignment of the coding sequences of PITG_22870 and PITG_08949. The inverted arrowhead indicates the position of sequence divergence between these sequences suggestive of a recombination event to generate alternative C-termini in the two predicted proteins (shown in Fig 1b).

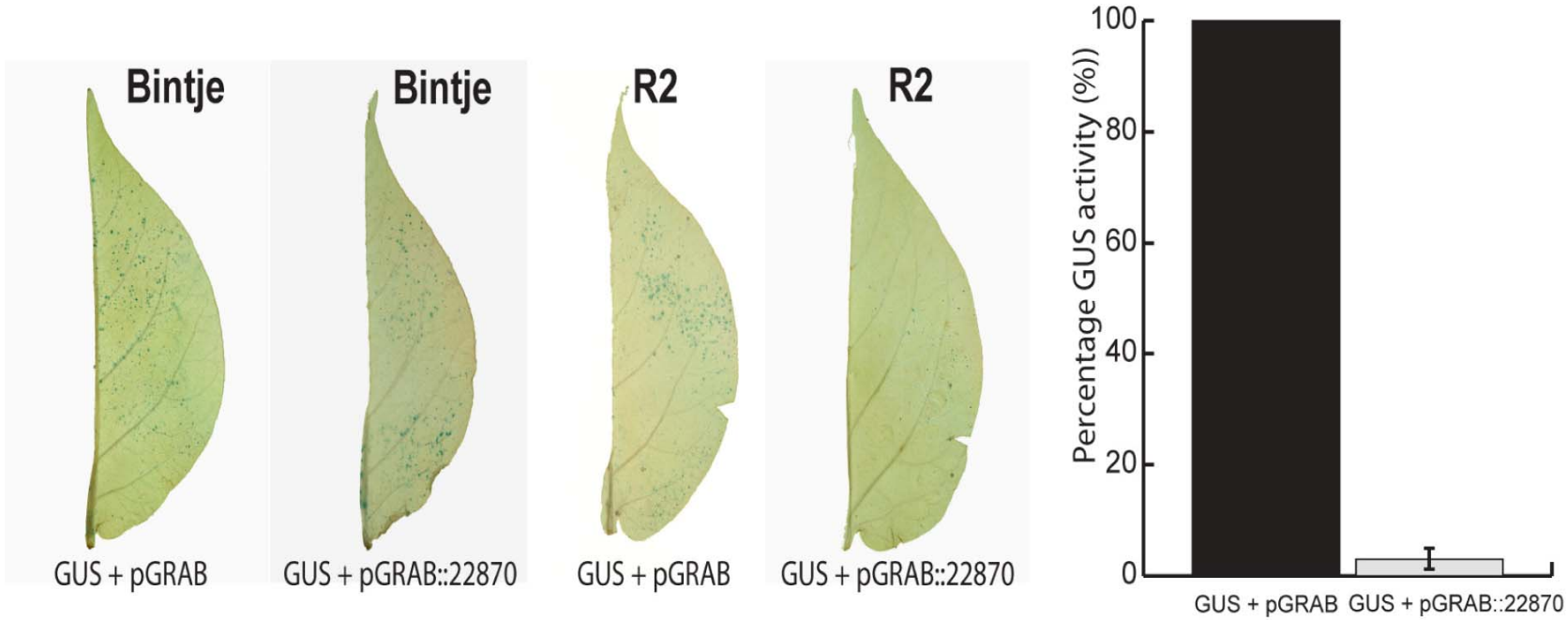


**Figure S3** Co-bombardment reveals R2-mediated recognition of PITG_22870 (*PiAVR2*)
GUS activity (blue specks) following bombardment of the *GUS* construct alone, or co-bombardment of *GUS* with PITG_22870 on cv Bintje or the *R2* potato differential 1512 c(16) as indicated. There is little visible difference in GUS staining on cv Bintje. However, considerably less GUS activity is observed on leaves of 1512 c(16) (R2), which is also represented in the graph to the right (for 6 pairs of half-leaves).

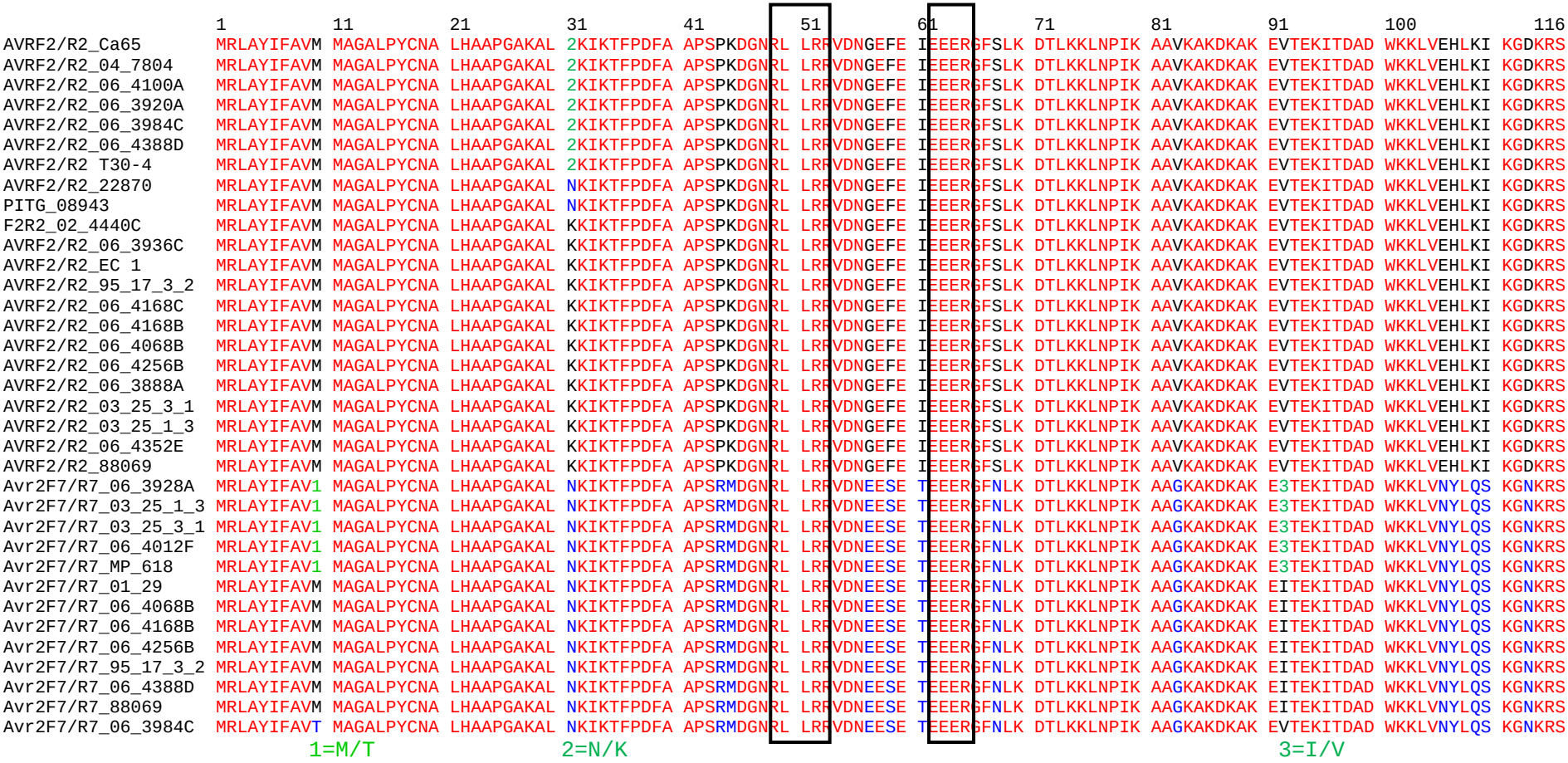


**Figure S4** Alignment of the R2-recognized PiAVR2 (amplified with AVR2F2/R2 primers) and unrecognized PiAVR2-like (amplified with avr2F7/R7 primers) protein sequences showing the amino acid changes within and between each form. The isolate names are preceded by the primer sequences that were used to amplify and sequence the PCR products. Numbers (in green) indicate isolates that are heterozygous as indicated. Details of each isolate are shown in Table S1. Primer locations and sequences are shown in Fig S1. Boxes indicate the RLLR and EER motifs.